US010822622B2

(12) **United States Patent**
Luo et al.

(10) **Patent No.: US 10,822,622 B2**
(45) **Date of Patent: Nov. 3, 2020**

(54) **METHODS FOR TREATING CELLS CONTAINING FUSION GENES**

(71) Applicant: **UNIVERSITY OF PITTSBURGH—OF THE COMMONWEALTH SYSTEM OF HIGHER EDUCATION**, Pittsburgh, PA (US)

(72) Inventors: **Jianhua Luo**, Wexford, PA (US); **Yanping Yu**, Wexford, PA (US); **Zhanghui Chen**, Hangzhou (CN); **George Konstantine Michalopoulos**, Pittsburgh, PA (US); **Joel Nelson**, Pittsburgh, PA (US)

(73) Assignee: **UNIVERSITY OF PITTSBURGH—OF THE COMMONWEALTH SYSTEM OF HIGHER EDUCATION**, Pittsburgh, PA (US)

(*) Notice: Subject to any disclaimer, the term of this patent is extended or adjusted under 35 U.S.C. 154(b) by 0 days.

(21) Appl. No.: **16/356,587**

(22) Filed: **Mar. 18, 2019**

(65) **Prior Publication Data**

US 2019/0203231 A1 Jul. 4, 2019

Related U.S. Application Data

(60) Division of application No. 15/406,472, filed on Jan. 13, 2017, now Pat. No. 10,308,960, which is a continuation of application No. PCT/US2015/041029, filed on Jul. 17, 2015, which is a continuation of application No. PCT/US2014/072268, filed on Dec. 23, 2014.

(60) Provisional application No. 62/025,923, filed on Jul. 17, 2014.

(51) **Int. Cl.**

C12N 15/90	(2006.01)
C12Q 1/6886	(2018.01)
C12N 15/63	(2006.01)
C12N 15/11	(2006.01)
A61K 31/522	(2006.01)
A61K 38/17	(2006.01)
A61K 48/00	(2006.01)
C12N 9/12	(2006.01)
C12N 9/22	(2006.01)

(52) **U.S. Cl.**

CPC ***C12N 15/907*** (2013.01); ***A61K 31/522*** (2013.01); ***A61K 38/1761*** (2013.01); ***A61K 48/0058*** (2013.01); ***C12N 9/1211*** (2013.01); ***C12N 9/22*** (2013.01); ***C12N 15/11*** (2013.01); ***C12N 15/111*** (2013.01); ***C12N 15/63*** (2013.01); ***C12Q 1/6886*** (2013.01); ***C12Y 207/01021*** (2013.01); *C12N 2310/10* (2013.01); *C12N 2310/20* (2017.05); *C12Q 2600/156* (2013.01)

(58) **Field of Classification Search**

CPC C12N 15/907

See application file for complete search history.

(56) **References Cited**

U.S. PATENT DOCUMENTS

9,932,641	B2	4/2018	Luo et al.
2008/0274909	A1	11/2008	Brothman
2012/0220672	A1	8/2012	Pestano et al.
2013/0079241	A1	3/2013	Luo et al.
2013/0225420	A1	8/2013	Albertson et al.

FOREIGN PATENT DOCUMENTS

WO	WO 2008/016374	A2	2/2008
WO	WO 2008/023087	A2	2/2008
WO	WO 2010/056337	A2	5/2010
WO	WO 2010/138460	A1	12/2010
WO	WO 2012/139134	A2	10/2012
WO	WO 2013/037118	A1	3/2013
WO	WO 2014/018673	A2	1/2014
WO	WO 2014/039556	A1	3/2014
WO	WO 2015/106341	A1	7/2015

OTHER PUBLICATIONS

U.S. Appl. No. 13/619,556, (US 2013/0079241), filed Sep. 14, 2012 (Mar. 28, 2013) (Abandoned).
U.S. Appl. No. 14/336,965, (US 2015/0050647), filed Jul. 21, 2014 (Feb. 19, 2015).
U.S. Appl. No. 15/199,056, (US 2016/0376666), filed Jun. 30, 2016 (Dec. 29, 2016).
U.S. Appl. No. 15/406,472, (U.S. Pat. No. 10,308,960), filed Jan. 13, 2017 (Jun. 4, 2019).
U.S. Appl. No. 15/896,818, filed Feb. 14, 2018.
U.S. Appl. No. 15/896,931, filed Feb. 14, 2018.
U.S. Appl. No. 13/619,556, Sep. 30, 2014 Notice of Abandonment.
(Continued)

Primary Examiner — Scott Long
(74) *Attorney, Agent, or Firm* — Baker Botts L.L.P.

(57) **ABSTRACT**

The present invention relates to methods for treating prostate cancer patients. It is based, at least in part, on the discovery that approximately 90% of men carrying at least one of the following fusion genes: TRMT11-GRIK2, SLC45A2-AMACR, MTOR-TP53BP1, LRRC59-FLJ60017, TMEM135-CCDC67 and CCNH-C5orf30 experienced prostate cancer recurrence, metastases and/or prostate cancer-specific death after radical prostatectomy (each examples of "progressive prostate cancer"), while these outcomes occurred in only 36% of men not carrying any of these fusion genes. It is also based, at least in part, on the discovery that a genome editing technique that specifically targets a fusion gene can induce cell death in a cancer cell that carries the fusion gene.

18 Claims, 69 Drawing Sheets

Specification includes a Sequence Listing.

(56) **References Cited**

OTHER PUBLICATIONS

U.S. Appl. No. 13/619,556, Jul. 3, 2014 Advisory Action.
U.S. Appl. No. 13/619,556, Jun. 19, 2014 Response to Final Office Action.
U.S. Appl. No. 13/619,556, Feb. 21, 2014 Final Office Action.
U.S. Appl. No. 13/619,556, Nov. 14, 2013 Response to Non-Final Office Action.
U.S. Appl. No. 13/619,556, Jul. 16, 2013 Non-Final Office Action.
U.S. Appl. No. 13/619,556, May 13, 2013 Response to Restriction Requirement.
U.S. Appl. No. 13/619,556, Mar. 12, 2013 Restriction Requirement.
U.S. Appl. No. 14/336,965, Jun. 7, 2017 Amendment and Request for Continued Examination (RCE).
U.S. Appl. No. 14/336,965, Feb. 7, 2017 Final Office Action.
U.S. Appl. No. 14/336,965, Nov. 2, 2016 Response to Non-Final Office Action.
U.S. Appl. No. 14/336,965, May 2, 2016 Non-Final Office Action.
U.S. Appl. No. 14/336,965, Feb. 3, 2016 Response to Restriction Requirement.
U.S. Appl. No. 14/336,965, Aug. 3, 2015 Restriction Requirement.
U.S. Appl. No. 15/199,056, Aug. 1, 2017 Response to Non-Final Office Action.
U.S. Appl. No. 15/199,056, May 3, 2017 Non-Final Office Action.
U.S. Appl. No. 15/199,056, Mar. 8, 2017 Response to Restriction Requirement.
U.S. Appl. No. 15/199,056, Mar. 3, 2017 Applicant Initiated Interview Summary.
U.S. Appl. No. 15/199,056, Nov. 9, 2016 Restriction Requirement.
U.S. Appl. No. 14/336,965, Mar. 20, 2018 Non-Final Office Action.
U.S. Appl. No. 15/199,056, Mar. 8, 2018 Notice of Allowance.
U.S. Appl. No. 15/199,056, Jan. 16, 2018 Issue Fee Payment.
U.S. Appl. No. 15/199,056, Oct. 16, 2017 Notice of Allowance.
U.S. Appl. No. 15/199,056, Aug. 25, 2017 Request for Continued Examination (RCE).
U.S. Appl. No. 15/199,056, Aug. 23, 2017 Notice of Allowance.
U.S. Appl. No. 15/406,472, Jun. 8, 2018 Restriction Requirement.
U.S. Appl. No. 15/406,472, Jul. 24, 2018 Response to Restriction Requirement.
U.S. Appl. No. 15/406,472, Sep. 11, 2018 Non-Final Office Action.
U.S. Appl. No. 15/406,472, Dec. 11, 2018 Response to Non-Final Office Action.
U.S. Appl. No. 15/406,472, Jan. 23, 2019 Notice of Allowance.
U.S. Appl. No. 15/406,472, Apr. 23, 2019 Issue Fee Payment.
Agarwal et al., (2003) Zinc metalloproteinase, ZMPSTE24, is mutated in mandibuloacral dysplasia, Human Molecular Genetics 12(16):1995-2001 (2003).
Ahn et al., "Fer Protein-Tyrosine Kinase Promotes Lung Adenocarcinoma Cell Invasion and Tumor Metastasis," Mol Cancer Res 11(8):952-963 (2013).
Anderson et al., "A simple method for the rapid generation of recombinant adenovirus vectors," Gene Therapy 7:1034-1038 (2000).
Antonarakis et al., "Changes in PSA Kinetics Predict Metastasis-Free Survival in Men with PSA-Recurrent Prostate Cancer Treated With Nonhormonal Agents: Combined Analysis of 4 Phase II Trials," Cancer 118:1533-1542 (2012).
Baca et al., "Punctuated Evolution of Prostate Cancer Genomes," Cell 153:666-677 (2013).
Bae, et al., "Low Frequency Mutation of the Ephrin Receptor A3 Gene in Hepatocellular Carcinoma", Neoplasma, 56(4):331-334 (2009).
Bar-Peled et al., "A Tumor Suppressor Complex with GAP Activity for the Rag GTPases That Signal Amino Acid Sufficiency to mTORC1," Science 340:1100-1106 (2013).
Berger et al., "The genomic complexity of primary human prostate cancer," Nature 4 70:214-220 (2011).
Bettendorf, et al., "Cytogenetic Changes and Loss of Heterozygosity in Atypical Adenomatous Hyperplasia, in Carcinoma of the Prostate and in Non-Neoplastic Prostate Tissue Using Comparative Genomic Hybridization and Multiplex-PCR", International Journal of Oncology, 26(1):267-274 (2005).
Blackford, et al., "Genetic Mutations Associated with Cigarette Smoking in Pancreatic Cancer", Cancer Research, 69(8):3681-3688 (2009).
Budd, et al., "Circulating Tumor Cells Versus Imaging-Predicting overall survival in Metastatic Breast Cancer", Clinical Cancer Research, 12(21):6403-6409 (2006).
Carver et al., "ETS rearrangements and prostate cancer initiation," Nature 457:E1; discussion E2-3 (2009).
Chen et al., "Targeting genomic rearrangements in tumor cells through Cas9-mediated insertion of a suicide gene," Nature Biotechnology, 35(6):543-550 (2017).
Chi et al., "ETV1 is a lineage survival factor that cooperates with KIT in gastrointestinal stromal tumours," Nature 467:849-853 (2010).
Clark et al., "ETS gene fusions in prostate cancer," Nat Rev Urol. 6:429-439 (2009).
Clifford, et al., "The EphA3 Receptor is Expressed in a Subset of Rhabdomyosarcoma Cell Lines and Suppresses Cell Adhesion and Migration", Journal of Cellular Biochemistry, 105:1250-1259 (2008).
Corban-Wilhelm et al., "Cytosine deaminase versus thymidine kinase: a comparison of the antitumor activity," Clinical and Experimental Medicine, 3(3):150-156 (2003).
Demichelis et al., "TMPRSS2:ERG gene fusion associated with lethal prostate cancer in a watchful waiting cohort," Oncogene, 26:4596-4599 (2007).
Derwent Abstract Accession No. 2013-E07845 (accessed on Sep. 21, 2016).
Edgren et al., "Identification of fusion genes in breast cancer by paired-end RNA-sequencing," Genome Biol. 12:R6 (2011).
El Gammal et al., "Chromosome 8p Deletions and 8q Gains are Associated with Tumor Progression and Poor Prognosis in Prostate Cancer," Clin Cancer Res 16:56-64 (2010).
Enard et al., "Intra- and Interspecific Variation in Primate Gene Expression Patterns," Science 296:340-343 (2002).
Enninga et al., "Sec13 Shuttles between the Nucleus and the Cytoplasm and Stably Interacts with Nup96 at the Nuclear Pore Complex," Molecular and Cellular Biology 23(20):7271-7284 (2003).
Esvelt et al., "Concerning RNA-guided gene drives for the alteration of wild populations," eLife 3:e03401 (2014).
Fisher et al., "A Novel Cyclin Associates with M015/CDK7 to Form the CDK-Activating Kinase," Cell 78:713-724 (1994).
Fitzgerald et al., "Association of TMPRSS2-ERG gene fusion with clinical characteristics and outcomes: results from a population-based study of prostate cancer," BMC Cancer 8:230 (2008).
Freedland et al., "Death in Patients With Recurrent Prostate Cancer After Radical Prostatectomy: Prostate-Specific Antigen Doubling Time Subgroups and Their Associated Contributions to All-Cause Mortality," J Clin Oncol. 25(13):1765-1771 (2007).
Golub, et al., "Molecular Classification of Cancer: Class Discovery and Class Prediction by Gene Expression Monitoring", Science, 286:531-537 (1999).
Green, et al., "Integrative analysis Reveals Selective 9p24.1 Amplification, Increased PD-1 Ligand Expression, and Further Induction Via JAK2 in Nodular Sclerosing Hodgkin Lymphoma and Primary Mediastinal Large B-Cell Lymphoma", Blood, 116(17):3268-3277 (2010).
Guo et al., "FER tyrosine kinase (FER) overexpression mediates resistance to quinacrine through EGF-dependent activation of NF-κB," PNAS USA 108(19):7968-7973 (2011).
Ha et al., "Identification of gene fusion transcripts by transcriptome sequencing in BRCA1-mutated breast cancers and cell lines," BMC Medical Genomics 4:75 (2011).
Hakkarainen et al., "A conditionally replicative adenovirus that codes for a TKGFP fusion protein (Ad5Delta24TK-GFP) for evaluation of the potency of oncolytic virotherapy combined with molecular chemotherapy," International Journal of Molecular Medicine, 18(4):751-759 (2006).
Han et al., "Interaction of integrin-linked kinase (ILK) and MCM7 mediating integrin α7 induced cell growth suppression," Cancer Research 70(11):4375-4384 (2010).

(56) **References Cited**

OTHER PUBLICATIONS

Han et al., "Metallothionein 1 h tumour suppressor activity in prostate cancer is mediated by euchromatin methyltransferase 1," The Journal of Pathology 230(2):184-193 (2013).
Hanczar, et al., "Small-Sample Precision of ROC-Related Estimates", Bioinformatics, 26(6):822-830 (2010).
Hanks, et al., "Pretreatment Prostate-Specific Antigen Doubling times: Clinical Utility of this Predictor of Prostate Cancer Behavior", Int. J. Radiation Oncology Biol. Phys., 34(3):549-553 (1996).
Hao et al., "Isolation and Sequence Analysis of a Novel Human Tyrosine Kinase Gene," Mol Cell Biol 9(4):1587-1593 (1989).
Heitzer et al., "Tumor-associated copy number changes in the circulation of patients with prostate cancer identified through whole-genome sequencing," Genome Medicine 5:30 (2013).
Hieronymus et al., "Copy number alteration burden predicts prostate cancer relapse,".
International Search Report and Written Opinion dated Apr. 1, 2015 in International Application No. PCT/US2014/072268.
International Search Report dated Oct. 17, 2016 in International Application No. PCT/US2016/046051.
International Search Report dated Oct. 7, 2015 in International Application No. PCT/US2015/041029.
Isaacs, "Molecular Markers for Prostate Cancer Metastasis", American Journal of Pathology, 150(5):1511-1521 (1997).
Ivanova et al., "FER kinase promotes breast cancer metastasis by regulating α6- and β1-integrin-dependent cell adhesion and anoikis resistance," Oncogene 32:5582-5592 (2013).
Jane-Valbuena et al., "An Oncogenic Role for ETV1 in Melanoma," Cancer Research 70(5):2075-2084 (2010).
Jemal et al., "Global Cancer Statistics," CA Cancer J Clin. 61(2):69-90 (2011).
Jemal, et al., "Global Cancer Statistic", CA Cancer J. Clin., 59:225-249 (2009).
Jemal, et al., "Global Cancer Statistic", CA Cancer J. Clin., 60:277-300 (2010).
Jeon et al., "A variant Ewing's sarcoma translocation (7;22) fuses the EWS gene to the ETS gene ETV1," Oncogene 10:1229-1234 (1995).
Jinek et al., "A Programmable Dual-RNA-Guided DNA Endonuclease in Adaptive Bacterial Immunity," Science 337:816-821 (2012).
Jing et al., "Expression of Myopodin Induces Suppression of Tumor Growth and Metastasis," The American Journal of Pathology 164(5):1799-1806 (2004).
Jung et al., "Discovery of ALK-PTPN3 Gene Fusion from Human Non-Small Cell Lung Carcinoma Cell Line Using Next Generation RNA Sequencing," Genes, Chromosomes & Cancer 51:590-597 (2012).
Kawakami et al., "FER overexpression is associated with poor postoperative prognosis and cancer-cell survival in non-small cell lung cancer," Int J Clin Exp Pathol 6(4):598-612 (2013).
Kim, et al., "Integrative analysis of Genomic Aberrations Associated with Prostate Cancer Progression", Cancer Research, 67(17):8229-8239 (2007).
Koutras, et al., "The Upgrade Role of HER3 and HER4 Receptors in Breast cancer", Critical Reviews in Oncology/Hematology, 74:73-78 (2010).
Krastev et al., "A systematic RNAi synthetic interaction screen reveals a link between p53 and snoRNP assembly," Nature Cell Biology 13(7):809-818 (2011).
Kraus, et al., "High-Resolution genomic Profiling of Occult Micrometastatic Tumor Cells", Genes, Chromosomes & cancer, 36:159-166 (2003).
Krolewski et al., "Identification and chromosomal mapping of new human tyrosine kinase genes," Oncogene 5:277-282 (1990).
Kwok et al., "FES Kinase Promotes Mast Cell Recruitment to Mammary Tumors via the Stem Cell Factor/KIT Receptor Signaling Axis," Mol. Cancer Res 10(7):881-891 (2012).
LaGrange et al., "Renal Cell Carcinoma Associated with TFE3 Gene Fusion in an Elderly Woman," Urology 70:590.e11-590.e12 (2007).
Lee, et al., "Somatic Mutation in Epidermal Growth Factor Receptor Signaling Pathway Genes in Non-Small Cell Lung Cancers", Journal of Thoracic Oncology, 5(11):1734-1740 (2010).
Li et al., "Fast and accurate long-read alignment with Burrows-Wheeler transform," Bioinformatics 26(5):589-595 (2010).
Li et al., "Identification of tyrosine-phosphorylated proteins associated with metastasis and functional analysis of FER in human hepatocellular carcinoma cells," BMC Cancer 9:366 (2009).
Liu et al., "Comprehensive Assessment of DNA Copy Number Alterations in Human Prostate Cancers Using Affymetrix 100K SNP Mapping Array," Genes, Chromosomes & Cancer 45:1018-1032 (2006).
Liu, et al., "Copy Number Analysis Indicates Monoclonal Origin of Lethal Metastatic Prostate Cancer", Nature Medicine, 15(5):559-565.
Loimas et al., "Human prostate carcinoma cells as targets for herpes simplex virus thymidine kinase-mediated suicide gene therapy," Cancer Gene Therapy, 8(2):137-144 (2001).
Luo et al., "(−)-Epigallocatechin-3-gallate induces Du 145 prostate cancer cell death via downregulation of inhibitor of DNA binding 2, a dominant negative helix-loop-helix protein," Cancer Science 101(3):707-712 (2010).
Luo et al., "Discovery and Classification of Fusion Transcripts in Prostate Cancer and Normal Prostate Tissue," Am J Pathol 185:1834-1845 (2015).
Luo et al., "Gene Expression Analysis of Prostate Cancers," Molecular Carcinog. 33:25-35 (2002).
Macoska, et al., "Evolution of 8p Loss in Transformed Human Prostate Epithelial cells", Cancer Genetics and Cytogenetics, 154:36-43 (2004).
Matsui, et al., "Molecular Characterization of a Consistent 4.5-Megabase Deletion at 4q28 in Prostate Cancer Cells", Cancer Genetics and Cytogenetics, 159:18-26 (2005).
McGarty, "CRISPRs and Cancer," White Paper No. 111, pp. 1-21 (Apr. 2014).
Mertens et al., "The Emerging Complexity of Gene Fusions in Cancer," Nature Reviews Cancer, 15:371-381 (2015).
Misago et al., "Molecular cloning and expression of cDNAs encoding human α-mannosidase II and a previously unrecognized α-mannosidase IIx isozyme," Proc Natl Acad Sci USA 92:11766-11770 (1995).
Miyata et al., "Feline sarcoma-related protein expression correlates with malignant aggressiveness and poor prognosis in renal cell carcinoma," Cancer Sci 104(6):681-686 (2013).
Mojica et al., "Intervening Sequences of Regularly Spaced Prokaryotic Repeats Derive from Foreign Genetic Elements," J Mol Evol 60:174-182 (2005).
Monaco, "Fatty Acid Metabolism in Breast Cancer Subtypes," Oncotarget 8(17):29487-29500 (2017).
Moremen et al., "Isolation, Characterization, and Expression of cDNAs Encoding Murine α-Mannosidase II, a Golgi Enzyme That Controls Conversion of High Mannose to Complex N-Glycans," J Cell Biol 115(6):1521-1534 (1991).
Moreno, et al., "Detection of Hematogenous Micrometastasis in Patients with Prostate Cancer", Cancer Research, 52:6110-6112 (1992).
Nam et al., "Expression of TMPRSS2 ERG Gene Fusion in Prostate Cancer Cells is an Important Prognostic Factor for Cancer Progression," Cancer Biology & Therapy 6(1):40-45 (2007).
Nellist et al., "Phosphorylation and binding partner analysis of the TSC1-TSC2 complex," Biochemical and Biophysical Research Communications 333:818-826 (2005).
Nunez, et al., "WWOX Protein Expression Varies Among Ovarian Carcinoma Histotypes and Correlates with Less Favorable Outcome", BMC Cancer, 5:64 (2005).
Pang, et al., "Cytogenetic and Expression Profiles Associated with Transformation to Androgen-Resistant Prostate Cancer", The Prostate, 66:157-172 (2006).
Parkin, et al., "Acquired Genomic Copy Number Aberrations and Survival in Adult Acute Myelogenous Leukemia", Blood, 116(23):4958-4967 (2010).
Parr-Sturgess et al., "Copper Modulates Zinc Metalloproteinase-Dependent Ectodomain Shedding of Key Signaling and Adhesion

(56) **References Cited**

OTHER PUBLICATIONS

Proteins and Promotes the Invasion of Prostate Cancer Epithelial Cells," Mol Cancer Res 10(10):1282-1293 (2012).
Partial Supplemental European Search Report dated Jul. 12, 2017 in EP Application No. 14875963.2.
Perner et al., "784-TMPRSS2-ERG Gene Fusion Defines a Metastatic Phenotype of Prostate Cancer," Eur Urol Suppl 8(4):316 (2009).
Prakash et al., "Expression of Conjoined Genes: Another Mechanism for Gene Regulation in Eukaryotes," PLoS One 5(10):e13284 (2010).
Ran et al., "Double Nicking by RNA-Guided CRISPR Cas9 for Enhanced Genome Editing Specificity," Cell, 154:1380-1389 (2013).
Ren et al., "Analysis of Integrin α7 Mutations in Prostate Cancer, Liver Cancer, Glioblastoma Multiforme, and Leiomyosarcoma," J Natl Cancer Inst 99:868-880 (2007).
Ren et al., "MCM7 amplification and overexpression are associated with prostate cancer progression," Oncogene 25:1090-1098 (2006).
Rickman et al., "SLC45A3-ELK4 is a novel and frequent erythroblast transformation-specific fusion transcript in prostate cancer," Cancer Research, 69(7):2734-2738 (2009).
Robin et al., "pROC: an open-source package for R and S+ to analyze and compare ROC curves," BMC Bioinformatics 12:77 (2011).
Rocha et al., "The Fer tyrosine kinase acts as a downstream interleukin-6 effector of androgen receptor activation in prostate cancer," Mol Cell Endocrinol 381:140-149 (2013).
Sander et al., "CRIRISPR-Cas systems for editing, regulating and targeting genomes," Nature Biotechnology, 32(4):347-355 (2014).
Savolainen et al., "A mouse model for α-methylacyl-CoA racemase deficiency: adjustment of bile acid synthesis and intolerance to dietary methyl-branched lipids," Hum Mol Genet 13(9):955-965 (2004).
Shchors et al., "Cell Death Inhibiting RNA (CDIR) Derived from a 3'-Untranslated Region Binds AUF1 and Heat Shock Protein 27*," The Journal of Biological Chemistry 277(49):47061-47072 (2002).
Shi et al., "Inhibition of prostate cancer growth and metastasis using small interference RNA specific for minichromosome complex maintenance component 7," Cancer Gene Therapy 17(10):694-699 (2010).
Siegel et al., "Cancer Statistics, 2012," CA Cancer J Clin. 62:10-29 (2012).
Siegel et al., "Cancer Statistics, 2015," CA Cancer J Clin 65:5-29 (2015).
Sinclair et al., "A Fluorescence in situ Hybridization Map of 6q Deletions in Acute Lymphocytic Leukemia: Identification and Analysis of a Candidate Tumor Suppressor Gene," Cancer Res. 64:4089-4098 (2004).
Smith et al., "A New Nucleoside Analog, 9-[[2-Hydroxy-1-(Hydroxymethyl)Ethoxy]Methyl]Guanine, Highly Active In Vitro Against Herpes Simplex Virus Types 1 and 2," Antimicrobial Agents and Chemotherapy 22:55-61 (1982).
Stephenson, et al., "Salvage Radiotherapy for Recurrent Prostate Cancer After Radical Prostatectomy", JAMA, 291(11):1325-1332 (2004).
Strassburger, et al., "Compatible Simultaneous Lower Confidence Bounds for the Holm Procedure and other Bonferroni-Based Closed Tests", Statistics in Medicine, 27:4914-4927 (2008).
Strausberg, et al., "Generation and Initial Analysis of More Than 15,000 Full-Length Human and Mouse cDNA Sequences", PNAS, 99(26):16899-16903 (2002).
Supplementary Partial European Search Report dated Apr. 10, 2018 in Application No. EP 15821594.
Swanson et al., "TMPRSS2/ERG Fusion Gene Expression Alters Chemo- and Radio-Responsiveness in Cell Culture Models of Androgen Independent Prostate Cancer," The Prostate 71:1548-1558 (2011).
Taylor et al., "Integrative Genomic Profiling of Human Prostate Cancer", Cancer Cell, 18:11-22, including supplementary material (2010).
Teixeira, et al., "Genomic analysis of Prostate Carcinoma Specimens Obtained via Ultrasound-guided Needle Biopsy May Be of Use in Preoperative Decision-Making", American Cancer Society, 101:1786-1793 (2004).
Tomlins et al., "Recurrent Fusion of TMPRSS2 and ETS Transcription Factor Genes in Prostate Cancer," Science 310:644-648 (2005).
Towns et al., "Transfer RNA Methytransferases and their Corresponding Modifications in Budding Yeast and Humans: Activities, Predications, and Potential Roles in Human Health," DNA and Cell Biology 31(4):434-454 (2012).
Trapnell et al., "Differential gene and transcript expression analysis of RNA-seq experiments with TopHat and Cufflinks," Nat Protoc. 7(3):562-578 (2012).
Trapnell et al., "TopHat: discovering splice junctions with RNA-Seq.," Bioinformatics 25(9):1105-1111 (2009).
Trapnell et al., "Transcript assembly and quantification by RNA-Seq reveals unannotated transcripts and isoform switching during cell differentiation," Nat. Biotechnol. 28(5):511-515 (2010).
Tsang, et al., "SCAPER, a Novel Cyclin A-Interacting Protein that Regulates Cell Cycle Progression", Journal of Cell Biology, 178(4):621-633 (2007).
Vitari et al., "COP1 is a tumour suppressor that causes degradation of ETS transcription factors," Nature 474:402-408 (2011).
Voisset et al., "The tyrosine kinase FES is an essential effector of KITD816V proliferation signal," Blood 110(7):2593-2599 (2007).
Wang et al., "Expression of variant TMPRSS2/ERG fusion messenger RNAs is associated with aggressive prostate cancer," Cancer Research, 66(17):8347-8351 (2006).
Wang et al., "p53-induced Gene 3 Mediates Cell Death Induced by Glutathione Peroxidase 3," J Biol Chem 287(20):16890-16902 (2012).
Watabe-Uchida et al., "The Rac Activator DOCK7 Regulates Neuronal Polarity through Local Phosphorylation of Stathmin/Op18," Neuron 51:727-739 (2006).
Wei et al., "High expression of FER tyrosine kinase predicts poor prognosis in clear cell renal cell carcinoma," Oncol Lett 5:473-478 (2013).
Weinberg et al., "A New World Order: Tailored Gene Targeting and Regulation Using CRISPR," Molecular Therapy 22(5):893 (2014).
Willardsen et al., "The ETS transcription factor Etv1 mediates FGF signaling to initiate proneural gene expression during Xenopus laevis retinal development," Mechanisms of Development 131:57-67 (2014).
Yakicier, et al., "Identification of Homozygous Deletions at Chromosome 16q23 in Aflatoxin B1 Exposed Hepatocellular Carcinoma", Oncogene, 20:5232-5238 (2001).
Yang et al., "mTOR kinase structure, mechanism and regulation," Nature 497:217-223 (2013).
Yang et al., "The Histone Demethylase JMJD2B is Regulated by Estrogen Receptor α and Hypoxia, and Is a Key Mediator of Estrogen Induced Growth," Cancer Res 70(16):6456-6466 (2010).
Yang, et al., "Deletion of the WWOX gene and Frequent Loss of its Protein Expression in Human Osteosarcoma", Cancer Letter, 291:31-38 (2010).
Youden, "Index for Rating Diagnostic Tests," Cancer 3:32-35 (1950).
Yu et al., "CSR1 Suppresses Tumor Growth and Metastasis of Prostate Cancer," American Journal of Pathology 168(2):597-607 (2006).
Yu et al., "Gene Expression Alterations in Prostate Cancer Predicting Tumor Aggression and Preceding Development of Malignancy," J Clin Oncol. 22(14):2790-2799 (2004).
Yu et al., "Genomic Copy Number Variations in the Genomes of Leukocytes Predict Prostate Cancer Clinical Outcomes," PloS ONE 10(8):E0135982 (2015).
Yu et al., "Glutathione Peroxidase 3, Deleted or Methylated in Prostate Cancer, Suppresses Prostate Cancer Growth and Metastasis," Cancer Res. 67(17):8043-8050 (2007).
Yu et al., "Novel fusion transcripts associate with progressive prostate cancer," The American Journal of Pathology, 184(10):2840-2849 (2014).

(56) **References Cited**

OTHER PUBLICATIONS

Yu, et al., "Genome Abnormalities Precede Prostate Cancer and Predict Clinical Relapse", The American Journal of Pathology, 180(6):2240-2248 (2012).

Zeng et al., "Visualizing Interchange Patterns in Massive Movement Data," Computer Graphics Forum 32(3):271-280 (2013).

Zha et al., "α-Methylacyl-CoA Racemase as an Androgen-Independent Growth Modifier in Prostate Cancer," Cancer research 63:7365-7376 (2003).

Zhao, et al., "Genome-Wide Characterization of Gene Expression Variations and DNA Copy Number Changes on Prostate cancer Cell Lines", The Prostate, 63:187-197 (2005).

Zhen et al., "Nuclear Import of Exogenous FGF1 Requires the ER-Protein LRRC59 and the Importins Kpnα1 and Kpnβ1," Traffic 13:650-664 (2012).

Zhu et al., "CSR1 induces cell death through inactivation of CPSF3," Oncogene 28:41-51 (2009).

Zhu et al., "Integrin Alpha 7 Interacts with High Temperature Requirement A2 (HtrA2) to Induce Prostate Cancer Cell Death," The American Journal of Pathology 177(3):1176-1186 (2010).

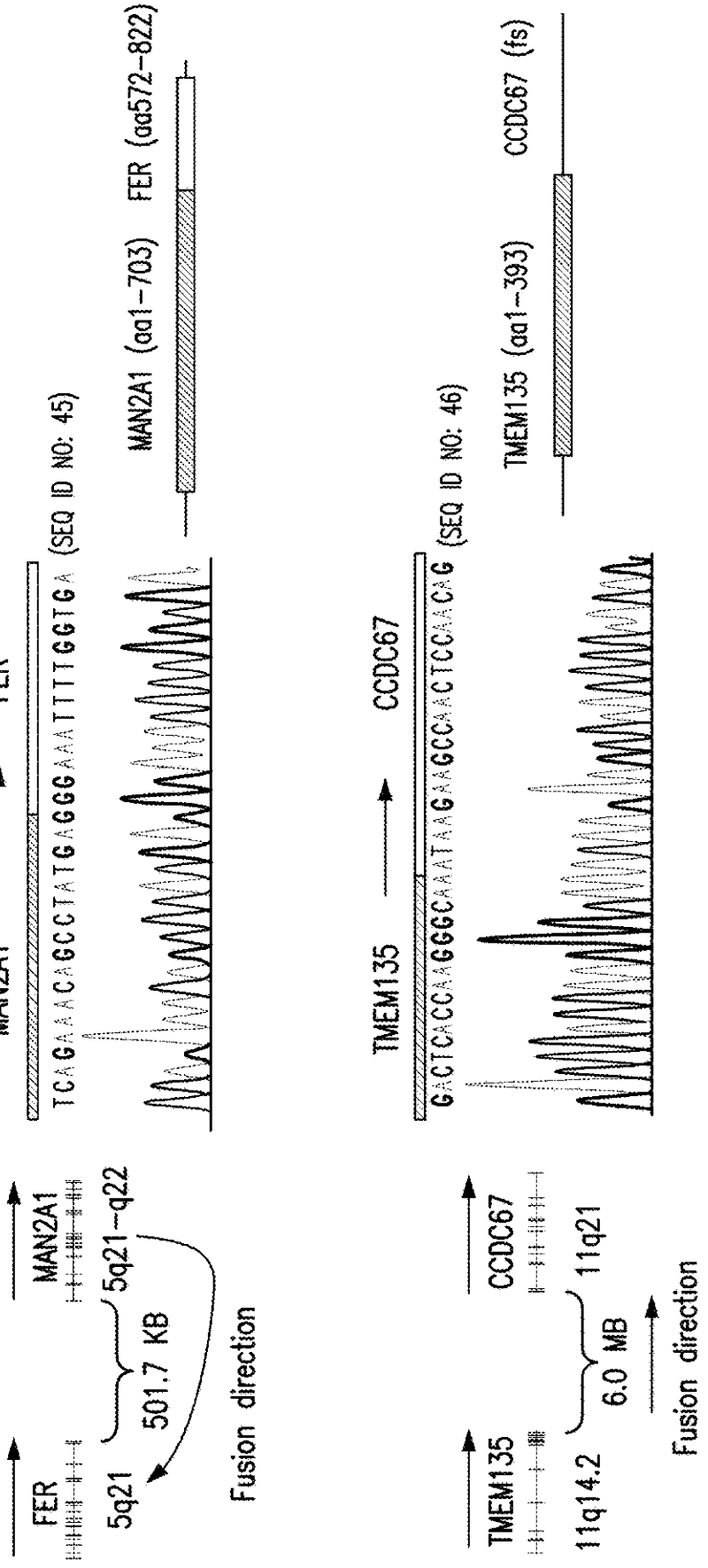
MAN2A1
FER
TCAGAAACAGCCTATGAGGGAAATTTTGGTGA (SEQ ID NO: 45)
MAN2A1 (aa1–703)
FER (aa572–822)
FER
MAN2A1
5q21
5q21–q22
501.7 KB
Fusion direction
TMEM135
CCDC67
GACTCACCAAGGGCAAATAAGAAGCCAACTCCAACAG (SEQ ID NO: 46)
TMEM135 (aa1–393)
CCDC67 (fs)
TMEM135
CCDC67
11q14.2
11q21
6.0 MB
Fusion direction

FIG. 1

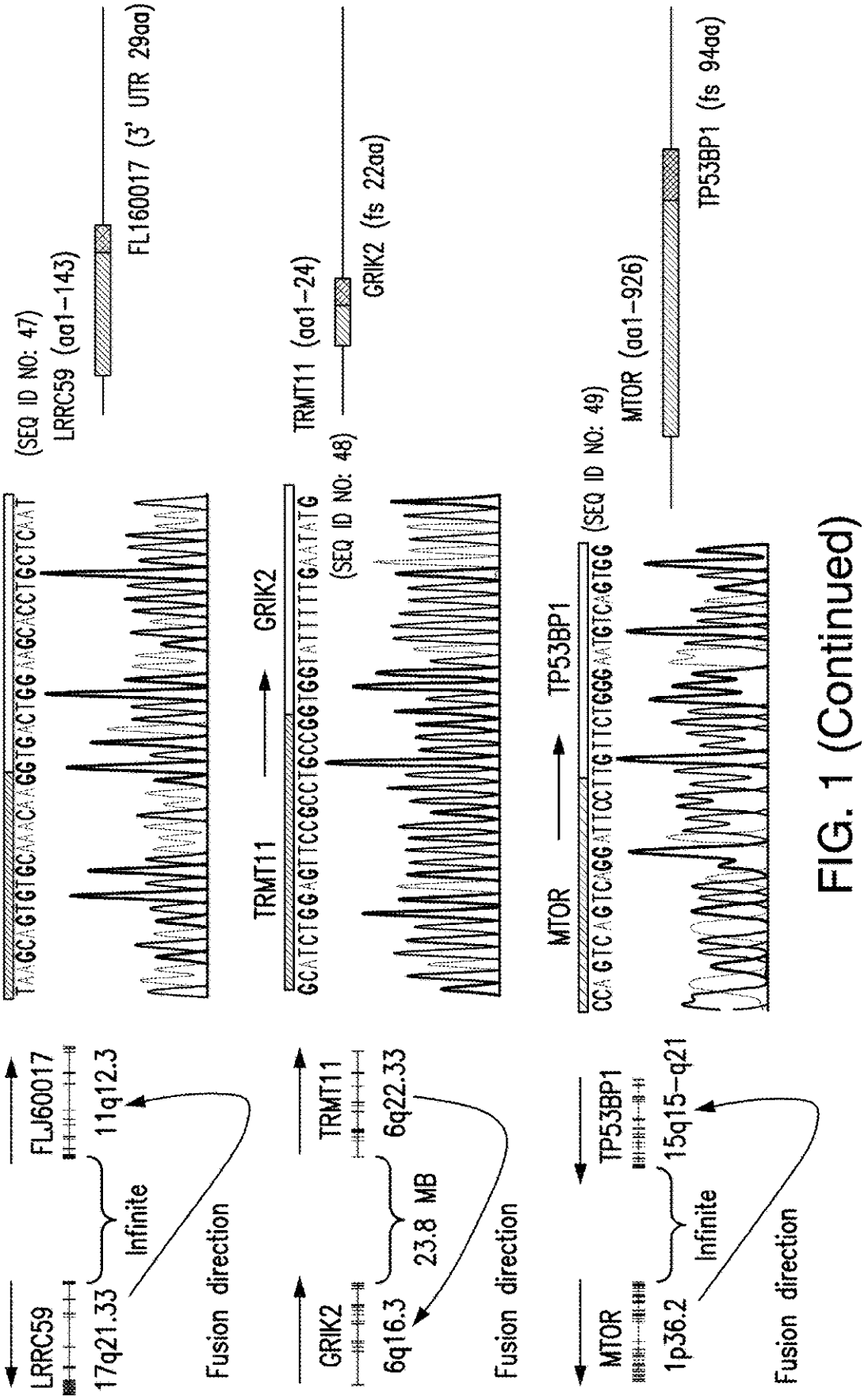

FIG. 1 (Continued)

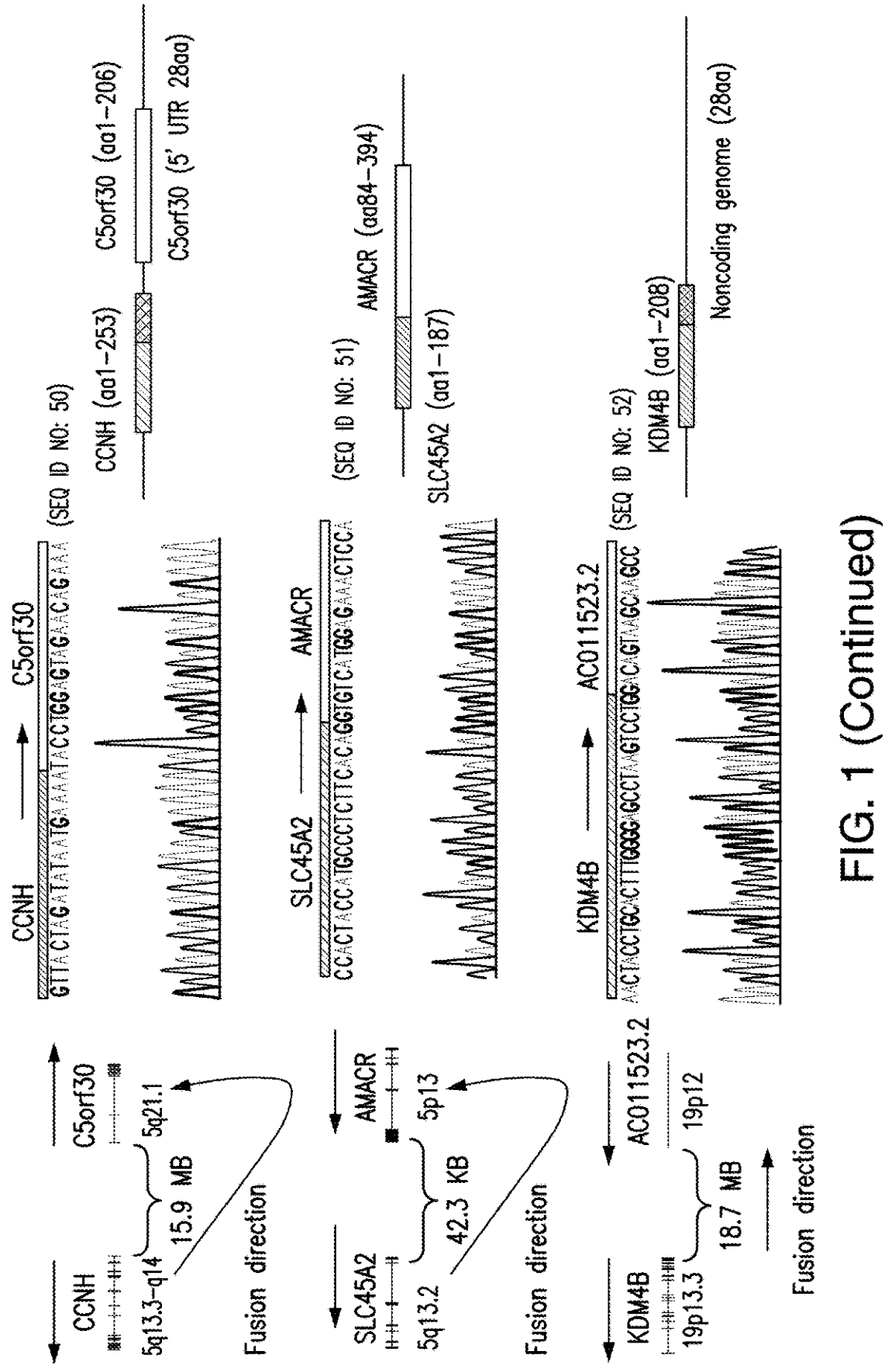

FIG. 1 (Continued)

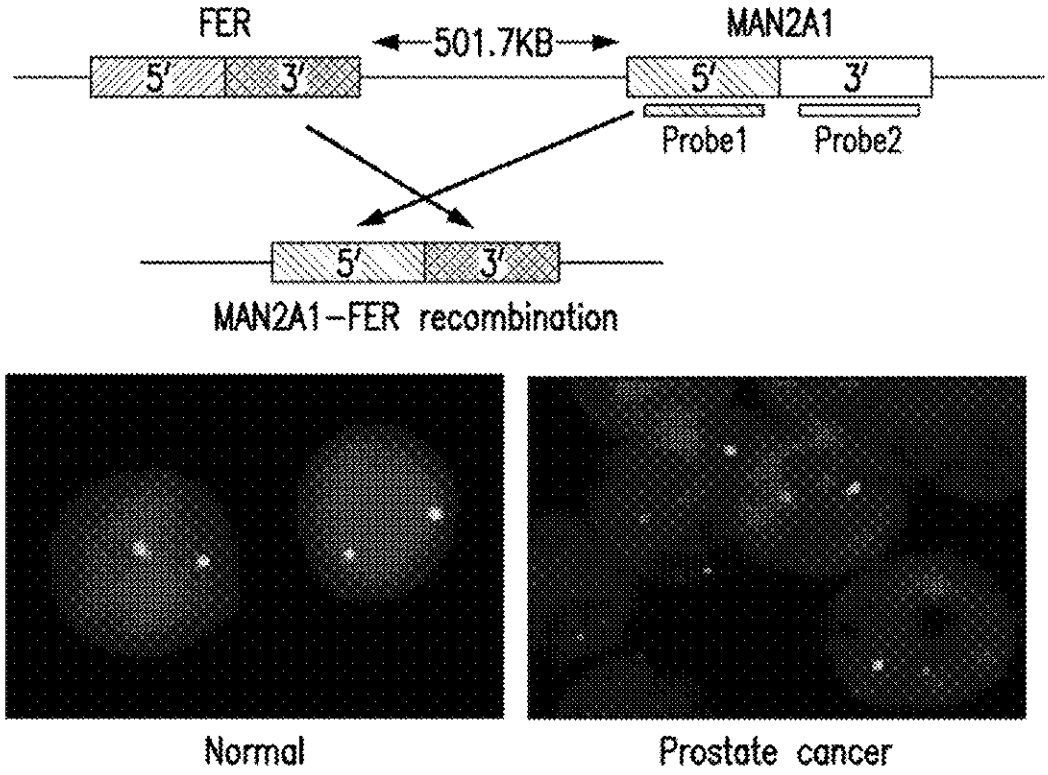
FER
501.7KB
MAN2A1
5′
3′
5′
3′
Probe1
Probe2
5′
3′
MAN2A1–FER recombination
Normal
Prostate cancer

FIG. 2A

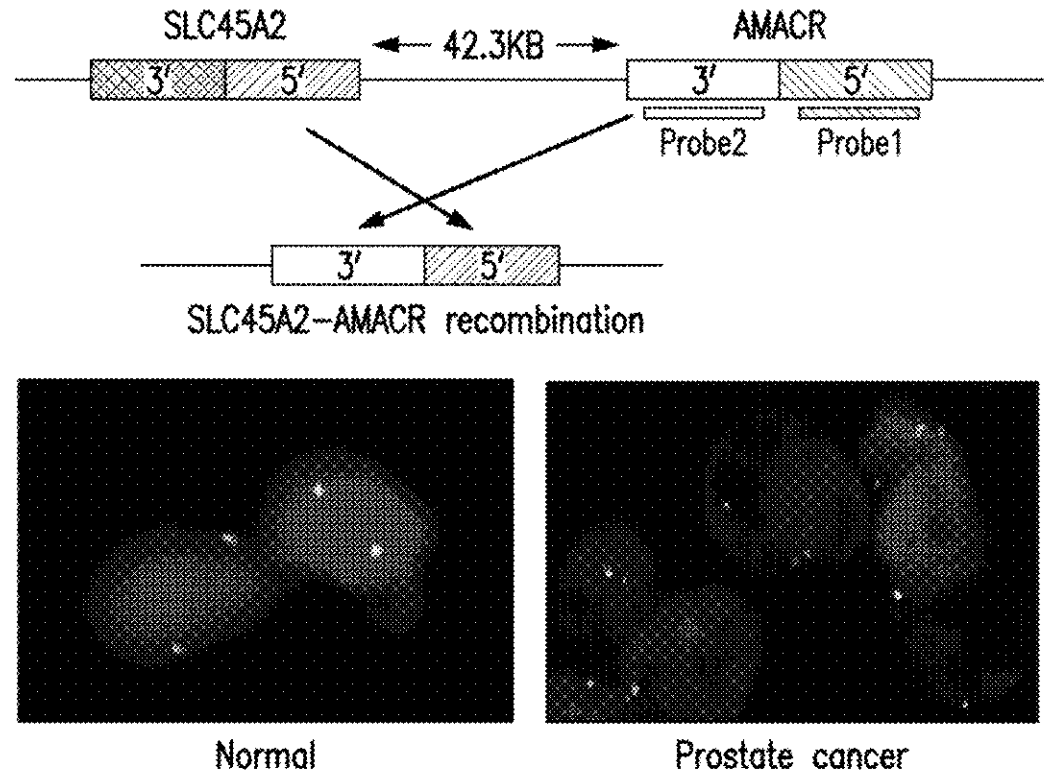
SLC45A2
42.3KB
AMACR
3′
5′
3′
5′
Probe2
Probe1
3′
5′
SLC45A2–AMACR recombination
Normal
Prostate cancer

FIG. 2B

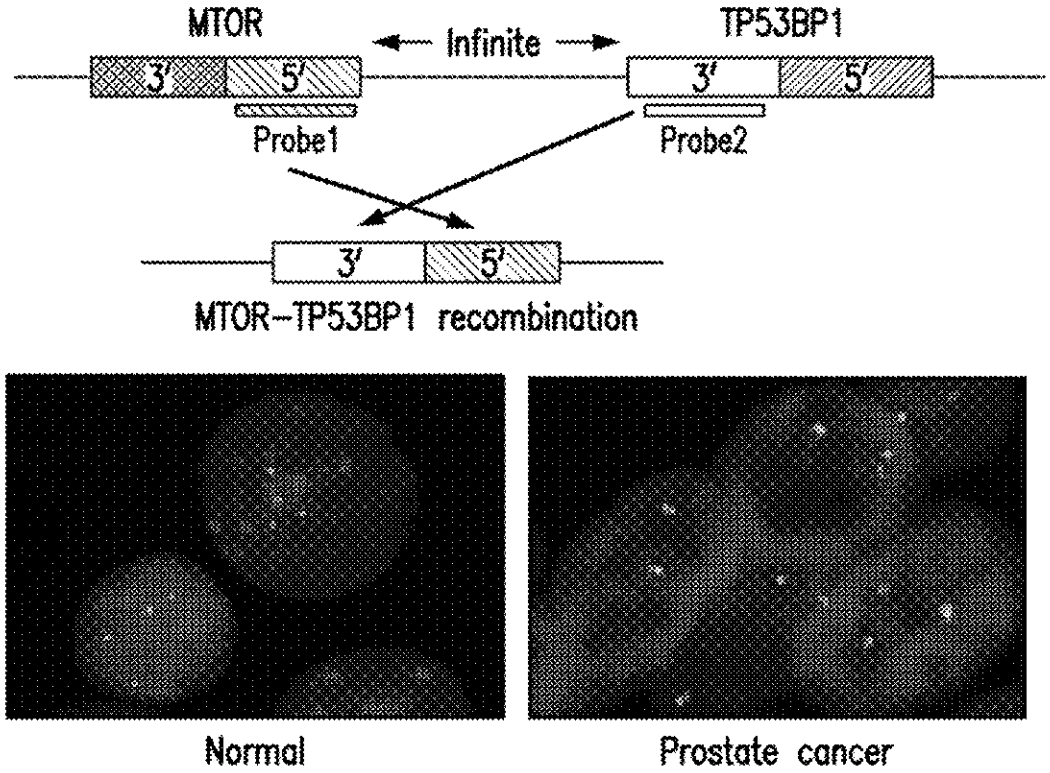
MTOR
Infinite
TP53BP1
3′
5′
3′
5′
Probe1
Probe2
3′
5′
MTOR-TP53BP1 recombination
Normal
Prostate cancer

FIG. 2C

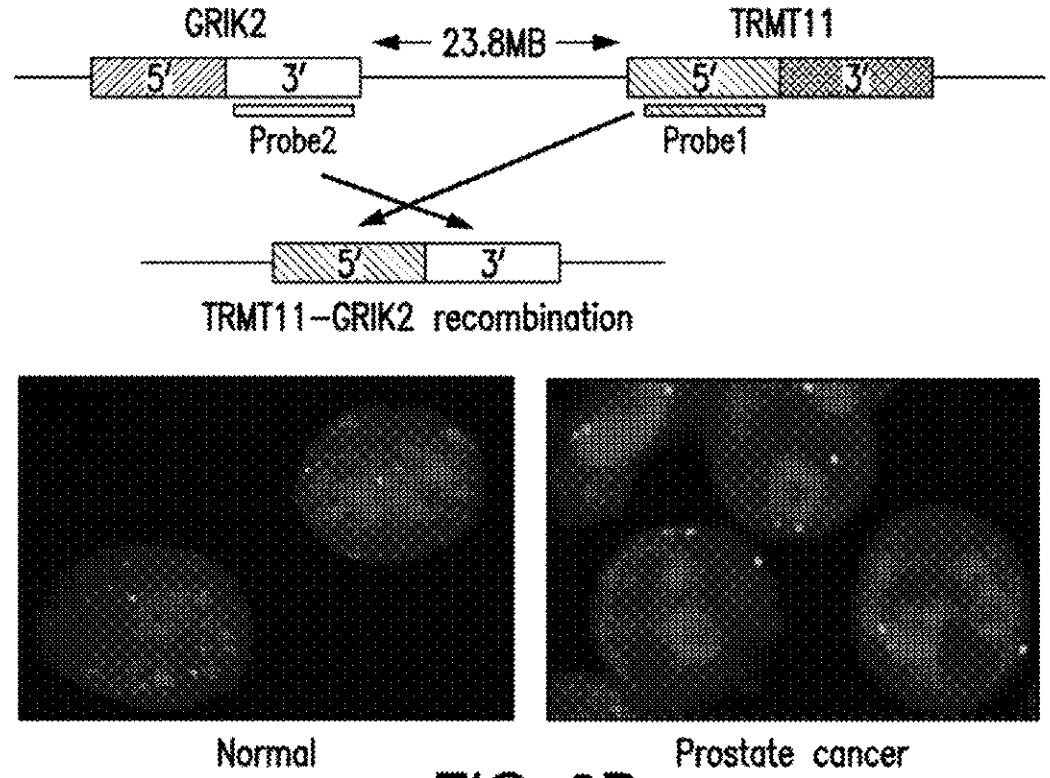
GRIK2
23.8MB
TRMT11
5′
3′
5′
3′
Probe2
Probe1
5′
3′
TRMT11-GRIK2 recombination
Normal
Prostate cancer

FIG. 2D

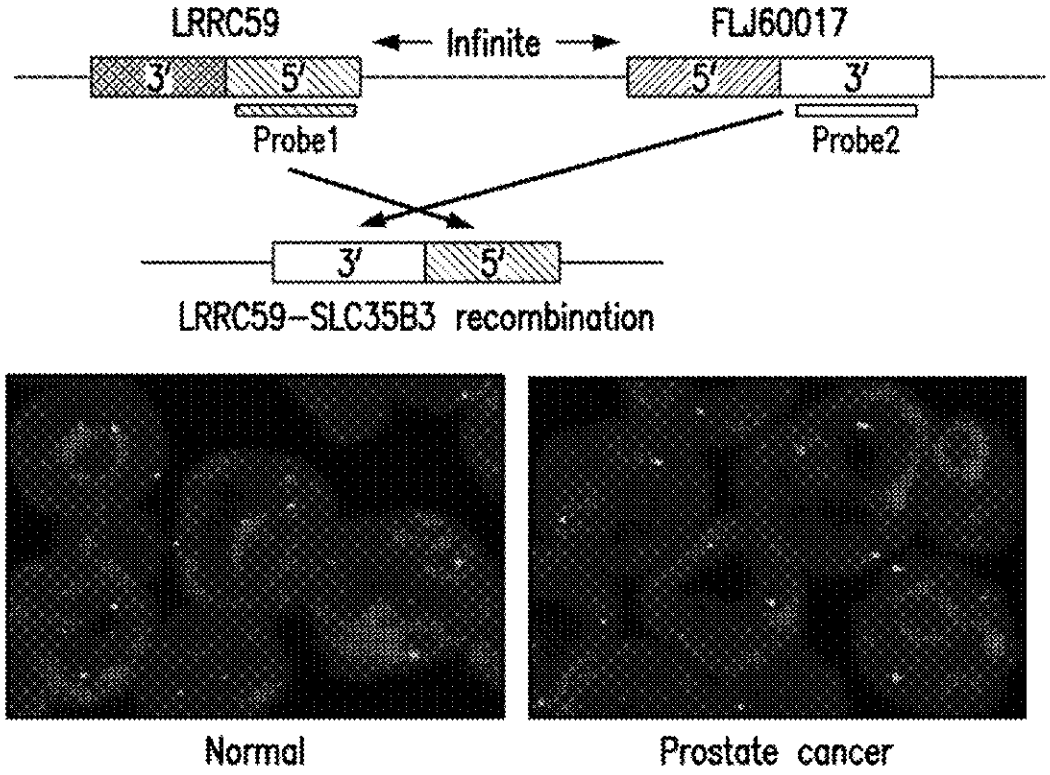
LRRC59
Infinite
FLJ60017
3′
5′
5′
3′
Probe1
Probe2
3′
5′
LRRC59–SLC35B3 recombination
Normal
Prostate cancer

FIG. 2E

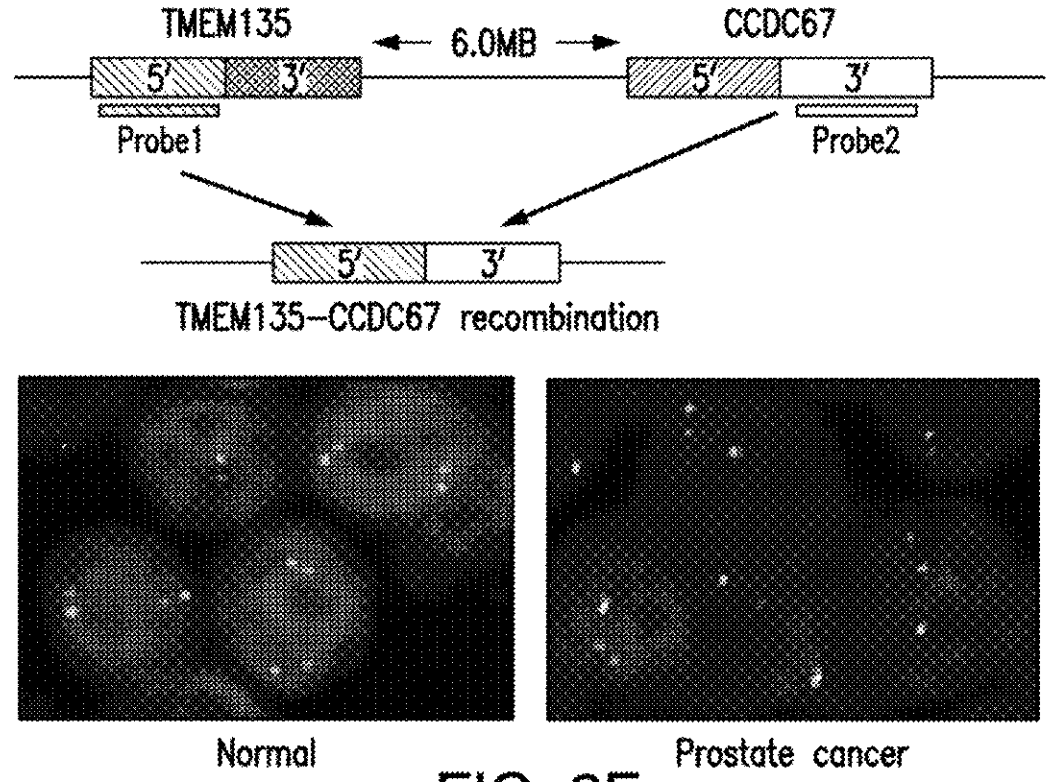
TMEM135
6.0MB
CCDC67
5′
3′
5′
3′
Probe1
Probe2
5′
3′
TMEM135–CCDC67 recombination
Normal
Prostate cancer

FIG. 2F

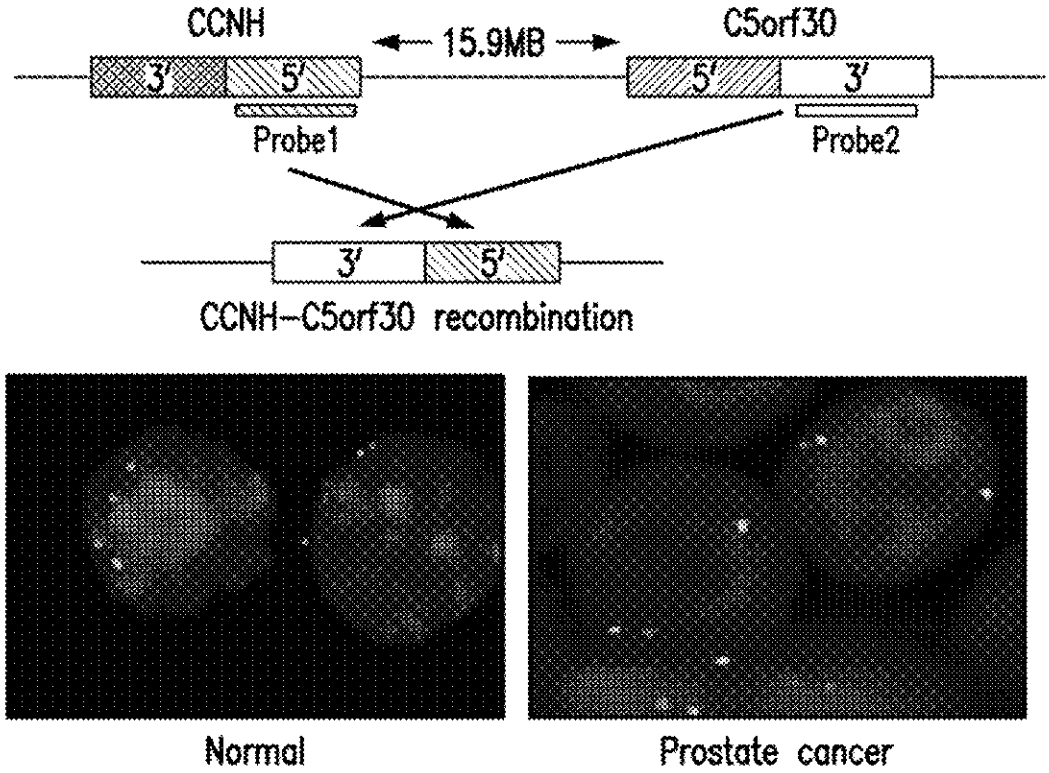
CCNH
15.9MB
C5orf30
3′
5′
5′
3′
Probe1
Probe2
3′
5′
CCNH-C5orf30 recombination
Normal
Prostate cancer

FIG. 2G

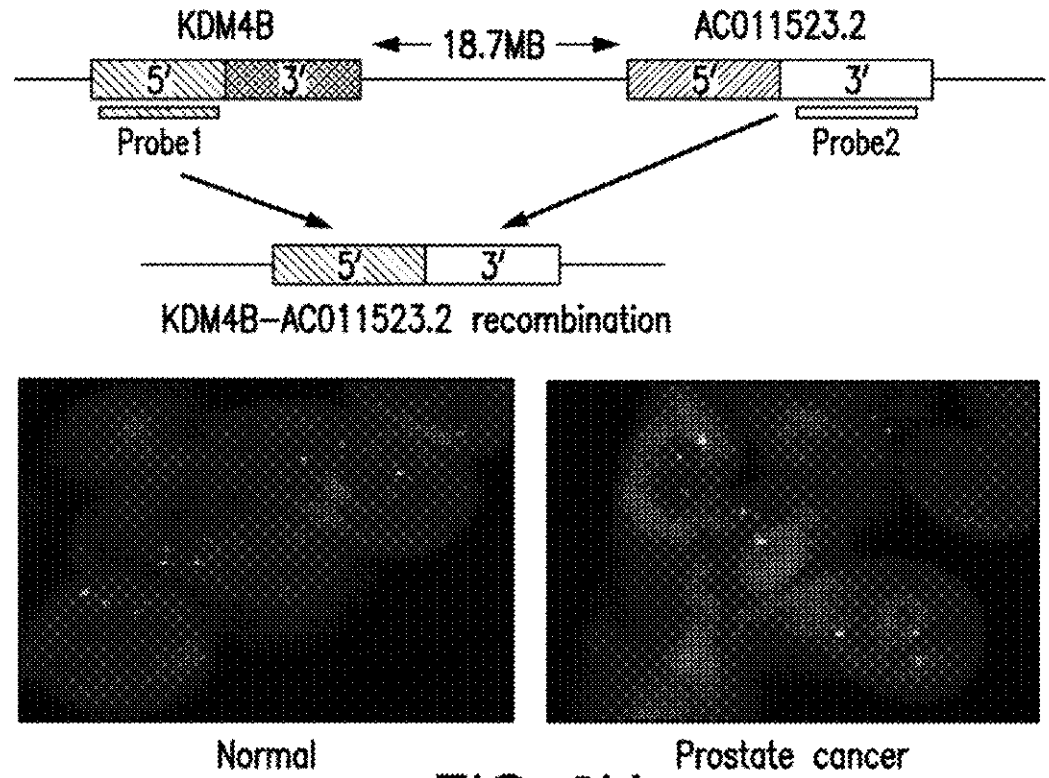
KDM4B
18.7MB
AC011523.2
5′
3′
5′
3′
Probe1
Probe2
5′
3′
KDM4B-AC011523.2 recombination
Normal
Prostate cancer

FIG. 2H

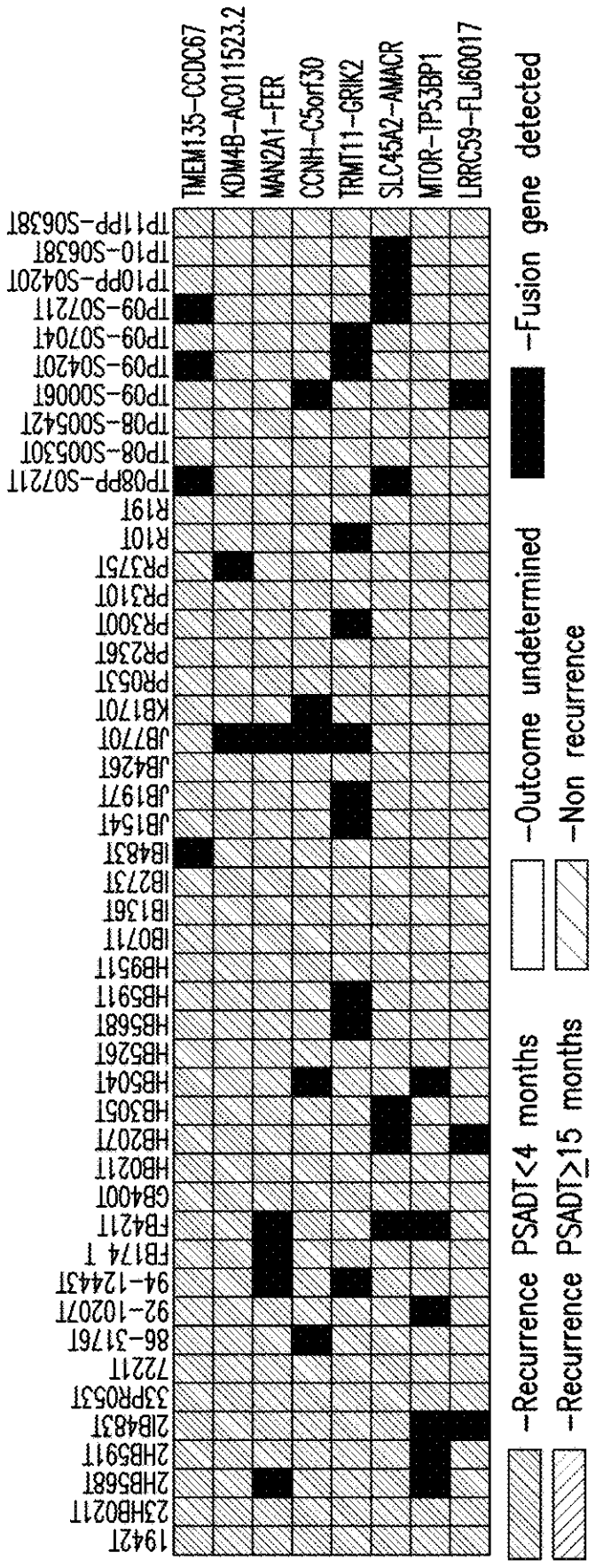
TMEM135-CCDC67
KDM4B-AC011523.2
MAN2A1-FER
CCNH-C5orf30
TRMT11-GRIK2
SLC45A2-AMACR
MTOR-TP53BP1
LRRC59-FLJ60017
Fusion gene detected
Outcome undetermined
Non recurrence
Recurrence PSADT<4 months
Recurrence PSADT≥15 months
TP11PP-S06381
TP10-S06381
TP10PP-S04201
TP09-S07211
TP09-S07041
TP09-S04201
TP09-S00061
TP08-S00542T
TP08-S00530T
TP08PP-S07211
R19T
R10T
PR375T
PR310T
PR300T
PR236T
PR053T
KB170T
JB770T
JB426T
JB197T
JB154T
IB483T
IB273T
IB136T
IB071T
HB951T
HB591T
HB568T
HB526T
HB504T
HB305T
HB207T
HB021T
CB400T
FB421T
FB174 T
94-12443T
92-10207T
86-3176T
7221T
33PR053T
21B483T
2HB591T
2HB568T
23HB021T
1942T

FIG. 3A

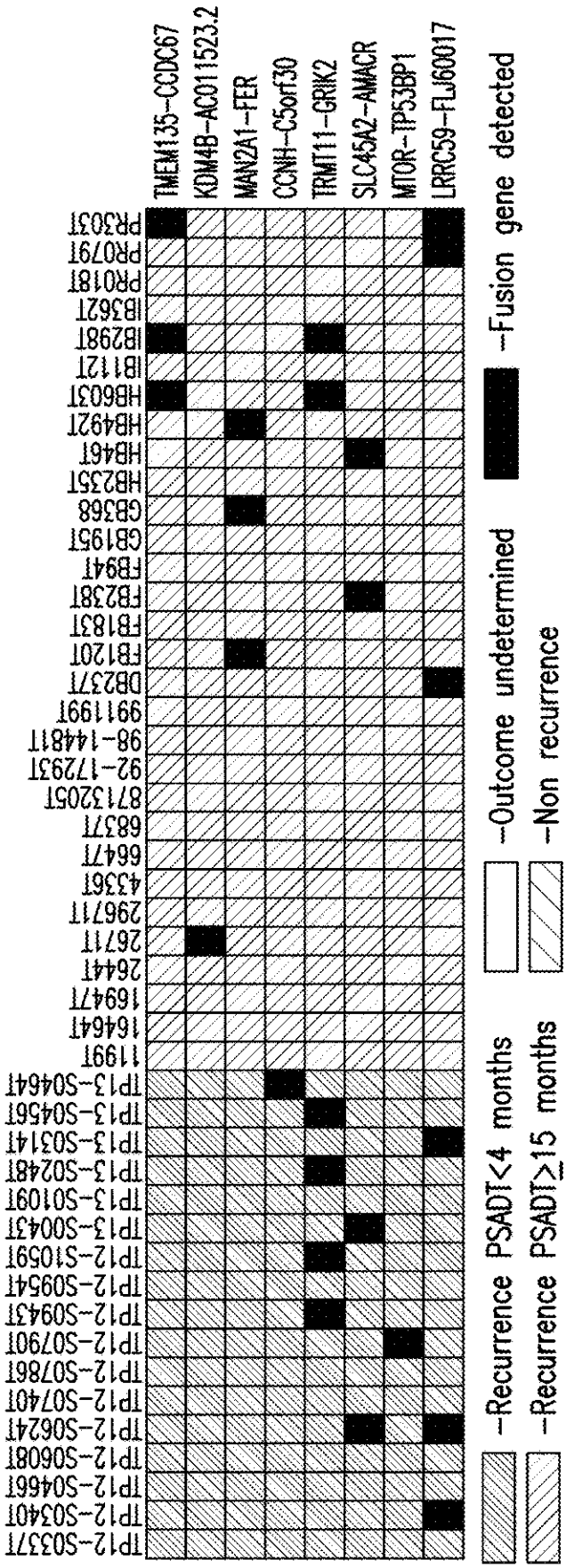

FIG. 3A (Continued)

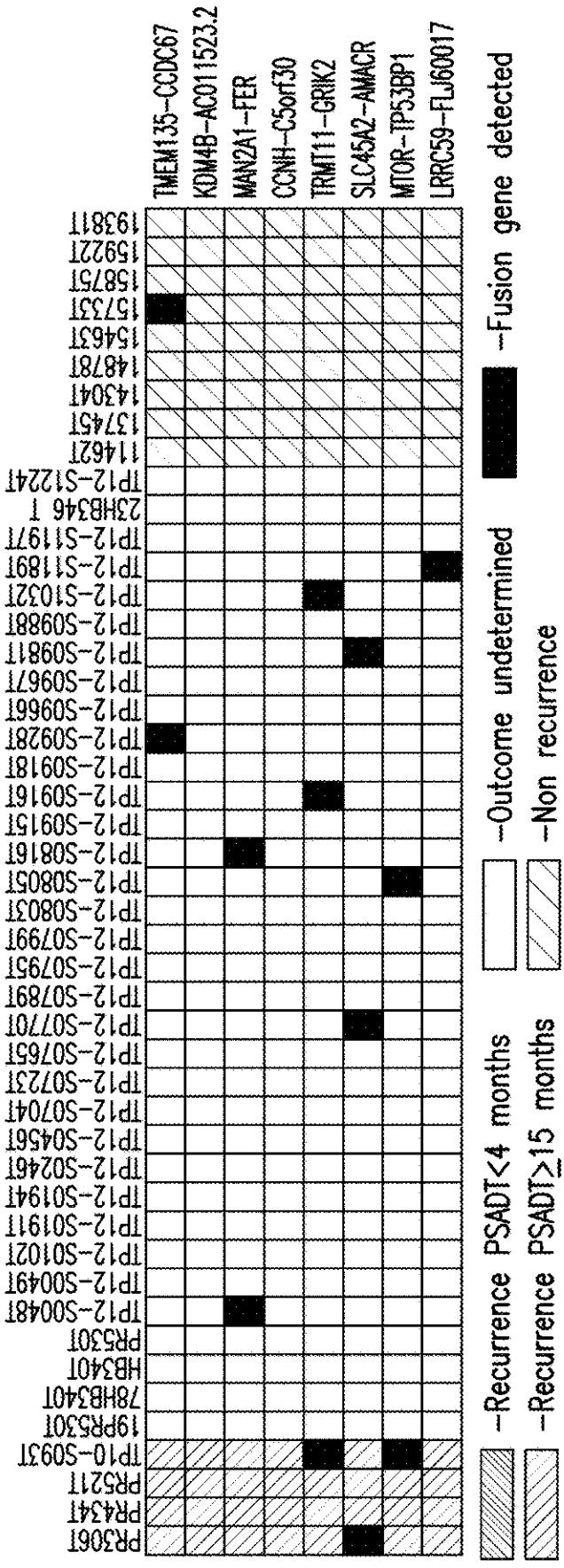

FIG. 3A (Continued)

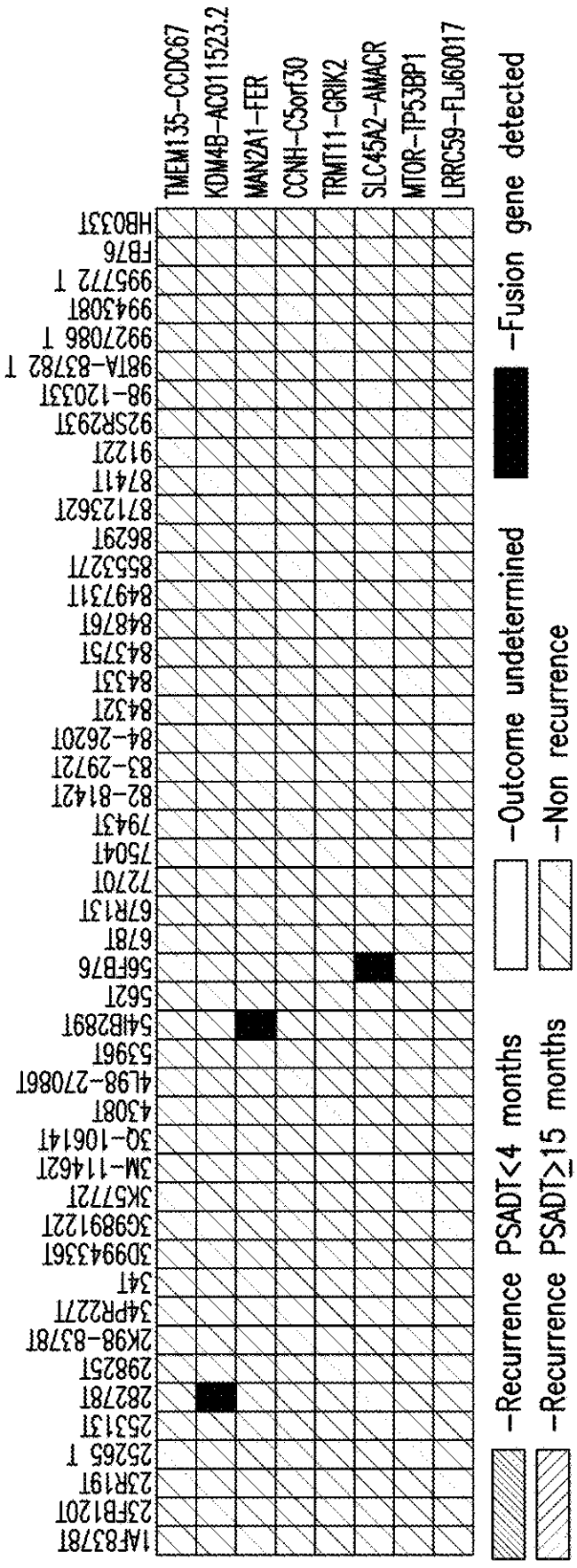

FIG. 3A (Continued)

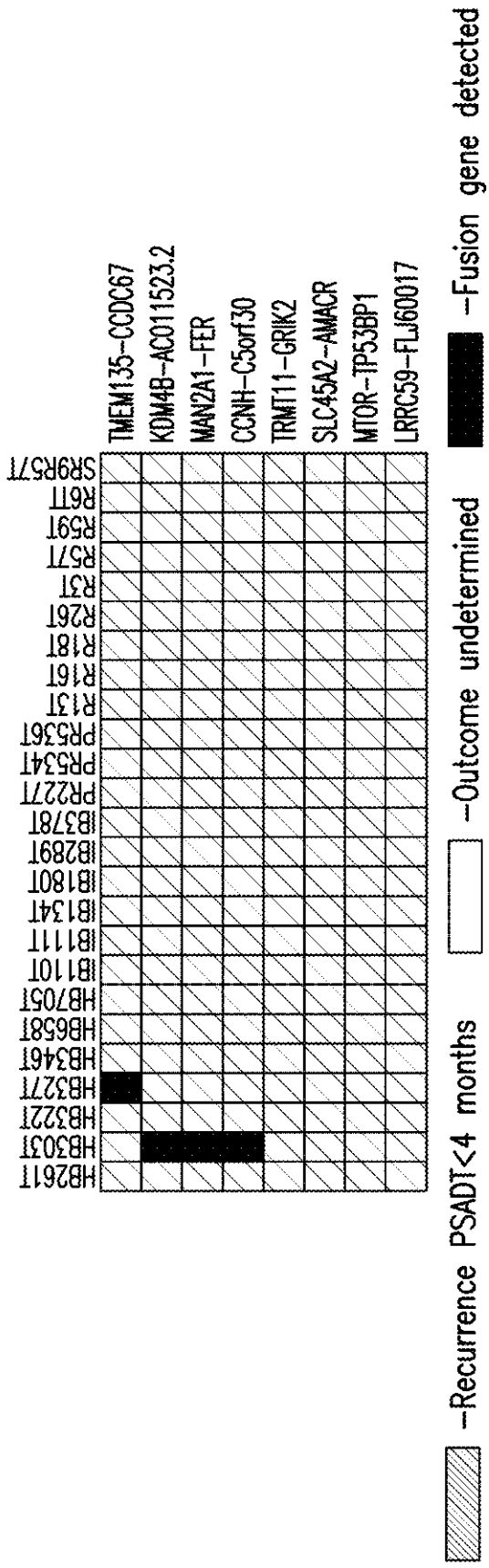

FIG. 3A (Continued)

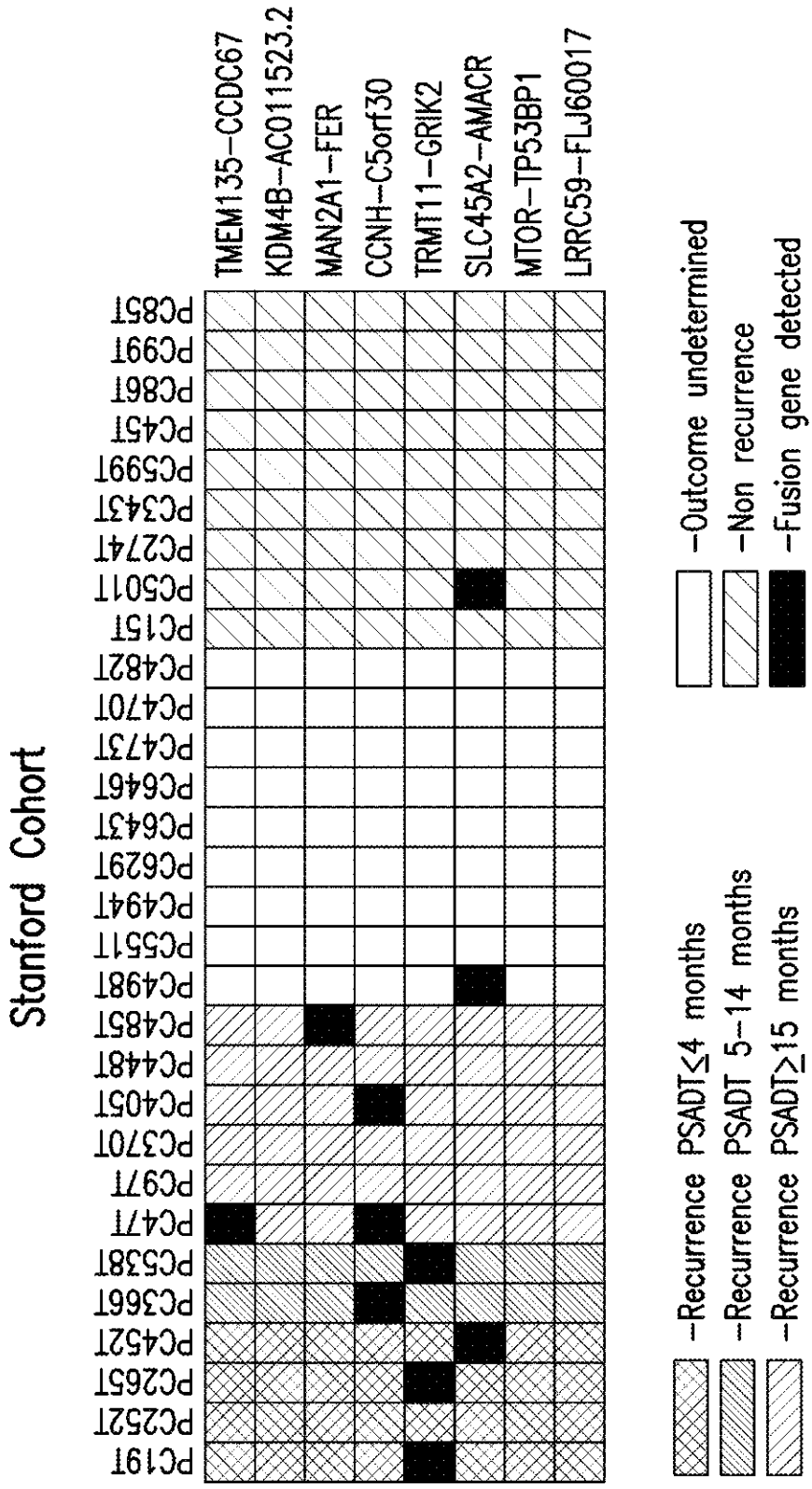

FIG. 3A (Continued)

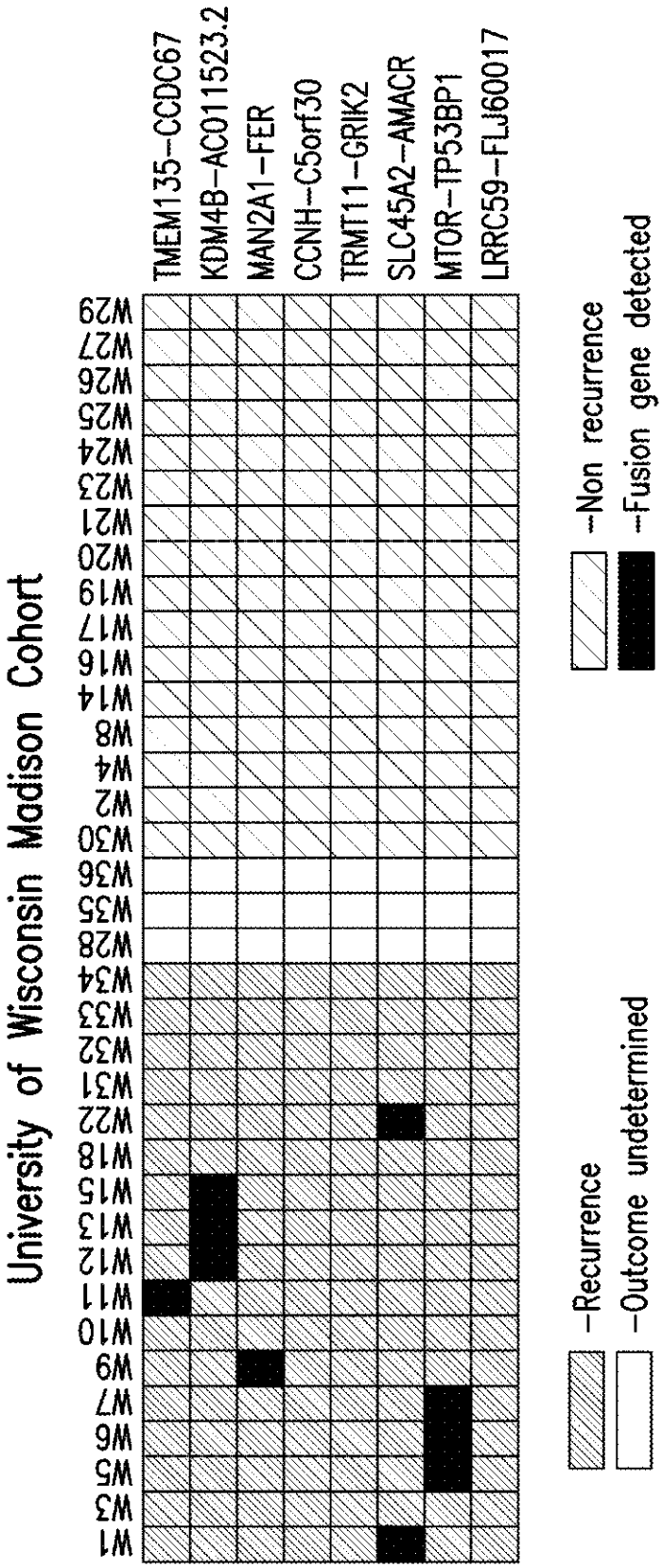

FIG. 3A (Continued)

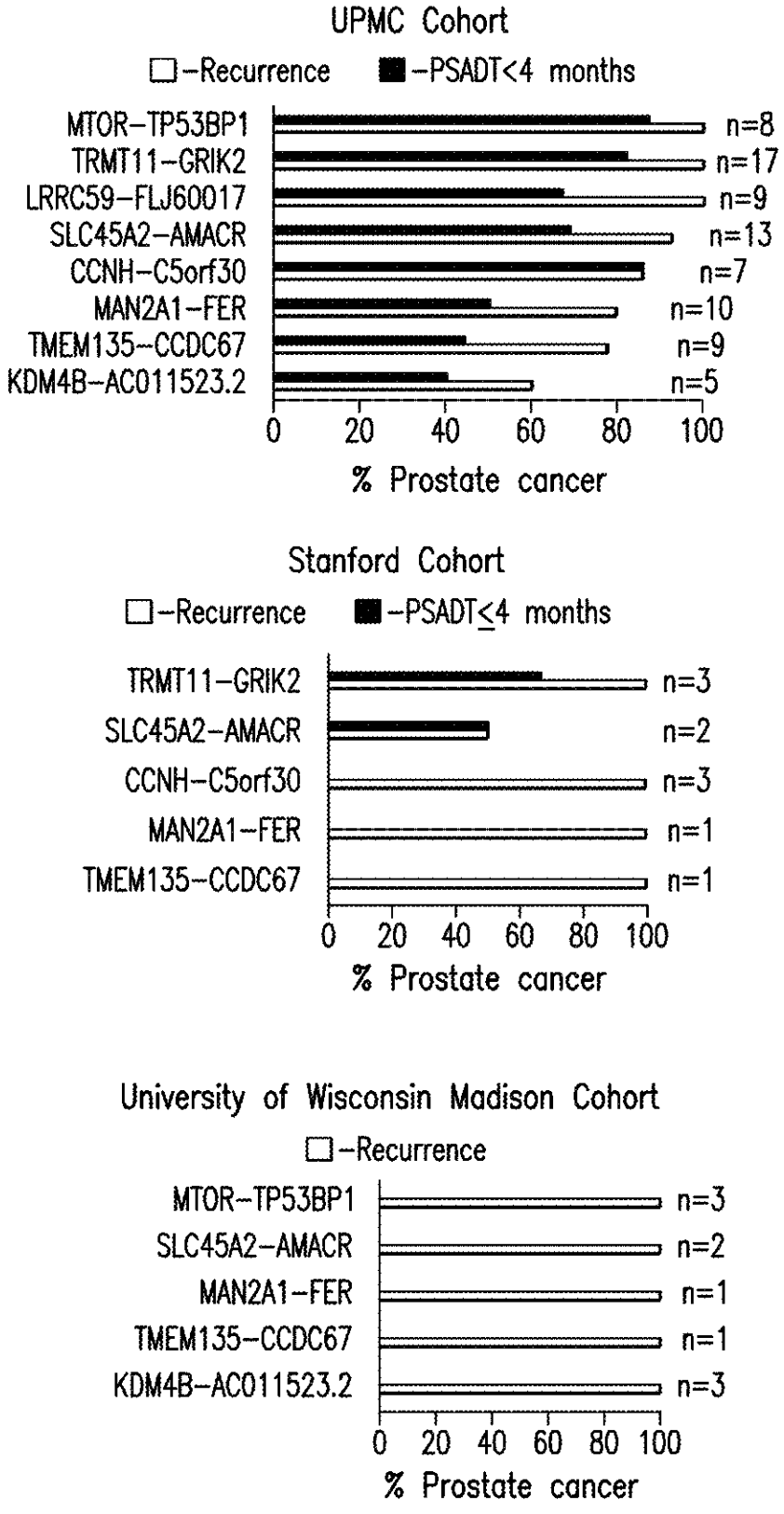
UPMC Cohort
□-Recurrence
■-PSADT<4 months
MTOR-TP53BP1
TRMT11-GRIK2
LRRC59-FLJ60017
SLC45A2-AMACR
CCNH-C5orf30
MAN2A1-FER
TMEM135-CCDC67
KDM4B-AC011523.2
n=8
n=17
n=9
n=13
n=7
n=10
n=9
n=5
0 20 40 60 80 100
% Prostate cancer
Stanford Cohort
□-Recurrence
■-PSADT≤4 months
TRMT11-GRIK2
SLC45A2-AMACR
CCNH-C5orf30
MAN2A1-FER
TMEM135-CCDC67
n=3
n=2
n=3
n=1
n=1
0 20 40 60 80 100
% Prostate cancer
University of Wisconsin Madison Cohort
□-Recurrence
MTOR-TP53BP1
SLC45A2-AMACR
MAN2A1-FER
TMEM135-CCDC67
KDM4B-AC011523.2
n=3
n=2
n=1
n=1
n=3
0 20 40 60 80 100
% Prostate cancer

FIG. 3B

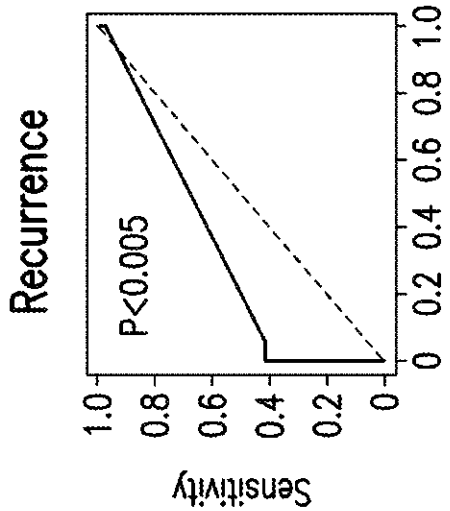
Recurrence
P<0.005
Sensitivity
1−Specificity
0
0.2
0.4
0.6
0.8
1.0

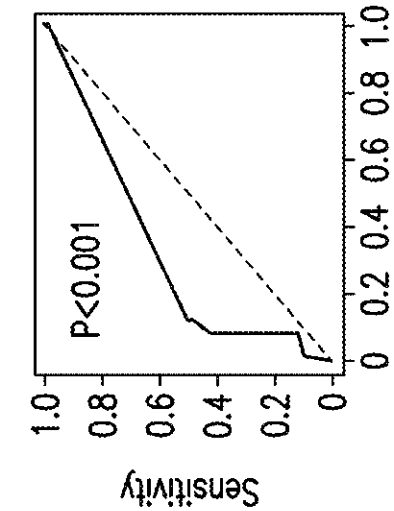
Short PSADT
P<0.001
Sensitivity
1−Specificity
0
0.2
0.4
0.6
0.8
1.0

FIG. 3C

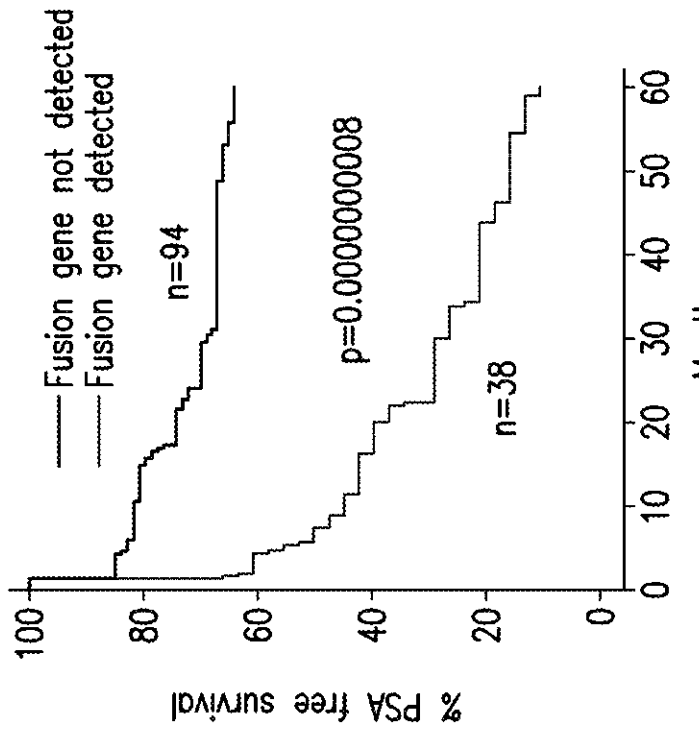
Fusion gene not detected
Fusion gene detected
n=94
p=0.0000000008
n=38
% PSA free survival
Months
0
20
40
60
80
100
0
10
20
30
40
50
60

FIG. 3D

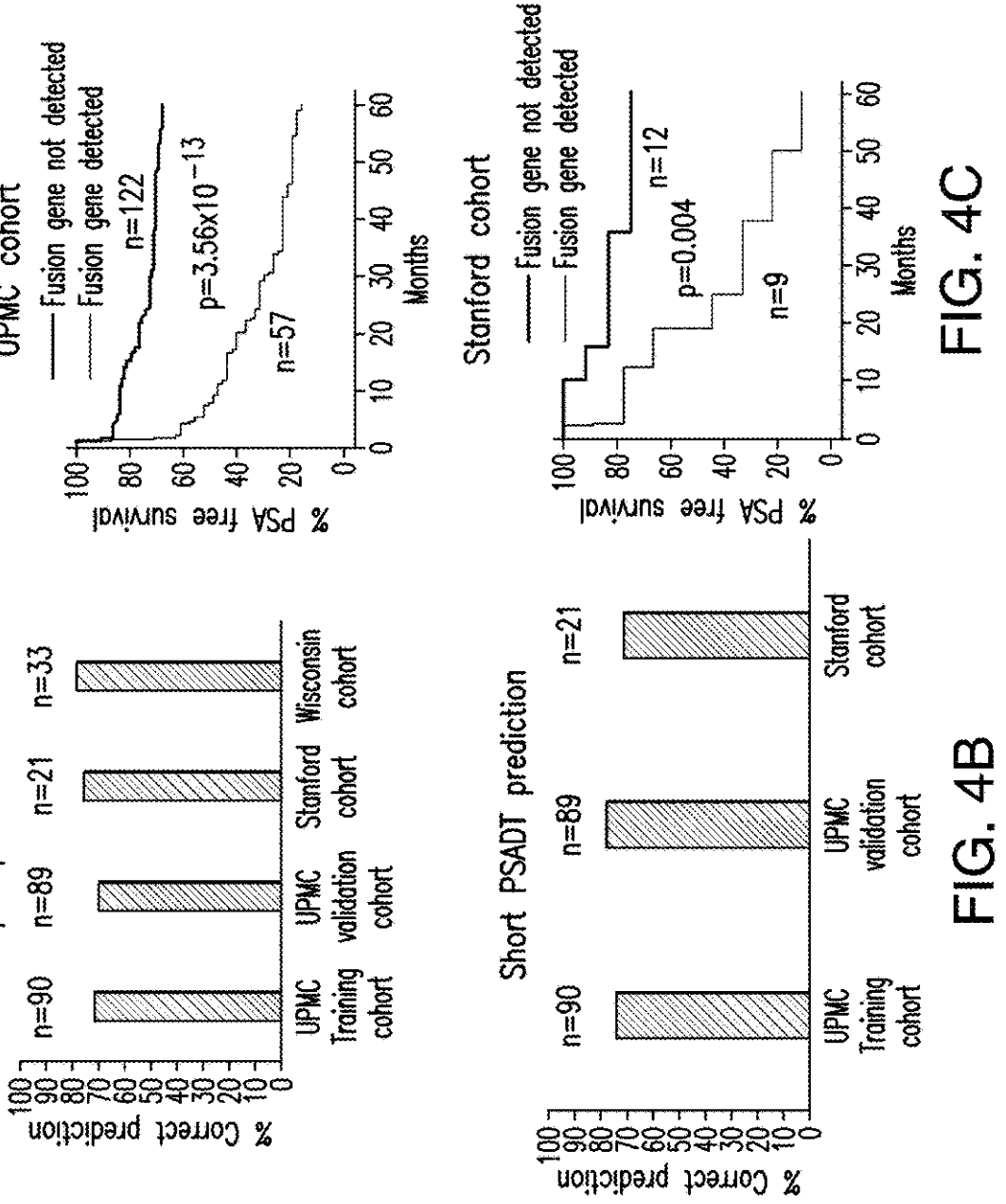

FIG. 4C

FIG. 4B

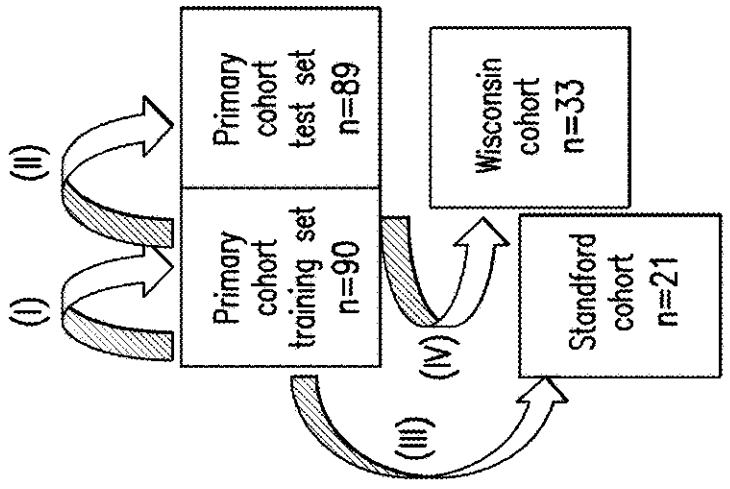

FIG. 4A

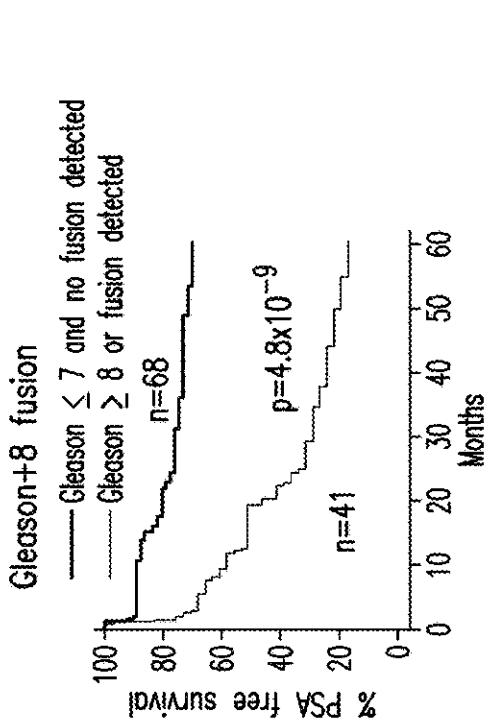
Gleason+8 fusion
Gleason ≤ 7 and no fusion detected
Gleason ≥ 8 or fusion detected
n=68
p=4.8x10^-9
n=41
% PSA free survival
Months

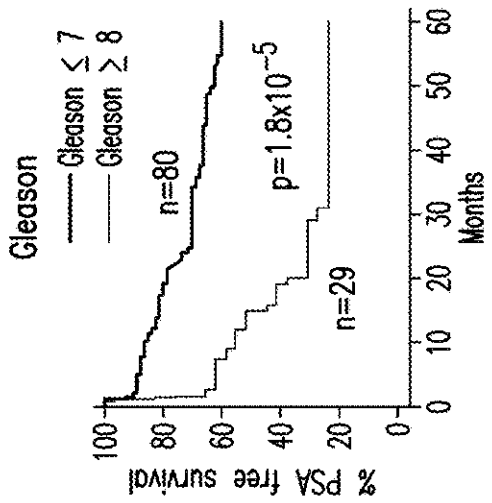
Gleason
Gleason ≤ 7
Gleason ≥ 8
n=80
p=1.8x10^-5
n=29
% PSA free survival
Months

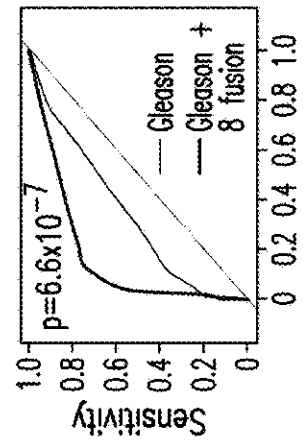
p=6.6x10^-7
Gleason
Gleason + 8 fusion
Sensitivity
1−Specificity

FIG. 5A

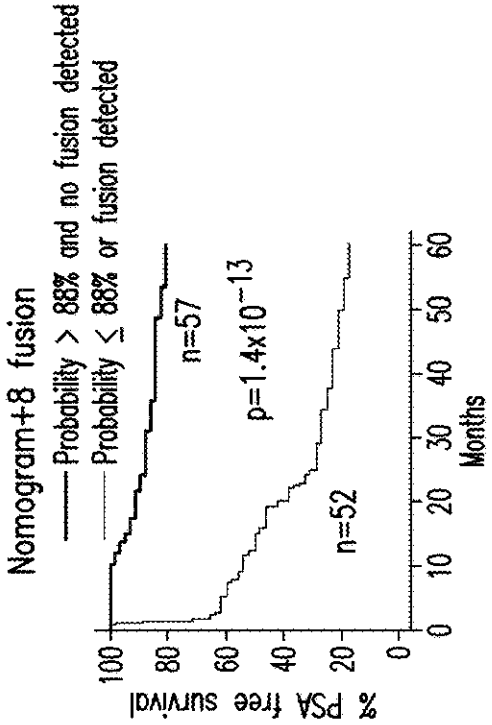
Nomogram+8 fusion
Probability > 88% and no fusion detected
Probability ≤ 88% or fusion detected
n=57
p=1.4x10^-13
n=52
% PSA free survival
Months

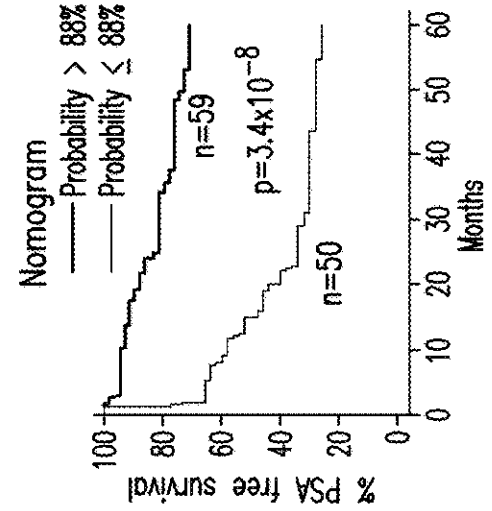
Nomogram
Probability > 88%
Probability ≤ 88%
n=59
p=3.4x10^-8
n=50
% PSA free survival
Months

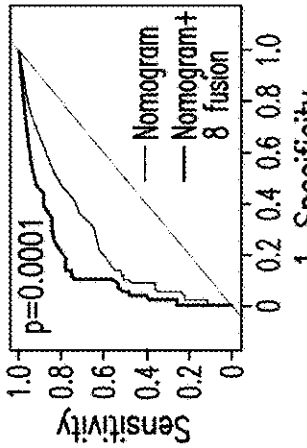
p=0.0001
Nomogram
Nomogram+ 8 fusion
Sensitivity
1−Specificity

FIG. 5B

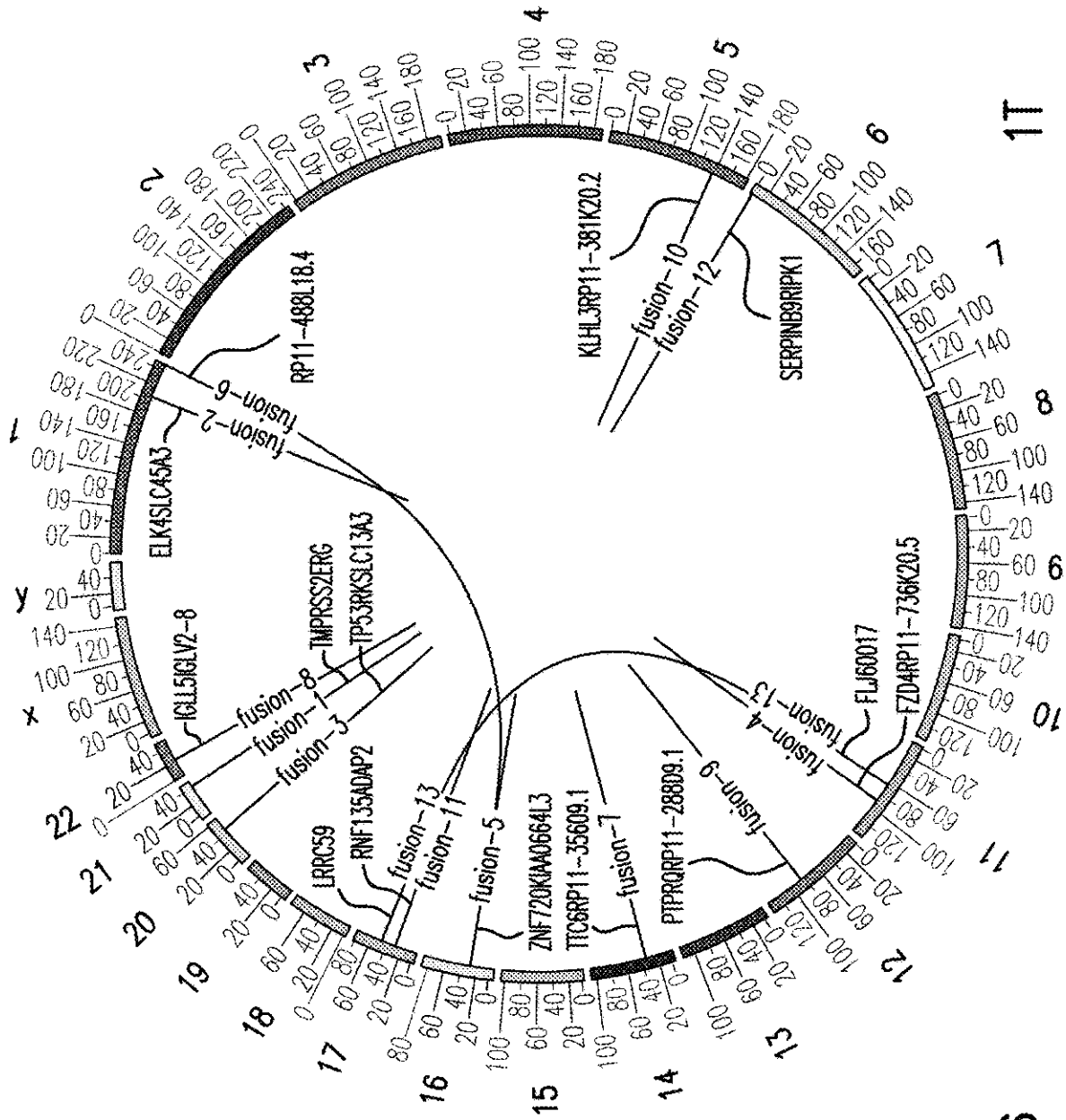
RP11-488L18.4
fusion-6
fusion-2
ELK4SLC45A3
IGLL5IGLV2-8
fusion-8
fusion-1
fusion-3
TMPRSS2ERG
TP53RKSLC13A3
LRRC59
RNF135ADAP2
fusion-13
fusion-11
fusion-5
ZNF720KIAA0664L3
TTC6RP11-35609.1
fusion-7
PTPRQRP11-28809.1
fusion-9
fusion-4
FLJ60017
FZD4RP11-736K20.5
KLHL3RP11-381K20.2
fusion-10
fusion-12
SERPINB9RIPK1

1T

FIG. 6

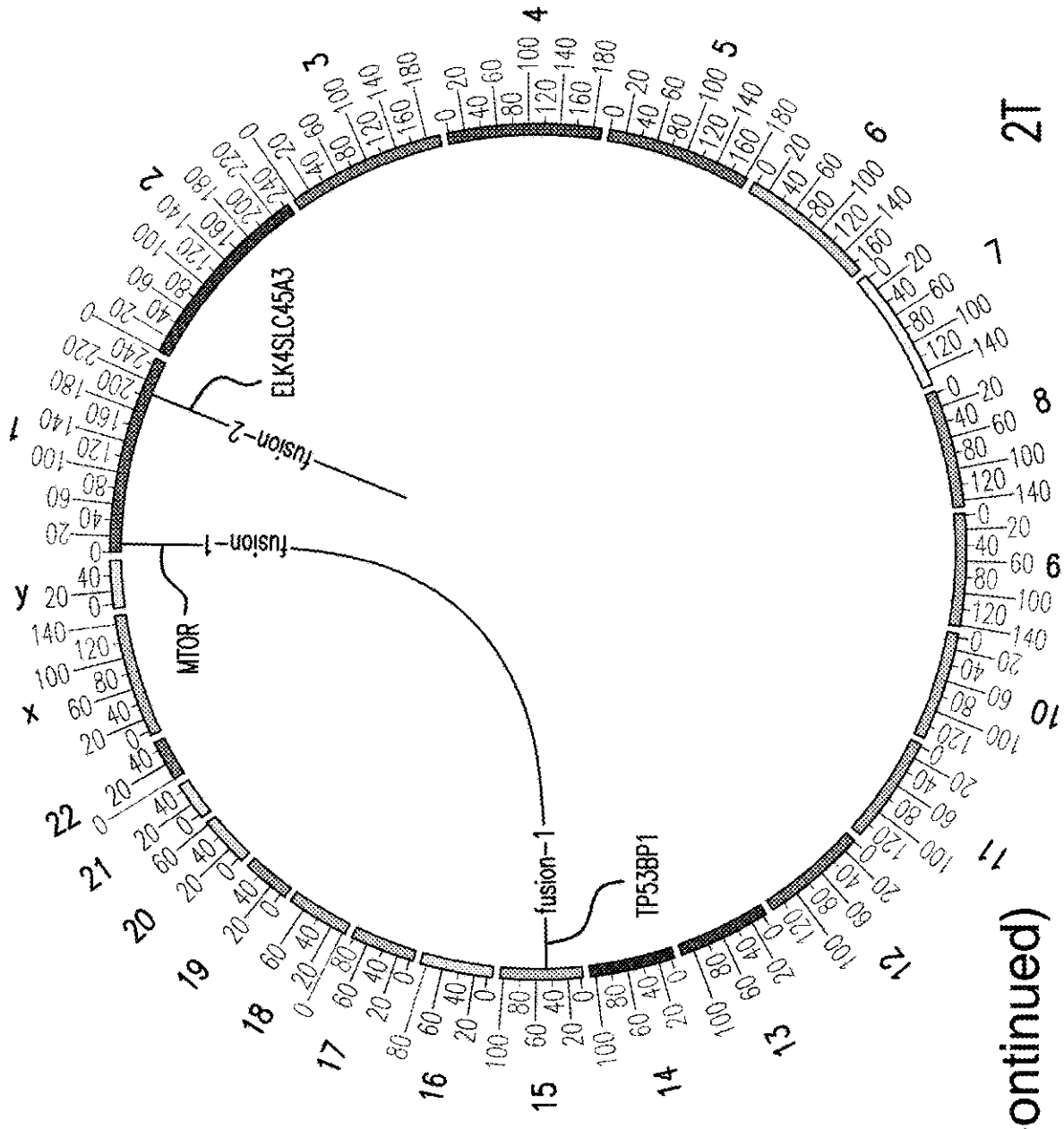

FIG. 6 (Continued)

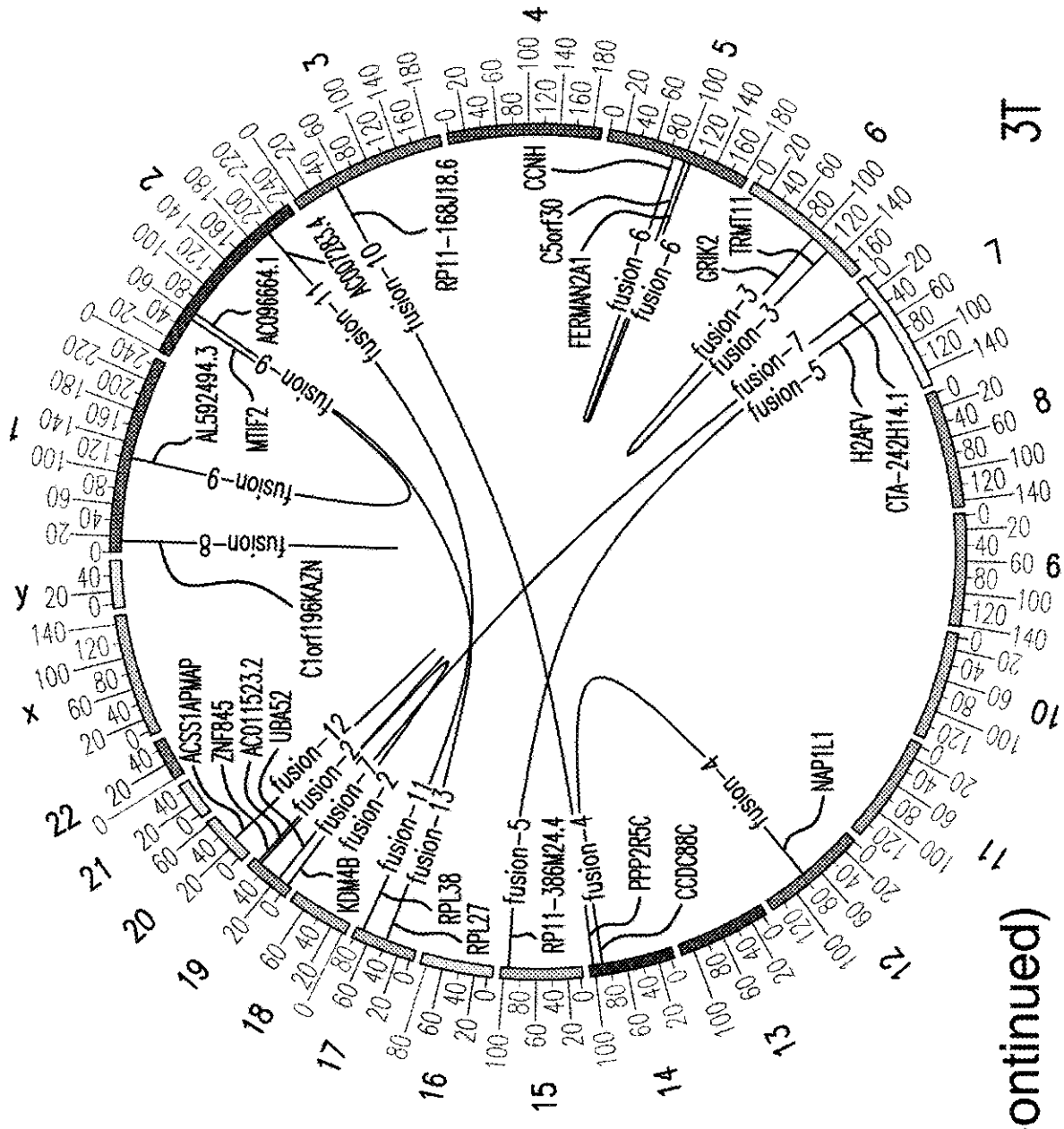

FIG. 6 (Continued)

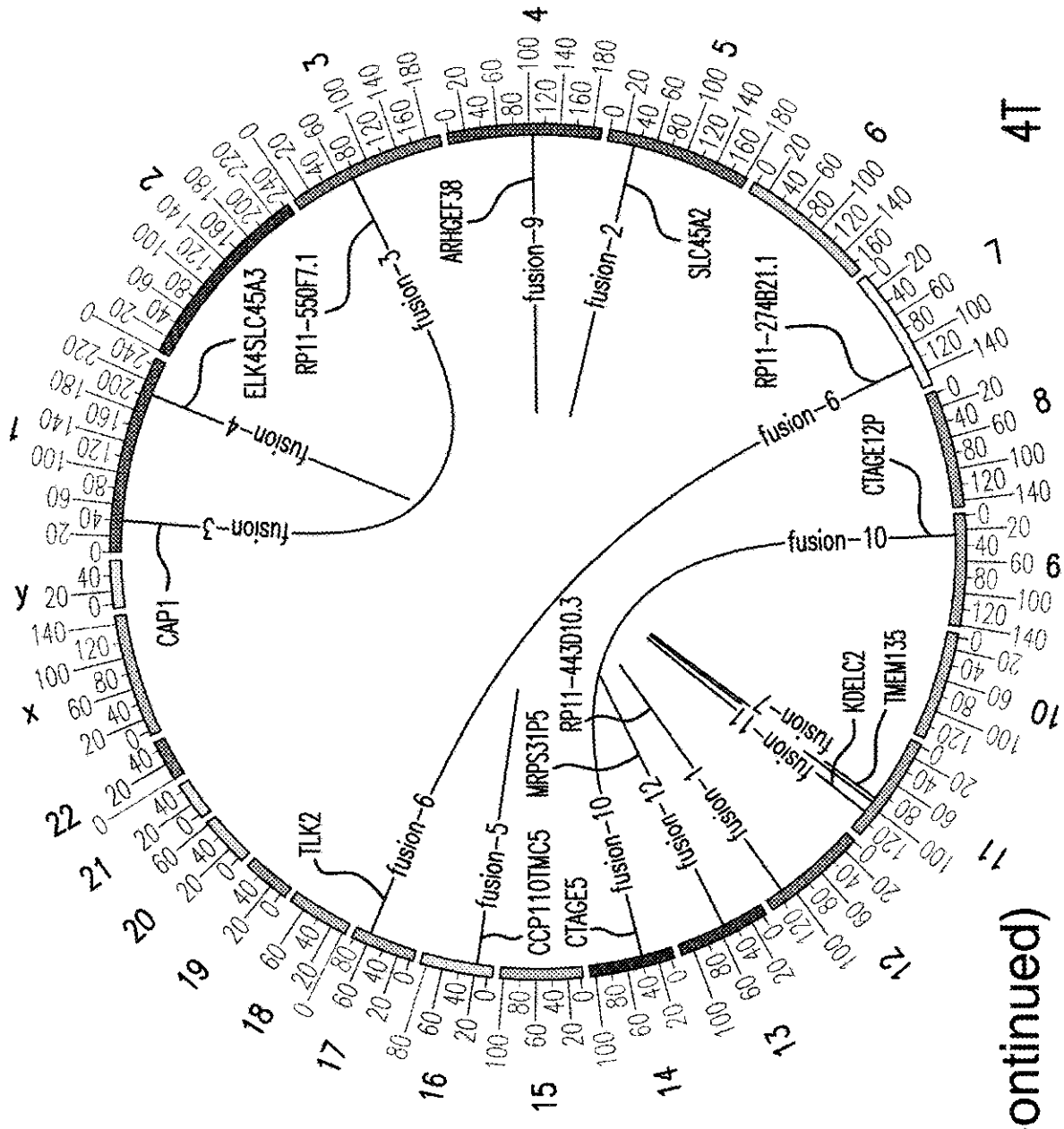

FIG. 6 (Continued)

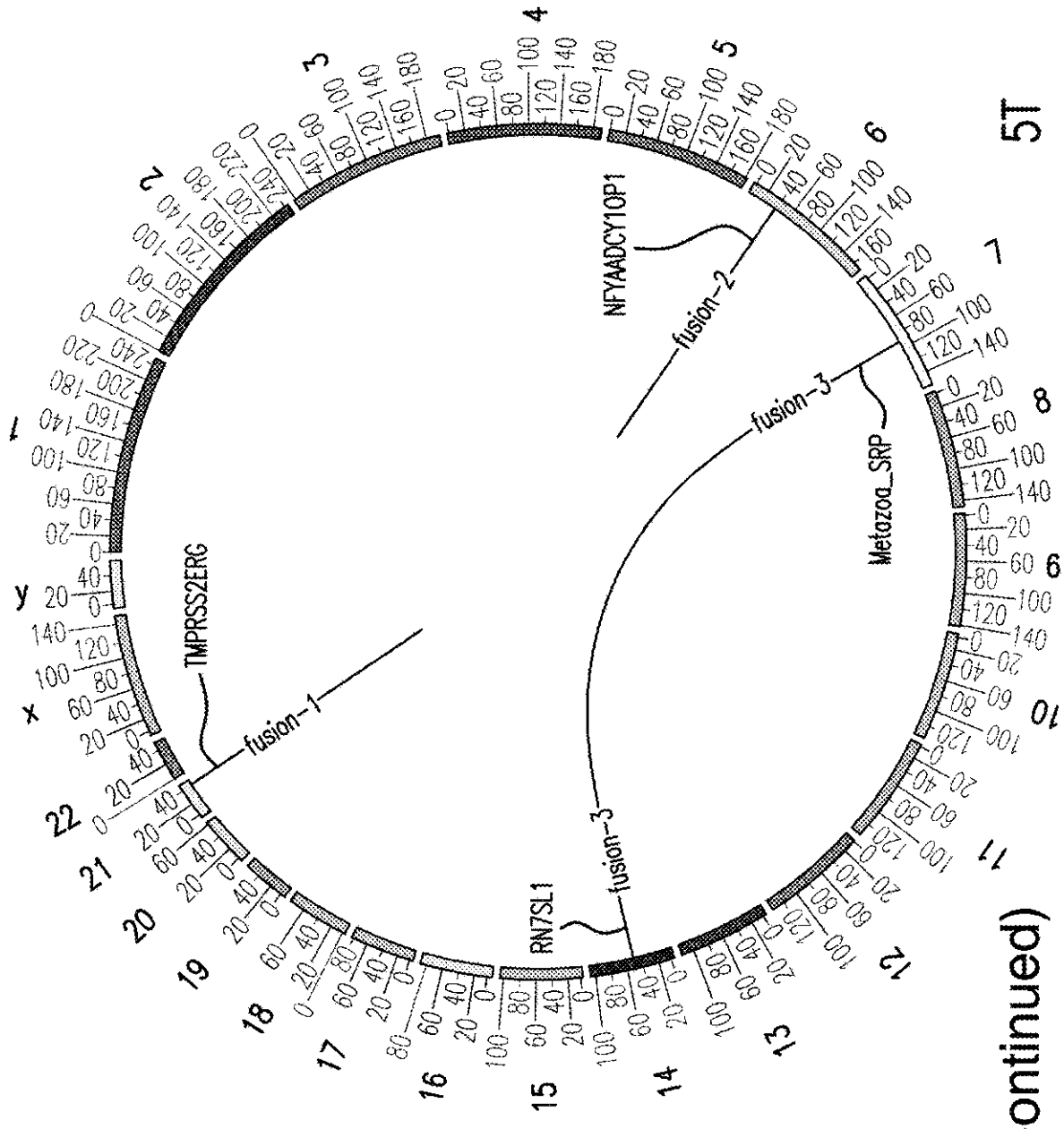

FIG. 6 (Continued)

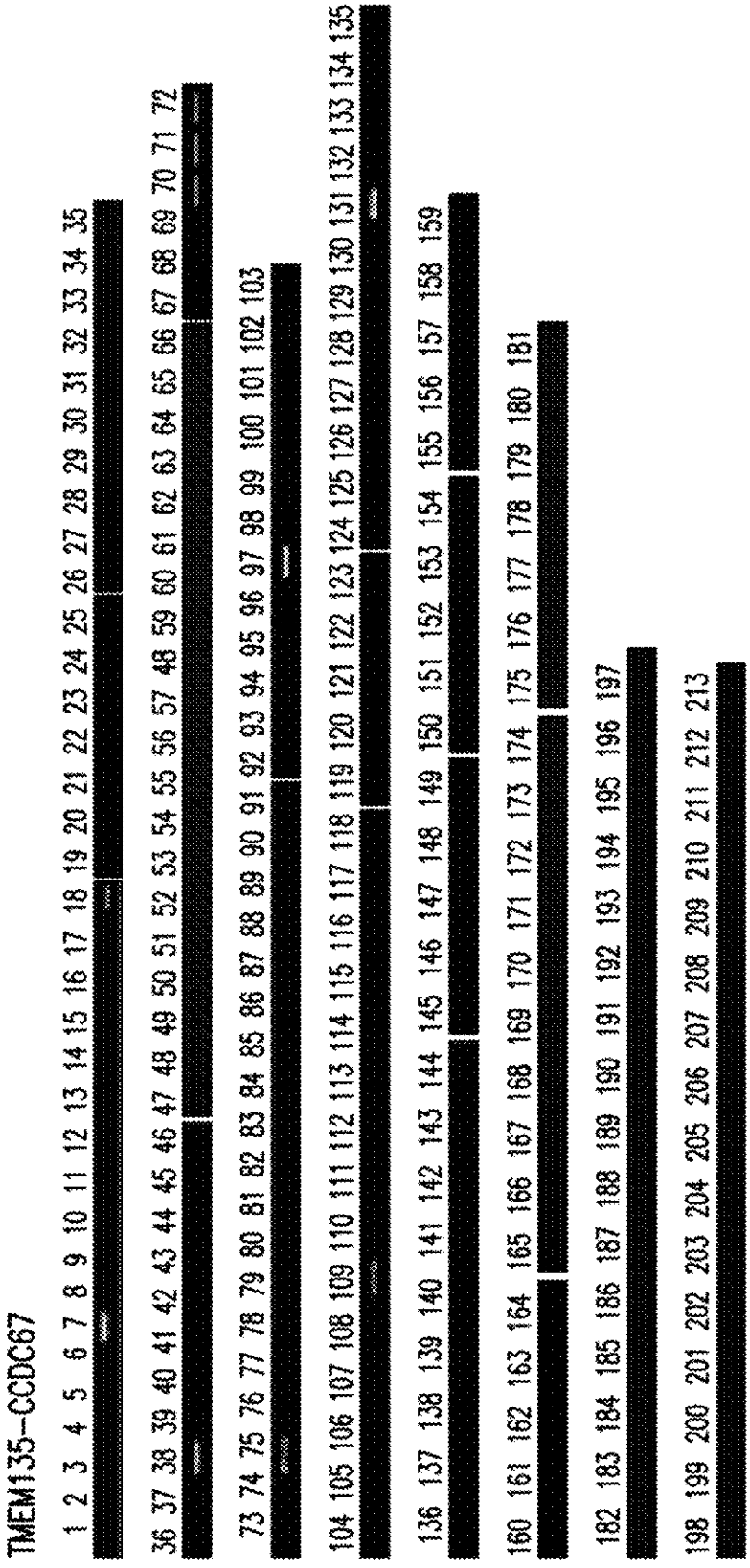
TMEM135-CCDC67
1 2 3 4 5 6 7 8 9 10 11 12 13 14 15 16 17 18 19 20 21 22 23 24 25 26 27 28 29 30 31 32 33 34 35
36 37 38 39 40 41 42 43 44 45 46 47 48 49 50 51 52 53 54 55 56 57 48 59 60 61 62 63 64 65 66 67 68 69 70 71 72
73 74 75 76 77 78 79 80 81 82 83 84 85 86 87 88 89 90 91 92 93 94 95 96 97 98 99 100 101 102 103
104 105 106 107 108 109 110 111 112 113 114 115 116 117 118 119 120 121 122 123 124 125 126 127 128 129 130 131 132 133 134 135
136 137 138 139 140 141 142 143 144 145 146 147 148 149 150 151 152 153 154 155 156 157 158 159
160 161 162 163 164 165 166 167 168 169 170 171 172 173 174 175 176 177 178 179 180 181
182 183 184 185 186 187 188 189 190 191 192 193 194 195 196 197
198 199 200 201 202 203 204 205 206 207 208 209 210 211 212 213

FIG. 7A

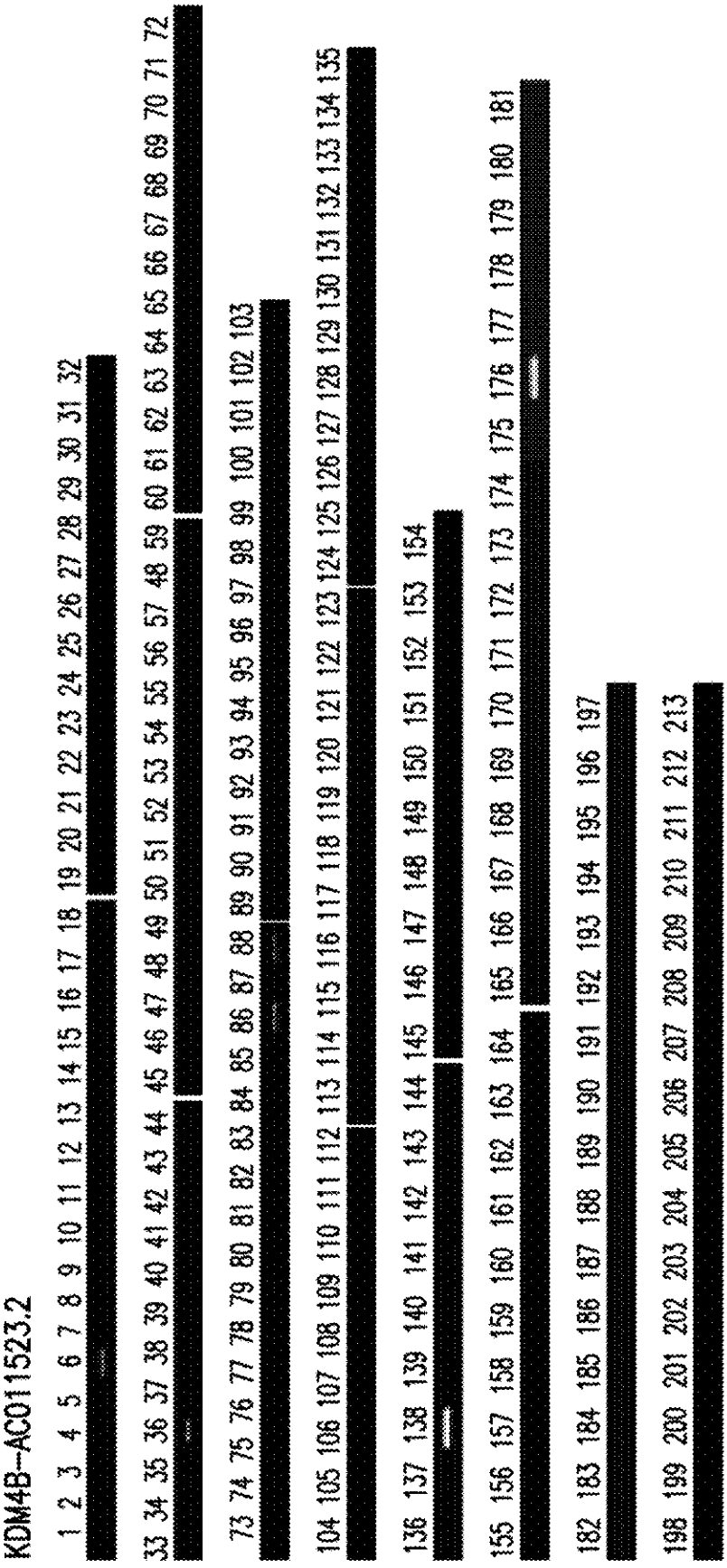

FIG. 7A (Continued)

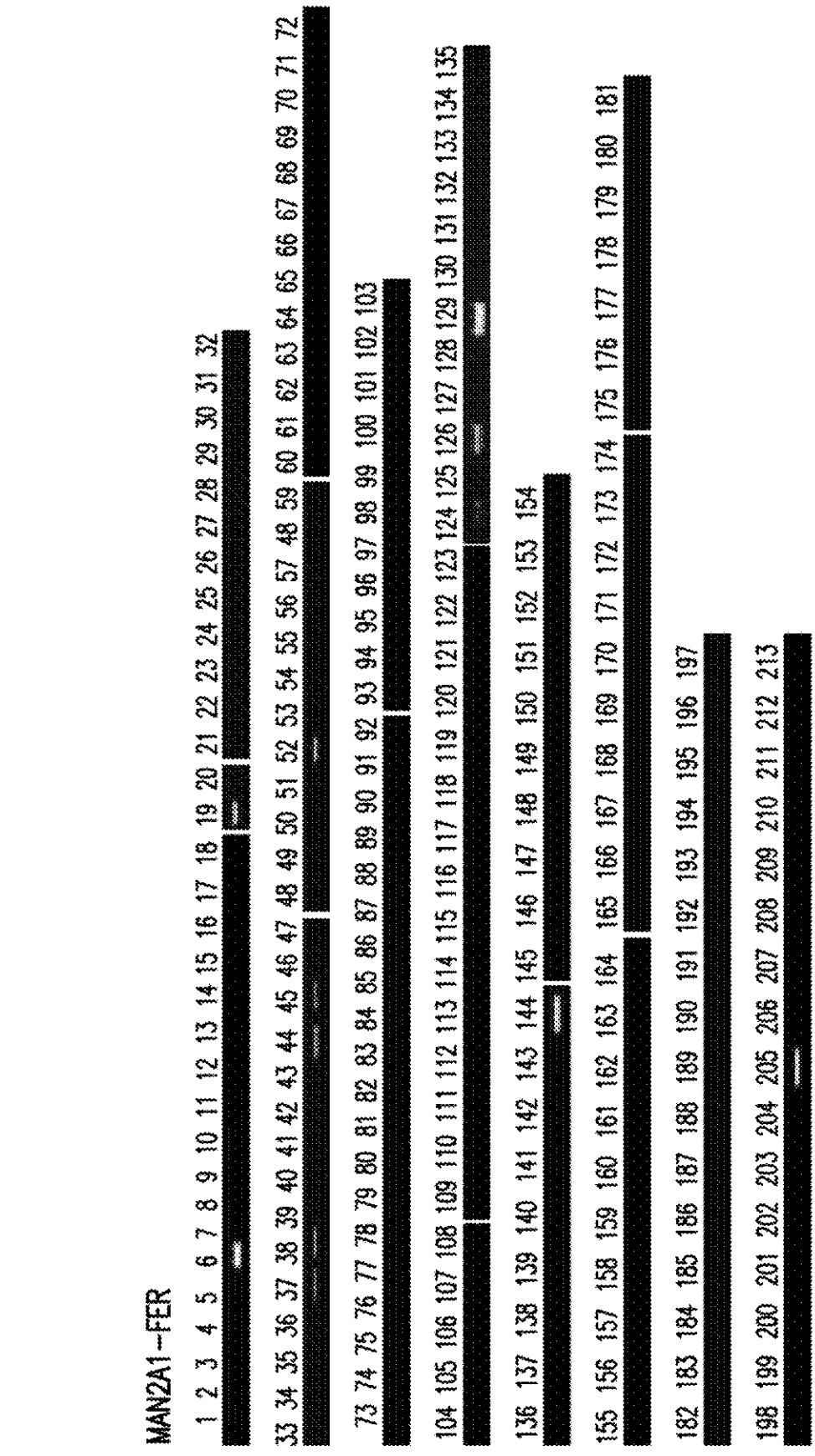

FIG. 7A (Continued)

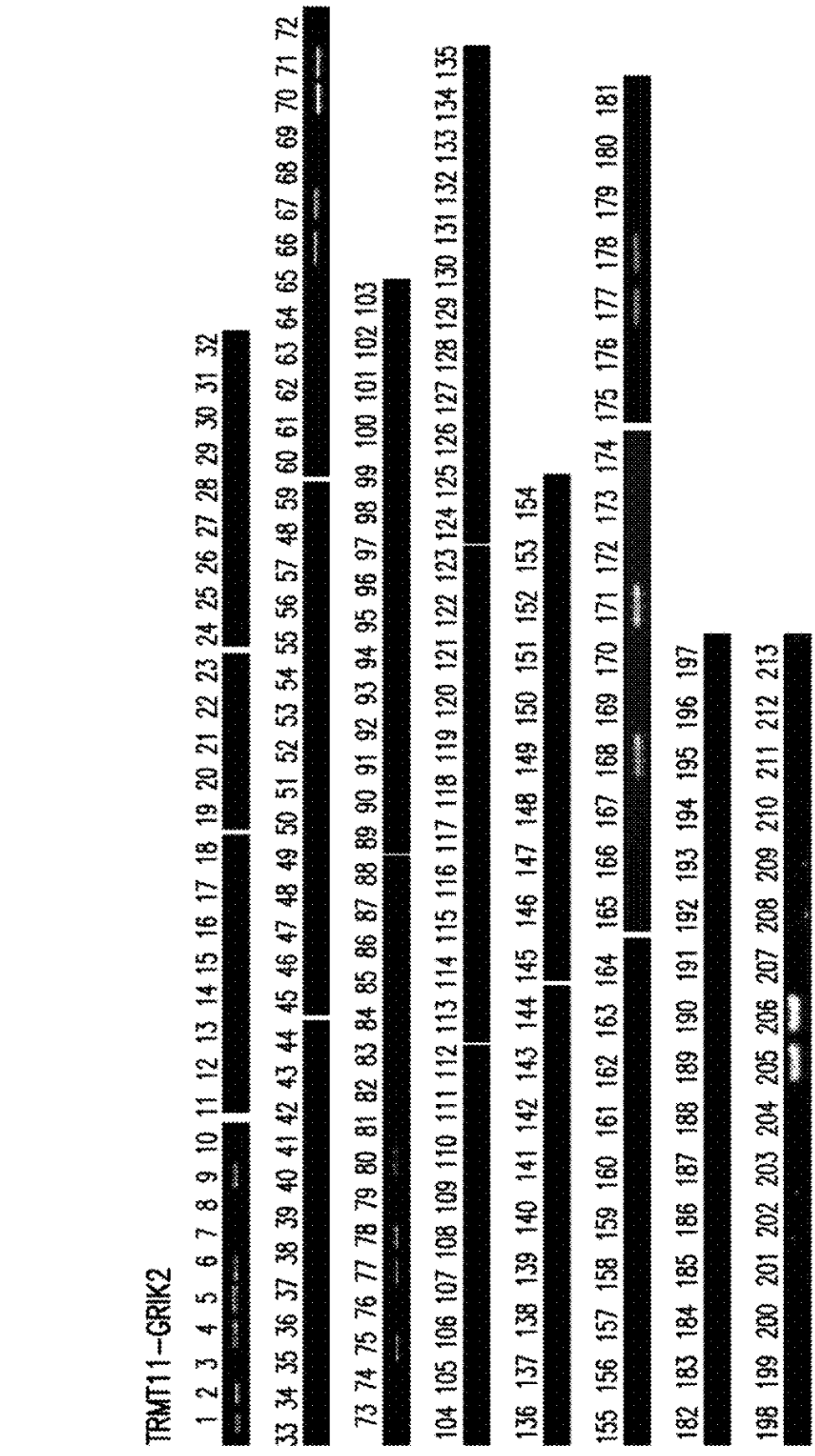

FIG. 7A (Continued)

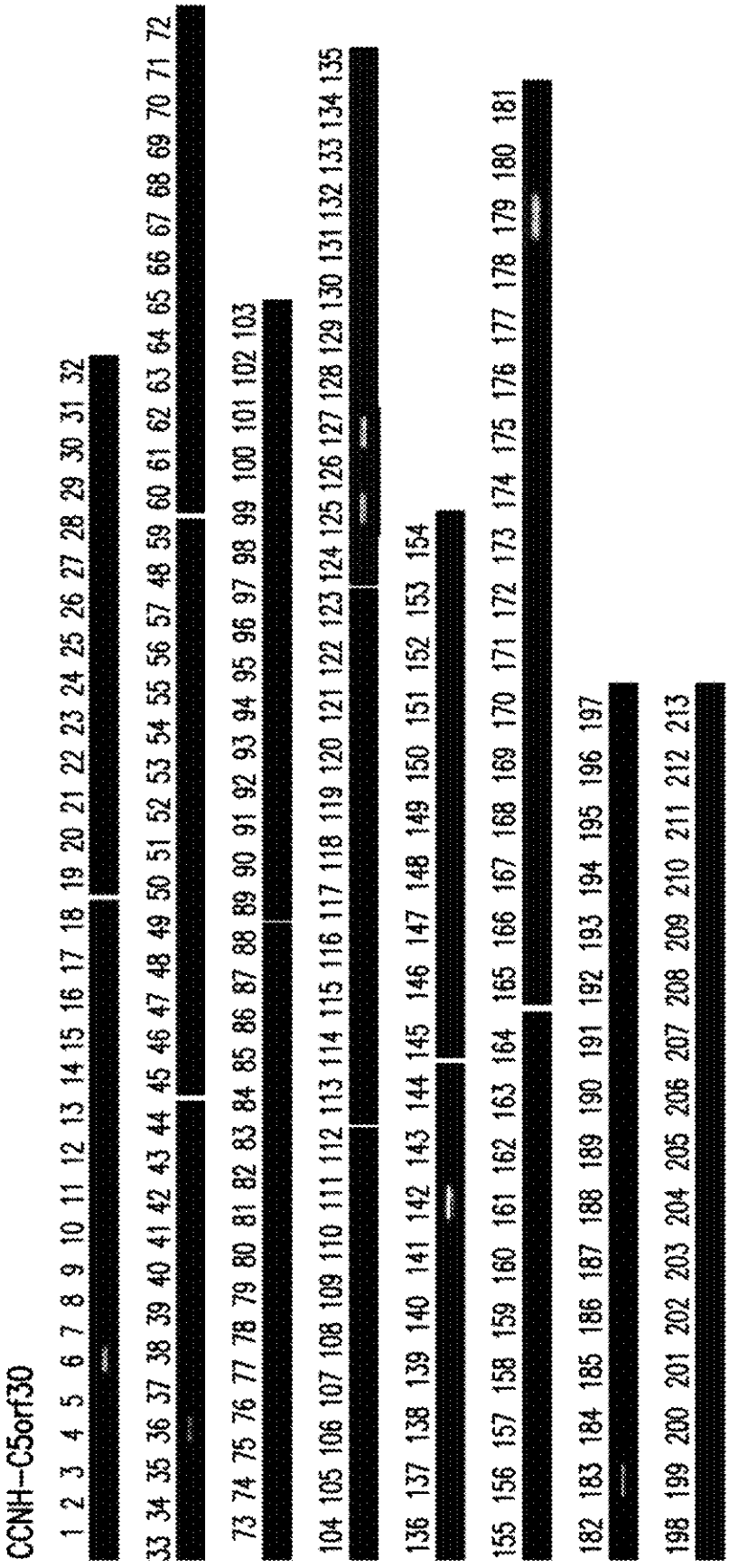

FIG. 7A (Continued)

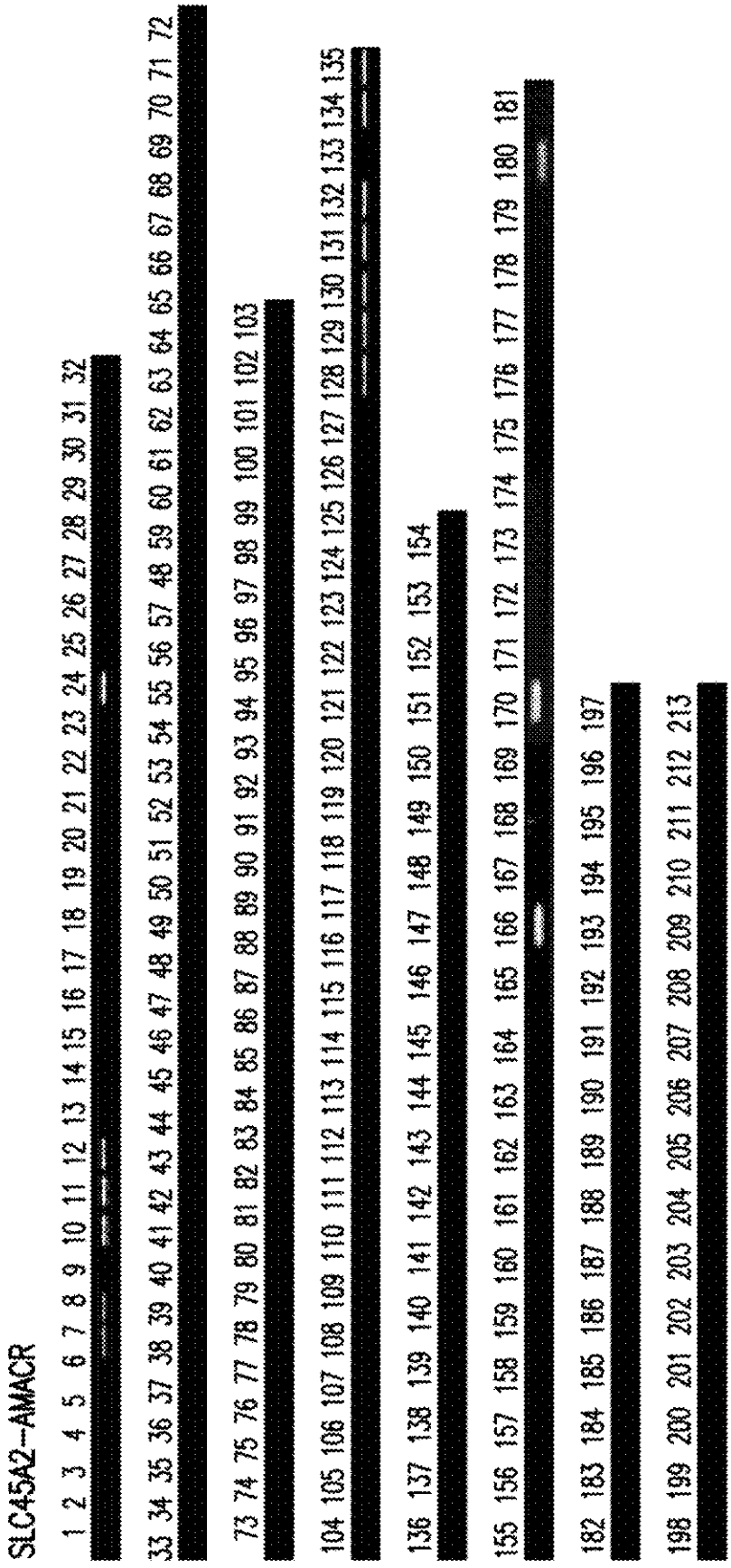

FIG. 7A (Continued)

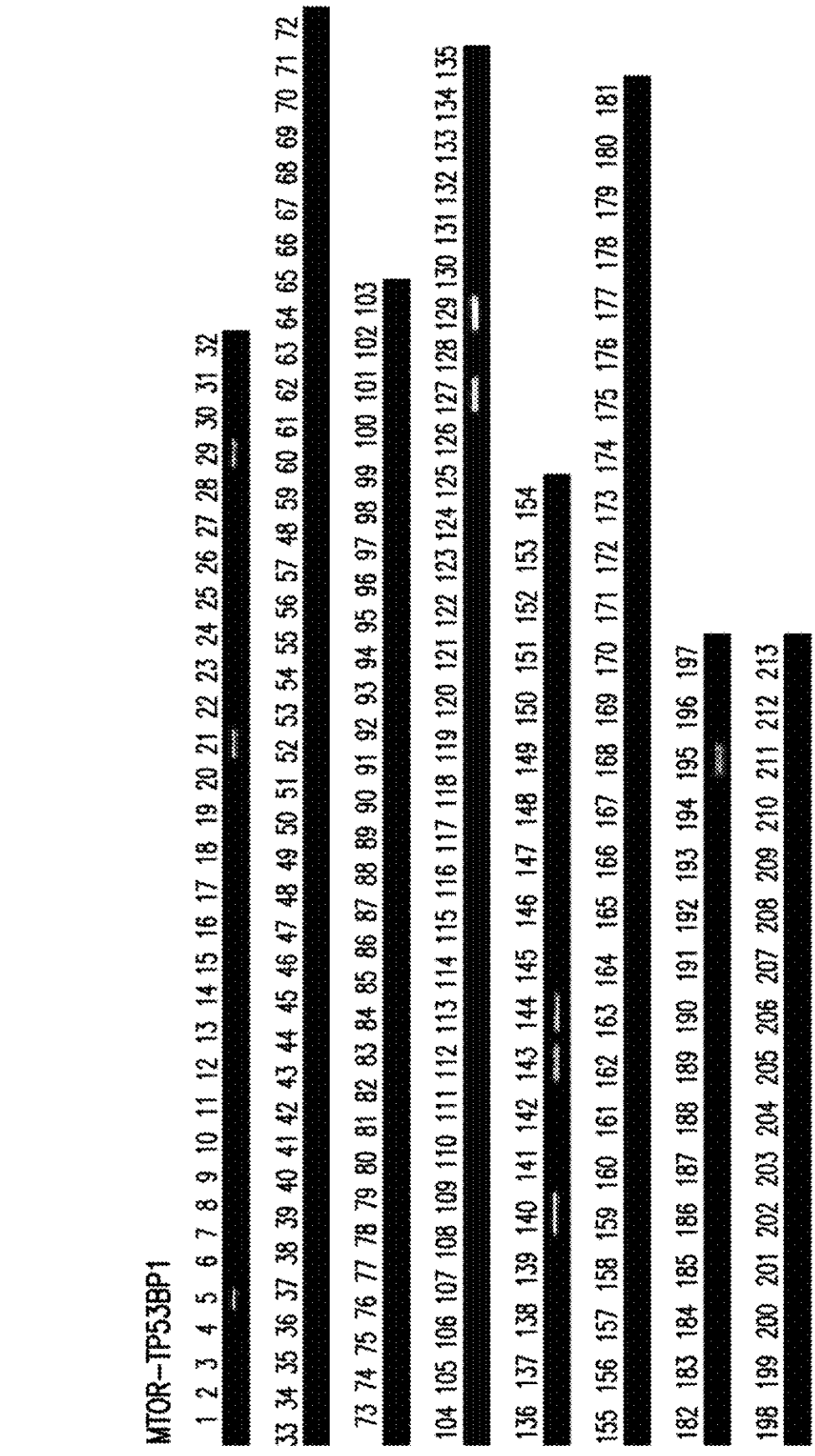

FIG. 7A (Continued)

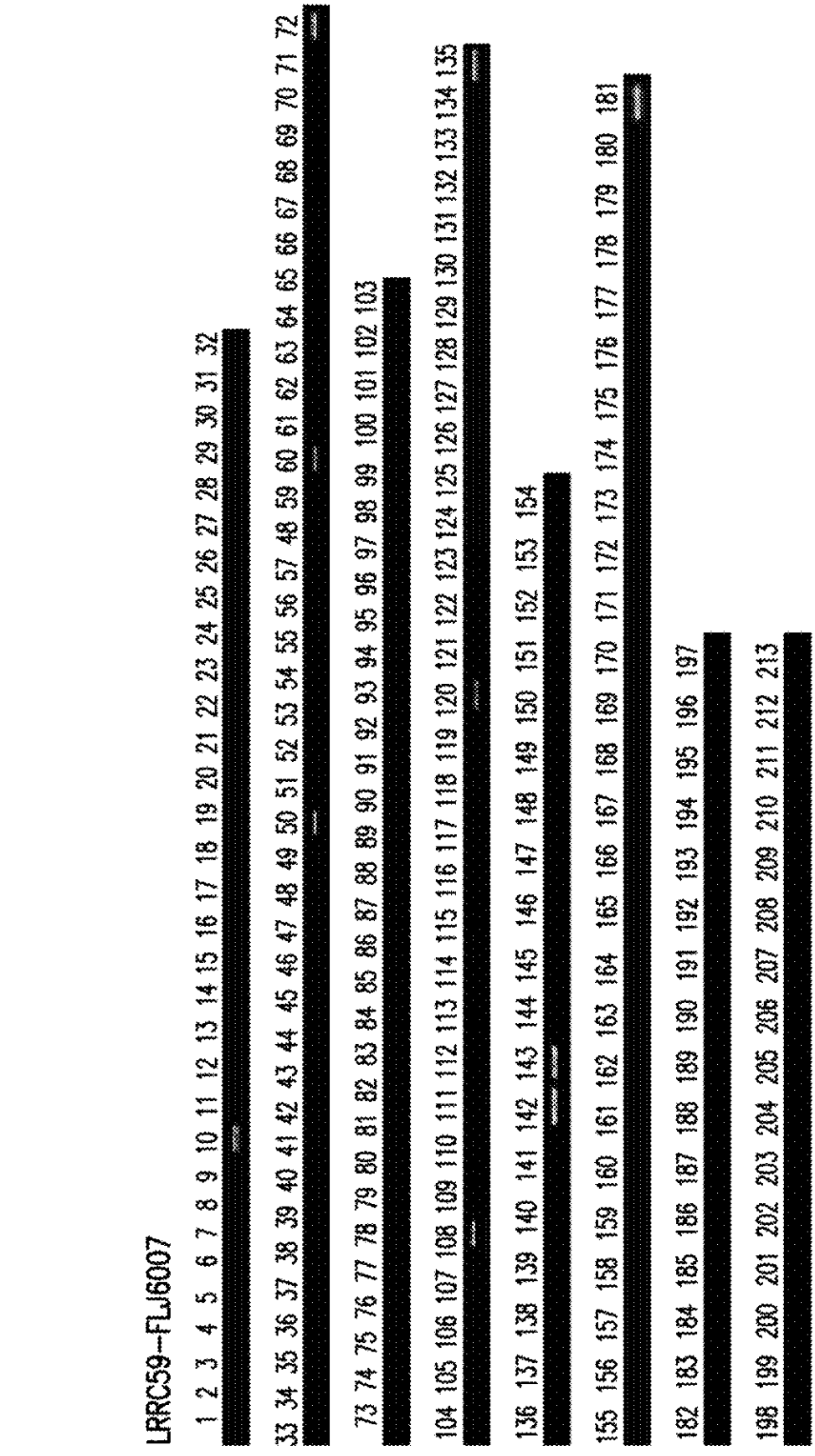

FIG. 7A (Continued)

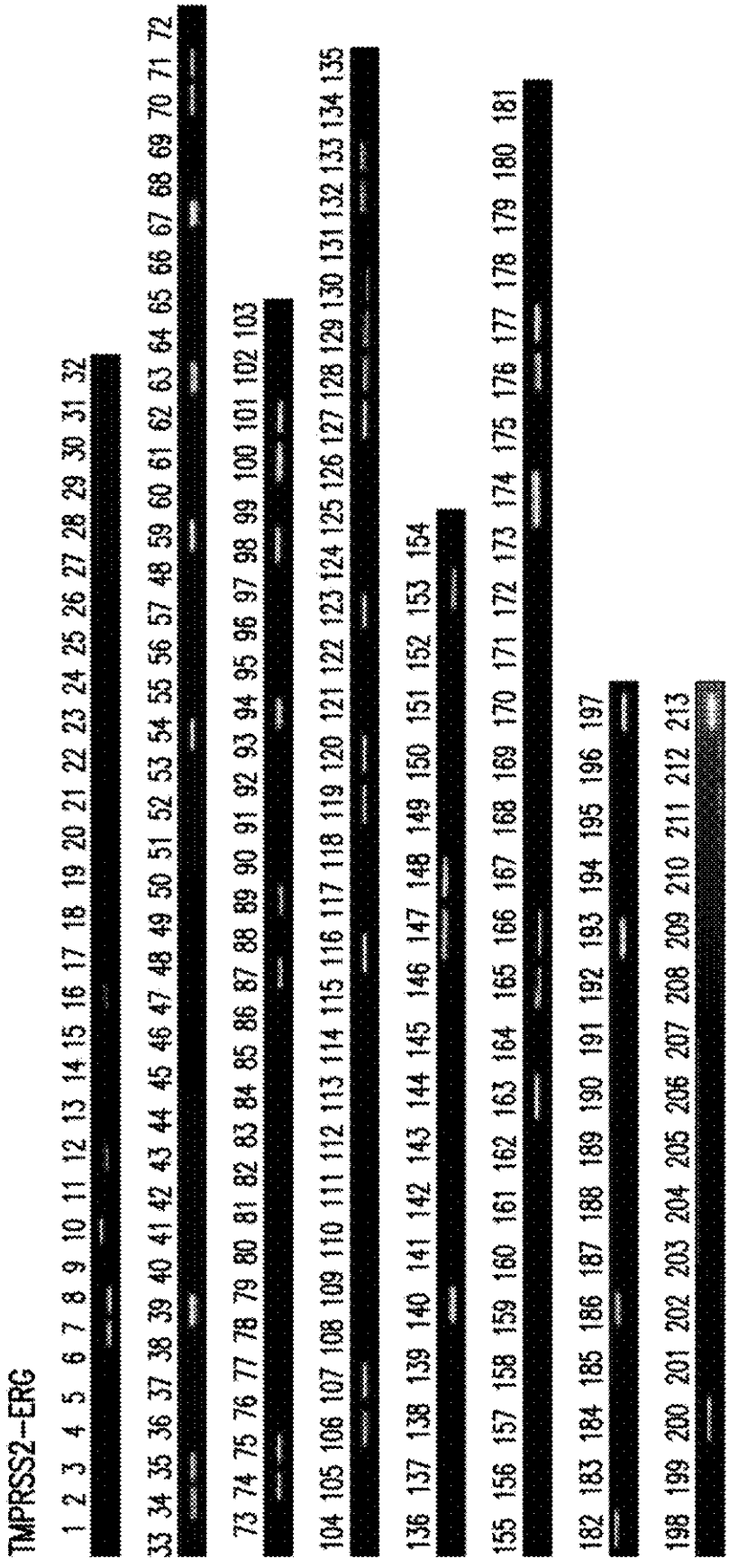

FIG. 7A (Continued)

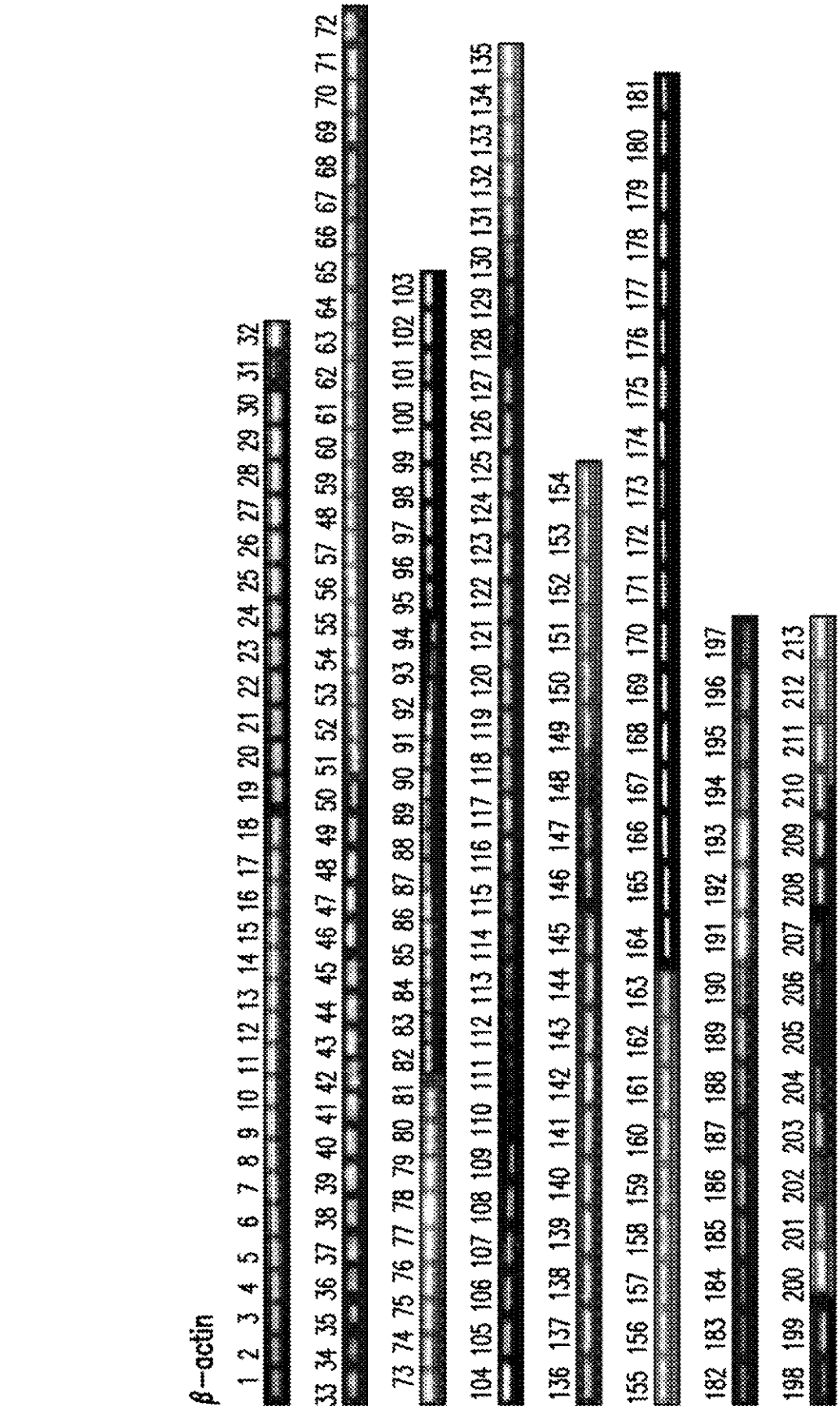

FIG. 7A (Continued)

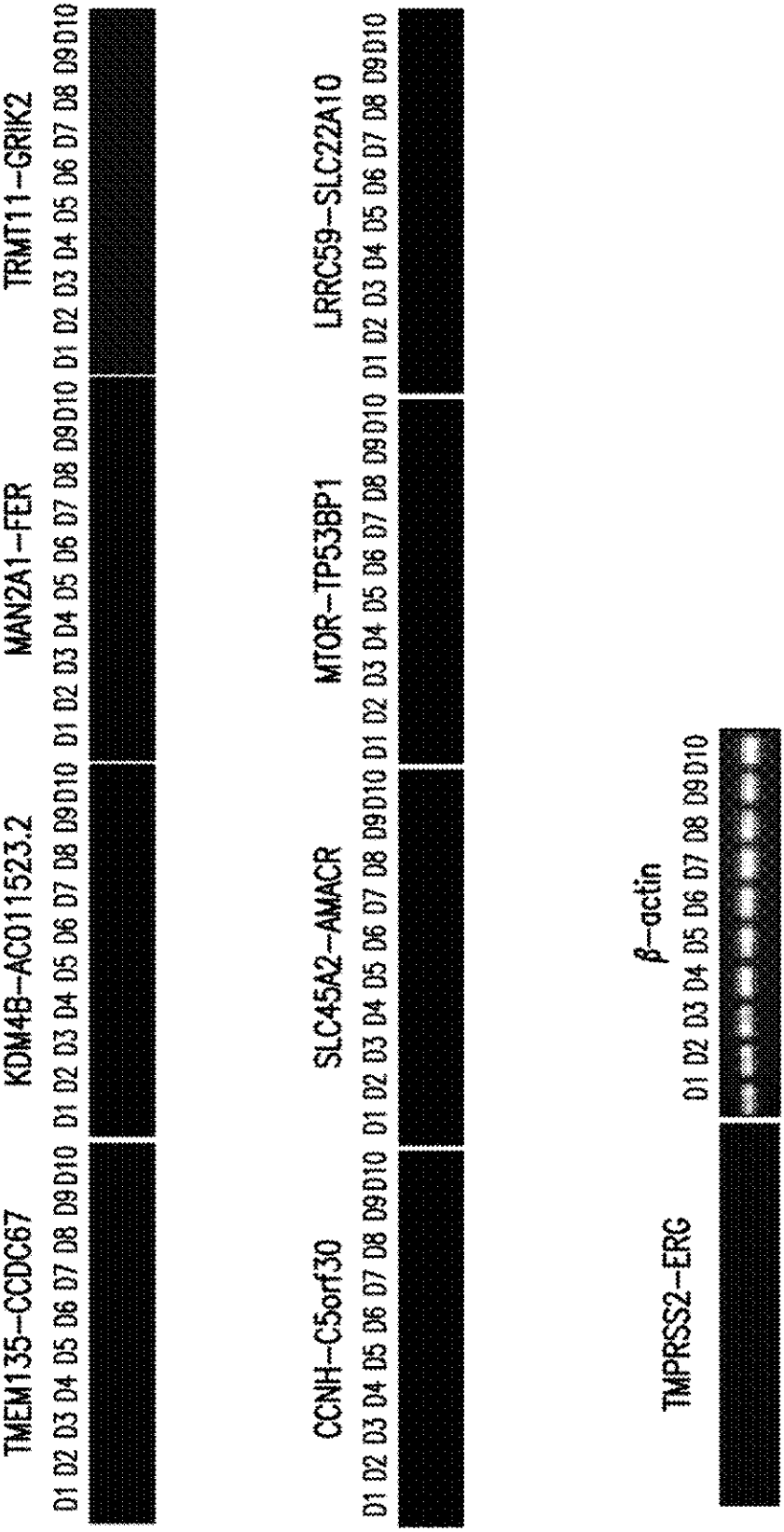
TMEM135–CCDC67
D1 D2 D3 D4 D5 D6 D7 D8 D9 D10
KDM4B–AC011523.2
D1 D2 D3 D4 D5 D6 D7 D8 D9 D10
MAN2A1–FER
D1 D2 D3 D4 D5 D6 D7 D8 D9 D10
TRMT11–GRIK2
D1 D2 D3 D4 D5 D6 D7 D8 D9 D10
CCNH–C5orf30
D1 D2 D3 D4 D5 D6 D7 D8 D9 D10
SLC45A2–AMACR
D1 D2 D3 D4 D5 D6 D7 D8 D9 D10
MTOR–TP53BP1
D1 D2 D3 D4 D5 D6 D7 D8 D9 D10
LRRC59–SLC22A10
D1 D2 D3 D4 D5 D6 D7 D8 D9 D10
TMPRSS2–ERG
β–actin
D1 D2 D3 D4 D5 D6 D7 D8 D9 D10

FIG. 7B

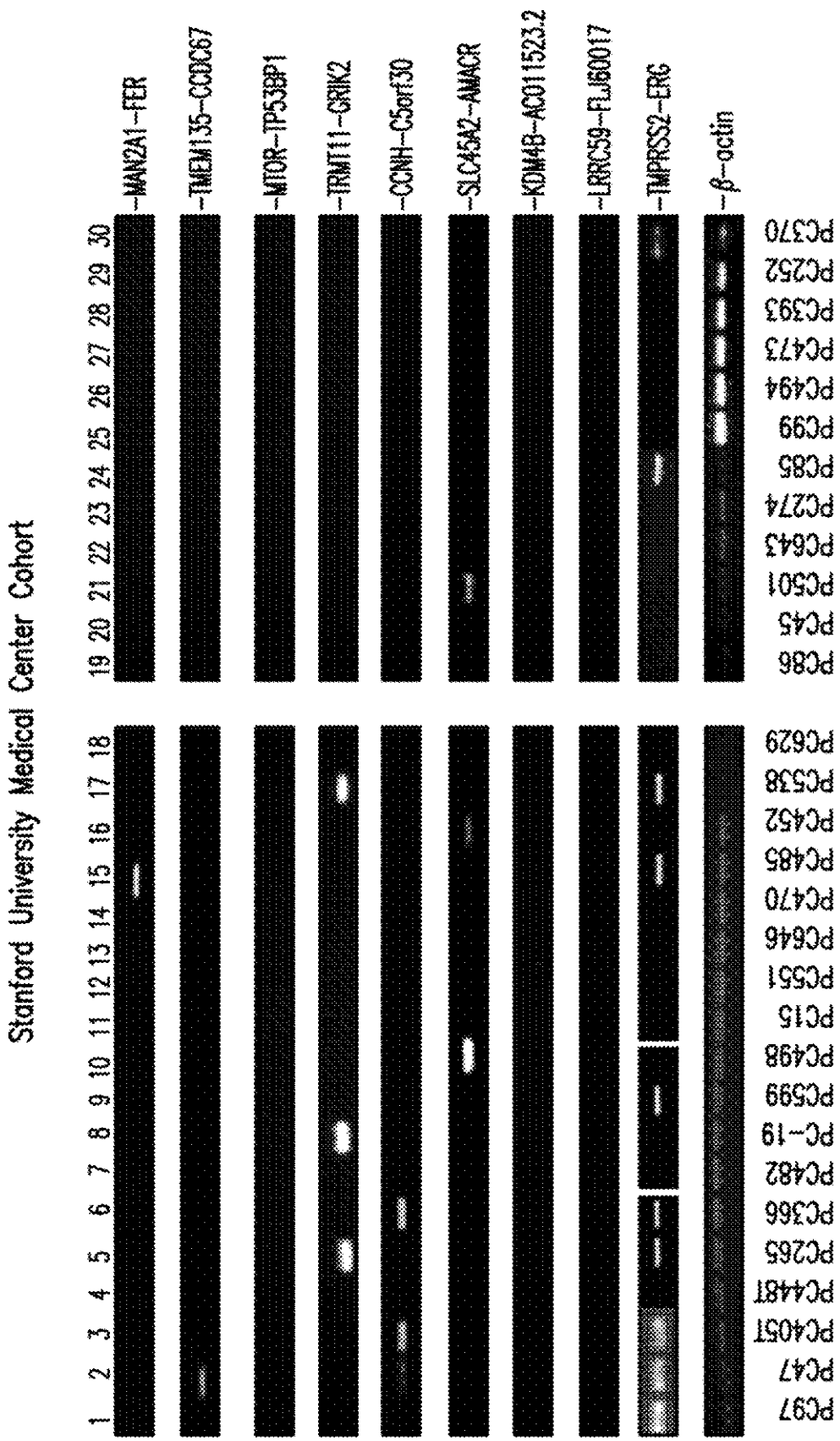
Stanford University Medical Center Cohort
1 2 3 4 5 6 7 8 9 10 11 12 13 14 15 16 17 18 19 20 21 22 23 24 25 26 27 28 29 30
-MAN2A1-FER
-TMEM135-CCDC67
-MTOR-TP53BP1
-TRMT11-GRIK2
-CCNH-C5orf30
-SLC45A2-AMACR
-KDM4B-AC011523.2
-LRRC59-FLJ60017
-TMPRSS2-ERG
-β-actin
PC97
PC47
PC405T
PC448T
PC265
PC366
PC482
PC-19
PC599
PC498
PC15
PC551
PC646
PC470
PC485
PC452
PC538
PC629
PC586
PC45
PC501
PC643
PC274
PC85
PC99
PC494
PC473
PC393
PC252
PC370

FIG. 8

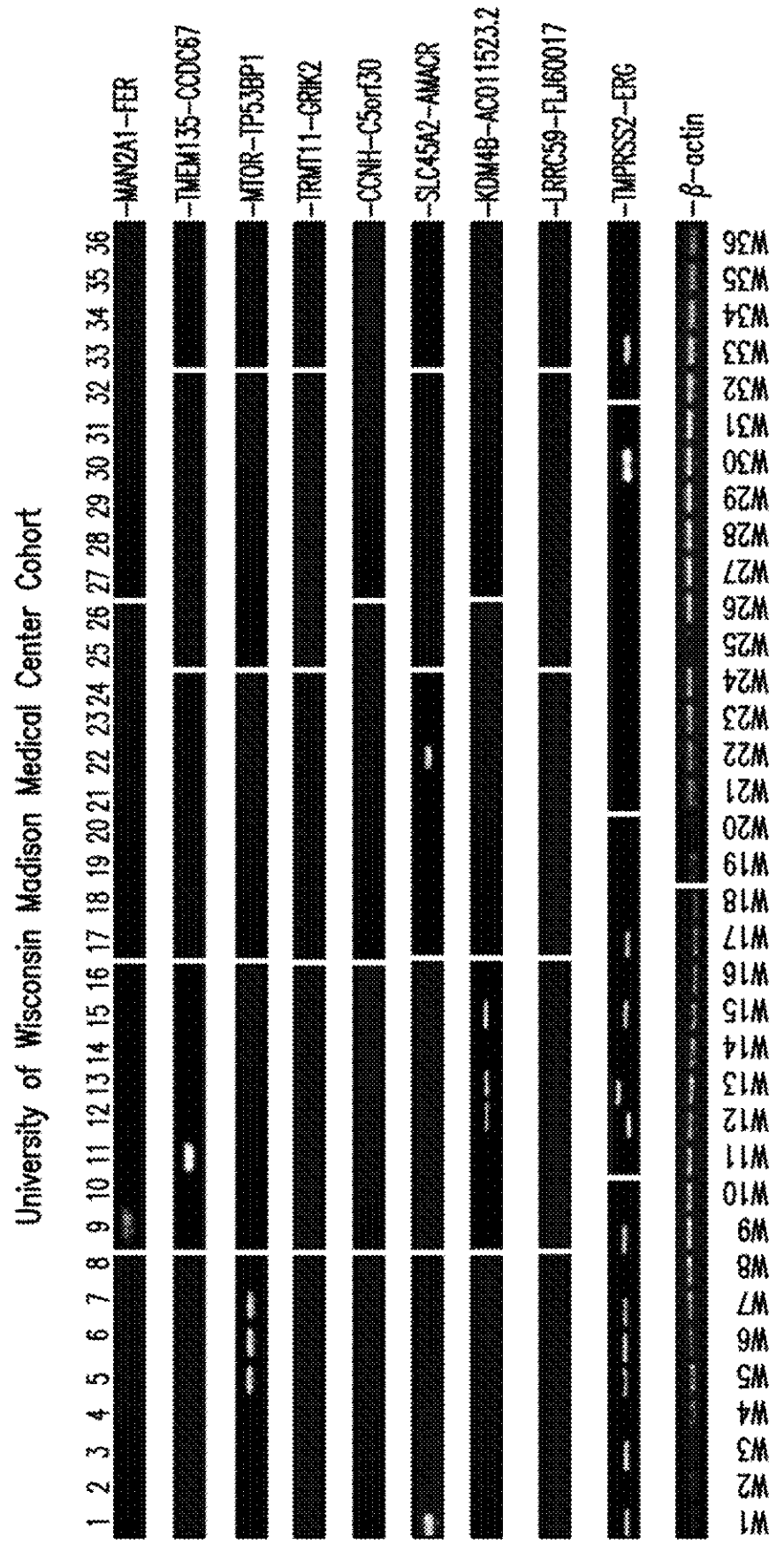
University of Wisconsin Madison Medical Center Cohort
1 2 3 4 5 6 7 8 9 10 11 12 13 14 15 16 17 18 19 20 21 22 23 24 25 26 27 28 29 30 31 32 33 34 35 36
MAN2A1-FER
TMEM135-CCDC67
MTOR-TP53BP1
TRMT11-GRIK2
CCNH-C5orf30
SLC45A2-AMACR
KDM4B-AC011523.2
LRRC59-FLJ60017
TMPRSS2-ERG
β-actin
W1 W2 W3 W4 W5 W6 W7 W8 W9 W10 W11 W12 W13 W14 W15 W16 W17 W18 W19 W20 W21 W22 W23 W24 W25 W26 W27 W28 W29 W30 W31 W32 W33 W34 W35 W36

FIG. 9

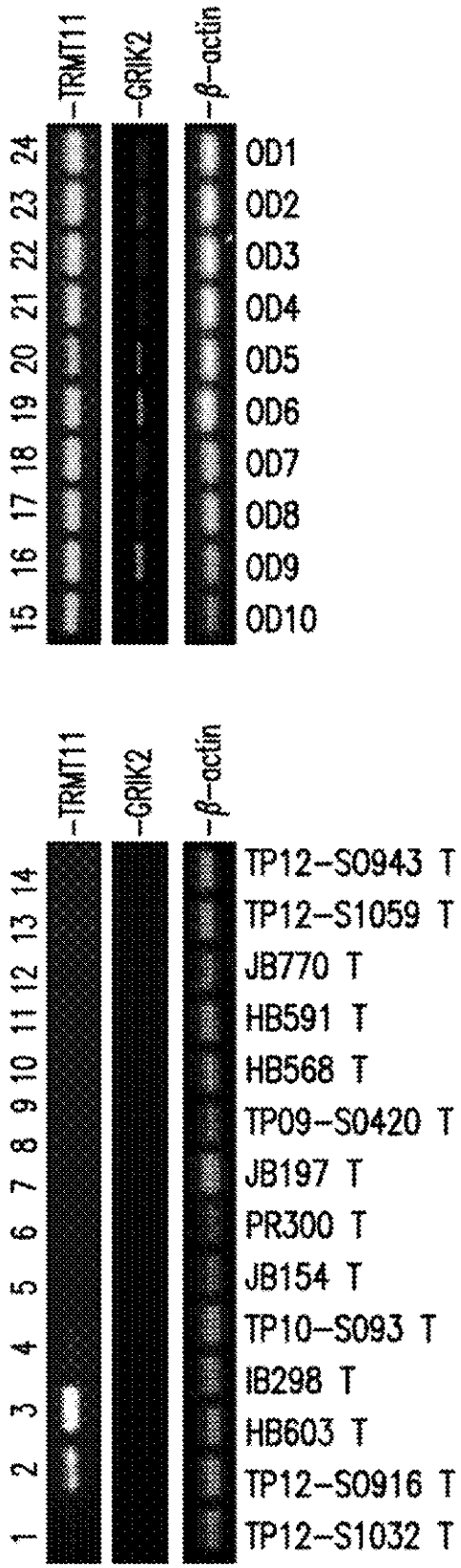
-TRMT11
-GRIK2
-β-actin
24 23 22 21 20 19 18 17 16 15
OD1
OD2
OD3
OD4
OD5
OD6
OD7
OD8
OD9
OD10
-TRMT11
-GRIK2
-β-actin
14 13 12 11 10 9 8 7 6 5 4 3 2 1
TP12-S0943 T
TP12-S1059 T
JB770 T
HB591 T
HB568 T
TP09-S0420 T
JB197 T
PR300 T
JB154 T
TP10-S093 T
IB298 T
HB603 T
TP12-S0916 T
TP12-S1032 T

FIG. 10

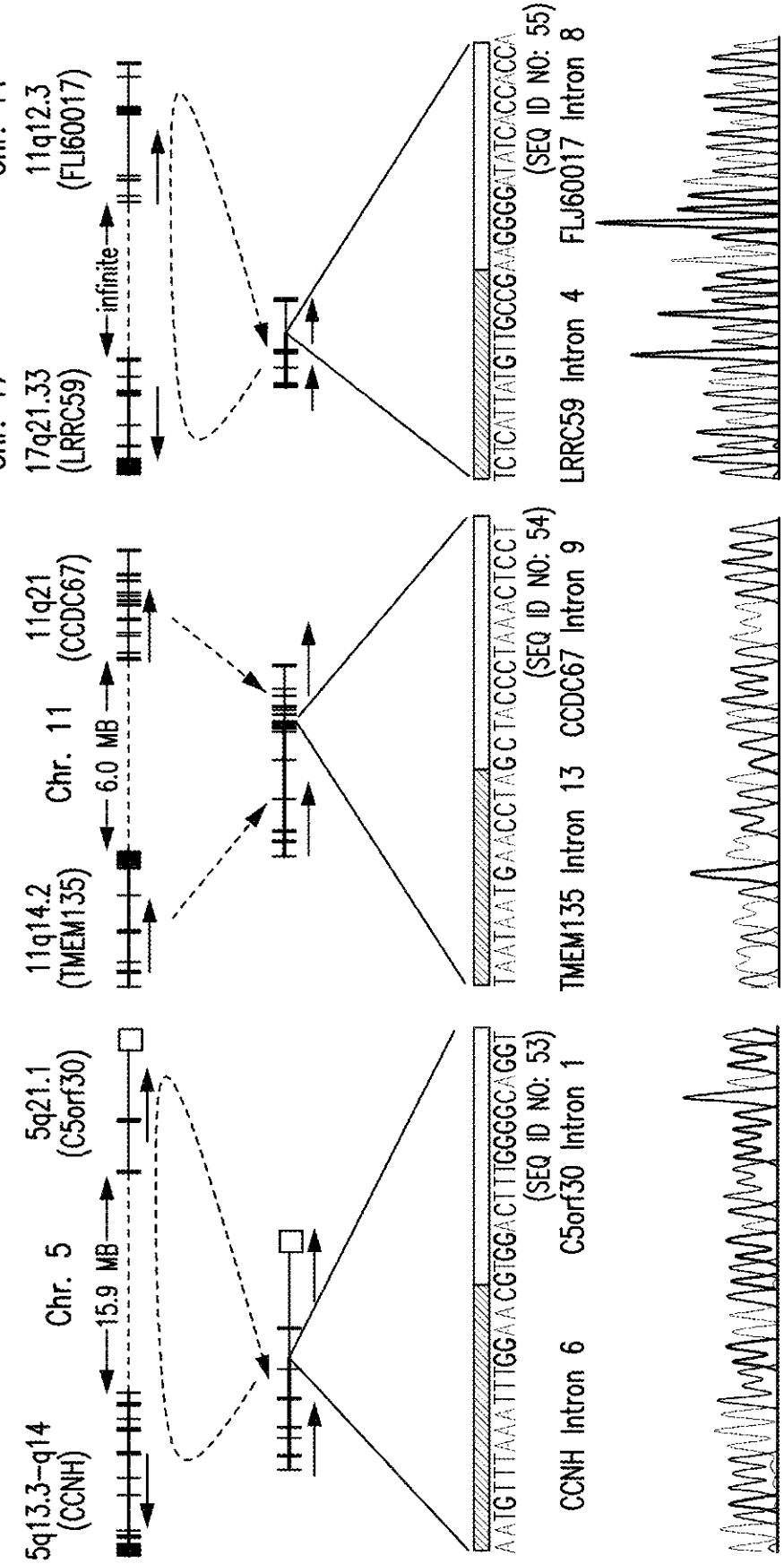
5q13.3–q14
(CCNH)
Chr. 5
15.9 MB
5q21.1
(C5orf30)
AATGTTTAAATTTGGAACGTGGACTTTGGGGCAGGT
(SEQ ID NO: 53)
CCNH Intron 6
C5orf30 Intron 1
11q14.2
(TMEM135)
Chr. 11
6.0 MB
11q21
(CCDC67)
TAATAAATGAACCTAGCTACCCTAAACTCCT
(SEQ ID NO: 54)
TMEM135 Intron 13
CCDC67 Intron 9
Chr. 17
17q21.33
(LRRC59)
infinite
Chr. 11
11q12.3
(FLJ60017)
TCTCATTATGTTGCCGAAGGGGTATCACCACCA
(SEQ ID NO: 55)
LRRC59 Intron 4
FLJ60017 Intron 8

FIG. 11

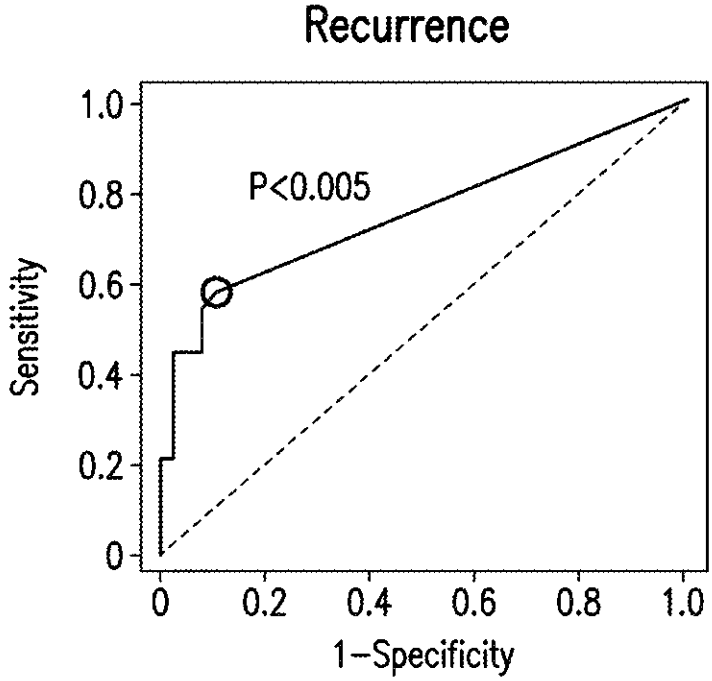

FIG. 12A

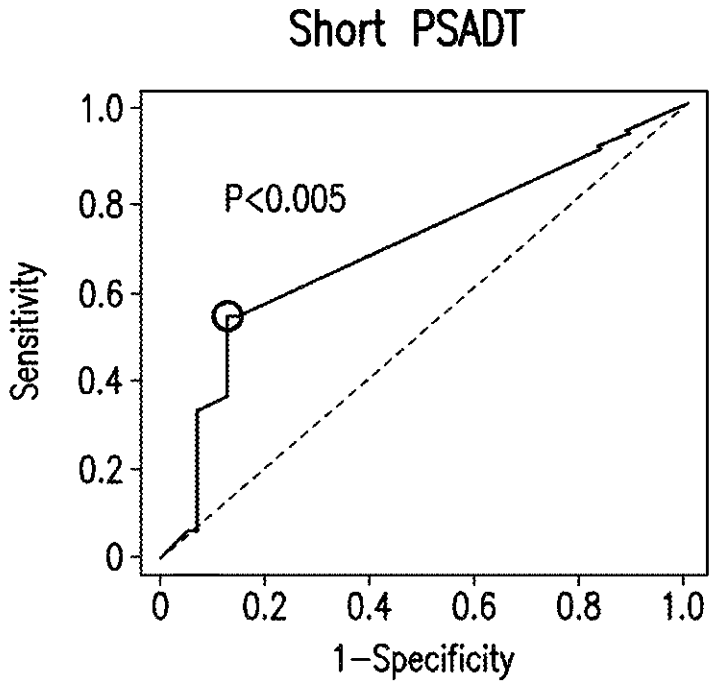

FIG. 12B

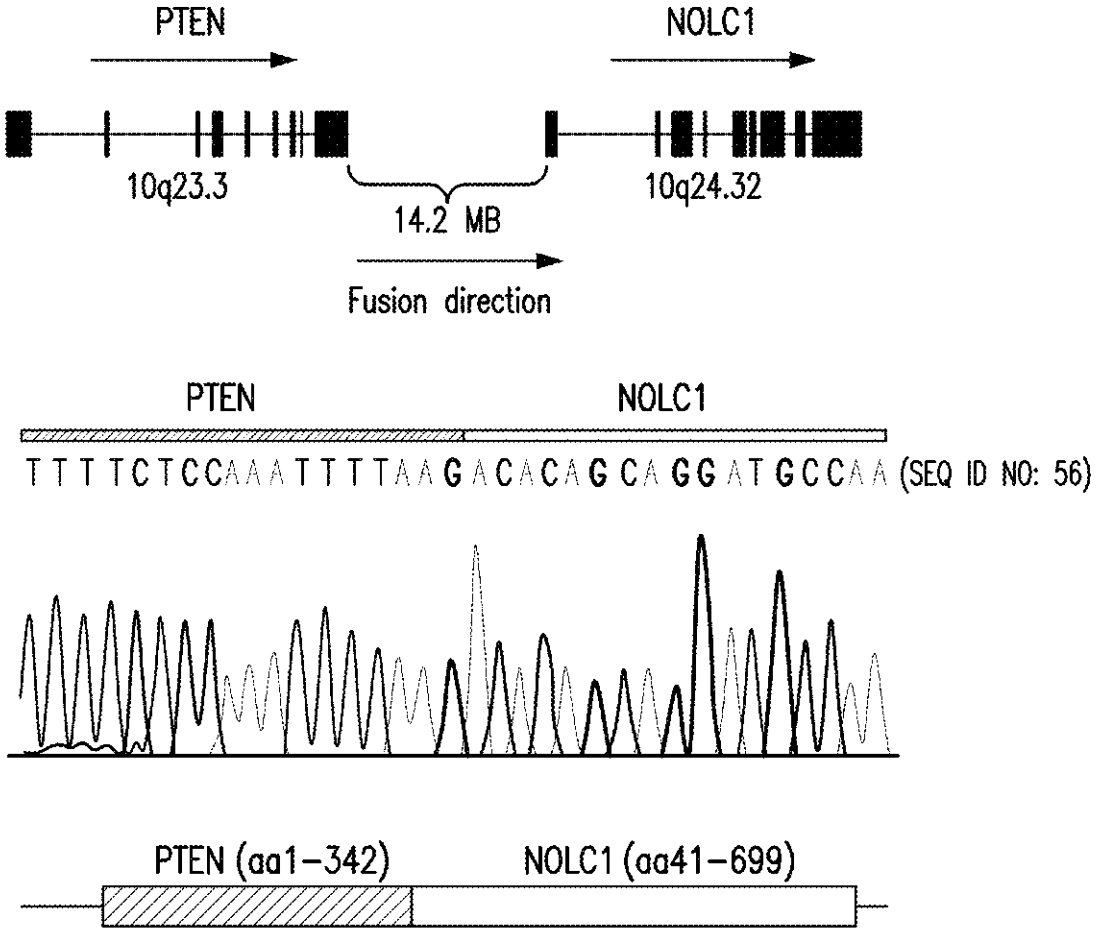
PTEN
NOLC1
10q23.3
14.2 MB
10q24.32
Fusion direction
PTEN
NOLC1
TTTTCTCCAAATTTTAAGACACAGCAGGATGCCAA (SEQ ID NO: 56)
PTEN (aa1-342)
NOLC1 (aa41-699)

FIG. 13A

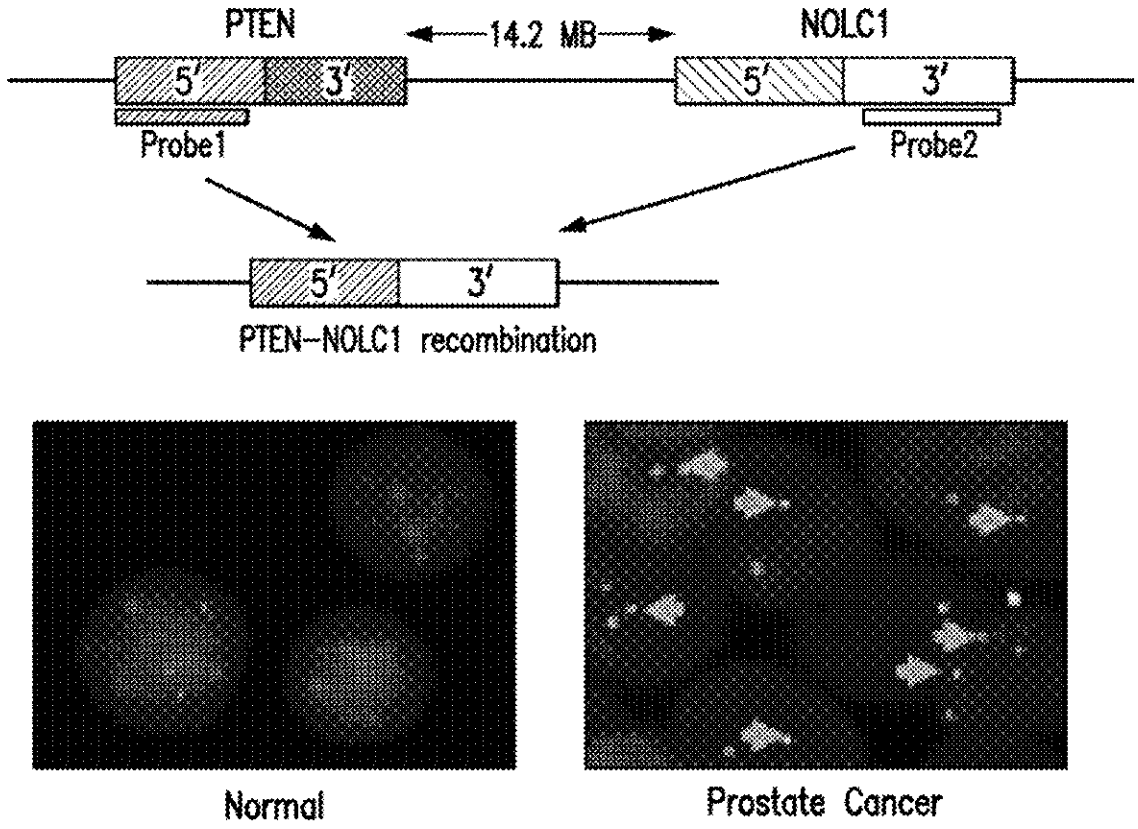
PTEN
14.2 MB
NOLC1
5′
3′
5′
3′
Probe1
Probe2
5′
3′
PTEN–NOLC1 recombination
Normal
Prostate Cancer

FIG. 13B

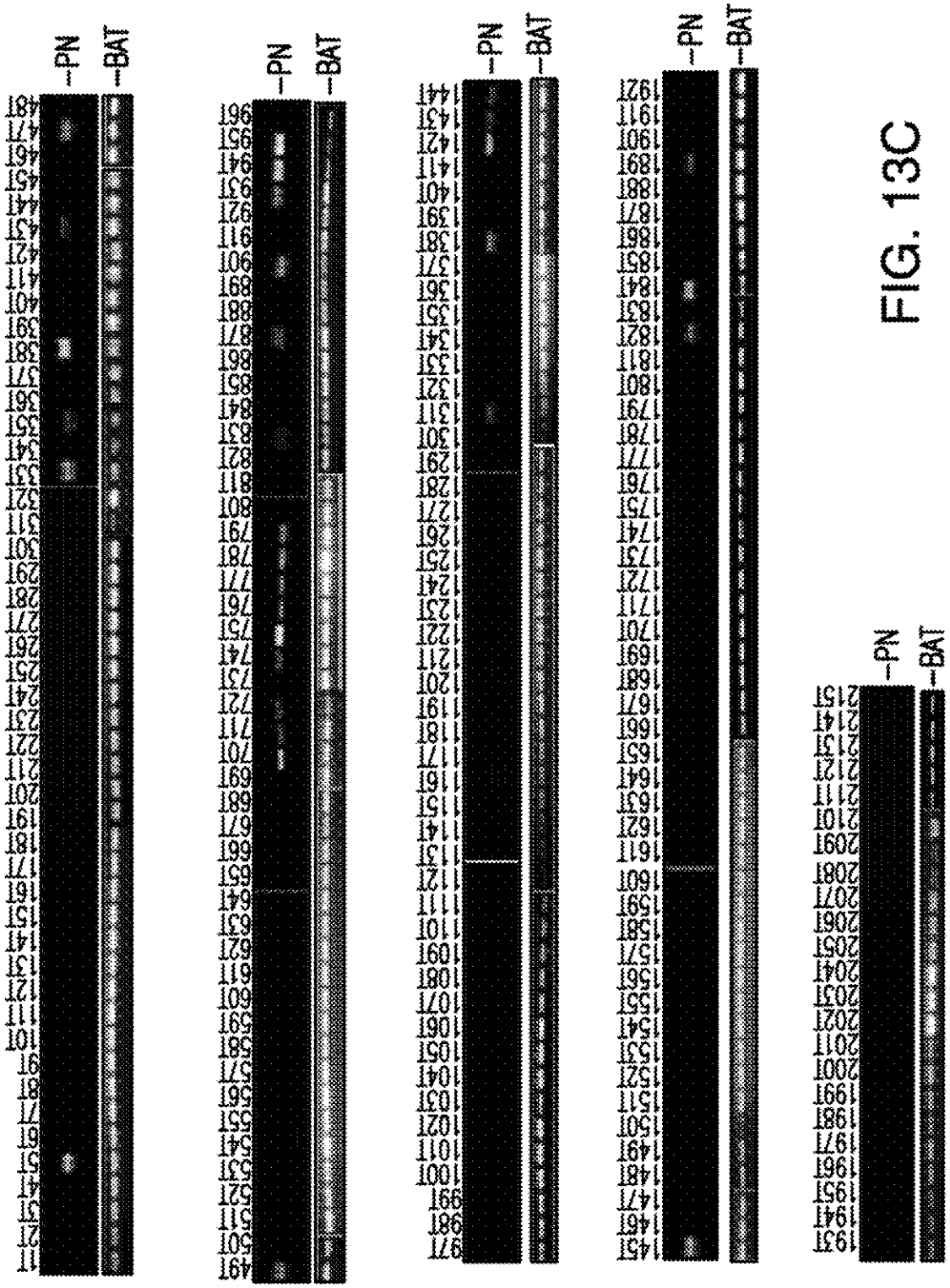

FIG. 13C

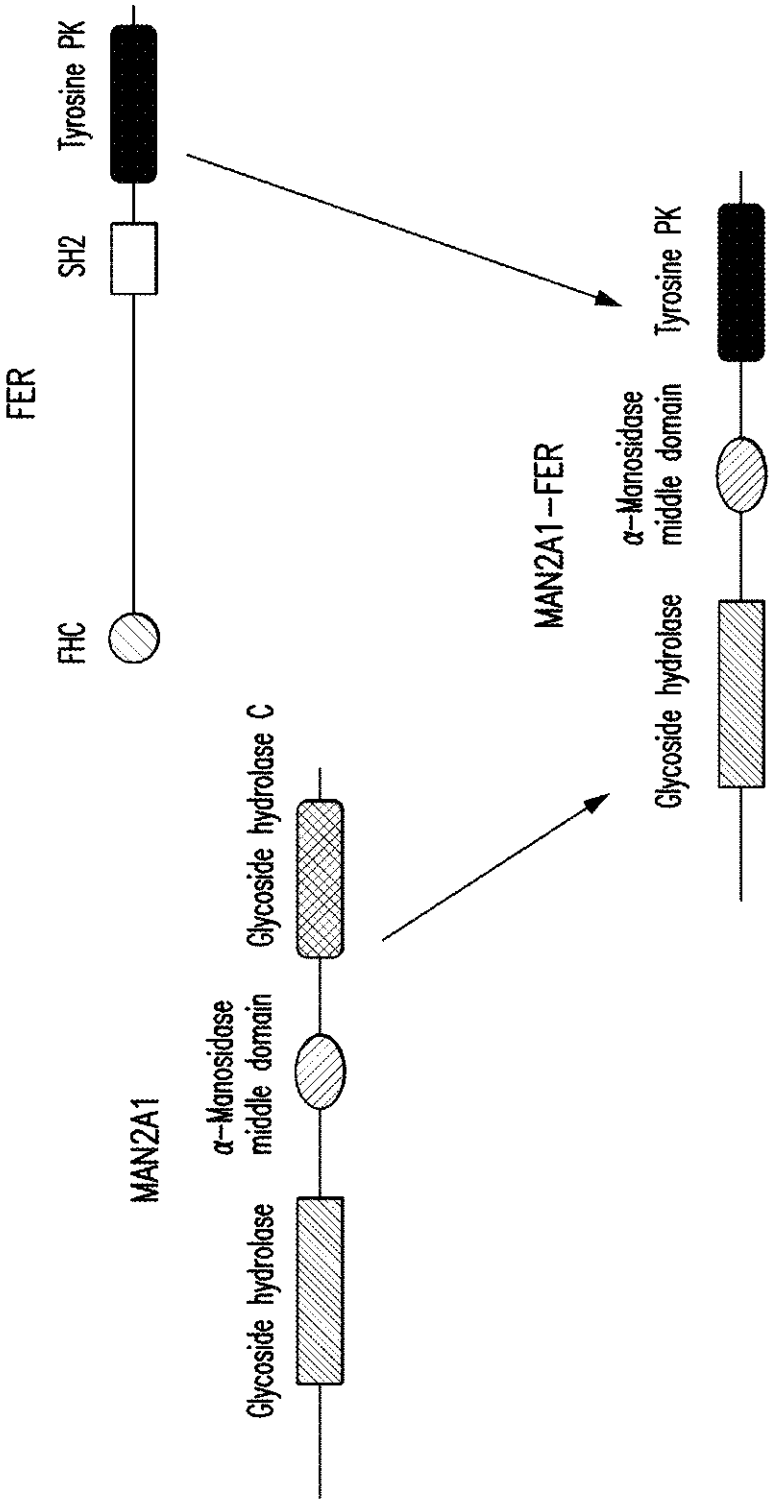
FER
FHC
SH2
Tyrosine PK
MAN2A1
Glycoside hydrolase
α-Manosidase middle domain
Glycoside hydrolase C
MAN2A1–FER
Glycoside hydrolase
α-Manosidase middle domain
Tyrosine PK

FIG. 14

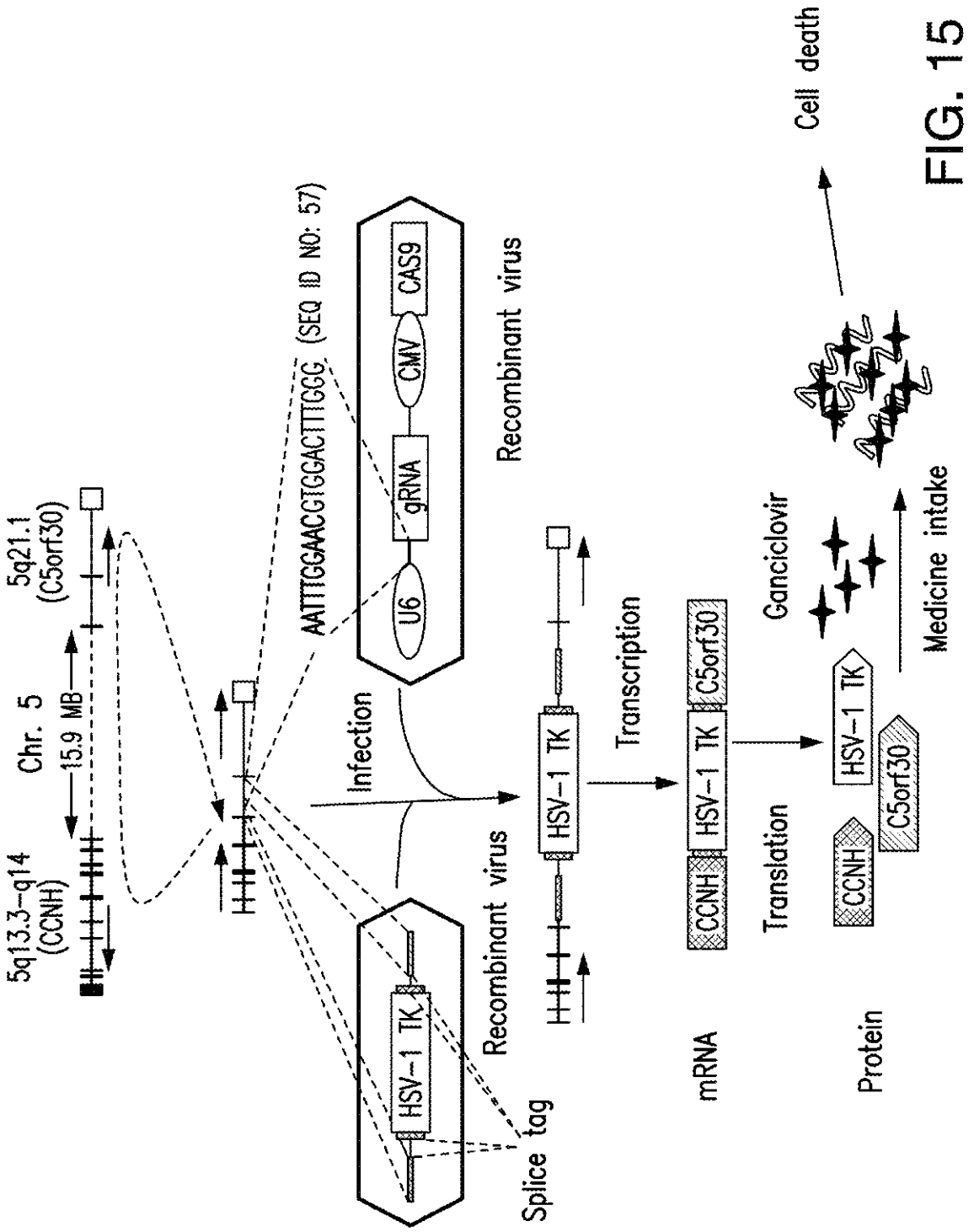
5q13.3–q14
(CCNH)
Chr. 5
15.9 MB
5q21.1
(C5orf30)
AATTTGGAACGTGGACTTTGGG (SEQ ID NO: 57)
U6
gRNA
CMV
CAS9
Recombinant virus
Infection
HSV–1 TK
Recombinant virus
Splice tag
HSV–1 TK
Transcription
CCNH
HSV–1 TK
C5orf30
mRNA
Translation
Ganciclovir
CCNH
HSV–1 TK
C5orf30
Protein
Medicine intake
Cell death

FIG. 15

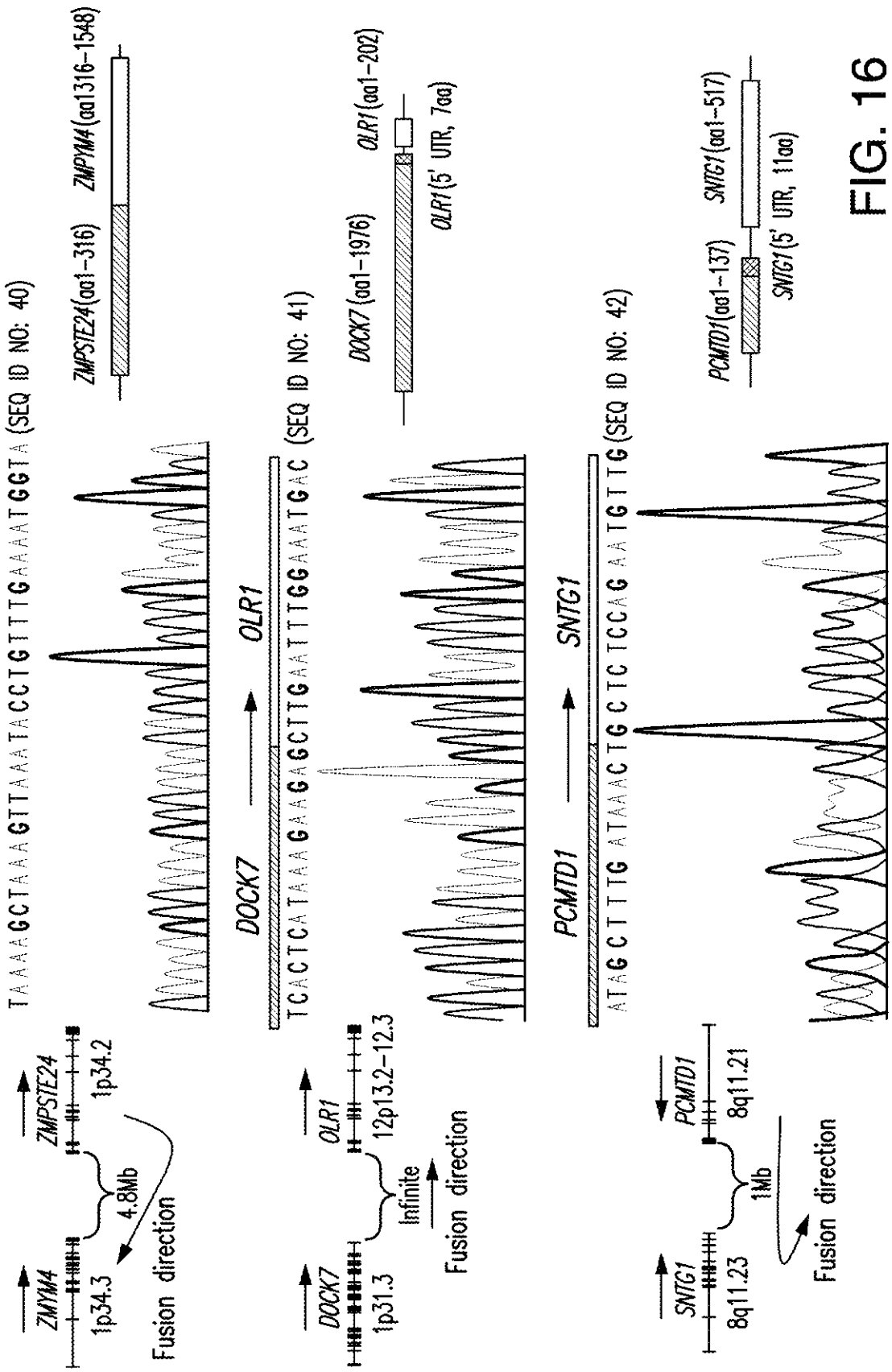
ZMPSTE24
ZMYM4
TAAAAGCTAAAGTTAAATACCTGTTTGAAAATGGTA (SEQ ID NO: 40)
ZMPSTE24(aa1-316)
ZMYM4(aa1316-1548)
ZMYM4
1p34.3
4.8Mb
ZMPSTE24
1p34.2
Fusion direction
DOCK7
OLR1
TCACTCATAAAGAAGAGCTTGAATTTGGAAATGAC (SEQ ID NO: 41)
DOCK7(aa1-1976)
OLR1(aa1-202)
OLR1(5' UTR, 7aa)
DOCK7
1p31.3
Infinite
OLR1
12p13.2-12.3
Fusion direction
PCMTD1
SNTG1
ATAGCTTTGATAAACTGCTCTCCAGAATGTTG (SEQ ID NO: 42)
PCMTD1(aa1-137)
SNTG1(aa1-517)
SNTG1(5' UTR, 11aa)
SNTG1
8q11.23
1Mb
PCMTD1
8q11.21
Fusion direction

FIG. 16

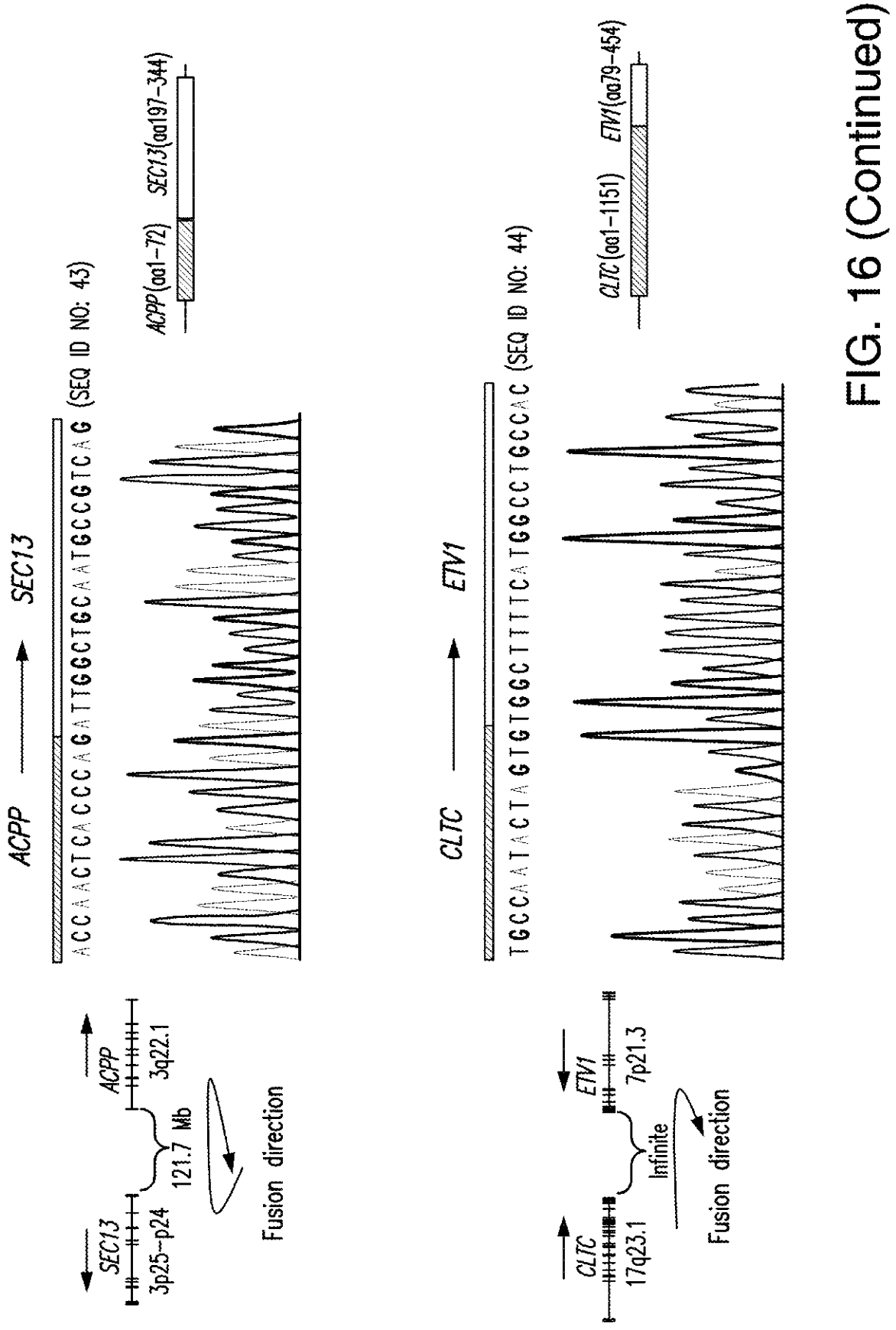

FIG. 16 (Continued)

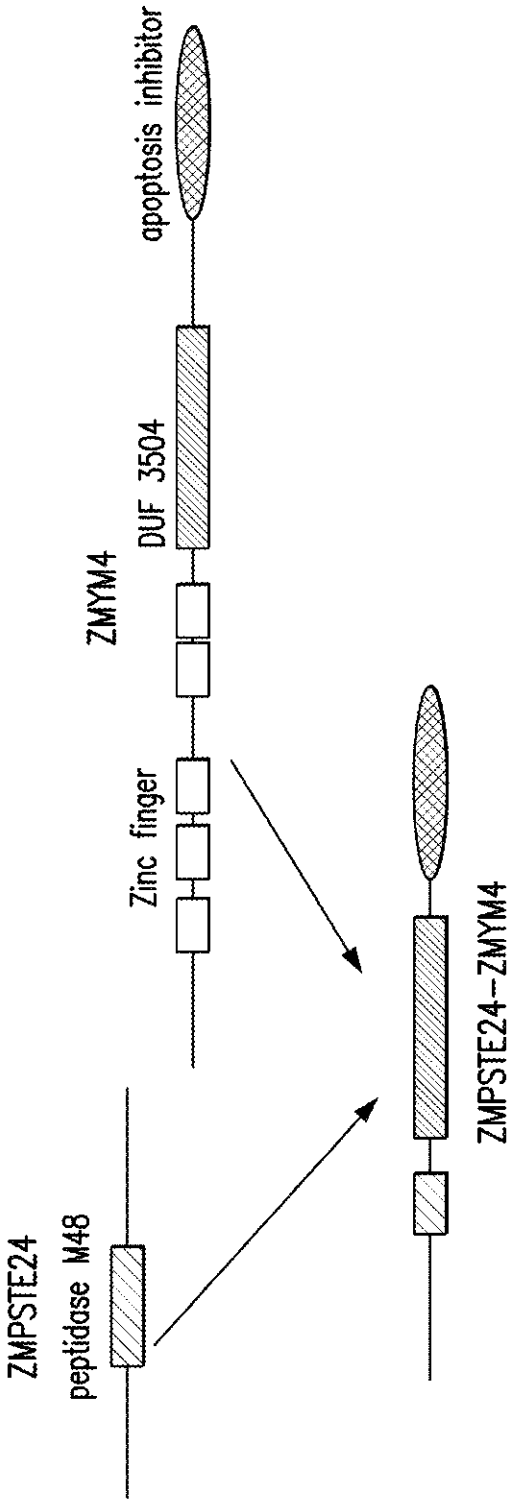
ZMPSTE24
peptidase M48
ZMYM4
Zinc finger
DUF 3504
apoptosis inhibitor
ZMPSTE24–ZMYM4

FIG. 17

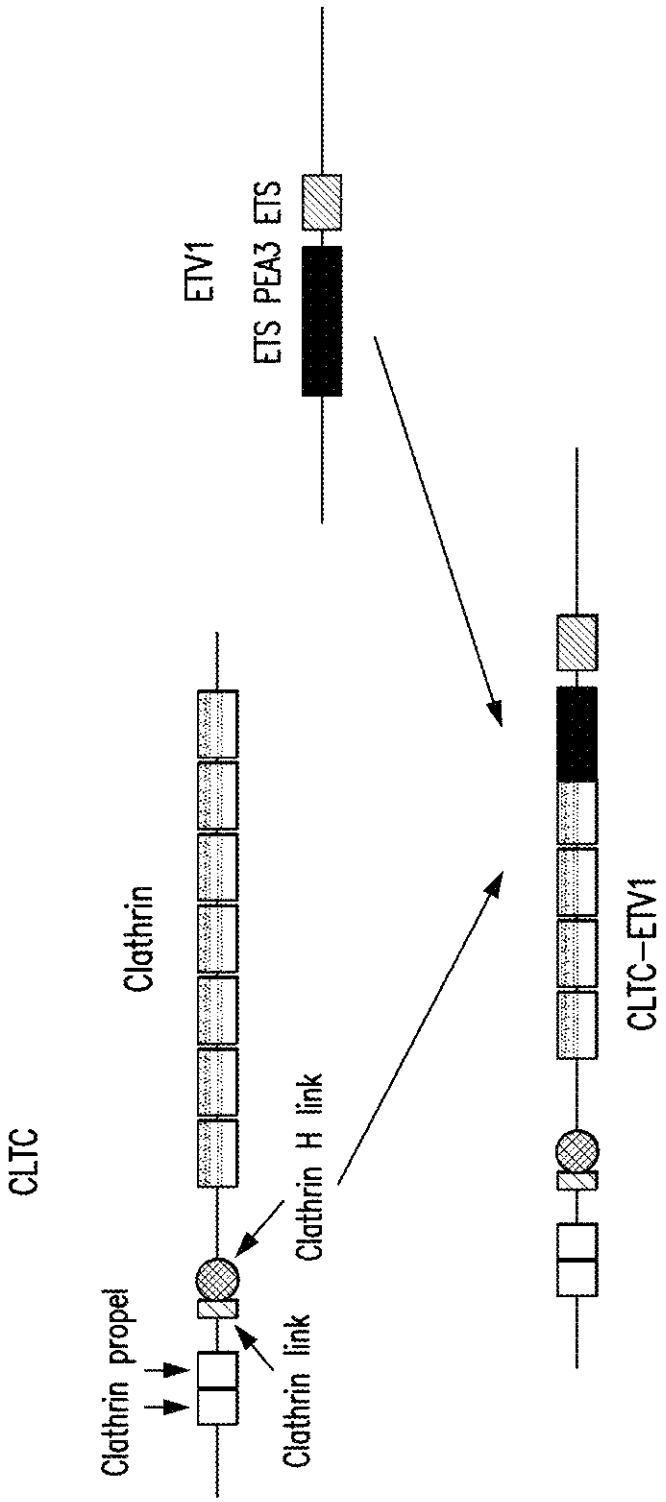
ETV1
ETS PEA3 ETS
CLTC
Clathrin
Clathrin H link
Clathrin propel
Clathrin link
CLTC-ETV1

FIG. 18

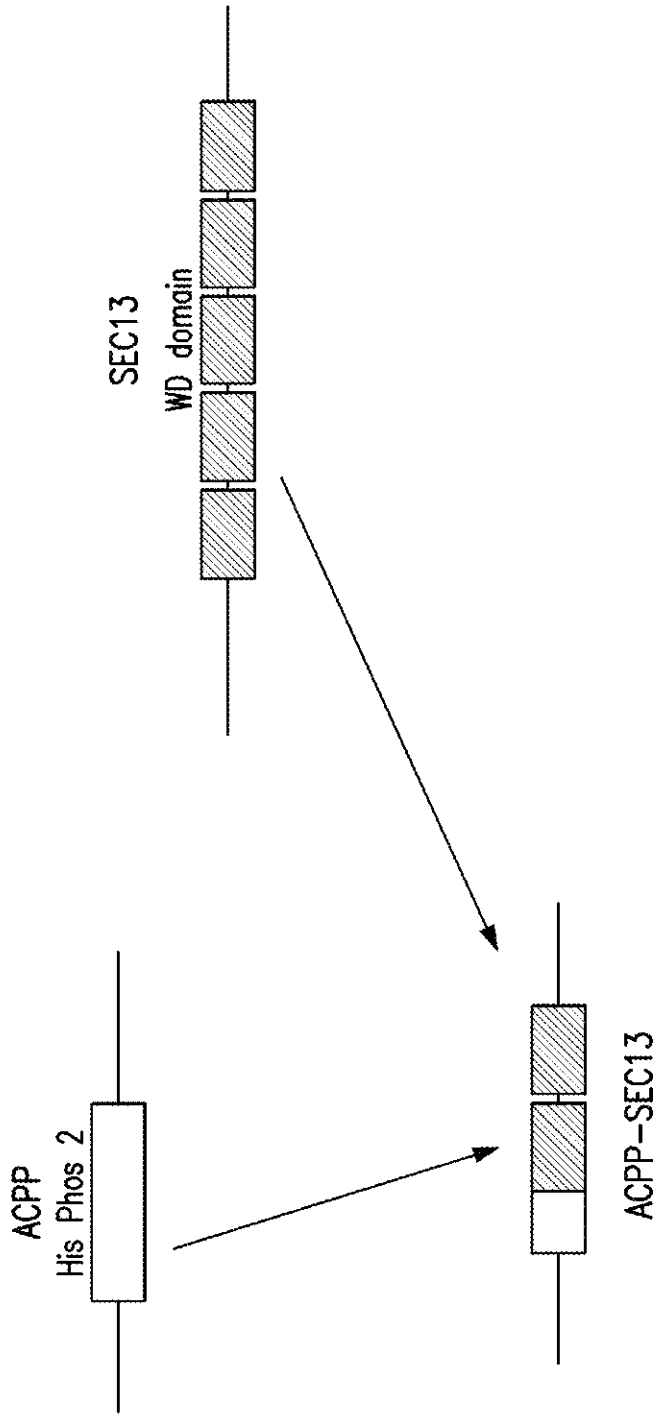

FIG. 19

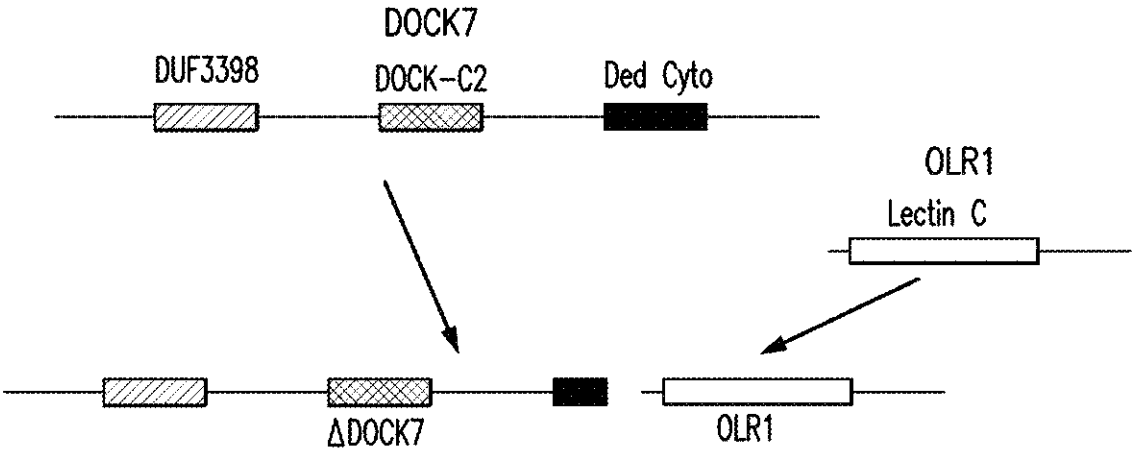
DOCK7
DUF3398
DOCK-C2
Ded Cyto
OLR1
Lectin C
ΔDOCK7
OLR1

FIG. 20

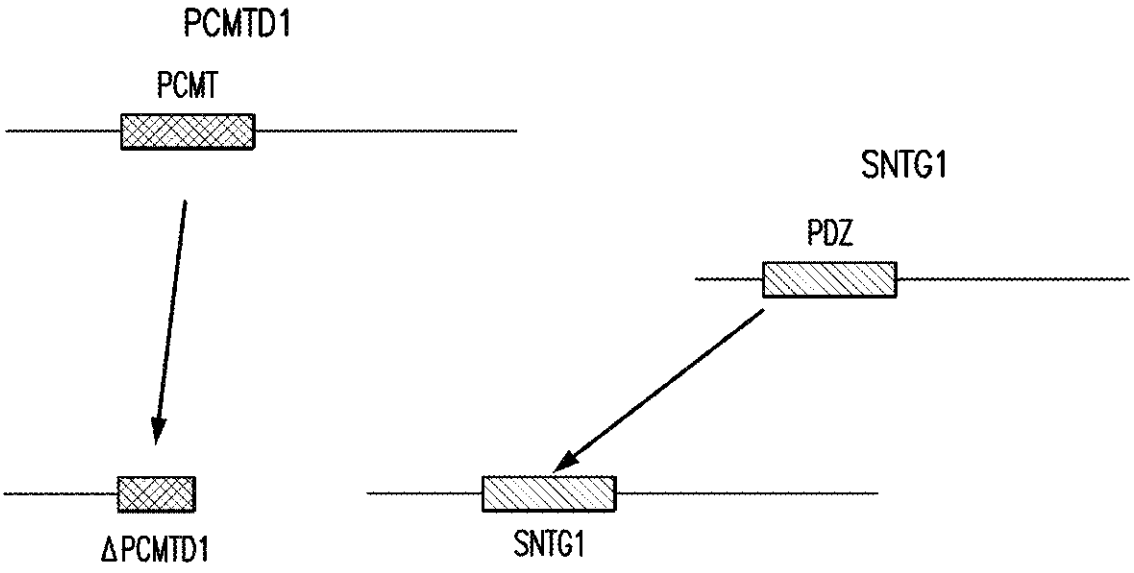
PCMTD1
PCMT
SNTG1
PDZ
ΔPCMTD1
SNTG1

FIG. 21

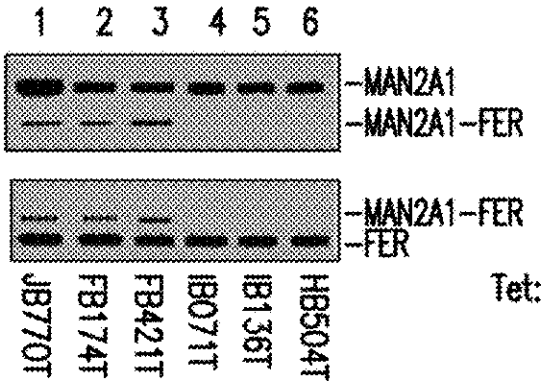

FIG. 22A

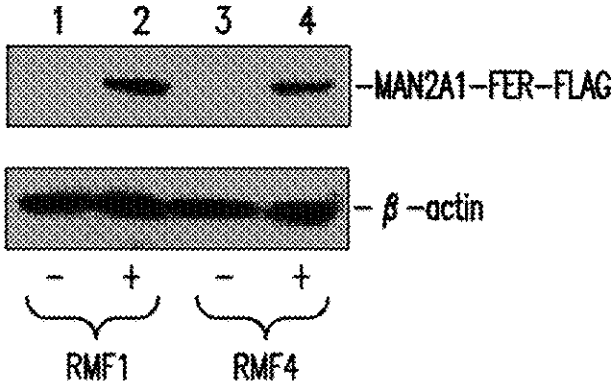

FIG. 22B

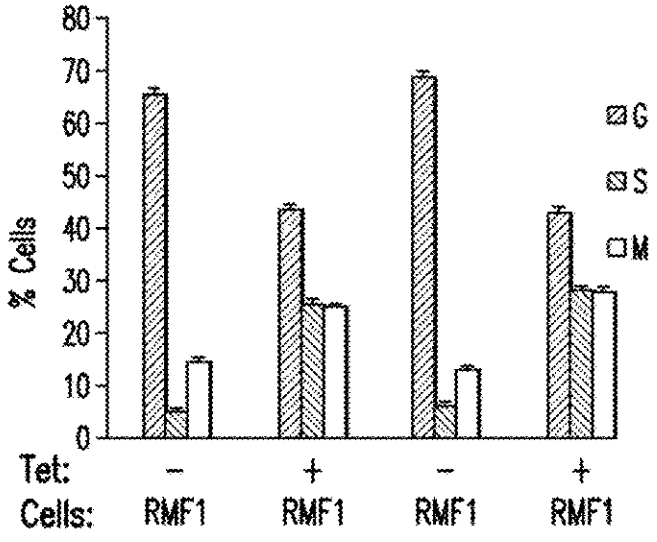

FIG. 22C

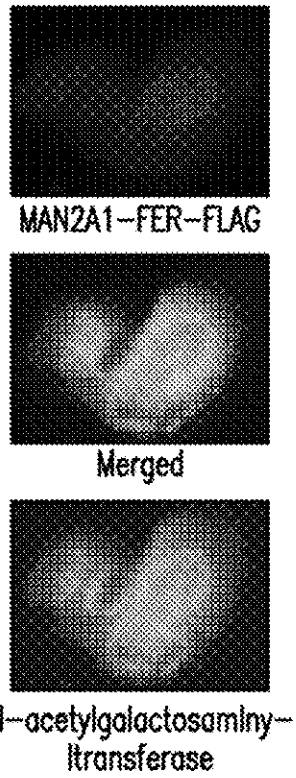

FIG. 22D

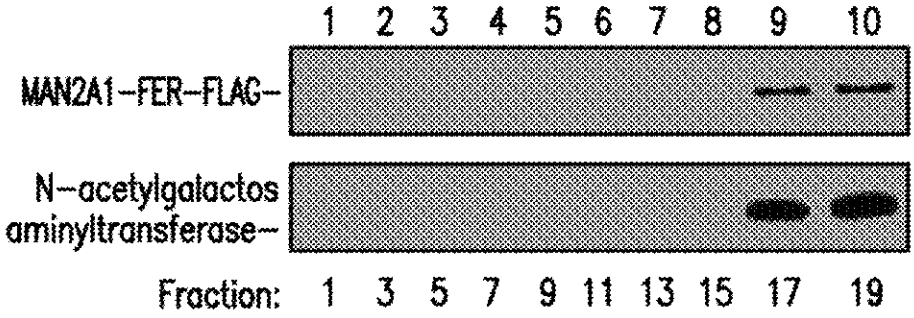

FIG. 22E

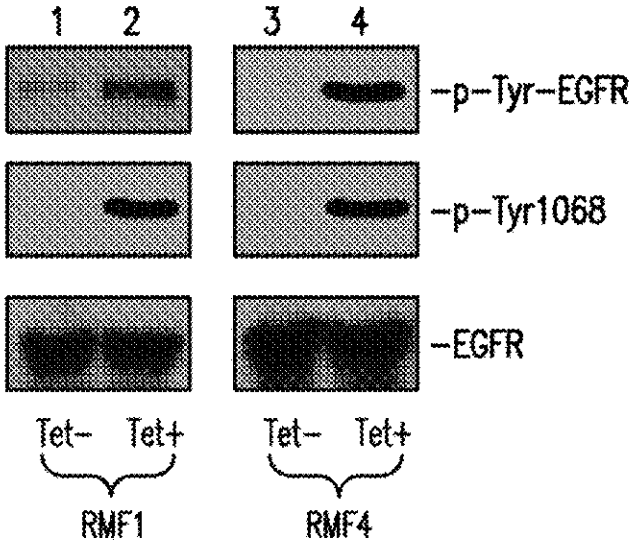

FIG. 22F

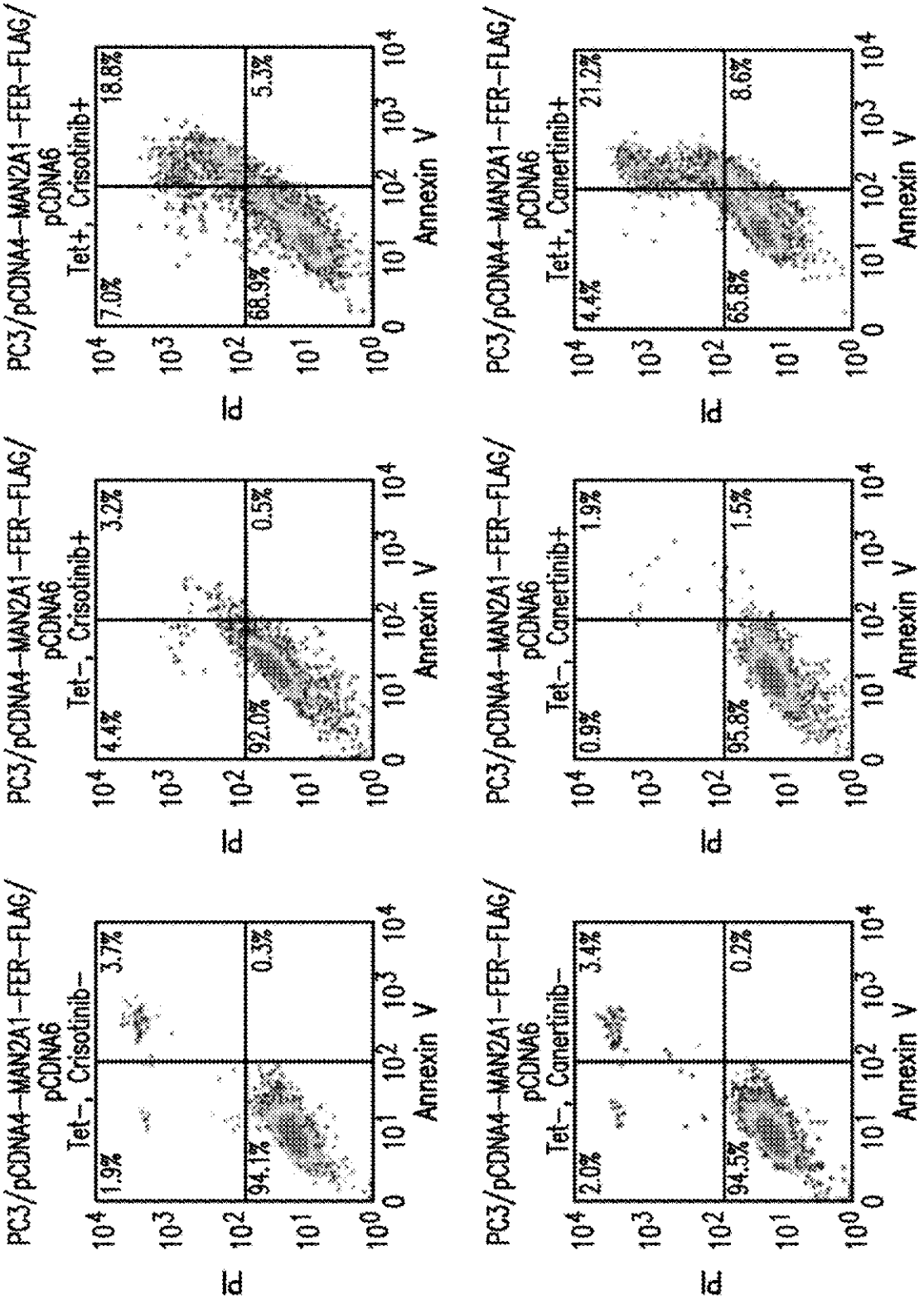
PC3/pCDNA4–MAN2A1–FER–FLAG/pCDNA6
Tet–, Crisotinib–
1.9%
3.7%
94.1%
0.3%
PC3/pCDNA4–MAN2A1–FER–FLAG/pCDNA6
Tet–, Crisotinib+
4.4%
3.2%
92.0%
0.5%
PC3/pCDNA4–MAN2A1–FER–FLAG/pCDNA6
Tet+, Crisotinib+
7.0%
18.8%
68.9%
5.3%
PC3/pCDNA4–MAN2A1–FER–FLAG/pCDNA6
Tet–, Canertinib–
2.0%
3.4%
94.5%
0.2%
PC3/pCDNA4–MAN2A1–FER–FLAG/pCDNA6
Tet–, Canertinib+
0.9%
1.9%
95.8%
1.5%
PC3/pCDNA4–MAN2A1–FER–FLAG/pCDNA6
Tet+, Canertinib+
4.4%
21.2%
65.8%
8.6%
PI
Annexin V

FIG. 23

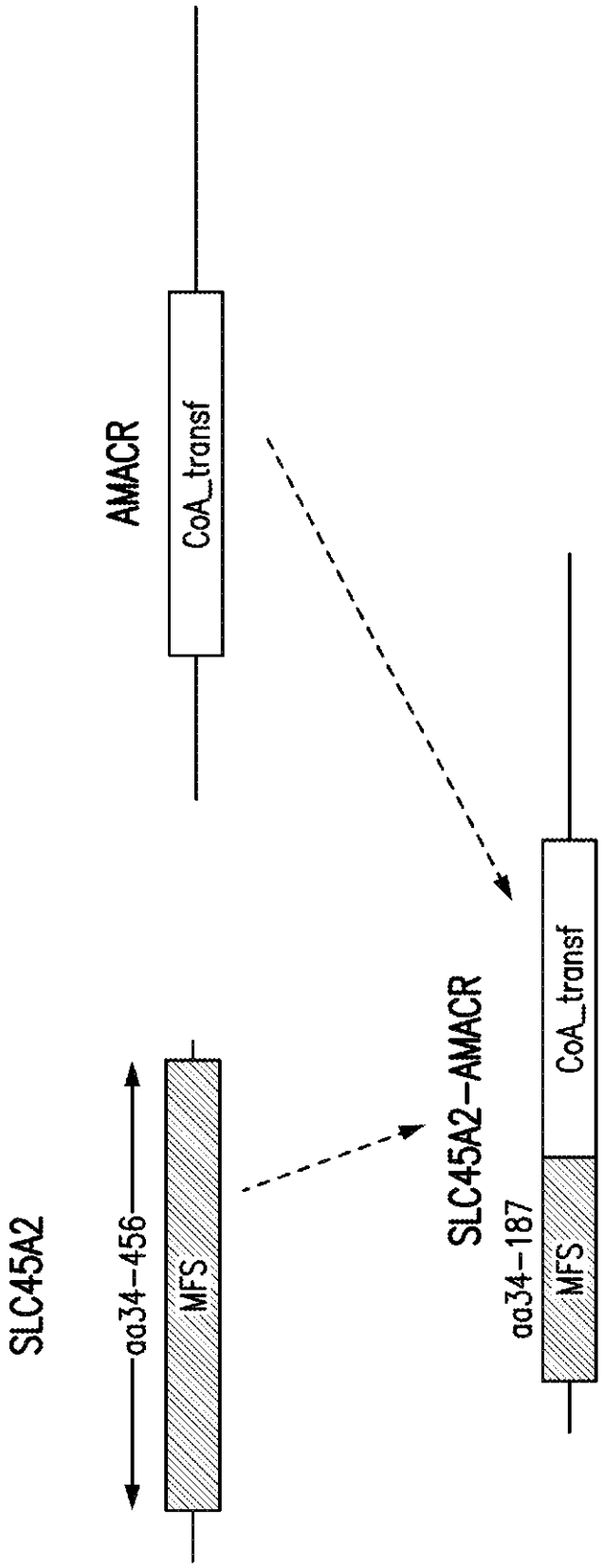
AMACR
CoA_transf
SLC45A2
aa34–456
MFS
SLC45A2–AMACR
CoA_transf
aa34–187
MFS

FIG. 24

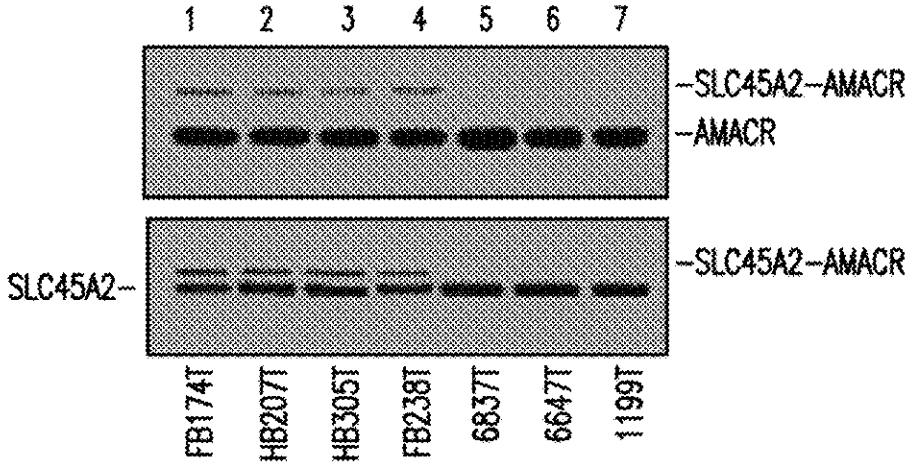

FIG. 25A

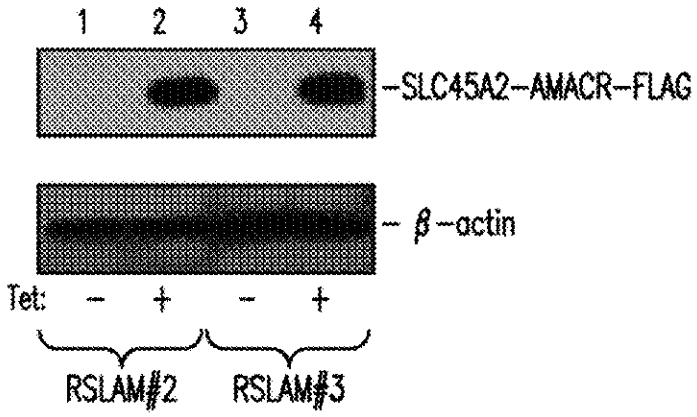

FIG. 25B

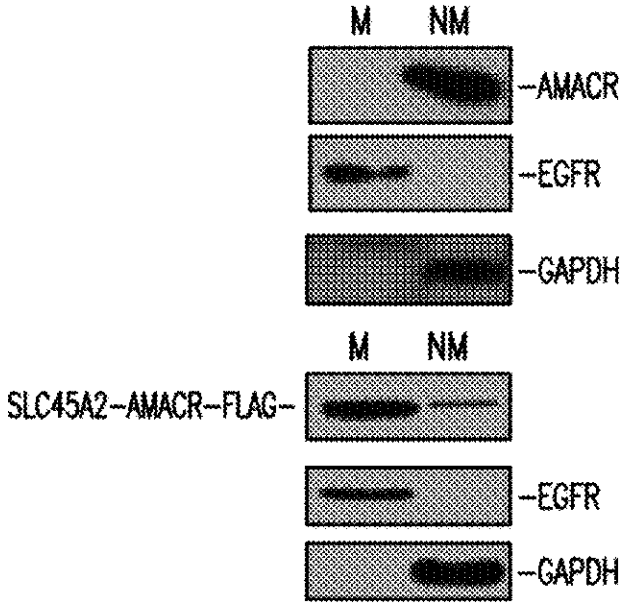

FIG. 25C

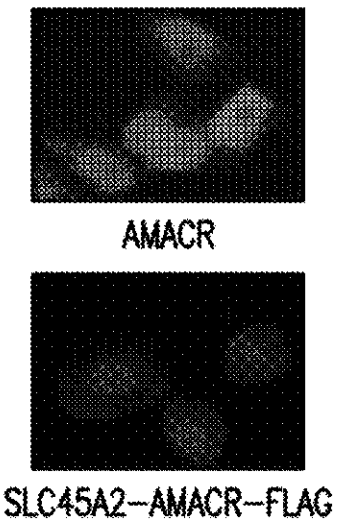

FIG. 25D

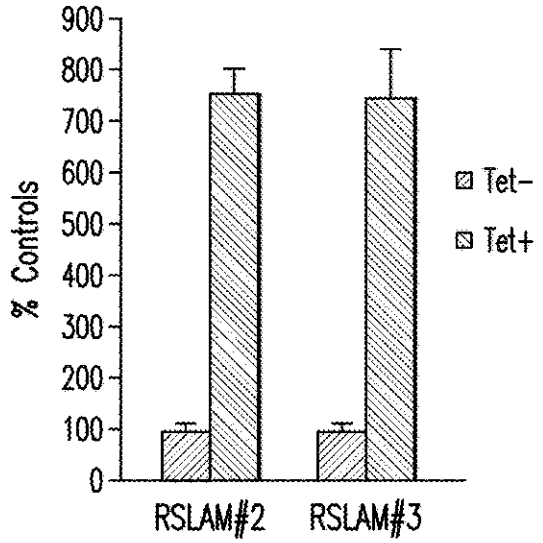

FIG. 25E

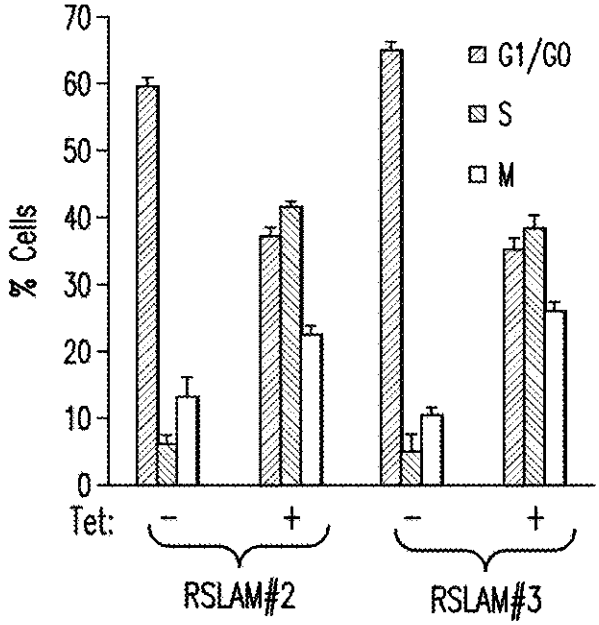

FIG. 25F

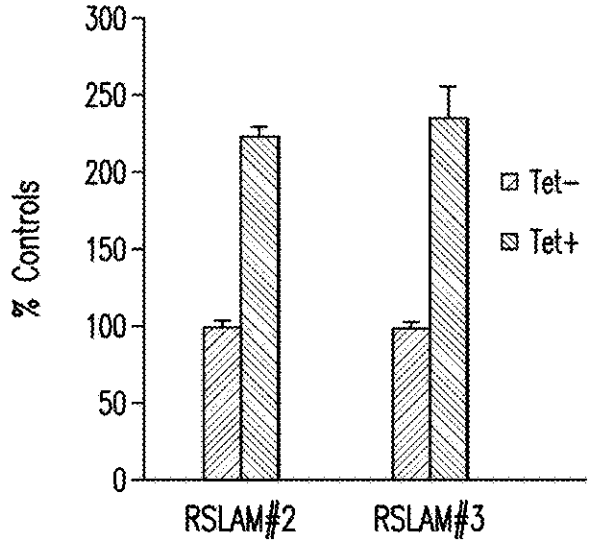

FIG. 25G

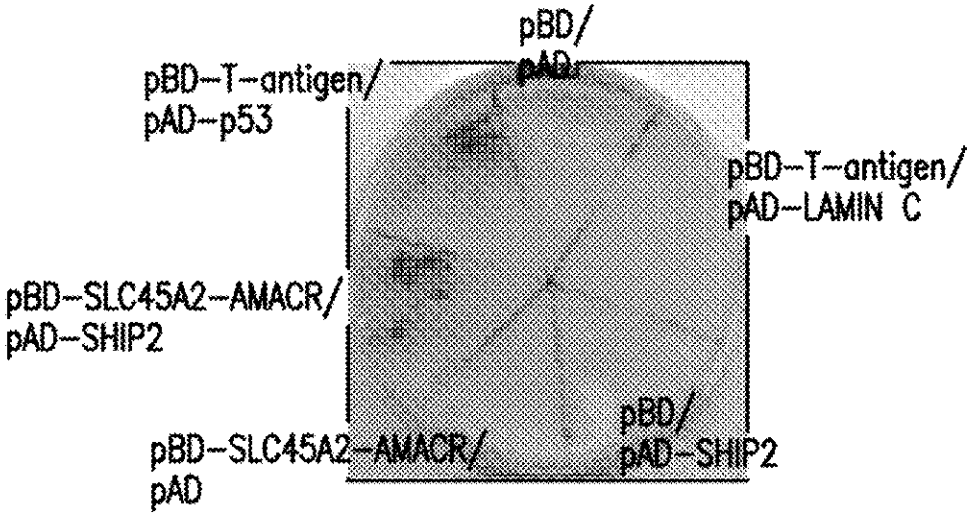

FIG. 25H

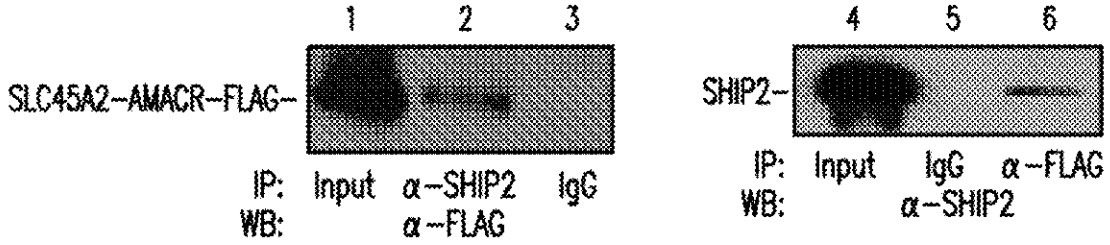

FIG. 25I

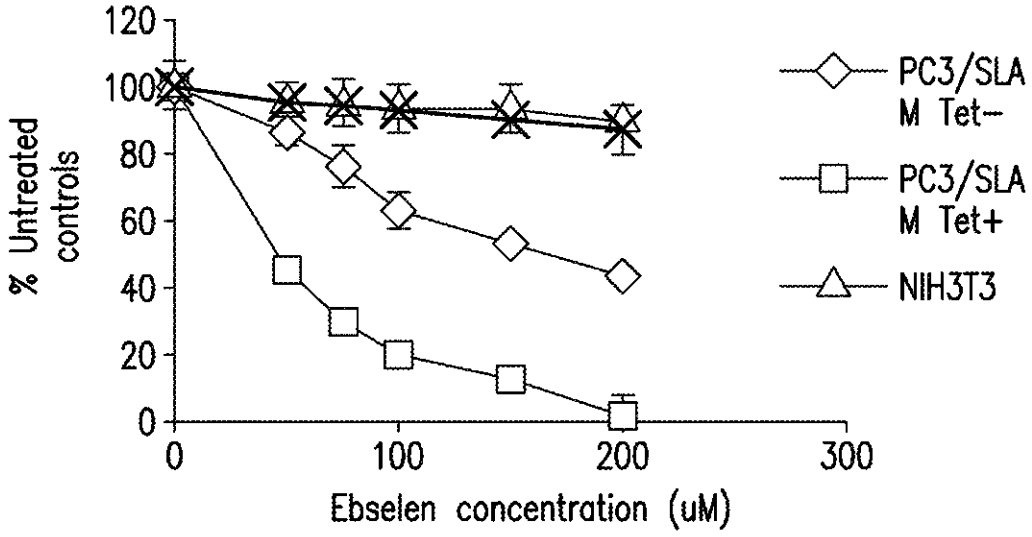
120
100
80
60
40
20
0
% Untreated controls
0
100
200
300
Ebselen concentration (uM)
PC3/SLA M Tet-
PC3/SLA M Tet+
NIH3T3

FIG. 26

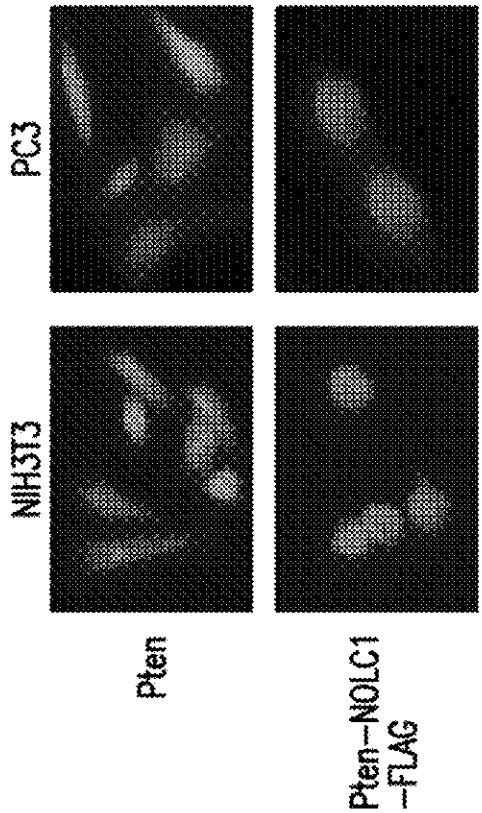

FIG. 27A

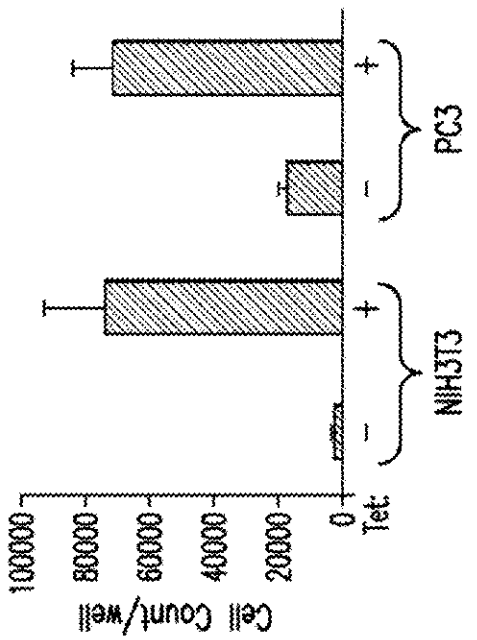

FIG. 27B

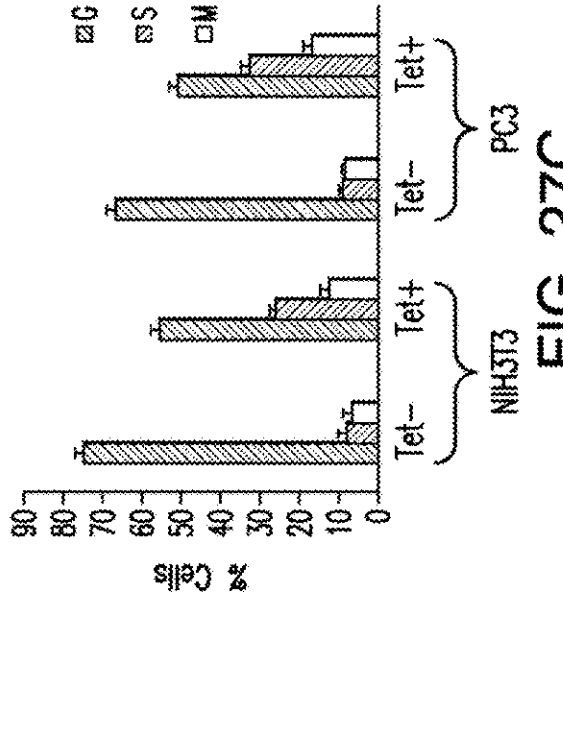

FIG. 27C

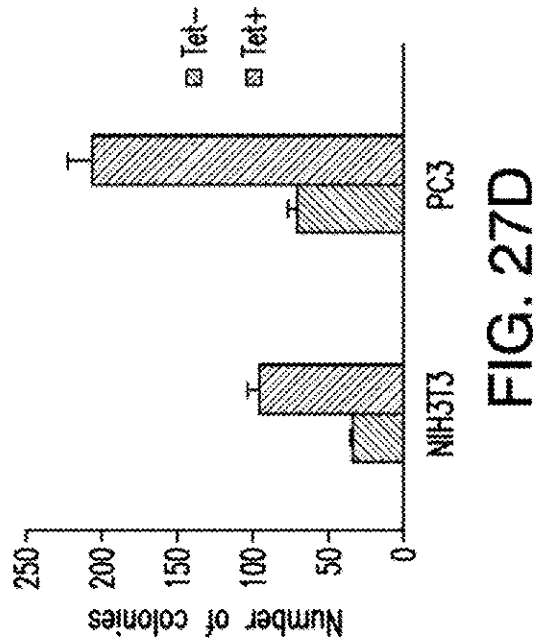

FIG. 27D

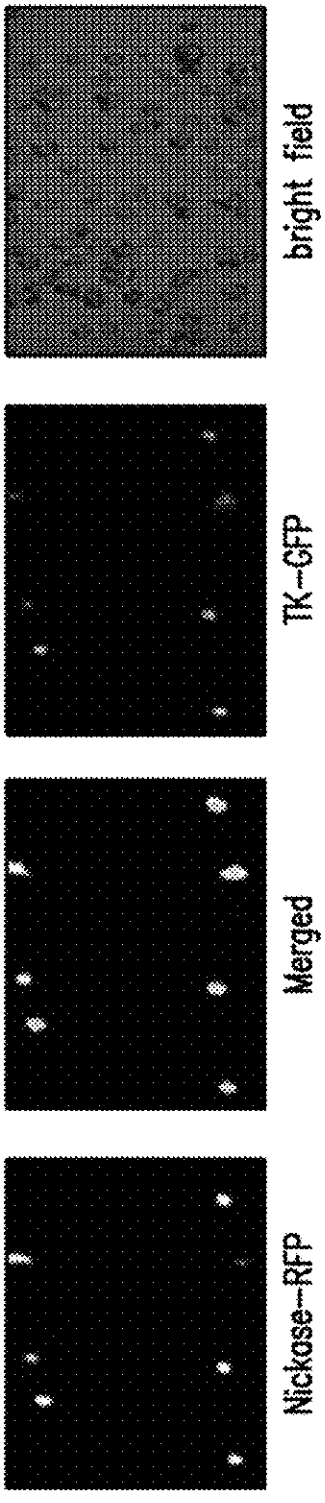

FIG. 28A

FIG. 28B

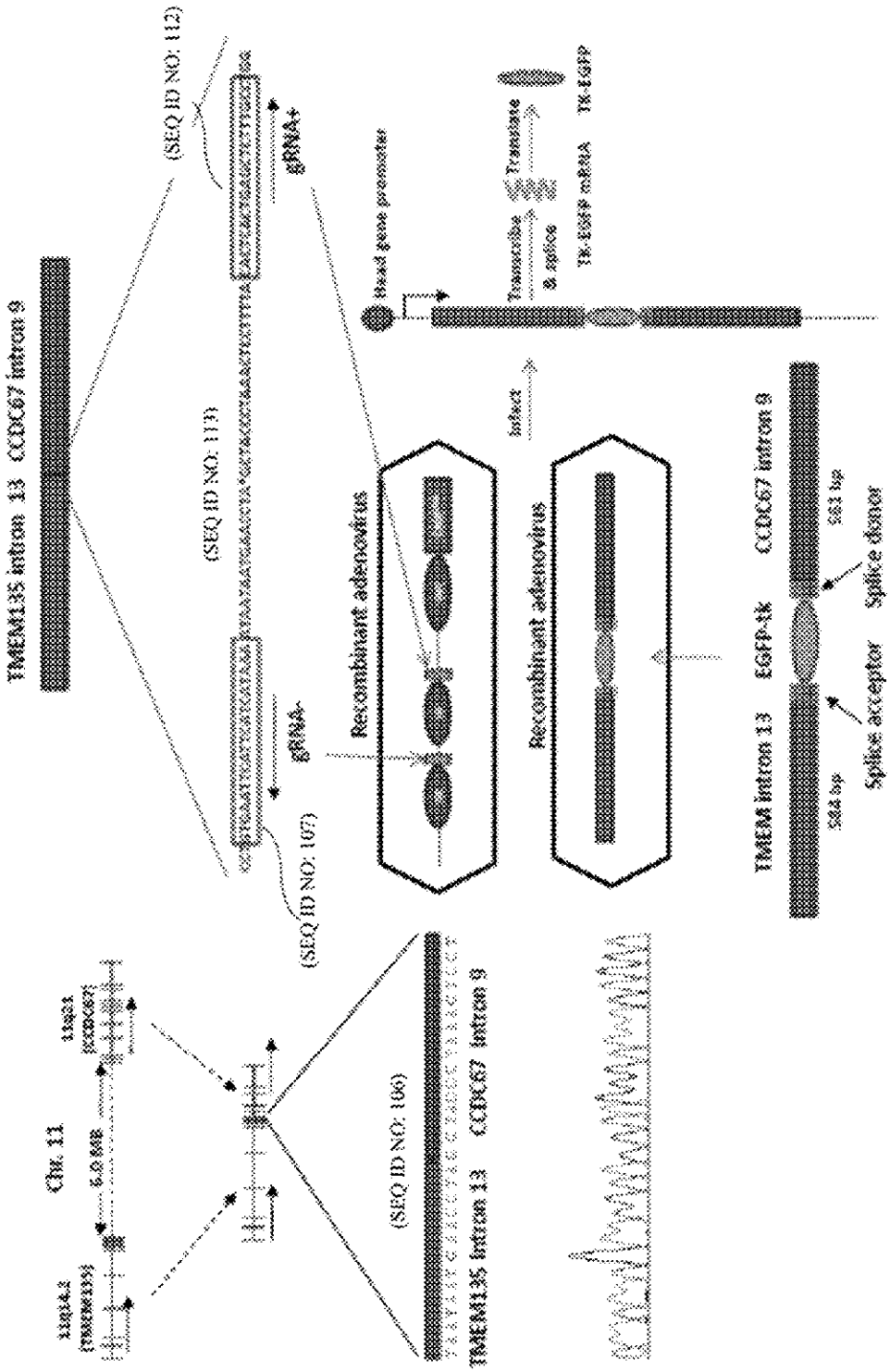

FIG. 29A

FIG. 29B

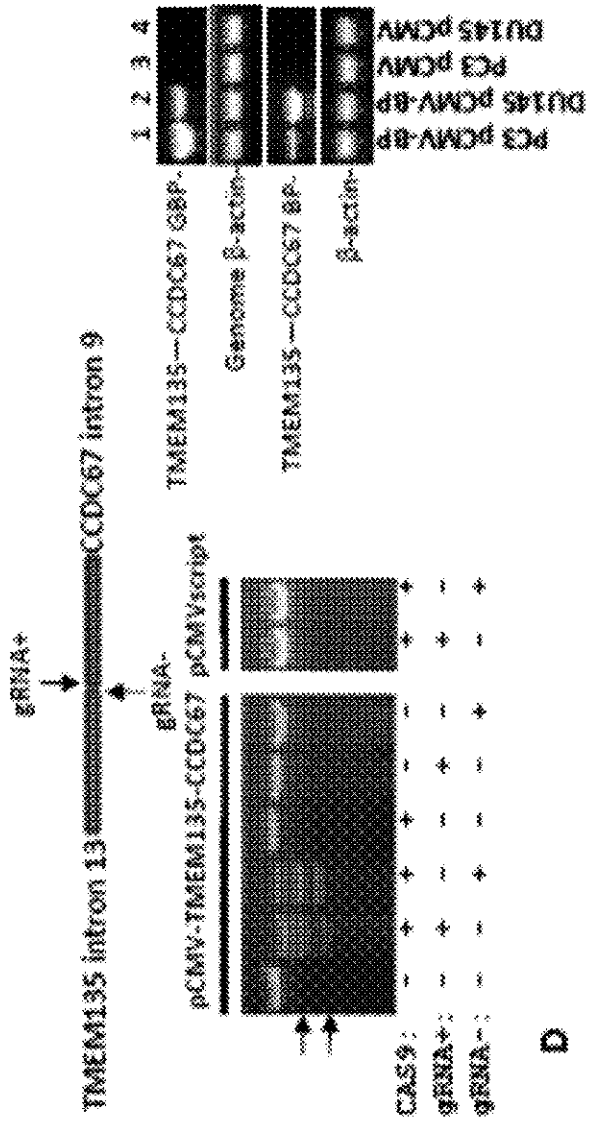

FIG. 30A

FIG. 30B

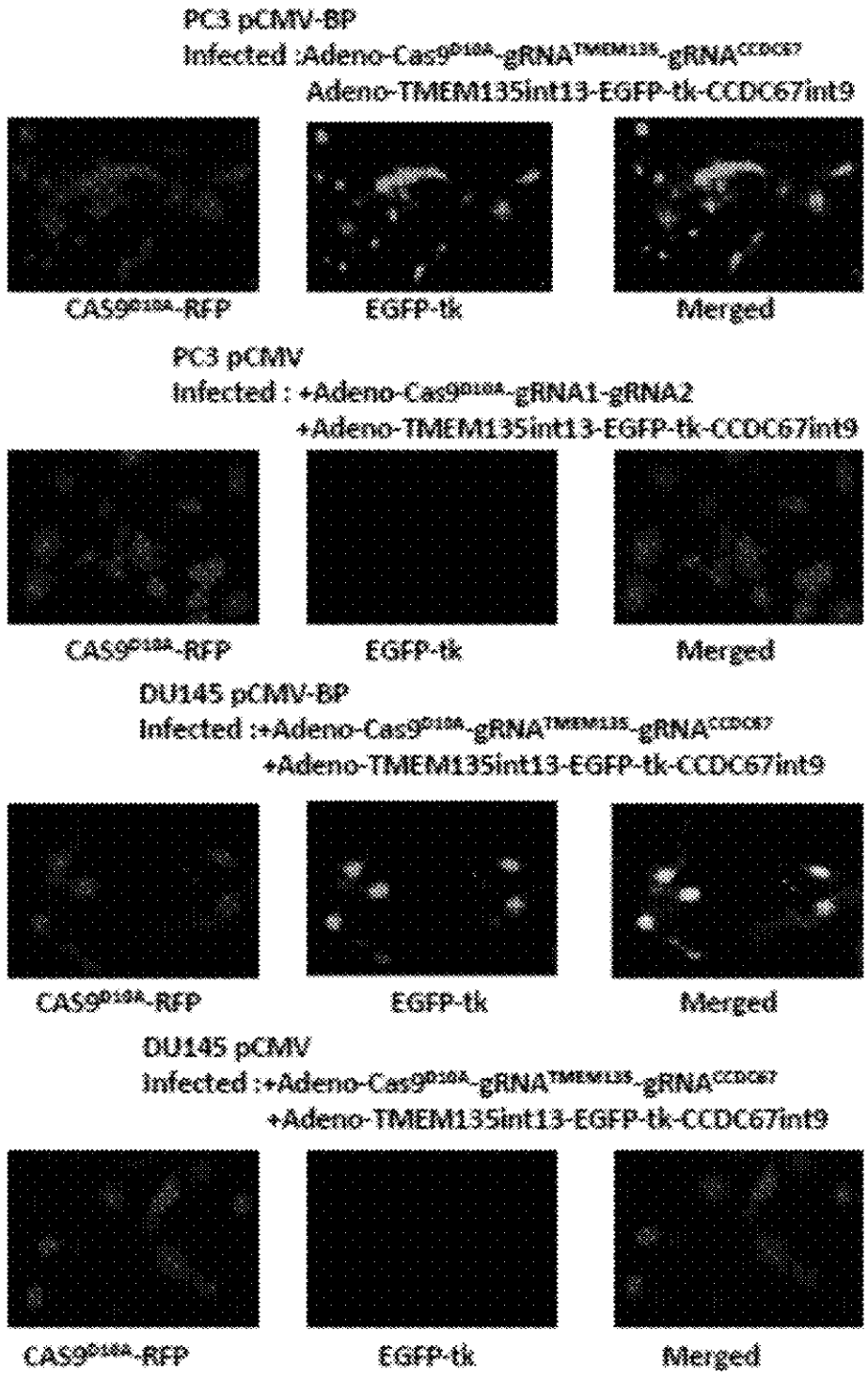
PC3 pCMV-BP
Infected :Adeno-Cas9^{D10A}-gRNA^{TMEM135}-gRNA^{CCDC67}
Adeno-TMEM135int13-EGFP-tk-CCDC67int9
CAS9^{D10A}-RFP
EGFP-tk
Merged
PC3 pCMV
Infected : +Adeno-Cas9^{D10A}-gRNA1-gRNA2
+Adeno-TMEM135int13-EGFP-tk-CCDC67int9
CAS9^{D10A}-RFP
EGFP-tk
Merged
DU145 pCMV-BP
Infected :+Adeno-Cas9^{D10A}-gRNA^{TMEM135}-gRNA^{CCDC67}
+Adeno-TMEM135int13-EGFP-tk-CCDC67int9
CAS9^{D10A}-RFP
EGFP-tk
Merged
DU145 pCMV
Infected :+Adeno-Cas9^{D10A}-gRNA^{TMEM135}-gRNA^{CCDC67}
+Adeno-TMEM135int13-EGFP-tk-CCDC67int9
CAS9^{D10A}-RFP
EGFP-tk
Merged

FIG. 30C

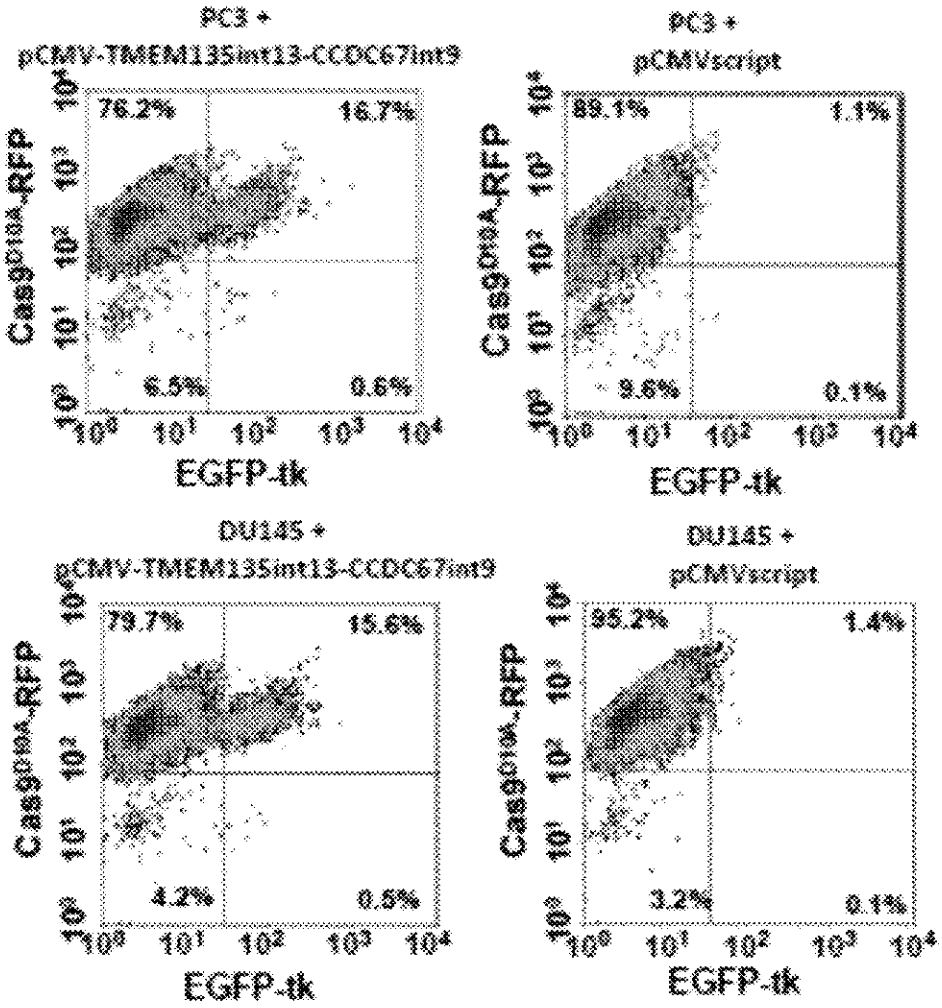
PC3 +
pCMV-TMEM135int13-CCDC67int9
76.2%
16.7%
6.5%
0.6%
Cas9D10A-RFP
EGFP-tk
PC3 +
pCMVscript
89.1%
1.1%
9.6%
0.1%
Cas9D10A-RFP
EGFP-tk
DU145 +
pCMV-TMEM135int13-CCDC67int9
79.7%
15.6%
4.2%
0.5%
Cas9D10A-RFP
EGFP-tk
DU145 +
pCMVscript
95.2%
1.4%
3.2%
0.1%
Cas9D10A-RFP
EGFP-tk

FIG. 30D

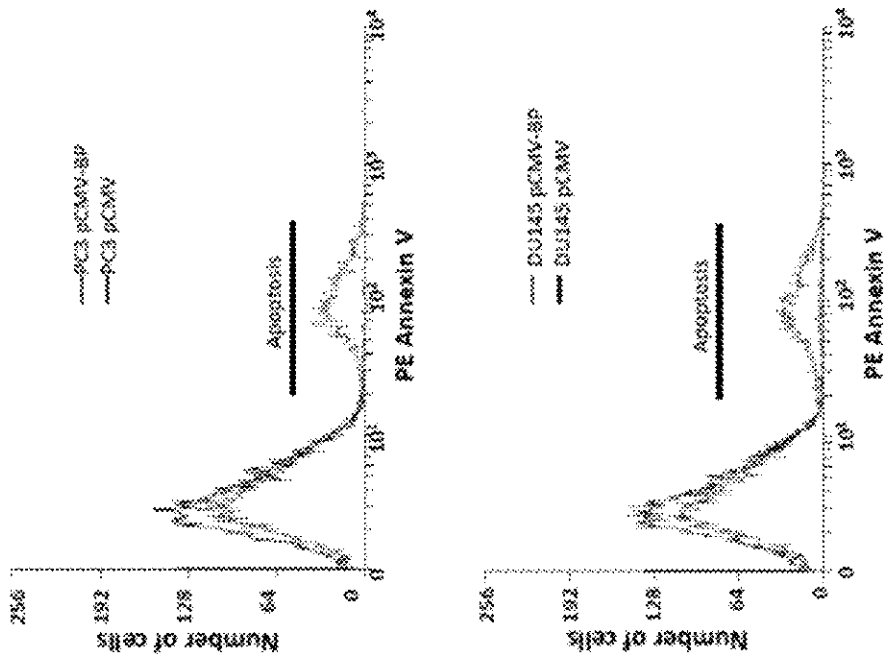

FIG. 31B

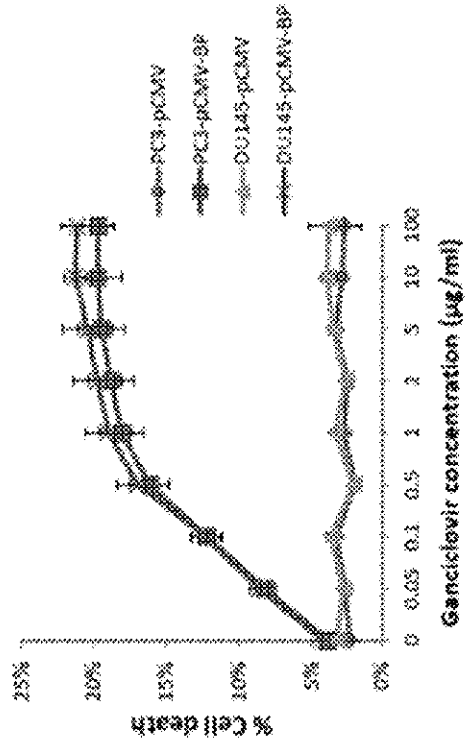

FIG. 31A

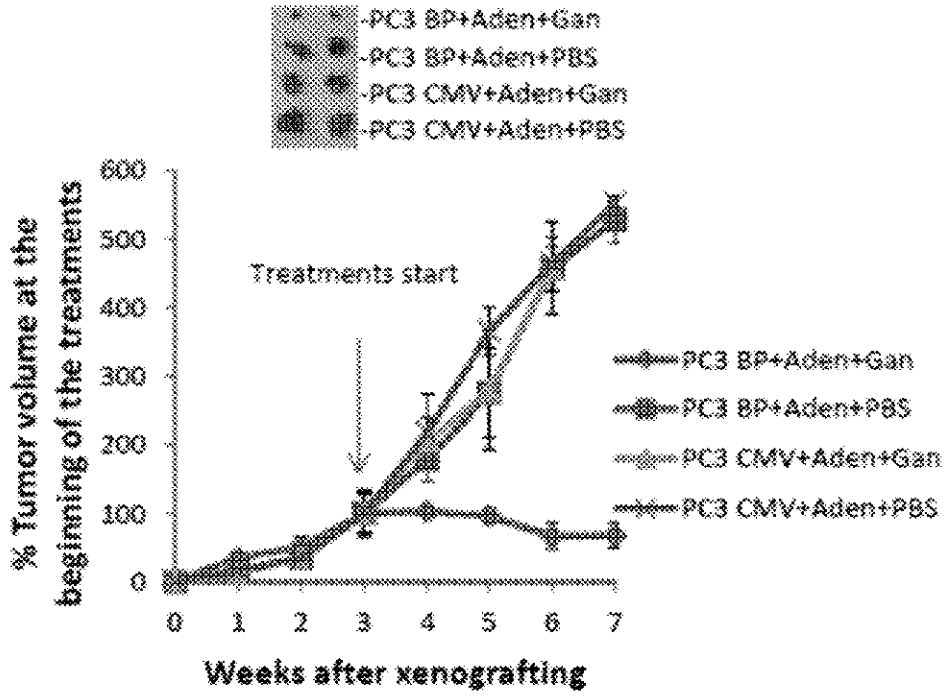

FIG. 32A

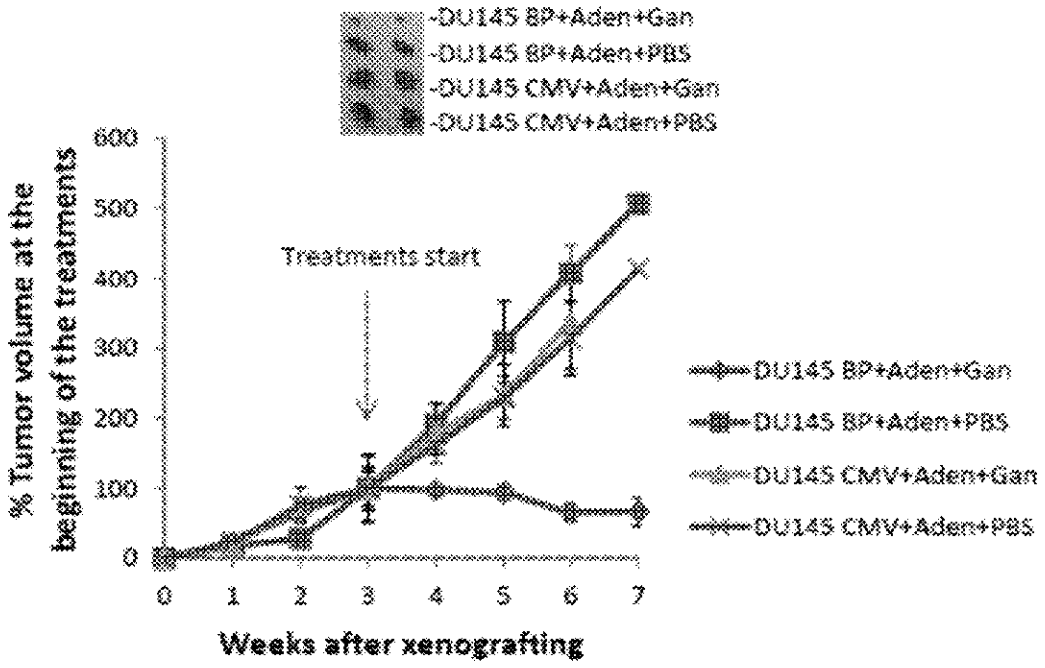

FIG. 32B

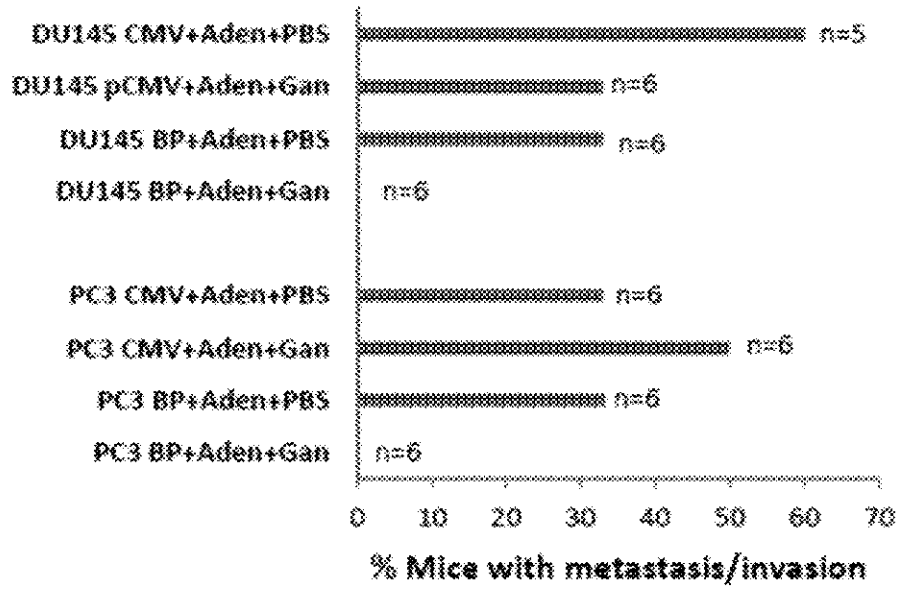

FIG. 32C

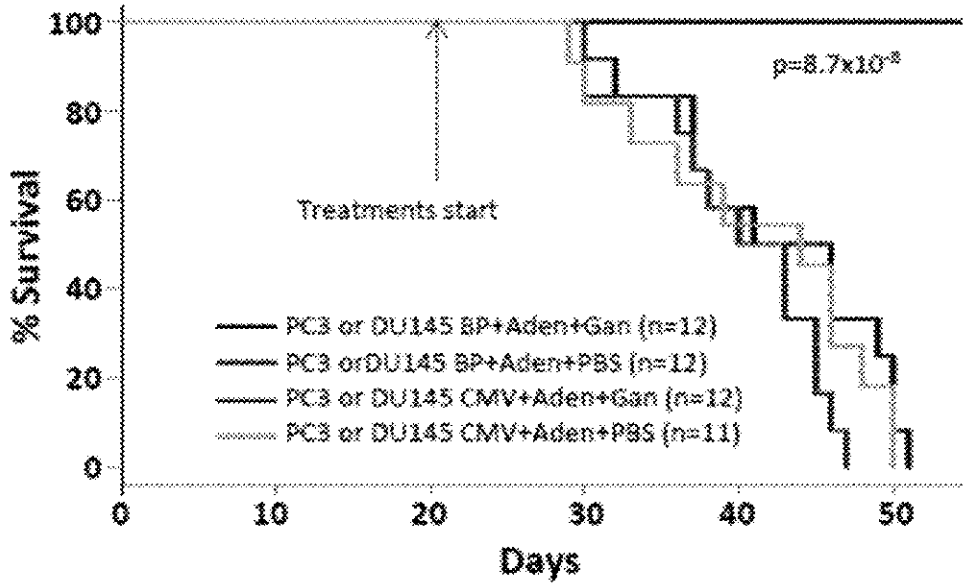

FIG. 32D

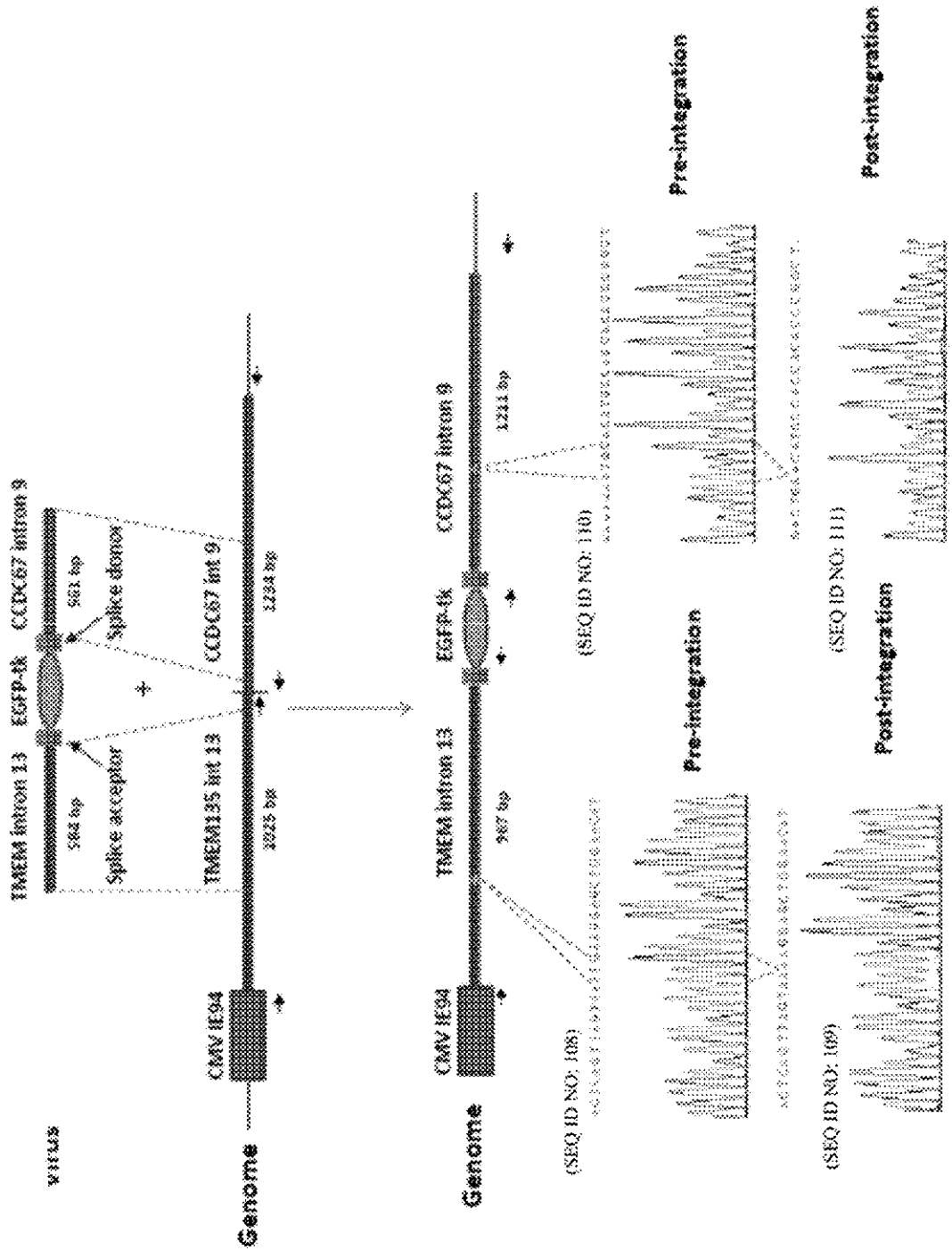
Virus
Genome
CMV IE94
TMEM135 int 13
CCDC67 int 9
Splice acceptor
Splice donor
EGFP-tk
TMEM intron 13
CCDC67 intron 9
Pre-integration
Post-integration
(SEQ ID NO: 108)
(SEQ ID NO: 109)
(SEQ ID NO: 110)
(SEQ ID NO: 111)

FIG. 33A

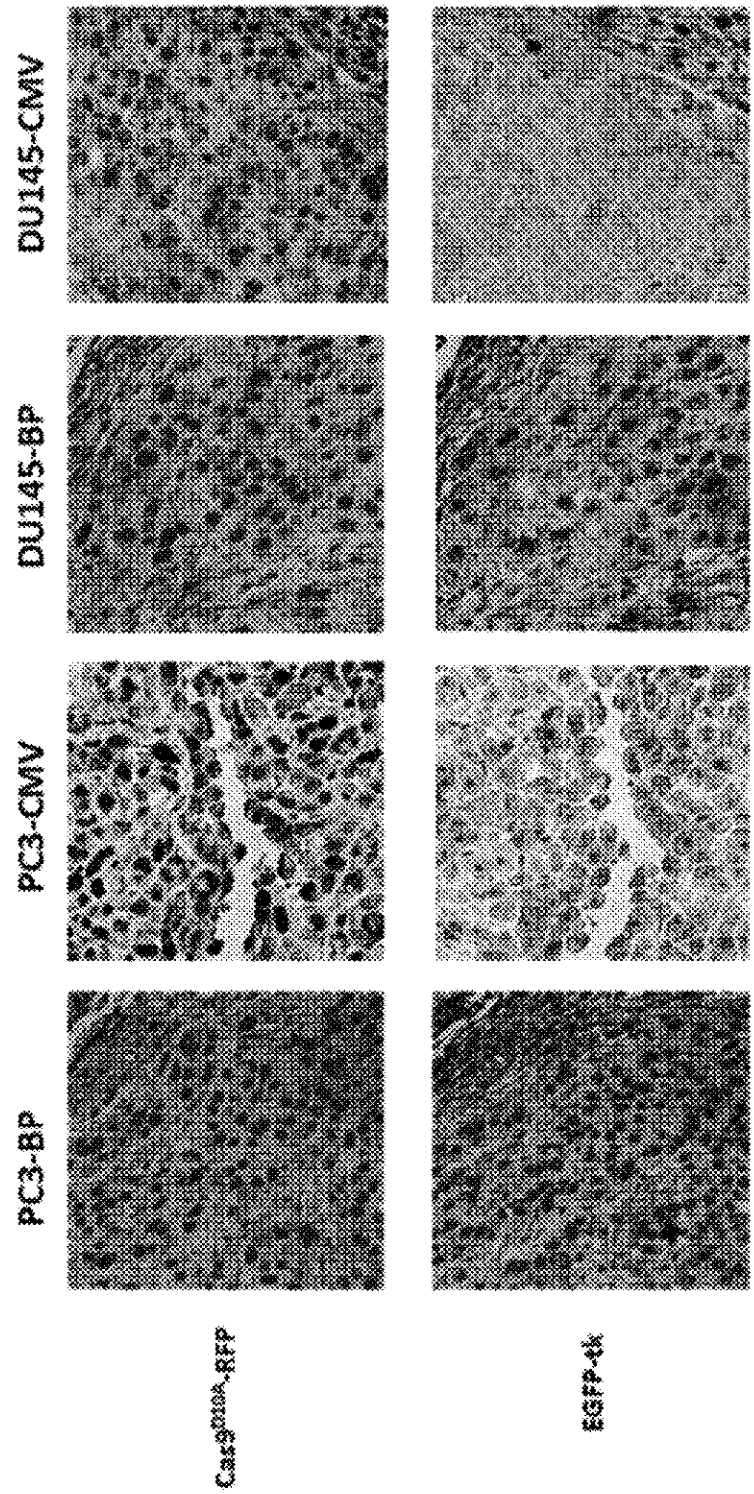

FIG. 33B

METHODS FOR TREATING CELLS CONTAINING FUSION GENES

PRIORITY CLAIM

This application is a divisional of U.S. patent application Ser. No. 15/406,472, filed Jan. 13, 2017, which is a continuation of International Application No. PCT/US2015/041029, filed Jul. 17, 2015, which claims priority to U.S. Provisional Patent Application Ser. No. 62/025,923, filed Jul. 17, 2014, and International Patent Application No. PCT/US2014/072268, filed Dec. 23, 2014, to each of which priority is claimed and the contents of which are incorporated by reference herein in their entireties.

GRANT INFORMATION

This invention was made with government support under Grant No. RO1 CA098249 and awarded by the National Cancer Institute of the National Institutes of Health. The government has certain rights in the invention.

SEQUENCE LISTING

The instant application contains a Sequence Listing which has been submitted electronically in ASCII format and is hereby incorporated by reference in its entirety. Said ASCII copy, created on Mar. 15, 2019, is named 072396_0753_SL.txt and is 27,292 bytes in size.

1. INTRODUCTION

The present invention relates to methods of treating prostate cancer patients carrying one or more specific fusion genes by performing genome targeting.

2. BACKGROUND OF THE INVENTION

Clustered regularly interspaced short palindromic repeats (CRISPR)/CRISPR-associated (Cas) were originally discovered to act as immunity defense mechanisms against foreign pathogens in prokaryotic cells (Mojica et al. (2005) J. of Molecular Evolution 60:174-182). Cas9, a protein for the type II CRISPR/Cas system, was found to exhibit DNA cleavage activity. The nuclease activity of Cas9 can be guided by a CRISPR RNA and a trans-activating CRISPR RNA complementary to a targeted sequence of DNA in the genome (Jinek et al. (2012) Science 337:816-821). Since trans-activating CRISPR RNA and CRISPR RNA can be made into a chimeric RNA containing the full function of both RNA species, artificial fusion RNA sequences, also called guide RNAs (gRNAs), were generated to target the activity of Cas9 to a target DNA sequence (Esvelt et al. (2014) eLife:e03401). A D10A mutation present in the catalytic domain of Cas9 converts it to a nickase that produces single nucleotide breaks at the target DNA (Jinek et al. (2012) Science 337:816-821). Double nicking of target DNA can increase genome editing specificity by 50-1500 fold (Ranet al. (2013) Cell 154:1380-1389), with the off-target rate as low as $1/10{,}000$. Such specificity can make somatic genomic targeting a viable approach in treating human diseases.

Despite a high incidence, only a fraction of men diagnosed with prostate cancer develop metastases and even fewer die from the disease. The majority of prostate cancers remain asymptomatic and clinically indolent. The precise mechanisms for the development of progressive, clinically concerning prostate cancer remain elusive. Furthermore, the inability to predict prostate cancer's potential aggressiveness has resulted in significant overtreatment of the disease. The dichotomous nature of prostate cancer—a subset of life-threatening malignancies in the larger background of histological alterations lacking the clinical features implicit with that label—is a fundamental challenge in disease management. Treatment of prostate cancer, particularly of those metastatic prostate cancers remains problematic. Therefore, there is a need in the art for methods of treating a subject that may develop progressive prostate cancer.

3. SUMMARY OF THE INVENTION

The present invention relates to methods for treating prostate cancer patients. It is based, at least in part, on the discovery that approximately 90% of men carrying at least one of the following fusion genes: TRMT11-GRIK2, SLC45A2-AMACR, MTOR-TP53BP1, LRRC59-FLJ60017, TMEM135-CCDC67 and CCNH-C5orf30 experienced prostate cancer recurrence, metastases and/or prostate cancer-specific death after radical prostatectomy (each examples of "progressive prostate cancer"), while these outcomes occurred in only 36% of men not carrying any of these fusion genes. It is also based, at least in part, on the discovery that a genome editing technique that specifically targets a fusion gene can induce cell death in a cancer cell having the fusion gene.

In various non-limiting embodiments, the present invention provides for methods of treating a subject that carries a fusion gene. In certain embodiments, a method of the present invention comprises performing a genome editing technique on one or more cancer cells, e.g., prostate cancer cells, of the subject. Non-limiting examples of such fusion genes include TRMT11-GRIK2, SLC45A2-AMACR, MTOR-TP53BP1, LRRC59-FLJ60017, TMEM135-CCDC67, KDM4B-AC011523.2, MAN2A1-FER, PTEN-NOLC1, CCNH-C5orf30, ZMPSTE24-ZMYM4, CLTC-ETV1, ACPP-SEC13, DOCK7-OLR1 and PCMTD1-SNTG1.

In certain non-limiting embodiments, the present invention further provides kits for performing methods of treating a subject that carries a fusion gene. In certain embodiments, a kit of the present invention can comprise one or more vectors or plasmids comprising a nucleic acid encoding a Cas protein, e.g., $Cas9^{D10A}$. In certain embodiments, the one or more vectors can further comprise one or more gRNAs specific to a fusion gene, e.g., specific to a breakpoint of a fusion gene and/or sequences flanking the breakpoint of a fusion gene.

In certain embodiments, a kit of the present invention can further include one or more vectors or plasmids comprising a nucleic acid, that when expressed results in cell death. In certain embodiments, the nucleic acid encodes HSV-1 thymidine kinase. In certain embodiments, this vector can further comprise one or more targeting sequences that are complementary to sequences within the fusion gene to promote homologous recombination and insertion of the nucleic acid. In certain embodiments, where the nucleic acid encodes HSV-1 thymidine kinase, the kit can further comprise ganciclovir and/or valganciclovir.

4. BRIEF DESCRIPTION OF THE FIGURES

FIG. 1. Unique fusion gene events. Left panel: Miniature diagrams of genome of the fusion genes, the transcription directions, the distances between the joining genes and

directions of the fusions. Middle panel: Representative sequencing chromograms of fusion genes. The joining gene sequences were indicated (SEQ ID NOs: 45-52). Right panel: Diagrams of translation products of fusion genes. Blue-driver gene translation product; Red-passenger gene translation product; Orange-novel translation products due to frameshift or translation products from a non-gene region.

FIG. **2**A-H. Fluorescence in situ hybridization suggests genome recombination in prostate cancer cells. (A) Schematic diagram of MAN2A1 and FER genome recombination and FISH probe positions. Representative FISH images were shown for normal prostate epithelial cells and cancer cells positive for MAN2A1-FER fusion. Orange denotes probe 1; Green denotes probe 2. (B) Schematic diagram of SLC45A2 and AMACR genome recombination and FISH probe positions. Representative FISH images were shown for normal prostate epithelial cells and cancer cells positive for SLC45A2-AMACR fusion. Orange denotes probe 1; Green denotes probe 2. (C) Schematic diagram of MTOR and TP53BP1 genome recombination and FISH probe positions. Representative FISH images were shown for normal prostate epithelial cells and cancer cells positive for MTOR-TP53BP1 fusion. Orange denotes probe 1; Green denotes probe 2. (D) Schematic diagram of TRMT11 and GRIK2 genome recombination and FISH probe positions. Representative FISH images were shown for normal prostate epithelial cells and cancer cells positive for TRMT11-GRIK2 fusion. Orange denotes probe 1; Green denotes probe 2. (E) Schematic diagram of LRRC59 and FLJ60017 genome recombination and FISH probe positions. Representative FISH images were shown for normal prostate epithelial cells and cancer cells positive for LRRC59-FLJ60017 fusion. Orange denotes probe 1; Green denotes probe 2. (F) Schematic diagram of TMEM135 and CCDC67 genome recombination and FISH probe positions. Representative FISH images were shown for normal prostate epithelial cells and cancer cells positive for TMEM135-CCDC67 fusion. Orange denotes probe 1; Green denotes probe 2. (G) Schematic diagram of CCNH and C5orf30 genome recombination and FISH probe positions. Representative FISH images were shown for normal prostate epithelial cells and cancer cells positive for CCNH-C5orf30 fusion. Orange denotes probe 1; Green denotes probe 2. (H) Schematic diagram of KDM4B and AC011523.2 genome recombination and FISH probe positions. Representative FISH images were shown for normal prostate epithelial cells and cancer cells positive for KDM4B-AC011523.2 fusion. Orange denotes probe 1; Green denotes probe 2.

FIG. **3**A-D. Fusion genes in prostate cancer are associated with aggressive prostate cancers. (A) Distribution of 8 prostate cancer samples positive for fusion genes. Samples from patients who experienced recurrence were indicated with grey (PSADT≥15 months) or dark grey (PSADT<4 months), samples from patients who have no recurrence at least 5 years with green, and samples from patients whose clinical follow-up is ongoing but less than 5 years with white (undetermined). (B) Correlation of fusion gene events with prostate cancer recurrence. Percentage of prostate cancer relapse when fusion gene was positive in the prostate cancer samples was plotted for each fusion gene. Percentage of prostate cancer experiencing recurrence from samples positive for fusion transcripts was plotted for each fusion transcript. Left, University of Pittsburgh Medical Center cohort; Middle, Stanford University Medical Center cohort; Right, University of Wisconsin Madison Medical Center cohort. (C) ROC analyses of a panel of 8 fusion genes predicting prostate cancer recurrence (top) and short PSADT (bottom). (D) Kaplan-Meier analysis of patients who are positive for any of TRMT11-GRIK2, SLC45A2-AMACR, MTOR-TP53BP1, LRRC59-FLJ60017, TMEM135-CCDC67 and CCNH-C5orf30 versus those who are negative for these fusion events.

FIG. **4**A-C. Fusion genes predict recurrence of prostate cancer. (A) Schema of training and validation steps in building fusion gene prediction models for prostate cancer recurrence and short PSADT. The algorithm of fusion gene prediction of prostate cancer recurrence and PSADT<4 months was obtained from 90 random-assigned prostate cancer samples from University of Pittsburgh Medical Center (I). The algorithm was then applied to 89 samples from University of Pittsburgh Medical Center (II), 21 samples from Stanford University Medical center (III) and 33 samples from University of Wisconsin Madison Medical Center (IV). (B) Prediction rate of prostate cancer recurrence (top) and PSADT<4 months using prostate cancer samples cohorts from University of Pittsburgh Medical Center, Stanford Medical Center, and University of Wisconsin Madison Medical Center, based on algorithm obtained from the 90-training sample cohort. (C) Kaplan-Meier analysis of patients who were positive for any of TRMT11-GRIK2, SLC45A2-AMACR, MTOR-TP53BP1, LRRC59-FLJ60017, TMEM135-CCDC67 and CCNH-C5orf30 versus those who were negative for these fusion events. Top, Kaplan-Meier analysis of prostate cancer sample cohort from University of Pittsburgh; P-value is indicated for the significant difference in survival between the group that is positive for at least one fusion transcript and the group that is negative. Bottom, Kaplan-Meier analysis of prostate cancer sample cohort from Stanford University Medical Center; P-value is indicated for the significant difference in survival between the group that is positive for at least one fusion transcript and the group that is negative.

FIG. **5**A-B. Combining status of fusion transcript and clinical/pathological parameter to improve prediction of prostate cancer recurrence. (A) Combining Gleason's grading and the status of 8 fusion transcripts in prostate cancer samples using LDA technique to predict the recurrence of prostate cancer. Left, ROC analysis of Gleason alone or Gleason plus the presence of fusion transcripts using LDA technique in the prediction of prostate cancer recurrence; P value (permutation test) is indicated for the significant difference between the ROC curve generated by Gleason alone and curve generated by Gleason plus the presence of fusion transcripts using LDA technique. Middle, Kaplan-Meier analysis of PSA free survival of prostate cancer patients with Gleason ≥8 versus <8 from combined UPMC testing, Wisconsin and Stanford data sets; P-value (Log-rank test) is indicated for the significant difference in survival between the group that has Gleason score at least 8 and the group that has score 7 or less. Right, Kaplan-Meier analysis of PSA free survival of prostate cancer patients with Gleason ≥8 or positive for any of the 8 fusion transcripts in the prostate cancer samples versus those <8 and negative for fusion transcripts using LDA from combined UPMC testing, Wisconsin and Stanford data sets. P-value (Log-rank test) is indicated for the significant difference in survival between the group that is positive for at least one fusion transcript or has Gleason ≥8 and the group that is negative for fusion transcript and has Gleason <8. (B) Combining nomogram and the status of 8 fusion transcripts in prostate cancer samples using LDA technique to predict the recurrence of prostate cancer. Left, ROC analysis of nomogram alone or nomogram plus the presence of fusion transcripts using LDA technique in the prediction of prostate cancer recur-

rence. P-value (permutation test) is indicated for the significant difference between the ROC curve generated by Nomogram alone and curve generated by Nomogram plus the presence of fusion transcripts using LDA technique. Middle, Kaplan-Meier analysis of PSA free survival of prostate cancer patients with probability >88 versus ≤88 from combined UPMC testing, Wisconsin and Stanford data sets; P-value (Log-rank test) is indicated for the significant difference in survival between the group that has probability >88 PSA free survival and the group that has ≤88 probability. Right, Kaplan-Meier analysis of PSA free survival of prostate cancer patients with Nomogram ≤88 or positive for any of the 8 fusion transcripts in the prostate cancer samples versus those >88 and negative for fusion transcripts using LDA from combined UPMC testing, Wisconsin and Stanford data sets. P-value (Log-rank test) is indicated for the significant difference in survival between the group that is negative for fusion transcript and has probability >88 PSA free survival and the group that is positive for fusion transcript or has ≤88 probability.

FIG. **6**. CIRCOS plots of prostate cancer functional genome translocation. Five prostate cancer functional translocations were based on RNA sequencing. Fourteen of these functional translocations were supported by whole genome sequencing analysis. Functional translocation is defined as at least one transcript identified in the translocation process. Translocations in non-gene area were excluded.

FIG. **7**A-B. Identification of fusion genes in 174 prostate samples. (A) RT-PCR of TMEM135-CCDC57, KDM4B-AC011523.2, MAN2A1-FER, TRMT11-GRIK2, CCNH-C5orf30, SLC45A2-AMACR, MTOR-TP53BP1, LRRC59-FLJ6001 and TMPRSS2-ERG were performed on 213 prostate cancer samples. RT-PCR of β-actin was used as quality control. The lane assignment is as follows: 1-TP12-S0943T, 2-TP12-S0916T, 3-TP12-S0967T, 4-TP12-S1059T, 5-TP10-S093T, 6-JB770T, 7-TP08PPS0721T, 8-TP10-S0638T, 9-TP12-S1032T, 10-TP12-S0624T, 11-TP12-S0981T, 12-TP10PPS0420T, 13-TP12-S0966T, 14-TP12-S0988T, 15-TP12-S0704T, 16-PR053T, 17-IB110T, 18-TP12-S0928T, 19-TP12-S0816T, 20-TP12-S0789T, 21-TP12-S0805T, 22-TP12-S0803T, 23-TP12-S0765T, 24-TP12-S0770T, 25-TP12-S0799T, 26-TP12-S0795T, 27-TP12-S0786T, 28-PR534T, 29-TP12-S0790T, 30-TP12-S0740T, 31-TP12-S0723T, 32-PR536T, 33-FB76, 34-IB378T, 35-IB180T, 36-HB303T, 37-GB368, 38-HB327T, 39-HB346T, 40-PR227T, 41-HB322T, 42-HB658T, 43-IB289T, 44-HB492T, 45-IB111T, 46-TP12-S0466T, 47-TP12-S0456T, 48-TP12-S0246T, 49-TP12-S0608T, 50-TP12-S0340T, 51-TP12-S0337T, 52-TP12-S0048T, 53-TP12-S0191T, 54-TP12-S0194T, 55-TP12-S0049T, 56-HB340T, 57-TP12-S0102T, 58-PR530T, 59-1942T, 60-TP12-S1189T, 61-13745T, 62-5396T, 63-8432T, 64-HB261T, 65-FB183T, 66-HB591T, 67-HB568T, 68-HB526T, 69-TP08-S00542T, 70-IB298T, 71-TP09-S0420T, 72-PR303T, 73-GB400T, 74-PR018T, 75-HB603T, 76-PR310T, 77-JB197T, 78-PR300T, 79-PR236T, 80-JB154T, 81-PR434T, 82-7504T, 83-25313T, 84-8629T, 85-7270T, 86-2671T, 87-4308T, 88-28278T, 89-TP12-S1224T, 90-TP12-S0918T, 91-TP12-S1197T, 92-TP12-S0915T, 93-16464T, 94-2644T, 95-1199T, 96-15922T, 97-15733T, 98-16947T, 99-19381T, 100-6837T, 101-9122T, 102-6647T, 103-4336T, 104-29671T, 105-11462T, 106-8741T, 107-IB362T, 108-PR079T, 109-IB483T, 110-IB071T, 111-GB195T, 112-PR521T, 113-TP08-S00530T, 114-7221T, 115-JB426T, 116-34T, 117-HB951T, 118-FB94T, 119-IB273T, 120-DB237T, 121-IB134T, 122-HB021T, 123-HB033T, 124-FB174 T, 125-KB170T, 126-FB120T, 127-HB504T, 128-HB305T, 129-FB421T, 130-TP09-S0721T, 131-FB238T, 132-HB46T, 133-TP11PP-S0638T, 134-PR306T, 135-HB207T, 136-HB235T, 137-IB112T, 138-IB136T, 139-PR375T, 140-2HB591T, 141-23HB021T, 142-TP09-S0006T, 143-2IB483T, 144-2HB568T, 145-M-11462T, 146-29825T, 147-3G989122T, 148-1AF8378T, 149-3Q-10614T, 150-4L98-27086T, 151-3D994336T, 152-3K5772T, 153-2K98-8378T, 154-14304T, 155-15463T, 156-15875T, 157-98TA-83782T, 158-562T, 159-14878T, 160-7943T, 161-995772T, 162-678T, 163-9927086T, 164-25265T, 165-HB705T, 166-33PR053T, 167-TP12-S0954T, 168-19PR530T, 169-34PR227T, 170-56FB76T, 171-TP09-S0704T, 172-78HB340T, 173-23FB120T, 174-23HB346T, 175-541B289T, 176-TP13-S0109T, 177-TP13-S0456T, 178-TP13-S0248T, 179-TP13-S0464T, 180-TP13-S0043T, 181-TP13-S0314T, 182-8433T, 183-863176T, 184-R6TT, 185-84876T, 186-994308T, 187-991199T, 188-9812033T, 189-855327T, 190-9814481T, 191-R3T, 192-R13T, 193-R19T, 194-84375T, 195-832972T, 196-9210207T, 197-R57T, 198-828142T, 199-R26T, 200-23R19T, 201-8713205T, 202-9217293T, 203-R18T, 204-8712362T, 205-9412443T, 206-R10T, 207-92SR293T, 208-R16T, 209-849731T, 210-67R13T, 211-842620T, 212-R59T, 213-SR9R57T. (B) RT-PCR of TMEM135-CCDC67, KDM4B-AC011523.2, MAN2A1-FER, TRMT11-GRIK2, CCNH-C5orf30, SLC45A2-AMACR, MTOR-TP53BP1 and LRRC59-FLJ60017 on 10 organ donor prostate tissues.

FIG. **8**. Identification of fusion genes in 30 prostate samples from Stanford University Medical Center. RT-PCR of TMEM135-CCDC67, KDM4B-AC011523.2, MAN2A1-FER, TRMT11-GRIK2, CCNH-C5orf30, SLC45A2-AMACR, MTOR-TP53BP1 and LRRC59-FLJ60017 were performed on 30 indicated prostate cancer samples. RT-PCR of β-actin was used as quality control.

FIG. **9**. Identification of fusion genes in 36 prostate samples from University of Wisconsin Madison Medical Center. RT-PCR of TMEM135-CCDC67, KDM4B-AC011523.2, MAN2A1-FER, TRMT11-GRIK2, CCNH-C5orf30, SLC45A2-AMACR, MTOR-TP53BP1 and LRRC59-FLJ60017 were performed on 36 indicated prostate cancer samples. RT-PCR of β-actin was used as quality control.

FIG. **10**. Inactivation of GRIK1 and TRMT11 RNA expression in prostate cancer positive for TRMT11-GRIK2 fusion. RT-PCR was performed on RNA from TRMT11-GRIK2 fusion gene positive prostate cancer samples using primers specific for GRIK2 and TRMT11. Products of RT-PCR using primers specific for β-actin were used as template normalization control.

FIG. **11**. Genome breakpoint analysis of fusion genes. Top panel: Miniature diagrams of genome of the fusion genes, the transcription directions, the distances between the joining genes and directions of the chromosome joining. Middle panel: Miniature of fusion genome and transcription direction. Bottom: Representative sequencing chromograms encompassing the joining breakpoint of chromosomes (SEQ ID NOs: 53-55).

FIG. **12**A-B. Prediction of prostate cancer recurrence and PSADT using a panel of 8 fusion genes. (A) ROC analyses of a panel of 8 fusion genes predicting prostate cancer recurrence using random assigned 90 prostate cancer samples from University of Pittsburgh Medical Center. Dotted line-random prediction; Black line-fusion prediction; Blue dot-optimal prediction. P-value (permutation test) is indicated for the significant difference between the ROC curve generated by fusion transcripts using LDA technique

and the baseline control curve. (B) ROC analyses of a panel of 8 fusion genes predicting prostate cancer short PSADT (<4 months). Dotted line-random prediction; Black line-fusion prediction; Blue dot-optimal prediction. P-value (permutation test) is indicated for the significant difference between the ROC curve generated by fusion transcripts using LDA technique and the baseline control curve.

FIG. **13**A-C. PTEN-NOLC1 fusion gene in prostate cancer. (A) PTEN-NOLC1 fusion transcript. Top panel: Miniature diagrams of genome of the PTEN and NOLC1 genes, the transcription direction, the distance between the joining genes and direction of the fusion. Middle panel: Representative sequencing chromogram of PTEN-NOLC1 transcript. The joining gene sequences were indicated (SEQ ID NO: 56). Lower panel: Diagram of translation product of fusion transcript. Blue-head gene translation product; Red-tail gene translation product. (B) Schematic diagram of PTEN and NOLC1 genome recombination and FISH probe positions. Representative FISH images were shown for normal prostate epithelial cells and cancer cells positive for TENNOLC1 fusion. Orange (asterisk *) denotes probe 1 (RP11-124B18); Green (plus sign +) denotes probe 2 (CTD-3082D22). Fusion joining signals are indicated by green arrows. (C) PTEN-NOLC1 expression in prostate cancer samples. RT-PCRs were performed in 215 samples of prostate cancer using primers specific for PTEN-NOLC1 (PN) fusion transcript. RT-PCRs using primers specific for β-actin (BAT) were performed as normalization controls.

FIG. **14**. Motif analysis of MAN2A1-FER. Diagram of functional domains of MAN2A1, FER and MAN2A1-FER fusion proteins.

FIG. **15**. Schematic diagram of Genome editing targeting at a fusion gene breakpoint in prostate cancer cells positive for CCNH-C5orf30 (SEQ ID NO: 57).

FIG. **16**. Schematic diagram of fusion genes. Left panel: Schematic diagram of genome of fusion partners. Genetic locus, distance between partners, transcription direction and fusion direction are indicated. Middle panel: Histogram of Sanger sequencing surrounding the fusion point of each fusion gene (SEQ ID NOs: 40-44). Right panel: Predicted protein products of fusion genes. Blue: Head gene protein; Yellow: frameshift translation; Red: tail.

FIG. **17**. Schematic diagram of ZMPSTE24-ZMYM5 fusion formation. Functional domains are indicated.

FIG. **18**. Schematic diagram of CLTC-ETV1 fusion formation. Functional domains are indicated.

FIG. **19**. Schematic diagram of ACPP-SEC13 fusion formation. Functional domains are indicated.

FIG. **20**. Schematic diagram of DOCK7-OLR1 fusion formation. Functional domains are indicated.

FIG. **21**. Schematic diagram of PCMTD1-SNTG1 fusion formation. Functional domains are indicated.

FIG. **22**A-F. Pro-growth activity of MAN2A1-FER. (A) Expression of MAN2A1-FER in primary Prostate cancer Samples. Immunoblottings were performed using antibodies specific for MAN2A1 (upper panel) or FER (lower panel) on MAN2A1-FER RNA positive (JB770T, FB174T and FB421T) or MAN2A1-FER negative (IB071T, IB136T and HB504T) samples. (B) Expression of MAN2A1-FER-FLAG in RWPE-1 cells. RWPE-1 cells were transfected with pCDNA4-MAN2A1-FER-FLAG/pCDNA6 vectors. Two stable cell lines (RMF1 and RMF4) were selected to demonstrate tetracycline induced expression of MAN2A1-FER-FLAG using anti-FLAG antibodies. (C) Expression of MAN2A1-FER-FLAG accelerates entry to S phase of cell cycle. Cell cycle phases were quantified by flow cytometry analysis of BrdU incorporation and propidium iodine labeling. (D) Co-localization of MAN2A1-FER-FLAG and Golgi resident enzyme N-acetylgalactosaminyltransferase. MAN2A1-FER-FLAG was labeled with FITZ conjugated antibodies specific for FLAG, while N-acetylgalactosaminyltransferase was labeled with Rhodamine-conjugated antibodies specific for N-acetylgalactosaminyltransferase. (E) Co-segregation of MAN2A1-FER-FLAG and Nacetylgalactosaminyltranferase in sucrose gradient ultra-centrifugation. (F) Expression of MAN2A1-FER-FLAG induced tyrosine phosphorylation of EGFR in the absence of EGFR ligand. RMF1 and RMF4 cells were serum starved for 72 hrs, and were subsequently induced with tetracycline (5 μg/ml) for 12 hrs. EGFR was immunoprecipitated with anti-EGFR antibodies, and immunoblotted with anti-phosphotyrosine or anti-pTyr1068 of EGFR or anti-EGFR antibodies.

FIG. **23**. Specific killing of MAN2A1-FER expressing cells by Crisotinib and Canertinib. Prostate cancer cell line PC3 was transformed with pCDNA4-MAN2A1-FER-FLAG/pCDNA6. Expression of MAN2A1-FER was induced with 5 μg/mL tetracycline. Cells not treated with tetracycline nor any drug were used as background controls. Upper panel: Crisotinib specifically kills cells expressing MAN2A1-FER. Lower panel: Canertinib specifically kills cells expressing MAN2A1-FER.

FIG. **24**. Schematic diagram of SLC45A2-AMACR chimera protein. Fusion between SLC45A2 and AMACR results in truncation of two-third of (MFS) domain in SLC45A2, but largely retains CoA-transferase domain of AMACR.

FIG. **25**A-I. Pro-growth activity of SLC45A2-AMACR. (A) Expression of SLC45A2-AMACR in primary Prostate cancer samples. Immunoblottings were performed using antibodies specific for AMACR (upper panel) or SLC45A2 (lower panel) on SLC45A2-AMACR RNA positive (FB174T, HB207T, HB305T and FB238T) or SLC45A2-AMACR negative (6637T, 6647T and 1199T) samples. (B) Expression of SLC45A2-AMACR-FLAG in RWPE-1 cells. RWPE-1 cells were transfected with pCDNA4-SLC45A2-AMACR-FLAG/pCDNA6 vectors. Two stable cell lines (RSLAM #2 and RSLAM #3) were selected to demonstrate tetracycline induced expression of SLC45A2-AMACR-FLAG using anti-FLAG antibodies. (C) SLC45A2-AMACR is primarily located in plasma membrane. Immunoblottings were performed on membranous fraction (M) and non-membranous fraction (NM) of RSLAM #2 cells treated without tetracycline (upper panel) or with tetracycline (lower panel), using antibodies specific for AMACR (upper panel) and for FLAG (lower panel). (D) Immunofluorescence staining of AMACR (upper panel) in RSLAM #2 cells treated without tetracycline using antibodies specific for AMACR or of SLC45A2-AMACR-FLAG in RSLAM #2 cells treated with tetracycline using antibodies specific for FLAG. (E) Expression of SLC45A2-AMACR increases cell growth in MTT assays. (F) Expression of SLC45A2-AMACR-FLAG accelerates entry to S phase of cell cycle. Cell cycle phases were quantified by flowcytometry analysis of BrdU incorporation and propidium iodine labeling. (G) Expression of SLC45A2-AMACR increases intracellular levels of PIP2(3,4). (H) Yeast Two-Hybrid validation of LC45A2-AMACR/SHIP2 interaction. (I) Co-immunoprecipitation of SHIP2 and SLC45A2-AMACR-FLAG in RSLAM #2 cells.

FIG. **26**. Ebselen specifically inhibits SLC45A2-AMACR expressing PC3 cells. Untransformed RWPE1, NIH3T3 cells and SLC45A2-AMACR transformed PC3 cells treated with (PC3/SLAM tet+) or without tetracycline (PC3/SLAM tet−) were applied with indicated concentration of Ebselen.

Cell growths relative to unapplied controls were examined. IC50 for PC3/SLAM tet+ is 37 μM, while for PC3/SLAM tet− is 173 μM. For NIH3T3 and RWPE1 cells, IC50s are >300 μM.

FIG. **27**A-D. PTEN-NOLC1 is localized in the nucleus and promotes cell growth. (A) Immunofluorescence staining of PTEN and PTEN-NOLC1-FLAG. NIH3T3 and PC3 cells were transformed with pCDNA4-Pten-NOLC1-FLAG/pCDNA6 and induced with tetracycline. Immunofluorescence staining were performed using antibodies specific for FLAG epitope. Uninduced NIH3T3 cells and PC3 cells transfected with pCMV-Pten immunostained with antibodies specific for Pten were controls. (B) Cell proliferation induced by Pten-NOLC1-FLAG. Cells (2000/well) from (A) were grown for 4 days with tetracycline. Cell numbers were then quantified. Cells not treated with tetracycline were negative controls. (C) Cell cycle analysis of NIH3T3 and PC3 cells transformed with pCDNA4-Pten-NOLC1-FLAG/pCDNA6. (D) Colony formation analysis of NIH3T3 and PC3 cells transformed with pCDNA4-Pten-NOLC1-FLAG/pCDNA6.

FIG. **28**A-B. Genetic therapy targeting at TMEM135-CCDC67 genome breakpoint. (A) Transfection of PC3 cells containing TMEM135-CCDC67 breakpoint with pTMEM135-CCDC67-TK-GFP and pNicKase-RFP-gRNA-TMEM135-CCDC67-BrkPt resulted in integration and expression of TK-GFP. (B) Treatment of ganciclovir of PC3 cells and PC3/TMEM135-CCDC67-BrkPt transfected with pTMEM135-CCDC67-TK-GFP and pNicKase-RFP-gRNA-TMEM135-CCDC67-BrkPt resulted in specific killing of TMEM135-CCDC67 breakpoint containing PC3 cells.

FIG. **29**A-B. Schema of strategy to introduce EGFP-tk into the breakpoint of TMEM135-CCDC67 fusion gene. (A) Diagram representation and Sanger sequencing of TMEM135-CCDC67 chromosome breakpoint. Direction of transcription is indicated by the arrows. (B) Schematic diagram of strategy to introduce EGFP-tk into the breakpoint of TMEM135-CCDC67. The locations of gRNA− and gRNA+ are indicated by boxes. These gRNAs were ligated with $Cas9^{D10A}$ into VQAd5-CMV shuttle vector and recombined into pAd5 virus. Separately, 584 bp of TMEM135 intron 13 sequence and 561 bp of CCDC67 intron 9 sequence were designed to sandwich a promoterless EGFP-tk cDNA, ligated into PAdlox shuttle vector and recombined into adenovirus. A splice acceptor and a splice donor from exon 14 of TMEM135 were inserted between TMEM intron 13 and EGFP-tk, and between EGFP-tk and CCDC67 intron 9, respectively, to allow proper EGFP-tk RNA splicing to occur. Cells containing TMEM135-CCDC67 chromosome breakpoint were infected with these recombinant viruses. The integrated EGFP-tk was transcribed by the fusion head gene promoter in these cells, spliced and translated into protein product of EGFP-tk, which in turn blocks DNA synthesis by converting ganciclovir to ganciclovir triphosphate.

FIG. **30**A-D. EGFP-tk integration and expression in cells expressing TMEM135-CCDC67 fusion breakpoint transcript. (A) gRNA mediated cleavage of pCMV-TMEM135int13-CCDC67int9. In vitro cleavage assays were performed on PVUI linearized pCMVTMEM135int13-CCDC67int9 vector using recombinant Cas9, *S. pyogenes* and in vitro transcribed gRNA− or gRNA+ as indicated. The cleavage generated 4317 and 3206 bp fragments of pCMV-TMEM135int13-CCDC67int9 vector for gRNA−, and 4414 and 3109 bp for gRNA+. (B) Genome integration and expression of TMEM135int13-CCDC67int9 breakpoint in PC3 and DU145 cells. Top panel: PCR products of TMEM135int13-CCDC67int9 breakpoint from the genome of indicated cells; Second from the top: PCR products of genomic β-actin from the genome of indicated cells. Third from the top: RT-PCR products of TMEM135int13-CCDC67int9 breakpoint from the mRNA of the indicated cells. Bottom panel: RT-PCR products of TMEM135int13-CCDC67int9 breakpoint from the mRNA of the indicated cells. PC3 Pcmvbp denotes PC3 cells transfected with pCMV-TMEM135int13-CCDC67int9). DU145 pCMVBP denotes DU145 cells transfected with pCMV-TMEM135int13-CCDC67int9, PC3 pCMV denotes PC3 transfected with pCMVscript. DU145 pCMV denotes DU145 cells transfected with pCMVscript. Primer sequences are listed in Table 18. (C) Infection of PC3 or DU145 cells containing TMEM135-CCDC67 breakpoint led to expression of EGFP-tk. PC3 or DU145 cells transformed with pCMV-TMEM135int13-CCDC67int9 were infected with pAD5-$Cas9^{D10A}$-$gRNA^{TMEM135int13}$-$gRNA^{CCDC67int9}$ and pAD-TMEM135int13-EGFP-tk-CCDC67int9. Expression of $Cas9^{D10A}$-RFP is indicated by red fluorescence, while expression EGFP-tk is indicated by green. PC3 or DU145 cells transformed with pCMVscript were used as controls. (D) Quantification of EGFP-tk integration/expression by flow cytometry.

FIG. **31**A-B. Treatment with nucleotide analogue ganciclovir kills cancer cells expressing EGFP-tk. (A) PC3 or DU145 cells containing the TMEM135-CCDC67 fusion gene were infected with pAD5-$Cas9^{D10A}$-$gRNA^{TMEM135int13}$-$gRNA^{CCDC67int9}$ and pAD-TMEM135int13-EGFP-tk-CCDC67int9. These cells were then incubated with various concentrations of ganciclovir for 24 hours. Cell deaths were then quantified with phycoerythrin labeled Annexin V through flow cytometer. PC3 or DU145 cells harboring no TMEM135-CCDC67 breakpoint were used as controls. (B) Representative sample of cell death induced by ganciclovir on cells infected with pAD5-$Cas9^{D10A}$-$gRNA^{TMEM135int13}$-$gRNA^{CCDC67int9}$ and pAD-TMEM135int13-EGFP-tk-CCDC67int9, and treated with 5 μg/ml ganciclovir. PC3 or DU145 cells harboring no TMEM135-CCDC67 breakpoint were used as controls. Apoptosis was indicated by Annexin V staining.

FIG. **32**A-D. Treatment of ganciclovir induced remission of xenografted prostate cancers in SCID mice. (A) PC3 cells harboring the TMEM135-CCDC67 breakpoint were xenografted into the subcutaneous regions of SCID mice. These tumors were allowed to grow for 3 week before the treatment. The indicated drugs were applied through peritoneal and local injections 3 times a week until all the mice from control treatments died off. The tumor volumes were measured weekly. PC3 BP denotes PC3 cells transformed with pCMV-TMEM135int13-CCDC67int9; Aden denotes treatment of pAD5-$Cas9^{D10A}$-$gRNA^{TMEM135int13}$-$gRNA^{CCDC67int9}$ and pAD-TMEM135int13-EGFP-tk-CCDC67int9; Gan denotes Ganciclovir; PBS denotes phosphate buffer saline. (B) DU145 cells harboring TMEM135-CCDC67 breakpoint were xenografted into the subcutaneous regions of SCID mice. These tumors were allowed to grow for 3 week before the treatment. The indicated drugs were applied through peritoneal and local injections 3 times a week until all the mice from control treatments died off. The tumor volumes were measured weekly. DU145 BP denotes DU145 cells transformed with pCMV-TMEM135int13-CCDC67int9; Aden denotes treatment of pAD5-$Cas9^{D10A}$-$gRNA^{TMEM135int13}$-$gRNA^{CCDC67int9}$ and pAD-TMEM135int13-EGFP-tk-CCDC67int9; Gan denotes Ganciclovir; PBS denotes

phosphate buffer saline. (C) Mice treated with TMEM135-CCDC67 breakpoint therapy were free of cancer metastasis. (D) Mice treated TMEM135-CCDC67 breakpoint therapy had no mortality.

FIG. **33**A-B. Evidence of EGFP-tk DNA integration and expression of EGFP-tk in xenografted PC3 cell cancer. (A) Schematic diagram for the detection of TMEM135int13-EGFP-tk-CCDC67int9 integration into TMEM135-CCDC67 breakpoint in the PC3 cell genome. Arrows indicate the primer position for PCR. Putative integration sites that generated mutations are indicated by yellow stars. The PCR products obtained from xenografted PC3 cells that contain TMEM135-CCDC67 breakpoint before virus treatment were used as reference control. PCR products obtained after viral (pAD5-Cas9^{D10A}-gRNA^{TMEM135int13}-gRNA^{CCDC67int9} and pADTMEM135int13-EGFP-tk-CCDC67int9) infections were sequenced. The positions of mutations due to DNA integration were detected through Sanger's sequencing. (B) Expression of Cas9^{D10A} and HSV1-tk in PC3 or DU145 cells that contain TMEM135-CCDC67 breakpoint (PC3-BP and DU145 BP, respectively) and their control counterparts (PC3-CMV and DU145 CMV).

5. DETAILED DESCRIPTION OF THE INVENTION

For clarity, and not by way of limitation, the detailed description of the invention is divided into the following subsections:

(i) fusion genes;
(ii) fusion gene detection;
(iii) methods of treatment;
(iv) genome editing techniques; and
(v) kits.

5.1 Fusion Genes

The term "fusion gene," as used herein, refers to a nucleic acid or protein sequence which combines elements of the recited genes or their RNA transcripts in a manner not found in the wild type/normal nucleic acid or protein sequences. For example, but not by way of limitation, in a fusion gene in the form of genomic DNA, the relative positions of portions of the genomic sequences of the recited genes is altered relative to the wild type/normal sequence (for example, as reflected in the NCBI chromosomal positions or sequences set forth herein). In a fusion gene in the form of mRNA, portions of RNA transcripts arising from both component genes are present (not necessarily in the same register as the wild-type transcript and possibly including portions normally not present in the normal mature transcript). In non-limiting embodiments, such a portion of genomic DNA or mRNA may comprise at least about 10 consecutive nucleotides, or at least about 20 consecutive nucleotides, or at least about 30 consecutive nucleotides, or at least 40 consecutive nucleotides. In a fusion gene in the form of a protein, portions of amino acid sequences arising from both component genes are present (not by way of limitation, at least about 5 consecutive amino acids or at least about 10 amino acids or at least about 20 amino acids or at least about 30 amino acids). In this paragraph, portions arising from both genes, transcripts or proteins do not refer to sequences which may happen to be identical in the wild type forms of both genes (that is to say, the portions are "unshared"). As such, a fusion gene represents, generally speaking, the splicing together or fusion of genomic elements not normally joined together.

The fusion gene TRMT11-GRIK2 is a fusion between the tRNA methyltransferase 11 homolog ("TRMT11") and glutamate receptor, ionotropic, kainate 2 ("GRIK2") genes. The human TRMT11 gene is typically located on chromosome 6q11.1 and the human GRIK2 gene is typically located on chromosome 6q16.3. In certain embodiments, the TRMT11 gene is the human gene having NCBI Gene ID No: 60487, sequence chromosome 6; NC_000006.11 (126307576 . . . 126360422) and/or the GRIK2 gene is the human gene having NCBI Gene ID No:2898, sequence chromosome 6; NC_000006.11 (101841584 . . . 102517958). In certain embodiments, the junction (also referred to herein as chromosomal breakpoint and/or junction fragment) of a TRMT11-GRIK2 fusion gene comprises a sequence as shown in FIG. **1** and/or Table 1.

The fusion gene SLC45A2-AMACR is a fusion between the solute carrier family 45, member 2 ("SLC45A2") and alpha-methylacyl-CoA racemase ("AMACR") genes. The human SLC45A2 gene is typically located on human chromosome 5p13.2 and the human AMACR gene is typically located on chromosome 5p13. In certain embodiments the SLC45A2 gene is the human gene having NCBI Gene ID No: 51151, sequence chromosome 5; NC_000005.9 (33944721 . . . 33984780, complement) and/or the AMACR gene is the human gene having NCBI Gene ID No:23600, sequence chromosome 5; NC_000005.9 (33987091 . . . 34008220, complement). In certain embodiments, the junction and/or junction fragment of a SLC45A2-AMACR fusion gene comprises a sequence as shown in FIG. **1** and/or Table 1.

The fusion gene MTOR-TP53BP1 is a fusion between the mechanistic target of rapamycin ("MTOR") and tumor protein p53 binding protein 1 ("TP53BP1") genes. The human MTOR gene is typically located on chromosome 1p36.2 and the human TP53BP1 gene is typically located on chromosome 15q15-q21. In certain embodiments, the MTOR gene is the human gene having NCBI Gene ID No:2475, sequence chromosome 1 NC_000001.10 (11166588 . . . 11322614, complement) and/or the TP53BP1gene is the human gene having NCBI Gene ID No: 7158, sequence chromosome 15; NC_000015.9 (43695262 . . . 43802707, complement). In certain embodiments, the junction and/or junction fragment of a MTOR-TP53BP1 fusion gene comprises a sequence as shown in FIG. **1** and/or Table 1.

The fusion gene LRRC59-FLJ60017 is a fusion between the leucine rich repeat containing 59 ("LRRC59") gene and the "FLJ60017" nucleic acid. The human LRRC59 gene is typically located on chromosome 17q21.33 and nucleic acid encoding human FLJ60017 is typically located on chromosome 11q12.3. In certain embodiments, the LRRC59 gene is the human gene having NCBI Gene ID No:55379, sequence chromosome 17; NC_000017.10 (48458594 . . . 48474914, complement) and/or FLJ60017 has a nucleic acid sequence as set forth in GeneBank AK_296299. In certain embodiments, the junction and/or junction fragment of a LRRC59-FLJ60017 fusion gene comprises a sequence as shown in FIG. **1**, FIG. **11** and/or Table 1.

The fusion gene TMEM135-CCDC67 is a fusion between the transmembrane protein 135 ("TMEM135") and coiled-coil domain containing 67 ("CCDC67") genes. The human TMEM135 gene is typically located on chromosome 11q14.2 and the human CCDC67 gene is typically located on chromosome 11q21. In certain embodiments the TMEM135 gene is the human gene having NCBI Gene ID No: 65084, sequence chromosome 11; NC-000011.9

(86748886 . . . 87039876) and/or the CCDC67 gene is the human gene having NCBI Gene ID No: 159989, sequence chromosome 11; NC-000011.9 (93063156 . . . 93171636). In certain embodiments, the junction and/or junction fragment of a TMEM135-CCDC67 fusion gene comprises a sequence as shown in FIG. **1**, FIG. **11**, FIG. **29** and/or Table 1.

The fusion gene CCNH-C5orf30 is a fusion between the cyclin H ("CCNH") and chromosome 5 open reading frame 30 ("C5orf30") genes. The human CCNH gene is typically located on chromosome 5q13.3-q14 and the human C5orf30gene is typically located on chromosome 5q21.1. In certain embodiments, the CCNH gene is the human gene having NCBI Gene ID No: 902, sequence chromosome 5; NC_000005.9 (86687310 . . . 86708850, complement) and/or the C5orf30gene is the human gene having NCBI Gene ID No: 90355, sequence chromosome 5; NC_000005.9 (102594442 . . . 102614361). In certain embodiments, the junction and/or junction fragment of a CCNH-C5orf30 fusion gene comprises a sequence as shown in FIG. **1**, FIG. **11** and/or Table 1.

The fusion gene KDM4B-AC011523.2 is a fusion between lysine (K)-specific demethylase 4B ("KDM4B") and chromosomal region "AC011523.2." The human KDM4B gene is typically located on chromosome 19p13.3 and the human AC011523.2 region is typically located on chromosome 19q13.4. In certain embodiments the KDM4B gene is the human gene having NCBI Gene ID NO: 23030, sequence chromosome 19; NC_000019.9 (4969123 . . . 5153609); and/or the AC011523.2 region comprises a sequence as shown in FIG. **1**. In certain embodiments, the junction and/or junction fragment of a KDM4B-AC011523.2 fusion gene comprises a sequence as shown in FIG. **1** and/or Table 1.

The fusion gene MAN2A1-FER is a fusion between mannosidase, alpha, class 2A, member 1 ("MAN2A1") and (fps/fes related) tyrosine kinase ("FER"). The human MAN2A1 gene is typically located on chromosome 5q21.3 and the human FER gene is typically located on chromosome 5q21. In certain embodiments, the MAN2A1gene is the human gene having NCBI Gene ID NO: 4124, sequence chromosome 5; NC_000005.9 (109025156 . . . 109203429) or NC_000005.9 (109034137 . . . 109035578); and/or the FER gene is the human gene having NCBI Gene ID NO: 2241, sequence chromosome 5: NC_000005.9 (108083523 . . . 108523373). In certain embodiments, the junction and/or junction fragment of a MAN2A1-FER fusion gene comprises a sequence as shown in FIG. **1** and/or Table 1.

The fusion gene PTEN-NOLC1 is a fusion between the phosphatase and tensin homolog ("PTEN") and nucleolar and coiled-body phosphoprotein 1 ("NOLC1"). The human PTEN gene is typically located on chromosome 10q23.3 and the human NOLC1 gene is typically located on chromosome 10q24.32. In certain embodiments, the PTEN gene is the human gene having NCBI Gene ID NO: 5728, sequence chromosome 10; NC_000010.11 (87863438 . . . 87970345) and/or the NOLC1 gene is the human gene having NCBI Gene ID NO: 9221, sequence chromosome 10; NC_000010.11 (102152176 . . . 102163871). In certain embodiments, the junction and/or junction fragment of a PTEN-NOLC1 fusion gene comprises a sequence as shown in FIG. **13** and/or Table 1.

The fusion gene ZMPSTE24-ZMYM4 is a fusion between zinc metallopeptidase STE24 ("ZMPSTE24") and zinc finger, MYM-type 4 ("ZMYM4"). The human ZMPSTE24 is typically located on chromosome 1p34 and the human ZMYM4 gene is typically located on chromosome 1p32-p34. In certain embodiments, the ZMPSTE24 gene is the human gene having NCBI Gene ID NO: 10269, sequence chromosome 1; NC_000001.11 (40258050 . . . 40294184) and/or the ZMYM4 gene is the human gene having NCBI Gene ID NO: 9202, sequence chromosome 1; NC_000001.11 (35268850 . . . 35421944). In certain embodiments, the junction and/or junction fragment of a ZMPSTE24-ZMYM4 fusion gene comprises a sequence as shown in FIG. **16**.

The fusion gene CLTC-ETV1 is a fusion between clathrin, heavy chain (Hc) ("CLTC") and ets variant 1 ("ETV1"). The human CLTC is typically located on chromosome 17q23.1 and the human ETV1 gene is typically located on chromosome 7p21.3. In certain embodiments, the CLTC gene is the human gene having NCBI Gene ID NO: 1213, sequence chromosome 17; NC_000017.11 (59619689 . . . 59696956) and/or the ETV1gene is the human gene having NCBI Gene ID NO: 2115, sequence chromosome 7; NC_000007.14 (13891229 . . . 13991425, complement). In certain embodiments, the junction and/or junction fragment of a CLTC-ETV1 fusion gene comprises a sequence as shown in FIG. **16** or a fragment thereof.

The fusion gene ACPP-SEC13 is a fusion between acid phosphatase, prostate ("ACPP") and SEC13 homolog ("SEC13"). The human ACPP is typically located on chromosome 3q22.1 and the human SEC13 gene is typically located on chromosome 3p25-p24. In certain embodiments, the ACPP gene is the human gene having NCBI Gene ID NO: 55, sequence chromosome 3; NC_000003.12 (132317367 . . . 132368302) and/or the SEC13 gene is the human gene having NCBI Gene ID NO: 6396, sequence chromosome 3; NC_000003.12 (10300929 . . . 10321188, complement). In certain embodiments, the junction and/or junction fragment of a ACPP-SEC13 fusion gene comprises a sequence as shown in FIG. **16**.

The fusion gene DOCK7-OLR1 is a fusion between dedicator of cytokinesis 7 ("DOCK7") and oxidized low density lipoprotein (lectin-like) receptor 1 ("OLR1"). The human DOCK7 is typically located on chromosome 1p31.3 and the human OLR1 gene is typically located on chromosome 12p13.2-p12.3. In certain embodiments, the DOCK7 gene is the human gene having NCBI Gene ID NO: 85440, sequence chromosome 1; NC_000001.11 (62454726 . . . 62688368, complement) and/or the OLR1 gene is the human gene having NCBI Gene ID NO: 4973, sequence chromosome 12; NC_000012.12 (10158300 . . . 10172191, complement). In certain embodiments, the junction and/or junction fragment of a DOCK7-OLR1 fusion gene comprises a sequence as shown in FIG. **16**.

The fusion gene PCMTD1-SNTG1 is a fusion between protein-L-isoaspartate (D-aspartate) O-methyltransferase domain containing 1 ("PCMTD1") and syntrophin, gamma 1 ("SNTG1"). The human PCMTD1 is typically located on chromosome 8q11.23 and the human SNTG1 gene is typically located on chromosome 8q11.21. In certain embodiments, the PCMTD1 gene is the human gene having NCBI Gene ID NO: 115294, sequence chromosome 8; NC_000008.11 (51817575 . . . 51899186, complement) and/or the SNTG1gene is the human gene having NCBI Gene ID NO: 54212, sequence chromosome 8; NC_000008.11 (49909789 . . . 50794118). In certain embodiments, the junction and/or junction fragment of a PCMTD1-SNTG1 fusion gene comprises a sequence as shown in FIG. **16**.

5.2 Fusion Gene Detection

Any of the foregoing fusion genes described above in section 5.1 may be identified and/or detected by methods

known in the art. The fusion genes may be detected by detecting a fusion gene manifested in a DNA molecule, an RNA molecule or a protein. In certain embodiments, a fusion gene can be detected by determining the presence of a DNA molecule, an RNA molecule or protein that is encoded by the fusion gene. For example, and not by way of limitation, the presence of a fusion gene may be detected by determining the presence of the protein encoded by the fusion gene.

The fusion gene may be detected in a sample of a subject. A "patient" or "subject," as used interchangeably herein, refers to a human or a non-human subject. Non-limiting examples of non-human subjects include non-human primates, dogs, cats, mice, etc. The subject may or may not be previously diagnosed as having prostate cancer.

In certain non-limiting embodiments, a sample includes, but is not limited to, cells in culture, cell supernatants, cell lysates, serum, blood plasma, biological fluid (e.g., blood, plasma, serum, stool, urine, lymphatic fluid, ascites, ductal lavage, saliva and cerebrospinal fluid) and tissue samples. The source of the sample may be solid tissue (e.g., from a fresh, frozen, and/or preserved organ, tissue sample, biopsy, or aspirate), blood or any blood constituents, bodily fluids (such as, e.g., urine, lymph, cerebral spinal fluid, amniotic fluid, peritoneal fluid or interstitial fluid), or cells from the individual, including circulating cancer cells. In certain non-limiting embodiments, the sample is obtained from a cancer. In certain embodiments, the sample may be a "biopsy sample" or "clinical sample," which are samples derived from a subject. In certain embodiments, the sample includes one or more prostate cancer cells from a subject. In certain embodiments, the one or more fusion genes can be detected in one or more samples obtained from a subject, e.g., in one or more prostate cancer cell samples.

In certain non-limiting embodiments, the fusion gene is detected by nucleic acid hybridization analysis.

In certain non-limiting embodiments, the fusion gene is detected by fluorescent in situ hybridization (FISH) analysis. FISH is a technique that can directly identify a specific sequence of DNA or RNA in a cell or biological sample and enables visual determination of the presence and/or expression of a fusion gene in a tissue sample. In certain non-limiting embodiments, where a fusion gene combines genes not typically present on the same chromosome, FISH analysis may demonstrate probes binding to the same chromosome. For example, and not by way of limitation, analysis may focus on the chromosome where one gene normally resides and then hybridization analysis may be performed to determine whether the other gene is present on that chromosome as well.

In certain non-limiting embodiments, the fusion gene is detected by DNA hybridization, such as, but not limited to, Southern blot analysis.

In certain non-limiting embodiments, the fusion gene is detected by RNA hybridization, such as, but not limited to, Northern blot analysis. In certain embodiments, Northern blot analysis can be used for the detection of a fusion gene, where an isolated RNA sample is run on a denaturing agarose gel, and transferred to a suitable support, such as activated cellulose, nitrocellulose or glass or nylon membranes. Radiolabeled cDNA or RNA is then hybridized to the preparation, washed and analyzed by autoradiography to detect the presence of a fusion gene in the RNA sample.

In certain non-limiting embodiments, the fusion gene is detected by nucleic acid sequencing analysis.

In certain non-limiting embodiments, the fusion gene is detected by probes present on a DNA array, chip or a microarray. For example, and not by way of limitation, oligonucleotides corresponding to one or more fusion genes can be immobilized on a chip which is then hybridized with labeled nucleic acids of a sample obtained from a subject. Positive hybridization signal is obtained with the sample containing the fusion gene transcripts.

In certain non-limiting embodiments, the fusion gene is detected by a method comprising Reverse Transcription Polymerase Chain Reaction ("RT-PCR"). In certain embodiments, the fusion gene is detected by a method comprising RT-PCR using the one or more pairs of primers disclosed herein (see, for example, Table 3).

In certain non-limiting embodiments, the fusion gene is detected by antibody binding analysis such as, but not limited to, Western Blot analysis and immunohistochemistry.

5.3 Methods of Treatment

The present invention provides methods of treating a subject carrying one or more fusion genes. Non-limiting examples of fusion genes are disclosed herein and in section 5.1. In certain embodiments, the methods of treatment include performing a targeted genome editing technique on one or more prostate cancer cells within the subject to produce an anti-cancer effect. Non-limiting examples of genome editing techniques are disclosed in section 5.4.

An "anti-cancer effect" refers to one or more of a reduction in aggregate cancer cell mass, a reduction in cancer cell growth rate, a reduction in cancer progression, a reduction in cancer cell proliferation, a reduction in tumor mass, a reduction in tumor volume, a reduction in tumor cell proliferation, a reduction in tumor growth rate and/or a reduction in tumor metastasis. In certain embodiments, an anti-cancer effect can refer to a complete response, a partial response, a stable disease (without progression or relapse), a response with a later relapse or progression-free survival in a patient diagnosed with cancer. In certain embodiments, an anti-cancer effect can refer to the induction of cell death, e.g., in one or more cells of the cancer, and/or the increase in cell death within a tumor mass.

In certain embodiments, a method of treating a subject comprises determining the presence of one or more fusion genes in a sample of the subject, where if one or more fusion genes are present in the sample then performing a targeted genome editing technique on one or more cells within the subject to produce an anti-cancer effect. In certain embodiments, the genome editing technique specifically targets the cells that carry the fusion gene, e.g., by specifically targeting a nucleic acid sequence of the fusion gene. Non-limiting examples of techniques for identifying and/or detecting a fusion gene are disclosed in section 5.2.

In certain embodiments, the method can include determining the presence or absence of one or more, two or more, three or more, four or more, five or more, six or more, seven or more, eight or more, nine or more, ten or more, eleven or more, twelve or more, thirteen or more or all fourteen of the fusion genes disclosed herein. In certain embodiments, the one or more fusion genes can be selected from the group consisting of TRMT11-GRIK2, SLC45A2-AMACR, MTOR-TP53BP1, LRRC59-FLJ60017, TMEM135-CCDC67, KDM4B-AC011523.2, MAN2A1-FER, PTEN-NOLC1, CCNH-C5orf30, ZMPSTE24-ZMYM4, CLTC-ETV1, ACPP-SEC13, DOCK7-OLR1, PCMTD1-SNTG1 or a combination thereof.

In certain embodiments, the fusion gene can be TMEM135-CCDC67.

In certain embodiments, the fusion gene can be CCNH-C5orf30.

In certain embodiments, the method of treating a subject comprises determining the presence of one or more fusion genes selected from the group consisting MAN2A1-FER, TMEM135-CCDC67, TRMT11-GRIK2, CCNH-C5orf30, LRRC59-FLJ60017, SLC45A2-AMACR, KDM4B-AC011523.2, PTEN-NOLC1, MTOR-TP53BP1 or a combination thereof in a sample of the subject, where if one or more fusion genes are detected in the sample then performing a targeted genome editing technique on one or more cancer cells within the subject, e.g., one or more prostate cancer cells, to produce an anti-cancer effect.

In certain embodiments, the method of treating a subject comprises determining the presence of one or more fusion genes selected from the group consisting of TRMT11-GRIK2, SLC45A2-AMACR, MTOR-TP53BP1, LRRC59-FLJ60017, TMEM135-CCDC67, KDM4B-AC011523.2, MAN2A1-FER, PTEN-NOLC1, CCNH-C5orf30, ZMP-STE24-ZMYM4, CLTC-ETV1, ACPP-SEC13, DOCK7-OLR1, PCMTD1-SNTG1 or a combination thereof in a sample of the subject, where if one or more fusion genes are detected in the sample then performing a genome editing technique targeting the fusion gene on one or more cancer cells within the subject, e.g., one or more prostate cancer cells, to produce an anti-cancer effect.

In certain embodiments, the method of treating a subject comprises determining the presence of one or more fusion genes selected from the group consisting of ZMPSTE24-ZMYM4, CLTC-ETV1, ACPP-SEC13, DOCK7-OLR1, PCMTD1-SNTG1 or a combination thereof in a sample of the subject, where if one or more fusion genes are detected in the sample then performing a targeted genome editing technique on one or more cancer cells within the subject, e.g., one or more prostate cancer cells, to produce an anti-cancer effect.

In certain embodiments, the sample in which the one or more fusion genes are detected is a prostate cancer sample.

In certain embodiments, the fusion gene in a sample is detected by genome sequencing. In certain embodiments, the fusion gene in a sample is detected by RNA sequencing. In certain embodiments, the fusion gene in a sample is detected by FISH.

5.4 Genome Editing Techniques

Genome editing is a technique in which endogenous chromosomal sequences present in one or more cells within a subject, can be edited, e.g., modified, using targeted endonucleases and single-stranded nucleic acids. The genome editing method can result in the insertion of a nucleic acid sequence at a specific region within the genome, the excision of a specific sequence from the genome and/or the replacement of a specific genomic sequence with a new nucleic acid sequence. A non-limiting example of a genome editing technique is the CRISPR/Cas 9 system. Non-limiting examples of such genome editing techniques are disclosed in PCT Application Nos. WO 2014/093701 and WO 2014/165825, the contents of which are hereby incorporated by reference in their entireties.

In certain embodiments, the genome editing technique can include the use of one or more guide RNAs (gRNAs), complementary to a specific sequence within a genome, e.g., a chromosomal breakpoint associated with a fusion gene, including protospacer adjacent motifs (PAMs), to guide a nuclease, e.g., an endonuclease, to the specific genomic sequence. A non-limiting example of an endonuclease includes the clustered, regularly interspaced short palindromic repeat (CRISPR) associated protein 9 (Cas9). In certain embodiments, the endonuclease can result in the cleavage of the targeted genome sequence and allow modification of the genome at the cleavage site through nonhomologous end joining (NHEJ) or homologous recombination.

In certain embodiments, the genome editing method and/or technique can be used to target a sequence of a fusion gene present in a cell, e.g., in a prostate cancer cell, to promote homologous recombination to insert a nucleic acid into the genome of the cell. For example, and not by way of limitation, the genome editing technique can be used to target the region where the two genes of the fusion gene are joined together (i.e., the junction and/or chromosomal breakpoint). As normal, non-cancerous, prostate cells do not contain the fusion gene, and therefore do not contain the chromosomal breakpoint associated with the fusion gene, prostate cancer cells can be specifically targeted using this genome editing technique. In certain embodiments, the genome editing technique can be used to target the junction (i.e., breakpoint) of a fusion gene selected from TRMT11-GRIK2, SLC45A2-AMACR, MTOR-TP53BP1, LRRC59-FLJ60017, TMEM135-CCDC67, KDM4B-AC011523.2, MAN2A1-FER, PTEN-NOLC1, CCNH-C5orf30, ZMP-STE24-ZMYM4, CLTC-ETV1, ACPP-SEC13, DOCK7-OLR1 and PCMTD1-SNTG1. For example, and not by way of limitation, the gRNAs can be designed to target (e.g., be complementary to) the sequences flanking the chromosomal breakpoint region (see, for example, FIGS. **15** and **29**) to guide an endonuclease, e.g., $Cas9^{D10A}$, to the chromosomal breakpoint region.

In certain embodiments, the disclosed genome editing technique can be used to promote homologous recombination with a sequence of a fusion gene, e.g., at a chromosomal breakpoint (junction) of a fusion gene, in one or more cells of a subject to allow the insertion of a nucleic acid sequence that when expressed results in the death, e.g., apoptosis, of the one or more cells. For example, and not by way of limitation, the nucleic acid sequence (also referred to herein as a donor nucleic acid) can encode the Herpes Simplex Virus 1 (HSV-1) thymidine kinase, Exotoxin A from *Pseudomonas aeruginosa*, Diphtheria toxin from *Corynebacterium diphtheri*, Ricin or abrin from *Ricinus communi* (castor oil plant), Cytosine deaminase from bacteria or yeast, Carboxyl esterase or Varicella Zoster virus (VZV) thymidine kinase. Additional non-limiting examples of nucleic acids and/or genes that can be inserted into the genome of a cell carrying a fusion gene to induce cell death are disclosed in Rajab et al. (2013) (J. of Genetics Syndromes and Gene Therapy, 4(9):187) and Zarogoulidis et al. (2013) (J. of Genetics Syndromes and Gene Therapy, 4(9):pii: 16849). In certain non-limiting embodiments, the nucleic acid sequence, e.g., the HSV-1 thymidine kinase nucleic acid sequence, is not operably linked to a regulatory sequence promoter (e.g., a promoter) and requires integration into the genome for expression. For example, and not by way of limitation, the promoter of the head gene of the fusion gene can promote the expression of the donor nucleic acid sequence.

In certain embodiments where a nucleic acid encoding HSV-1 thymidine kinase is inserted in the genome of one or more cells of a subject, a therapeutically effective amount of the guanine derivative, ganciclovir, or its oral homolog, valganciclovir, can be administered to the subject. HSV-1 thymidine kinase can phosphorylate and convert ganciclovir and/or valganciclovir into the triphosphate forms of ganciclovir and/or valganciclovir in the one or more cells of the

subject. The triphosphate form of ganciclovir and/or valganciclovir acts as competitive inhibitor of deoxyguanosine triphosphate (dGTP) and is a poor substrate of DNA elongation, and can result in the inhibition of DNA synthesis. The inhibition of DNA synthesis, in turn, can result in the reduction and/or inhibition of growth and/or survival and/or cell death of prostate cancer cells that contain the targeted chromosomal breakpoint and the integrated HSV-1 thymidine kinase nucleic acid sequence. This genome editing method can be used to produce an anti-cancer effect in a subject, e.g., a prostate cancer subject, that has been determined to have a fusion gene and/or an increased risk for progressive prostate cancer.

In certain embodiments, a genome editing technique of the present disclosure can include the introduction of an expression vector comprising a nucleic acid sequence that encodes a Cas protein or a mutant thereof, e.g., $Cas9^{D10A}$, into one or more cells of the subject, e.g., prostate cancer cells, carrying a fusion gene. In certain embodiments, the vector can further comprise one or more gRNAs for targeting the Cas9 protein to a specific nucleic acid sequence within the genome.

In certain embodiments, the one or more gRNAs can hybridize to a target sequence within a fusion gene. For example, and not by way of limitation, the one or more gRNAs can target the chromosomal breakpoint of a fusion gene and/or target the one or more sequences that flank the chromosomal breakpoint region. Non-limiting examples of sequences of fusion gene chromosomal breakpoints are disclosed herein and within the Figures (see, for example, Table 1). In certain embodiments, one gRNA can be complementary to a region within one of the genes of the fusion gene and another gRNA can be complementary to a region within the other gene of the fusion gene. For example, and not by way of limitation, one gRNA can be complementary to a region within the TMEM135 gene of the TMEM135-CCDC67 fusion gene and another gRNA can be complementary to a region within the CCDC67 gene. In certain embodiments, one gRNA can be complementary to a region upstream of the chromosomal breakpoint of a fusion gene and another gRNA can be complementary to a region downstream of the chromosomal breakpoint. In certain embodiments, genome sequencing can be performed to determine the regions of the fusion gene that can be targeted by the gRNAs. In certain embodiment, the regions of the genes that are targeted by the gRNAs can be introns and/or exons.

In certain embodiments, the nucleic acid sequence encoding the Cas protein can be operably linked to a regulatory element, and when transcribed, the one or more gRNAs can direct the Cas protein to the target sequence in the genome and induce cleavage of the genomic loci by the Cas protein. In certain embodiments, the Cas9 protein cut about 3-4 nucleotides upstream of the PAM sequence present adjacent to the target sequence. In certain embodiments, the regulatory element operably linked to the nucleic acid sequence encoding the Cas protein can be a promoter, e.g., an inducible promoter such as a doxycycline inducible promoter. The term "operably linked," when applied to DNA sequences, for example in an expression vector, indicates that the sequences are arranged so that they function cooperatively in order to achieve their intended purposes, i.e., a promoter sequence allows for initiation of transcription that proceeds through a linked coding sequence as far as the termination signal.

In certain embodiments, the Cas9 enzyme encoded by a vector of the present invention can comprise one or more mutations. The mutations may be artificially introduced mutations or gain- or loss-of-function mutations. Non-limiting examples of such mutations include mutations in a catalytic domain of the Cas9 protein, e.g., the RuvC and HNH catalytic domains, such as the D10 mutation within the RuvC catalytic domain and the H840 in the HNH catalytic domain. In certain embodiments, a mutation in one of the catalytic domains of the Cas9 protein results in the Cas9 protein functioning as a "nickase," where the mutated Cas9 protein cuts only one strand of the target DNA, creating a single-strand break or "nick." In certain embodiments, the use of a mutated Cas9 protein, e.g., $Cas9^{D10A}$, allows the use of two gRNAs to promote cleavage of both strands of the target DNA. Additional non-limiting examples of Cas9 mutations include VP64, KRAB and SID4X.

In certain embodiments, the genome editing technique of the present disclosure can further include introducing into the one or more cells an additional vector comprising a nucleic acid, that when expressed results in the death, e.g., apoptosis, of the one or more cells. In certain embodiments, this vector can further comprise one or more targeting sequences that are complementary (e.g., can hybridize) to the same and/or adjacent to the genomic sequences targeted by the gRNAs to allow homologous recombination to occur and insertion of the nucleic acid sequence (i.e., donor nucleic acid sequence) into the genome. In certain embodiments, the additional vector can further comprise one or more splice tag sequences of an exon/intron junction of a gene that makes up the fusion gene. In certain embodiments, the targeting sequences can be complementary to an intron, exon sequence and/or intron/extron splicing sequence within a gene of the fusion gene. In certain embodiments, one targeting sequence can be complementary to a region within one of the genes of the fusion gene targeted by the gRNAs and a second targeting sequence can be complementary to a region within the other gene of the fusion gene, to allow homologous recombination between the vector comprising the donor nucleic acid and the genome sequence cleaved by the Cas9 protein. For example, and not by way of limitation, one targeting sequence can be complementary to a region within the TMEM135 gene of the TMEM135-CCDC67 fusion gene and another targeting sequence can be complementary to a region within the CCDC67 gene. In certain embodiments, one targeting sequence can be complementary to a region upstream of the cleavage site generated by the Cas9 protein and another targeting sequence can be complementary to a region downstream of the chromosomal breakpoint. Non-limiting examples of the types of nucleic acid sequences that can be inserted into the genome are disclosed above. In certain embodiments, the nucleic acid that is to be inserted into the genome encodes HSV-1 thymidine kinase. Additional non-limiting examples of nucleic acids and/or genes that can be inserted into the genome of a cell carrying a fusion gene to induce cell death are set forth above.

The vectors for use in the present disclosure can be any vector known in the art. For example, and not by way of limitation, the vector can be derived from plasmids, cosmids, viral vectors and yeast artificial chromosomes. In certain embodiments, the vector can be a recombinant molecule that contains DNA sequences from several sources. In certain embodiments, the vector can include additional segments such as, but not limited to, promoters, transcription terminators, enhancers, internal ribosome entry sites, untranslated regions, polyadenylation signals, selectable markers, origins of replication and the like. In certain embodiments, the vectors can be introduced into the one or more cells by any technique known in the art such as by transfection and transduction. In certain embodiments, the vectors can be introduced by adenovirus transduction.

TABLE 1

Fusion gene junction sequences and siRNA sequences targeting the fusion gene junctions.

MAN2A1-FER

MAN2A1 FER
*GCAAATACTATTTCAGA**AACAGCCTATGAGGGAAATTTTGGTGA**AGTATATAAGGGC*
ACA (SEQ ID NO: 1)

siRNA sequence for MAN2A1-FER:
Sense Strand: 5' RCrArGrCrCrUrArUrGrArGrGrGrArArArUrUrUrUrGrGrUGA (SEQ ID NO: 2)

Antisense Strand: 5' RUrCrArCrCrArArArArUrUrUrCrCrCrUrCrArUrArGrGrCrUrGrUrU (SEQ ID NO: 3)

SLC45A2-AMACR

SLC45A2 AMACR
*TCCACTAC**CATGCCCTCTTCACAGGTGTCATGGAG**AAACTCCAGCTGGGCCCAGAG*
A (SEQ ID NO: 4)

siRNA sequence for SLC45A2-AMACR:
Sense Strand: 5' RUrGrCrCrCrUrCrUrUrCrArCrArGrGrUrGrUrCrArUrGrGrAG (SEQ ID NO: 5)

Antisense Strand: 5' RCrUrCrCrArUrGrArCrArCrCrUrGrUrGrArArGrArGrGrGrCrArUrG (SEQ ID NO: 6)

MTOR-TP53BP1

MTOR TP53BP1
*TGTCAGAATCC**AAGTCAAGTCAGGATTCCT**TGTTCTGGGAATG**TCAGTGGAATCTG*
CTCCTGC (SEQ ID NO: 7)

siRNA sequence for MTOR-TP53BP1:
Sense Strand: 5' RGrUrCrArGrGrArUrUrCrCrUrUrGrUrUrCrUrGrGrGrArATG (SEQ ID NO: 8)

Antisense Strand: 5' RCrArUrUrCrCrCrArGrArArCrArArGrGrArArUrCrCrUrGrArCrUrU (SEQ ID NO: 9)

TMEM135-CCDC67

TMEM135 CCDC67
*TTTT**AAGACTCACCAAGGGCAA**ATAAGAAGC*CAACTCCAACAGGTGGAAGAGTACC
A (SEQ ID NO: 10)

siRNA sequence for TMEM135-CCDC67:
Sense Strand: 5' RGrArCrUrCrArCrCrArArGrGrGrCrArArArUrArArGrArAGC (SEQ ID NO: 11)

Antisense Strand: 5' RGrCrUrUrCrUrUrArUrUrUrGrCrCrCrUrUrGrGrUrGrArGrUrCrUrU (SEQ ID NO: 12)

CCNH-C5orf30

CCNH C5ORF30
*TGTCACAGTTACTAGATA**TAATGAACTTCACAGAA**TACCTGGAGTAGAACAGA*AAAATTATTATG
TCT (SEQ ID NO: 13)

siRNA sequence for CCNH-C5orf30:
Sense Strand: 5' RArUrGrArArArArUrArCrCrUrGrGrArGrUrArGrArArCrAGA (SEQ ID NO: 14)

Antisense Strand: 5 RUrCrUrGrUrUrCrUrArCrUrCrCrArGrGrUrArUrUrUrUrCrArUrUrA (SEQ ID NO: 15)

KDM4B-AC011523.2

KDM4B AC011523.2
*AACTACCTGCACTTTG**GGGAGCCTAAGTCCTGGACAGTAAGCA**AGCCTGGATCTGA*
GAGA (SEQ ID NO: 16)

siRNA sequence for KDM4-AC011523.2:
Sense Strand: 5' RGrArGrCrCrUrArArGrUrCrCrUrGrGrArCrArGrUrArArGrCA (SEQ ID NO: 17)

Antisense Strand: 5' RUrGrCrUrUrArCrUrGrUrCrCrArGrGrArCrUrUrArGrGrCrUrCr CrC (SEQ ID NO: 18)

TABLE 1-continued

Fusion gene junction sequences and siRNA sequences targeting the fusion gene junctions.

TRMT11-GRIK2
TRMT11 GRIK2 *AGCATCTGGAG**TTCCGCCTGCCGGTGGTATTTTTGAAT**ATGTGGAATCTGGCCCAA* TGGGAGCTG (SEQ ID NO: 19)
siRNA sequence for TRMT11-GRIK2: Sense Strand: 5' RCrCrGrCrCrUrGrCrCrGrGrUrGrGrUrArUrUrUrUrGrAAT (SEQ ID NO: 20)
Antisense Strand: 5' RArUrUrCrArArArArArUrArCrCrArCrCrGrGrCrArGrGrCrGrGrArA (SEQ ID NO: 21)
LRRC59-FLJ60017
LRRC69 FLJ60017 *CTGCTTGGATGAGAAGCAGTGTAAGCAGTGTGG**AAACAAGGTGACTGGAAGCACC*** ***TGCTC**AATGGCTG (SEQ ID NO: 22)
siRNA sequence for LRRC59-FLJ60017: Sense Strand: 5' RArCrArArGrGrUrGrArCrUrGrGrArArGrCrArCrCrUrGrCTC (SEQ ID NO: 23)
Antisense Strand: 5' RGrArGrCrArGrGrUrGrCrUrUrCrCrArGrUrCrArCrCrUrUrGrUrUrU (SEQ ID NO: 24)
PTEN-NOLC1
PTEN NOLC1 *AAGCCAACCGATACTT**TTCTCCAAATTTTAAGA**CACAGCAGGA*TGCCAATGCCTCTT CCCTCTTAGAC (SEQ ID NO: 25)
siRNA sequence for PTEN-NOLC1: Sense Strand: 5' RCrUrCrCrArArArUrUrUrUrArArGrArCrArCrArGrCrArGGA (SEQ ID NO: 26)
Antisense Strand: 5' RUrCrCrUrGrCrUrGrUrGrUrCrUrUrArArArArUrUrUrGrGrArGrArA (SEQ ID NO: 27)

The head gene is italicized and the tail gene is non-italicized. Targeted sequences are underlined and bolded.

5.4.1 Particular Non-Limiting Examples

In certain embodiments, a genome editing technique of the present invention comprises introducing into one or more cells of a subject: (i) a vector comprising a nucleic acid sequence that encodes a Cas9 protein, or mutant thereof; (ii) a vector comprising one or more gRNAs that are complementary to one or more target sequences of a fusion gene, that when expressed induce Cas9-mediated DNA cleavage within the fusion gene; and (iii) a vector comprising a donor nucleic acid sequence, that when expressed results in cell death, and one or more targeting sequences that are complementary to one or more sequences of the fusion gene to promote homologous recombination and the insertion of the donor nucleic acid sequence into the fusion gene.

In certain embodiments, a genome editing technique of the present invention comprises introducing into one or more cells of a subject: (i) a vector comprising a nucleic acid sequence that encodes a Cas9 protein, or mutant thereof, and one or more gRNAs that are complementary to one or more target sequences of a fusion gene, wherein when transcribed, the one or more gRNAs direct sequence-specific binding of a Cas9 protein to the one or more target sequences of the fusion gene to promote cleavage of the fusion gene; and (ii) a vector comprising a donor nucleic acid sequence, that when expressed results in cell death, and one or more targeting sequences that are complementary to one or more sequences of the fusion gene to promote homologous recombination and the insertion of the donor nucleic acid sequence into the fusion gene.

In certain embodiments, a genome editing technique of the present invention comprises introducing into one or more cells of a subject: (i) a vector comprising a nucleic acid sequence that encodes Cas9 protein, or mutant thereof, and one or more gRNAs that are complementary to one or more target sequences of a fusion gene, wherein when transcribed, the one or more gRNAs direct sequence-specific binding of a Cas9 protein to the one or more target sequences of the fusion gene to promote cleavage of the fusion gene; and (ii) a vector comprising a donor nucleic acid sequence encoding HSV-1 thymidine kinase and one or more targeting sequences that are complementary to one or more sequences of the fusion gene to promote homologous recombination and the insertion of the donor nucleic acid sequence encoding HSV-1 thymidine kinase into the fusion gene. In certain embodiments, the genome editing technique further comprises the administration of a therapeutically effective amount of ganciclovir and/or valganciclovir.

5.5 Kits

The present invention further provides kits for treating a subject that carries one or more of the fusion genes disclosed herein. In certain embodiments, the present disclosure provides kits for performing a targeted genome editing tech-

nique on one or more cancer cells, e.g., prostate cancer cells, within the subject that carries one or more of the fusion genes disclosed herein.

Types of kits include, but are not limited to, packaged fusion gene-specific probe and primer sets (e.g., TaqMan probe/primer sets), arrays/microarrays, antibodies, which further contain one or more probes, primers, or other reagents for detecting one or more fusion genes and/or can comprise means for performing a genome editing technique.

In certain embodiments, the kit can include means for performing the genome editing techniques disclosed herein. For example, and not by way of limitation, a kit of the present disclosure can include a container comprising one or more vectors or plasmids comprising a nucleic acid encoding a Cas protein, e.g., $Cas9^{D10A}$. In certain embodiments, the nucleic acid encoding the Cas protein can be operably linked to a regulatory element such as a promoter. In certain embodiments, the one or more vectors can further comprise one or more gRNAs specific to a fusion gene, e.g., specific to a breakpoint of a fusion gene and/or sequences flanking the breakpoint of a fusion gene.

In certain embodiments, a kit of the present invention can include, optionally in the same container as the vector comprising the nucleic acid encoding a Cas protein or in another container, one or more vectors or plasmids comprising a nucleic acid, that when expressed (in the presence of absence of a compound) results in cell death. For example, and not by way of limitation, the nucleic acid sequence can encode the Herpes Simplex Virus 1 (HSV-1) thymidine kinase, Exotoxin A from *Pseudomonas aeruginosa*, Diphtheria toxin from *Corynebacterium diphtheri*, Ricin or abrin from *Ricinus communi* (castor oil plant), Cytosine deaminase from bacteria or yeast, Carboxyl esterase or Varicella Zoster virus (VZV) thymidine kinase. In certain embodiments, this vector can further comprise one or more targeting sequences that are complementary to sequences within the fusion gene to promote homologous recombination and insertion of the donor nucleic acid.

In certain embodiments, where the donor nucleic acid encodes HSV-1 thymidine kinase, the kit can further comprise ganciclovir and/or valganciclovir.

In certain non-limiting embodiments, a kit of the present disclosure can further comprise one or more nucleic acid primers or probes and/or antibody probes for use in carrying out any of the above-listed methods. Said probes may be detectably labeled, for example with a biotin, colorimetric, fluorescent or radioactive marker. A nucleic acid primer may be provided as part of a pair, for example for use in polymerase chain reaction. In certain non-limiting embodiments, a nucleic acid primer may be at least about 10 nucleotides or at least about 15 nucleotides or at least about 20 nucleotides in length and/or up to about 200 nucleotides or up to about 150 nucleotides or up to about 100 nucleotides or up to about 75 nucleotides or up to about 50 nucleotides in length. An nucleic acid probe may be an oligonucleotide probe and/or a probe suitable for FISH analysis. In specific non-limiting embodiments, the kit comprises primers and/or probes for analysis of at least two, at least three, at least four, at least five, six, seven, eight, nine, ten, eleven, twelve, thirteen, fourteen of TRMT11-GRIK2, SLC45A2-AMACR, MTOR-TP53BP1, LRRC59-FLJ60017, TMEM135-CCDC67, KDM4B-AC011523.2, MAN2A1-FER, PTEN-NOLC1, CCNH-C5orf30, ZMPSTE24-ZMYM4, CLTC-ETV1, ACPP-SEC13, DOCK7-OLR1 and PCMTD1-SNTG1.

In certain non-limiting embodiments, the nucleic acid primers and/or probes may be immobilized on a solid surface, substrate or support, for example, on a nucleic acid microarray, wherein the position of each primer and/or probe bound to the solid surface or support is known and identifiable. The nucleic acid primers and/or probes can be affixed to a substrate, such as glass, plastic, paper, nylon or other type of membrane, filter, chip, bead, or any other suitable solid support. The nucleic acid primers and/or probes can be synthesized directly on the substrate, or synthesized separate from the substrate and then affixed to the substrate. The arrays can be prepared using known methods.

In non-limiting embodiments, a kit provides nucleic acid probes for FISH analysis of one or more fusion gene selected from the group consisting of: TRMT11-GRIK2, SLC45A2-AMACR, MTOR-TP53BP1, LRRC59-FLJ60017, TMEM135-CCDC67, CCNH-C5orf30, TRMT11-GRIK2, SLC45A2-AMACR, KDM4B-AC011523.2, MAN2A1-FER, PTEN-NOLC1, MTOR-TP53BP1, ZMPSTE24-ZMYM4, CLTC-ETV1, ACPP-SEC13, DOCK7-OLR1 or PCMTD1-SNTG1. In non-limiting embodiments, a kit provides nucleic acid probes for FISH analysis of one or more fusion gene selected from the group consisting of: TRMT11-GRIK2, SLC45A2-AMACR, MTOR-TP53BP1, LRRC59-FLJ60017, TMEM135-CCDC67, PTEN-NOLC1 and CCNH-C5orf30, and TRMT11-GRIK2, SLC45A2-AMACR, KDM4B-AC011523.2, MAN2A1-FER and MTOR-TP53BP1. In specific non-limiting embodiments, probes to detect a fusion gene may be provided such that separate probes each bind to the two components of the fusion gene or a probe may bind to a "junction" that encompasses the boundary between the spliced genes. For example, and not by way of limitation, the junction is the region where the two genes are joined together. In specific non-limiting embodiments, the kit comprises said probes for analysis of at least two, at least three, at least four or all five of ZMPSTE24-ZMYM4, CLTC-ETV1, ACPP-SEC13, DOCK7-OLR1 or PCMTD1-SNTG1. An example of FISH analysis used to identify a fusion gene is provided in Example 1 below.

In non-limiting embodiments, a kit provides nucleic acid primers for PCR analysis of one or more fusion gene selected from the group consisting of: TRMT11-GRIK2, SLC45A2-AMACR, MTOR-TP53BP1, LRRC59-FLJ60017, TMEM135-CCDC67, PTEN-NOLC1, CCNH-C5orf30, TRMT11-GRIK2, SLC45A2-AMACR, KDM4B-AC011523.2, MAN2A1-FER or MTOR-TP53BP1. In non-limiting embodiments, a kit provides nucleic acid primers for PCR analysis of one or more fusion gene selected from the group consisting of: ZMPSTE24-ZMYM4, CLTC-ETV1, ACPP-SEC13, DOCK7-OLR1or PCMTD1-SNTG1. In specific non-limiting embodiments, the kit comprises said primers for analysis of at least two, at least three, at least four, at least five, six, seven, eight, nine, ten, eleven, twelve, thirteen, fourteen of TRMT11-GRIK2, SLC45A2-AMACR, MTOR-TP53BP1, LRRC59-FLJ60017, TMEM135-CCDC67, KDM4B-AC011523.2, MAN2A1-FER, PTEN-NOLC1, CCNH-C5orf30, ZMPSTE24-ZMYM4, CLTC-ETV1, ACPP-SEC13, DOCK7-OLR1 and PCMTD1-SNTG1.

The following Examples are offered to more fully illustrate the disclosure, but are not to be construed as limiting the scope thereof.

6. EXAMPLE 1: TRANSLOCATION AND FUSION GENE EVENTS IN PROGRESSIVE PROSTATE CANCER

6.1 Abstract

Importance:

Prediction of prostate cancer clinical outcome remains a major challenge after the diagnosis. An accurate and reproducible test predicting the behavior of prostate cancer is urgently needed.

Objective:

To identify biomarkers that are predictive of prostate cancer recurrence or prostate cancer related death.

Design:

Genome DNA and/or total RNA from Nineteen specimens of prostate cancer (T), matched adjacent benign prostate tissues (AT), matched bloods (B) and organ donor prostates (OD) were sequenced. Eight novel fusion genes were discovered and validated. These 8 novel fusion genes were then analyzed on 174 prostate samples, including 164 prostate cancer and 10 healthy prostate organ donor samples. Up to 15 years of clinical follow-ups on prostate cancer patients were conducted.

Setting:

University of Pittsburgh Medical Center, Presbyterian and Shadyside Campus.

Participants:

One hundred sixty-four prostate cancer patients underwent radical prostatectomy from 1998-2012 were selected for fusion gene expression analysis. 80.5% (132/164) patients had been followed-up for at least 5 years.

Main Measure:

To identify the presence of any of the following fusion genes in prostate cancer samples: TMEM135-CCDC67, KDM4B-AC011523.2, MAN2A1-FER, TRMT11-GRIK2, CCNH-C5orf30, SLC45A2-AMACR, MTOR-TP53BP1 and LRRC59-FLJ60017.

Results:

Approximately 90% of men carrying at least one of six of these fusion genes (TRMT11-GRIK2, SLC45A2-AMACR, MTOR-TP53BP1, LRRC59-FLJ60017, TMEM135-CCDC67 and CCNH-C5orf30) experienced prostate cancer recurrence, metastases and/or prostate cancer-specific death after radical prostatectomy, while these outcomes occurred in only 36% of men not carrying those fusion genes. Four fusion genes occurred exclusively in prostate cancer samples from patients who experienced recurrence or prostate cancer related death. The formation of these fusion genes is the result of genome recombination events.

Conclusion and Relevance:

These findings suggest that the formation of these fusion genes are associated with prostate cancer recurrence and may drive the progression.

6.2. Introduction

Despite a high incidence[1, 2], only a fraction of men diagnosed with prostate cancer develop metastases and even fewer die from the disease. The majority of prostate cancers remain asymptomatic and clinically indolent. The precise mechanisms for the development of progressive, clinically concerning prostate cancer remain elusive. Furthermore, the inability to predict prostate cancer's potential aggressiveness has resulted in significant overtreatment of the disease. The dichotomous nature of prostate cancer—a subset of life-threatening malignancies in the larger background of histological alterations lacking the clinical features implicit with that label—is a fundamental challenge in disease management.

To identify genome markers for prostate cancer, whole genome sequencing was performed on 14 prostate tissue samples from 5 prostate cancer patients: five prostate cancers (T) from patients who experienced poor clinical outcomes (reoccurrence with fast rise of prostate cancer antigen doubling time (PSADT<4 months)), five matched blood (B) samples and four matched benign prostate tissues from the prostate cancer patients (AT) (Table 2). In one patient, normal adjacent prostate tissue was not available. An average of 200 GB was sequenced per sample to achieve 33 fold coverage of the entire genome. Total RNA from all T and AT samples was sequenced to achieve >1333 (average 400 million reads/sample) fold coverage per gene. Total RNA from four age-matched, entirely histologically benign prostate tissues harvested from healthy organ donors was similarly sequenced as a tissue control. The sequencing data were aligned to human reference genome HG19[3]. Fusion genes were then identified and validated. We hypothesize that these fusion genes from cancer samples that prove metastatic are associated poor clinical outcome for prostate cancer patients. A prediction model for prostate cancer recurrence and short post-operative prostate specific antigen doubling time (PSADT) was built. This model was then applied to 89 additional prostate cancer samples from University of Pittsburgh Medical Center, 30 samples from Stanford University Medical Center, and 36 samples from University of Wisconsin Madison Medical Center with follow-up ranging from 1 to 15 years. One hundred twenty-seven of these samples are from patients who experienced prostate cancer recurrence after radical prostatectomy, and 106 are from patients with no evidence of recurrence for at least 5 years after the surgery. The remaining 46 samples are from patients who had less than 5 years of follow-up and had not yet experienced biochemical recurrence.

The newly validated fusion genes were then analyzed on 164 prostate cancer samples with clinical follow-up ranging from 2 to 15 years. Seventy-eight of these samples are from patients who experienced prostate cancer recurrence after radical prostatectomy, while 54 are from patients had no recurrence for at least 5 years after the surgery. The remainder samples are from patients who had radical prostatectomy less than 5 years ago. Association of fusion gene expression with prostate cancer recurrence was analyzed.

6.3 Methods

Tissue Samples.

Nineteen specimens of prostate cancer (T), matched adjacent benign prostate tissues (AT), matched bloods (B) and organ donor prostates (OD) were obtained from University of Pittsburgh Tissue Bank in compliance with institutional regulatory guidelines (Table 2). To ensure high purity (≥80%) of tumor cells, needle-microdissection was performed by pathologists to isolate the tumor cells from adjacent normal tissues (≥3 mm distance from the tumor). For AT and OD samples, similar needle-microdissections were performed to achieve 80% epithelial purity. Genomic DNA of these tissues was extracted using a commercially available tissue and blood DNA extraction kit (Qiagen, Hilden, Germany). The protocols of tissue procurement and procedure were approved by Institution Board of Review of University of Pittsburgh.

Whole Genome and Transcriptome Sequencing Library Preparation.

To prepare the genomic DNA libraries, 50 ng DNA was subjected to the tagmentation reactions using the NEXTERA DNA sample prep kit (Madison, Wis.) for 5 min at 55° C. The DNA was then amplified with adaptor and sequencing primers for 9 cycles of the following procedure: 95° C. for 10s, 62° C. for 30s and 72° C. for 3 min. The PCR products were purified with Ampure beads. The quality of genomic DNA libraries was then analyzed with qPCR using Illumina sequencing primers and quantified with Agilent 2000 bioanalyzer. For transcriptome sequencing, total RNA was extracted from prostate samples using Trizol, and

treated with DNAse1. Ribosomal RNA was then removed from the samples using RIBO-ZERO™ Magnetic kit (Epicentre, Madison, Wis.). The RNA was reverse-transcribed to cDNA and amplified using TRUSEQ™ RNA Sample Prep Kit v2 from Illumina, Inc (San Diego, Calif.). The library preparation process such as adenylation, ligation and amplification was performed following the manual provided by the manufacturer. The quantity and quality of the libraries were assessed as those described in genome DNA library preparation.

Whole Genome and Transcriptome Sequencing.

The Illumina whole genome sequencing system was applied to the analysis. The operation procedures strictly followed the manufacturer's instructions. Briefly, DNA libraries were hybridized to flowcells and subjected to primer extension and bridge amplification in an automatic cBot process for 4 h to generate clusters of DNA sequencing templates. These clustered flowcells were then subjected to the sequencing analysis in the Illumina HiSeq2000 system. All samples were sequenced with paired-end runs for 200 cycles.

Read Alignment.

Whole genome DNA-seq reads from 5 Ts, 4 ATs and 5 Bs were aligned by BWA[3] version 1.4.1 against the UCSC hg19 human reference genome allowing maximal 2 base mismatches per (100 nucleotide) read. After alignment, the average coverage of whole genome is above 30× for all 14 samples. Picard tool (http://picard.sourceforge.net) was applied to remove duplicate reads after the alignment. RNA-seq reads (from 5 T, 4 matched AT and 4 OD samples) were at an average of 1333× coverage. Whole transcriptome RNA-seq reads were aligned with the UCSC hg19 reference genome using Tophat[4-6] version 1.4.1. Maximal 2 mismatches per read were allowed.

Fusion Gene Detection.

To identify fusion gene events, we applied a Fusioncatcher (v0.97) algorithm[7] on RNA sequencing samples. The analysis results by the software had been validated with high precision rate in breast cancer cell lines. Both BOWTIE and BLAT alignment were applied in the analysis and were plotted with CIRCOS software[8]. The preliminary list of candidate fusion transcripts are filtered in Fusioncatcher based on the existing biological knowledge of the literature including: (1) If the genes are known to be the other's paralog in Ensembl; (2) If one of the fusion transcripts are the partner's pseudogene; (3) If one of the fusion transcripts are micro/transfer/small-nuclear RNA; (4) If the fusion transcript is known to be a false positive event (e.g., Conjoin gene database[21]); (5) If it has been found in healthy samples (Illumina Body Map 2.0 [http://www.ebi.ac.uk/arrayexpress/experiments/E-MTAB-513/]); (6) If the head and tail genes are overlapping with each other on the same strand. Fusion genes were visualized with CIRCOS software[8] as shown in FIG. **6**.

TABLE 2

Case	TNM	Margin	Relapse	Relapse fast	Relapse simple	Gleason	Age	Gender	Race
Case 1	T3bN1MX	Negative	fast	f	y	7	50s	M	W
Case 2	T3aN0MX	Negative	slow	nf	y	7	60s	M	W
Case 3	T2cN0MX	Negative	fast	f	y	8	60s	M	W
Case 4	T3bN1MX	Negative	fast	f	y	10	50s	M	W
Case 5	T3bN1MX	Negative	fast	f	y	10	50s	M	W

	PSA pre-operative	Time to progression (Months)	PSADT	Radiology follow-up	Time interval of follow-up (Months)	Length of follow-up (Months)	Additional treatment
Case	14.6	1.41	3.7	NEGATIVE	2.76	29.09	ADT
Case 1	4.1	43.75	39.96	NO	2.56	133.3	RT
Case 2	2.38	33.76	2.99	NEGATIVE	3.42	33.93	RT
Case 3	29.3	1.35	0.93	POSITIVE FOR BONE METASTASIS	1.02	15.48	ADT, CHEMO
Case 4							
Case 5	9.17	1.35	1.83	POSITIVE FOR BONE METASTASIS	2.4	149.6	ADT

Machine Learning Classifier to Predict Relapse Status.

8 fusion genes from 5 tumor samples validated by RT-PCR, Sanger sequencing and Fluorescence In-situ Hybridization (FISH) analyses were used as features to predict the relapse status (fast vs non-fast and relapse vs non-relapse) in a large validation cohort (PSADT<4 months vs PSADT>15 months or non-recurrent). The presence for each fusion pair was coded either as 1 or 0 to represent whether the fusion gene exist in the sample. Linear discriminant analysis (LDA) was used to build a classifier. In light of relatively rare occurrence of the fusion transcripts (4.4%-9.0%) in our 90-sample Pittsburgh training cohort, we also applied a simple prediction rule based on the presence in any subset of the eight fusion genes (i.e., a patient is predicted as recurrence if any fusion transcript in a designated subset exists). Leave-one-out cross validation (LOOCV) was applied to construct the model and evaluate the prediction performance. ROC curves were constructed by varying the parameters in the LDA classifier construction and the optimal prediction model was selected with the best Youden index (=sensitivity+specificity−1)[22], and was then evaluated in a 89-sample Pittsburgh test cohort, a 21-sample Stanford test cohort and a 30-sample Wisconsin test cohort. To compare the statistical significance of AUC difference between two models, a bootstrap test is used to generate p-values[23]. To compare accuracy of two models, a test for equal proportions using "prop.test" in R is applied.

To demonstrate the potential translational predictive value of these fusion transcripts, information of Nomogram estimated five-year PSA free survival probability and Gleason scores of the patients was incorporated into our prediction models. The following models were generated: (I) 8 fusion transcripts alone, (II) Gleason scores alone, (III) Nomogram values alone, (IV) Gleason scores+8 fusion transcripts, (V) Nomogram values+8 fusion transcripts. Complete information of prediction accuracy, sensitivity, specificity and Youden index for these eight models is available in Tables 7-16.

RT-PCR.

To verify fusion genes detected by transcriptome and whole genome sequencing, total RNA was reverse-transcribed with random hexamer. Double strand cDNA was synthesized as described previously[9, 10]. PCRs were performed using primers indicated in Table 3 using the following condition: 94° C. for 5 min, followed by 30 cycles of 94° C. for 30 seconds, 61° C. for 1 min and 72° C. for 2 min.

TABLE 3

Primer sequences for RT-PCR.

Fusion genes	Sequences
TMEM135-CCDC67	5'-GAGACCATCTTACTGGAAGTTCC-3' (SEQ ID NO: 58)/ 5'-TGGTACTCTTCCACCTGTTGG-3' (SEQ ID NO: 59)
Mtor-TP53BP1	5'-TTGGCATGATAGACCAGTCCC-3' (SEQ ID NO: 60)/ 5'-CAGCACCAAGGGAATGTGTAG-3' (SEQ ID NO: 61)
TRMT11-GRIK2	5'-GCGCTGTCGTGTACCCTTAAC-3' (SEQ ID NO: 62)/ 5'-GGTAAGGGTAGTATTGGGTAGC-3' (SEQ ID NO: 63)
CCNH-C5orf30	5'-CCAGGGCTGGAATTACTATGG-3' (SEQ ID NO: 64)/ 5'-AAGCACCAGTCTGCACAATCC-3' (SEQ ID NO: 65)
SLC45A2-AMACR	5'-TTGATGTCTGCTCCCATCAGG-3' (SEQ ID NO: 66)/ 5'-TGATATCGTGGCCAGCTAACC-3' (SEQ ID NO: 67)
KDM4B-AC011523.2	5'-AACACGCCCTACCTGTACTTC-3' (SEQ ID NO: 68)/ 5'-CTGAGCAAAGACAGCAACACC-3' (SEQ ID NO: 69)
MAN2A1-FER	5'-TGGAAGTTCAAGTCAGCGCAG-3' (SEQ ID NO: 70)/ 5'-GCTGTCTTTGTGTGCAAACTCC-3' (SEQ ID NO: 71)
LRRC59-FLJ60017	5'-GTGACTGCTTGGATGAGAAGC-3' (SEQ ID NO: 72)/ 5'-CCAGCATGCAGCTTTTCTGAG-3' (SEQ ID NO: 73)
TMPRSS2-ERG	5'-AGTAGGCGCGAGCTAAGCAGG-3' (SEQ ID NO: 74)/ 5'-GGGACAGTCTGAATCATGTCC-3' (SEQ ID NO: 75)
β-actin	5'-TCAAGATCATTGCTCCTCCTGAGC-3' (SEQ ID NO: 76)/ 5'-TGCTGTCACCTTCACCGTTCCAGT-3' (SEQ ID NO: 77)

Fluorescence In-Situ Hybridization.

Formalin-fixed and paraffin-embedded tissue slides (5 microns) were placed in 2×SSC at 37° C. for 30 min. Slides were then removed and dehydrated in 70% and 85% ethanol for 2 min each at room temperature, and air dried. The DNA from the selected clones (Table 4) was extracted using Nucleobond Ax kit (Macherey-Nagel, Easton, Pa.). The biotin-labeled probes were prepared using standard nick-translation procedure and hybridized to sample slides as described previously[11, 12].

TABLE 4

Bacterial artificial chromosome clone for FISH.

Fusion genes	Probe 1	Probe 2
TMEM135-CCDC67	RP11-80F20	RP11-1034E22
Mtor-TP53BP1	RP4-647M16	RP11-114F23
TRMT11-GRIK2	RP11-92N18	RP11-70I17
CCNH-C5orf30	RP11-111M24	RP11-244M13
SLC45A2-AMACR	RP11-179D3	RP11-1072I21
KDM4B-AC011523.2	RP11-241K5	RP11-655K24
MAN2A1-FER	RP11-452L20	RP11-328A14
LRRC59-SLC35B3	RP11-269I10	RP11-360D22
LRRC59-FLJ60017	RP11-269I10	CTD-2116N11

6.4. Results

Fusion Genes Discovered by RNA and Whole Genome Sequencing.

A total of 76 RNA fusion events were identified in prostate cancer samples by the Fusioncatcher[7] program. Thirteen of these fusion events were suggested by genome sequencing. To control for tissue-based fusion gene events, fusion genes present in any of the four age-matched organ donor prostate tissues were eliminated (Table 5). Further, fusion genes with less than 20 kb between each element and read in the cis direction were also eliminated. As a result of this filtering, 28 of 76 fusion gene events were identified as prostate cancer specific (Table 6 and FIG. **6**). Among these fusion events, TMPRSS2-ERG, the most common prostate cancer fusion gene[13-15], was found in two prostate cancer samples. Majority of the fusion events identified are novel and not reported in the literature. None of the 29 fusion genes were identified in the matched AT transcriptome analysis. To validate these fusion genes, RT-PCR was performed using primers specific for fusion gene regions

encompassing the fusion breakpoints and the PCR products were sequenced. Eight of these fusion gene events were validated through sequencing (FIG. **1**).

Five of the eight fusion events resulted in truncation of a driver gene and frameshift in translation of a passenger gene. One of the fusion genes produced a truncated cyclin H and an independent open reading frame of a novel protein whose function is not known. Two fusion events, however, produced chimera proteins that possibly retain at least partial function of both genes. One of these fusion products is N-terminus 703 amino acids of α-Mannosidase 2A (MAN2A1) fusing to the C-terminus 250 amino acids of FER, a Feline tyrosine kinase. The fusion protein retains the glycoside hydrolase domain but has its manosidase domain replaced with a tyrosine kinase domain from FER. Another fusion protein product produces a chimera of membrane-associated transporter protein (SLC45A20) and alpha-methylacyl-CoA racemase (AMACR). The chimera protein has 5 of its 10 transmembrane domains deleted from SLC45A2 and replaced with methyl-acyl CoA transferase domain from AMACR. Interestingly, both MAN2A1-FER and SLC45A2-AMACR fusions are in the trans-direction, eliminating the possibility of a fusion event from simple chromosome deletion or collapse of extremely large RNA transcript.

Fluorescence In Situ Hybridization Suggests Genome Recombination Underlying Fusion Gene Formation.

To investigate the mechanism of these fusion events, fluorescence in situ hybridization (FISH) was performed on prostate cancer tissues where the fusion gene was present. Using the probes surrounding MAN2A1 breakpoint, a physical separation of signals between 5' and 3' MAN2A1 in cancer cells containing the fusion gene was observed, in contrast to the overlapping nature of these signals in the wild type alleles in normal prostate epithelial cells (FIG. **2**). Similar "break-apart" hybridization occurred in SLC45A2-AMACR positive prostate cancer samples (FIG. **2**B). These findings indicate that MAN2A1-FER and SLC45A2-AMACR fusions are the result of chromosome recombination. Interestingly, in prostate cancer cells containing "break-apart" signals of MAN2A1, only 31% of the cells retained the 3' end signal, suggesting that the recombination of genome DNA in most prostate cancer cells results in truncation of the C-terminus of MAN2A1. A similar "collateral loss" of the N-terminus of AMACR was found in prostate cancer cells expressing SLC45A2-AMACR fusion (29% retaining the N-terminus signal of AMACR). Other FISH analyses confirm that genome translocations occur in cancer cells expressing TRMT11-GRIK2, MTOR-TP53BP1, LRRC59-FLJ60017, TMEM137-CCDC67, CCNH-C5orf30 and KDM4B-AC011523.2 fusion genes (FIGS. **2**C-G). These fusion genes are either separated by a large segment of genome DNA (TRMT11-GRIK2, TMEM135-CCDC67, CCNH-C5orf30 and KDM4B-AC011523.2) or located in separate chromosomes (MTOR-TP53BP1 and LRRC59-FLJ60017). The joining signals of hybridizations in prostate cancer cells suggest that these fusion genes were relocated to juxtapose to their fusion partners. Finally, genomic breakpoints were identified in 3 fusion pair through Sanger sequencing of the cancer genomic DNA (CCNH-C5orf30, TMEM135-CCDC67 and LRRC59-FLJ60017) (FIG. **11**).

Fusion Genes Association with Prostate Cancer Recurrence.

A genomic alteration in prostate cancer without clinical consequence is of limited significance. Therefore, the association of these fusion genes with prostate cancer progression was investigated in prostate cancer specimens obtained from 213 men and from entirely benign prostate tissues obtained from 10 organ donors free of urological disease aged 20 to 70. The prostate cancer samples were linked to the clinical outcomes after radical prostatectomy: those with no detectable prostate specific antigen (PSA) recurrence after a minimum of five years of observation, those whose clinical outcomes remain unknown and those who had an observed PSA recurrence within five years. For 179 of the 223 prostate cancer samples, clinical outcome data after radical prostatectomy were available, and 81 had no detectable prostate specific antigen (PSA) recurrence after a minimum of five years of follow-up, while 98 developed biochemical recurrence (defined as a measurable PSA ≥0.2 ng/ml). Only 7.4% (6/81) primary prostate cancers expressed one of the fusion genes in non-recurrent patients. In contrast, 52% (51/98) primary prostate cancers expressed at least one fusion in patients who developed recurrence (FIG. **3** and FIG. **7**A). No fusion genes were detected in benign prostate tissues obtained from healthy organ donors (FIG. **7**B). Three fusion events were observed exclusively in recurrent prostate cancer after radical prostatectomy (TRMT11-GRIK2, MTOR-TP53BP1 and LRRC59-FLJ60017; FIGS. **3**A and B).

Fisher's exact test showed a significant difference in recurrent status between patients with at least one of the 8 fusion transcripts and those without ($p=6.8\times10^{16}$). In the combined UPMC, Stanford and Wisconsin data sets, 91% (69/76) of patients positive for one of the fusion transcripts experienced prostate cancer recurrence in 5 years after prostate resection. Based on the hypothesis that the presence of at least one of the 8 fusion transcripts would indicate a recurrence for a prostate cancer patient, a prostate cancer prediction model was built and tested, using 90 randomly selected prostate cancer samples from University of Pittsburgh Medical Center (training set). This training cohort yielded an accuracy of prostate cancer recurrence prediction of 71% with 89% specificity and 58% sensitivity ($p<0.005$) (FIG. **12**A, Table 10). When this model was applied to a separate cohort of 89 samples (test set), the model correctly predicted recurrence in 70% of patients. To further validate this model, we tested its performance in a 30-patient (21 with qualified clinical follow-up) cohort from Stanford University Medical Center and a 36-patient (30 with qualified clinical follow-up) cohort from University of Wisconsin Madison Medical Center (FIG. **3**, FIG. **8** and FIG. **9**). Once again, the model correctly predicted recurrence with 76.2% accuracy and with 89% specificity and 67% sensitivity on the prostate cancer cohort from Stanford, and 80% accuracy and with 100% specificity and 63% sensitivity on the cohort from Wisconsin (Table 11).

Similar to the dichotomous nature of prostate cancer in general, recurrent prostate cancer can progress in an indolent or aggressive manner. A PSA doubling time (PSADT) less than four months after radical prostatectomy is strongly associated with the early development of metastatic disease and prostate cancer-specific death, whereas these events are rare and remote in men with a PSADT of greater than 15 months[16, 17]. Strong association was found between the fusion genes (e.g., TRMT11-GRIK2, SLC45A2-AMACR, MTOR-TP53BP1, LRRC59-FLJ60017, TMEM135-CCDC67 and CCNH-C5orf30) with prostate cancer recurrence ($p=4.2\times10^{-9}$) and a PSADT less than four months ($p=6\times10^{-9}$). To examine whether these fusion gene events have prognostic value for prostate cancer clinical outcome, receiver operator curve (ROC) analyses with varying weights of fusion genes were performed. As shown in FIG.

3C, the panel of eight fusion genes correctly predicted 74.4% for PSA doubling time less than four months in the 90-sample training cohort, and 67% for prostate cancer recurrence. To optimize the prediction model, six fusion genes were selected for an improved association with disease-free survival after radical prostatectomy. When the same algorithm was applied to a separate 89-sample test set from University of Pittsburgh Medical Center and 21-sample cohort from Stanford University Medical Center, the prediction rate for PSADT<4 months was found to be 78% and 71%, respectively (FIG. 4B). As shown in FIG. 3D, 89.5% of patients had an observed disease recurrence within five years of radical prostatectomy if they carried any of the six fusion genes. In addition, and as shown in FIG. 4C, 84.2% of patients had an observed disease recurrence within five years of radical prostatectomy if they carried any of the eight fusion genes. No patient survived five years without recurrence if their primary prostate cancer contained a TRMT11-GRIK2 or MTOR-TP53BP1 fusion gene. In contrast, 68% patients were free of disease recurrence if any of the novel fusion genes were not detected in their primary prostate cancer. Similar findings were also identified in the Stanford cohort: 88.9% patients experienced recurrence of prostate cancer if they carried any fusion transcript, while 66.7% patients were free of the disease recurrence if they are negative.

TABLE 5

Fusion gene 1	Fusion_gene2	read pairs	Validation Status
SORBS1	RP11-476E15.3	25	
AHCY	RP11-292F22.3	25	
DCUN1D3	ERI2	12	
MACF1	KIAA0754	11	
C10orf68	CCDC7	11	RT-PCR and sequencing
RP11-166D19.1	BLID	7	
ASS1	ASS1P9	6	
BACH1	BACH1-IT1	6	RT-PCR
MPDZ	RP11-272P10.2	5	
LIG3	RPS-837J1.2	4	
ACAD8	GLB1L3	4	RT-PCR
IGSF9B	RP11-259P6.1	3	
EYA1	RP11-1102P16.1	3	
TTC33	PRKAA1	3	RT-PCR
DNAH1	GLYCTK	3	
PSPC1	ZMYM5	3	
HSP90AB3P	RP11-759L5.2	3	
LSAMP	RP11-384F7.2	3	
RNF4	FAM193A	81	RT-PCR
AHCY	RP11-292F22.3	9	
LSAMP	RP11-384F7.2	8	
CBLL1	AC002467.7	4	
FNBP4	Y_RNA	4	
TBCE	RP11-293G6_A.2	4	
TRIM58	RP11-634B7.4	4	
DCUN1D3	ERI2	4	
PHPT1	MAMDC4	3	
TRIP6	SLC12A9	3	
NAT14	ZNF628	3	
TLL2	RP11-35J23.5	3	
UFSP2	Y_RNA	3	
TSPAN33	Y_RNA	3	
CADM3	DARC	3	
KIF27	RP11-213G2.3	3	
RABL6	KIAA1984	3	
ZNF615	ZNF350	3	
ZYG11A	RP4-631H13.2	3	
RP11-522L3.6	MTND4P32	3	
MTND3P10	AC012363.10	3	
RP11-464F9.1	BMS1P4	3	
RNF4	FAM193A	14	RT-PCR
GBP3	Y_RNA	3	
NACA	PRIM1	1	

TABLE 5-continued

Fusion gene 1	Fusion_gene2	read pairs	Validation Status
AHCY	RP11-292F22.3	3	
GBP3	Y_RNA	3	
HARS2	ZMAT2	2	RT-PCR and sequencing
EED	C11orf73	1	RT-PCR
CNPY3	RP3-475N16.1	1	RT-PCR
RN7SL2	Metazoa_SRP	1	
SLC16A8	BAIAP2L2	2	RT-PCR
KLK4	KLKP1	2	RT-PCR and sequencing
ZNF137P	ZNF701	1	RT-PCR
AZGP1	GJC3	1	RT-PCR
USP7	RP11-252I13.1	1	
TRRAP	AC004893.11	1	
C6orf47	BAG6	1	RT-PCR
TTTY15	USP9Y	9	
AC005077.12	LINC00174	2	
ADCK4	NUMBL	2	
ZNF606	C19orf18	2	
SLC45A3	ELK4	3	RT-PCR and sequencing

The most frequent fusion events in prostate cancer are TRMT11-GRIK2 (7.9%, or 22/279) and SLC45A2-AMACR (7.2%, or 20/279) (FIGS. 3A, 7-9). TRMT11-GRIK2 fusion represents a giant truncation of TRMT11, a tRNA methyltransferase, and elimination of GRIK2, a glutamate receptor but reported to possess tumor suppressor activity[18]. Indeed, GRIK2 was not expressed in prostate cancer samples that contain TRMT11-GRIK2 fusions, while it was detected in organ donor prostate samples (FIG. 10). Only 4 of 14 samples with TRMT11-GRIK2 expressed full length non-fusion TRMT11. Thus, the fusion event of TRMT11-GRIK2 represents a loss of function instead of a gain.

Combining Detection of Fusion Transcripts and Clinical/Pathological Parameters Improved the Prediction Rate of Prostate Cancer Recurrence.

Prostate cancer samples with at least one fusion transcript correlate with more advanced stage of prostate cancer (p=0.004), Lymph node involvement status (P=0.005) and lower nomogram scores (p=0.0003) (Table 12). Gleason grading alone produced a prostate cancer recurrence prediction rate of 61.1%, with 85.7% specificity and 39.6% sensitivity in the 90-sample UPMC training cohort, when Gleason ≥8 was used as cutoff to predict prostate cancer recurrence. The Gleason model yielded prediction accuracy ranging from 57-60% in 3 separate testing cohorts (Tables 13 and 14). However, when fusion transcript status was combined with Gleason Grade >8, improvement of prediction was found for all 4 cohorts: 72% for the UPMC training cohort, 74% for the UPMC test cohort, 76% for the Stanford cohort and 90% for the Wisconsin cohort. ROC showed a significant larger AUC (area under the curve) (0.84 versus 0.67, P=6.6×10-7) and higher testing accuracy (77.7% versus 59.7%, P=0.0019) (FIG. 5A) when Gleason score was combined with detection of any of 8 fusion transcripts. Similarly, Nomogram prediction of prostate cancer recurrence has the best accuracy of 76% with 68.8% sensitivity and 83.3% specificity in the analysis of 90-sample UPMC training cohort (Table 15). When this model was applied to UPMC testing, Stanford and Wisconsin cohorts independently, the results showed that the prediction accuracy ranged from 60% to 75% among the 3 cohorts (Table 16). When Nomogram was combined with the status of 8 fusion transcripts using LDA technique to build a classifier, the accuracy of prediction improves to 81-83% among the testing cohorts (Table 16). ROC showed an increase of AUC

from 0.76 to 0.87 (P=0.0001) and an improvement of accuracy from 69% to 81% (P=0.026, FIG. 5B). As a result, we concluded that classifier combining Nomogram and the 8 fusion gene panel generated the best prediction accuracy that outperforms each diagnostic tool alone.

6.5. Discussion

Transcriptome and whole genome sequencings revealed numerous fusion RNA transcripts occurring not just in prostate cancer but also in healthy organ donor prostate samples (Table 17). Some of these fusion events are verifiable by sequencing on the cDNA products. The functions of these new transcripts are not known. Since most of these chimeric RNA transcripts in healthy individuals are the splicing products of two adjacent genes, they are likely the new isoforms of the existing genes. These previously defined independent "genes" in the transcript could be one of the preferred spliced isoforms of the existing larger genes.

TABLE 6

Putative fusion transcripts from 5 prostate cancer samples

Fusion gene 1	Fusion gene2	Gene 1 breakpoint	Gene2 breakpoint	Reads	in DNAseq	Distance
1T						
HTMPRSS2	ERG	21: 42870046: –	21: 39817544: –	8	2	3052502
FZD4	RP11-736K20.5	11: 86665843: –	11: 86633140: –	7	0	32703
ZNF720	RP11-488L18.4	16: 31734674: +	1: 247363495: –	3	0	Inf
RP11-356O9.1	TTC6	14: 38033571: +	14: 38075868: +	12	0	42297
IGLV2-8	IGLL5	22: 23165779: +	22: 23235961: +	5	0	70182
RP11-381K20.2	KLHL3	5: 137150022: –	5: 137056273: –	3	0	93749
ADAP2	RNF135	17: 29286022: +	17: 29311635: +	3	0	25613
LRRC59	FLJ60017	17: 48469759: –	11: 63129852: +	3	7	Inf
RIPK1	SERPINB9	6: 3064293: +	6: 2900855: –	5	24	163438
Fusion gene 1	Fusion gene2	Gene 1 breakpoint	Gene2 breakpoint	Read pairs	in DNAseq	Distance
2T						
MTOR	TP53BP1	1: 11290982: –	15: 43773220: –	12	2	Inf
3T						
MAN2A1	FER	5: 109153139: +	5: 108380381: +	7	4	772758
KDM4B	AC011523.2	19: 5047680: +	19: 51354167: +	7	0	46306487
TRMT11	GRIK2	6: 126307768: +	6: 102069824: +	11	0	24237944
NAP1L1	CCDC88C	12: 76444311: –	14: 91850880: –	3	2	Inf
RP11-386M24.4	H2AFV	15: 93277091: –	7: 44874151: –	6	0	Inf
CCNH	C5orf30	5: 86697519: –	5: 102601609: +	3	8	15904090
UBA52	CTA-242H14.1	19: 18685741: +	7: 252729331: –	3	3	Inf
C1orf196	KAZN	1: 14507087: +	1: 14925479: +	3	0	418392
MTIF2	AL592494.3	2: 55473480: –	1: 121244615: +	6	0	Inf
RP11-168J18.6	PPP2R5C	3: 52408762: +	14: 102368056: +	3	2	Inf
RPL38	AC007283.4	17: 72205448: +	2: 202027232: –	3	0	Inf
ACSS1	APMAP	20: 24988402: –	20: 24964655: –	3	0	23747
4T						
RP11-443D10.3	ACACB	12: 109551220: +	12: 109577202: +	4	0	25982
SLC45A2	AMACR	5: 33982341: –	5: 34006004: –	3	0	23663
RP11-550F7.1	CAP1	3: 76483671: +	1: 40529899: +	7	9	Inf
TMC5	CCP110	16: 19508485: +	16: 19539189: +	6	0	30704
TLK2	RP11-274B21.1	17: 60631098: +	7: 128248237: +	6	126	Inf
TMEM135	CCDC67	11: 87030419: +	11: 93127625: +	7	26	6097206
Fusion gene 1	Fusion gene2	Gene 1 breakpoint	Gene2 breakpoint	Spanning_pairs	in DNAseq	Distance
5T						
TMPRSS2	ERG	21: 42870046: –	21: 39947671: –	12	2	2922375

This analysis reveals significant number of cancer specific fusion gene events. These fusions are not detectable in either organ donor prostate or benign prostate tissues from prostate cancer patients. Most of these fusion transcripts appear to express in low abundance, with only an average 6.6 reads of these fusion transcripts detected in >1333× sequencing. Indeed, when the coverage was reduced to 600× in simulation studies, only MTOR-TP53BP1 was detected consistently. The characteristics of these fusion genes are that they either have a large distance between the joining genes or have trans-direction of fusion that could only occur when chromosome recombination happens. In either scenario, DNA alteration in genome level must be the underlying mechanism.

Although the association between the eight novel fusion transcripts and prostate cancer recurrence is striking, the biological roles of these fusion transcripts are not yet elucidated. Given the known function of the genes contributing to the fusion transcripts, their formation may have impact on several cell pathways such as RNA stability[24] (TRMT11-GRIK2), protein glycosylation[25] (MAN2A1-FER), cell cycle progression[26,27, 28] (CCNH-C5orf50 and MTORTP53BP1), fibroblast growth factor nuclear import[29] (LRRC59-FLJ60017), histone demethylation[30] (KDM4B-AC011523.2), and fatty acid metabolism[31] (SLC45A2-AMACR). Many of these pathways appear to be fundamental to cell growth and survival.

Two of the fusion genes are of particular interest: MAN2A1-FER and SLC45A2-AMACR. First, MAN2A1 is a mannosidase critical in glycosylation of proteins[19]. It is usually located in Golgi apparatus. The truncation in MAN2A1-FER replaces the mannosidase domain with a tyrosine kinase domain from FER[20], while leaves the glycosyl transferase domain intact. The chimera protein likely loses the mannosidase function. The new kinase domain in MAN2A1-FER may confer the chimera protein a tyrosine kinase activity. Thus, the impact of this fusion gene could be profound: abnormal glycosylation and phosphorylation in hundreds of secreted or plasma membrane proteins. It may impact on cell-cell interactions and signal transduction, and generate a new immune response to the cancer cells. Second, AMACR is a racemase that catalyzes 2R stereoisomers of phytanic and pristanic acid to their S counterparts. AMACR is essential for β-oxidation of branch fatty acid in mitochondria. SLC45A2 is a transmembrane solute carrier known for its protective role in melanoma. SLC45A2-AMACR chimeric protein has 5 transmembrane domains of SLC45A2 truncated and replaced with a largely intact racemase. SLC45A2-AMACR also loses the mitochondria target site in AMACR. Presumably, the fusion protein would be located in the plasma membrane. It is of interest that all prostate cancer samples with SLC45A2-AMACR fusion proved highly aggressive. Identification of the signaling pathways of this chimeric protein may gain critical insight into the behavior of prostate cancer.

Even though the prevalence of each fusion transcript in prostate cancer samples is low (ranging from 2.9% to 7.9%), up to 60% of prostate cancers that later recurred and had short PSADT were positive for at least one of these fusion transcripts. The specificity of these fusion transcripts in predicting prostate cancer recurrence appears remarkably high, ranging from 89-100% among 4 separate prediction cohorts. There were no long term recurrence-free survivors if the primary tumor contained either TRMT11-GRIK2, MTOR-TP53BP1 or LRRC59-FLJ60017 fusion transcripts.

To our knowledge, this is the first report showing that a set of fusion genes is strongly associated with poor prognosis of prostate cancer. This discovery may have salient impact on clinical practice in light of the limit of serum PSA and Gleason's grading from biopsy samples in predicting prostate cancer clinical outcome. Detection of one of these prostate cancer recurrence association fusion genes in prostate cancer sample may warrant a more aggressive treatment regimen. The fusion RNA and chimera proteins validated in this study may lay down the foundation for future molecular targeting therapy for prostate cancer patients carrying these genes.

TABLE 7

Clinical and pathological characteristics of 213 cases of prostate cancer from UPMC cohort

Sample	Type	TNM	Margin	Recurrence	Recurrence fast	Recurrence simple	Gleason	Age	Sex	Race	PSA pre-operative	Time to progession (Months)	PSADT (months)	Radiology follow-up	Length of follow-up (Months)	Additional Treatment
11462T	T	T3aN0MX	Negative	none	nf	n	7.0	50s	M	W	25.0	N/A	N/A	NEGATIVE	158.0	None
1199T	T	T3bN0MX	Negative	slow	nf	y	8.0	50s	M	W	40.0	15.0	33.7	NEGATIVE	150.0	NK
13745T	T	T1cN0MX	Negative	none	nf	n	7.0	60s	M	W	6.8	N/A	N/A	NO	151.0	None
14304T	T	T2BN0MX	Negative	none	nf	n	6.0	50s	M	W	7.8	N/A	N/A	NO	156.0	None
14878T	T	T2bN0MX	Negative	none	nf	n	8.0	60s	M	W	6.2	N/A	N/A	NO	151.0	None
15463T	T	T2bN0MX	Negative	none	nf	n	7.0	60s	M	W	7.8	N/A	N/A	NO	149.0	None
15733T	T	T2bN0MX	Negative	none	nf	n	7.0	50s	M	W	6.4	N/A	N/A	NO	152.0	None
15875T	T	T3bN0MX	Negative	none	nf	n	7.0	40s	M	W	5.6	N/A	N/A	NO	154.0	None
15922T	T	T3aN0MX	Negative	none	nf	n	7.0	60s	M	W	16.0	N/A	N/A	NO	154.0	None
16464T	T	T3bN0MX	Negative	slow	nf	y	7.0	60s	M	W	8.5	88.5	24.6	NEGATIVE	149.0	NK
16947T	T	T3aN1MX	Negative	slow	nf	y	8.0	70s	M	W	6.1	31.0	15.6	NEGATIVE	148.0	NK
19381T	T	T2bN0MX	Negative	none	nf	n	6.0	50s	M	AA	2.5	N/A	N/A	NO	154.0	None
1942T	T	T3bN0MX	Positive	fast	f	y	9.0	60s	M	W	7.5	80.1	14.8	NEGATIVE	157.0	NK
19PR530T	T	T2cN0MX	Negative	ND	ND	ND	7.0	60s	M	W	4.4	N/A	N/A	not done	21.0	None
1AF8378T	T	T3aN0MX	Negative	none	nf	n	6.0	60s	M	W	12.9	N/A	N/A	NO	153.0	None
23FB120T	T	T3bN0MX	Negative	none	nf	n	7.0	60s	M	W	11.4	N/A	N/A	NEGATIVE	104.0	None
23HB021T	T	T2bN0MX	Negative	Fast	f	y	7.0	50s	M	W	6.4	23.0	3.0	NEGATIVE	78.0	ADT, RT
23R19T	T	T2bN0MX	Negative	none	nf	n	7.0	50s	M	W	7.2	N/A	NA	NO	151.0	None
23HB8346T	T	T2cN0MX	Negative	ND	ND	ND	6.0	60s	M	W	7.3	N/A	N/A	NO	34.0	None
25265T	T	T3bN0MX	Negative	none	nf	n	7.0	60s	M	W	3.4	N/A	N/A	NO	156.0	None
25313T	T	T3bN0MX	Negative	none	nf	n	8.0	50s	M	W	9.5	N/A	N/A	NO	156.0	None
2644T	T	T3aN0MX	Negative	slow	nf	y	9.0	50s	M	W	11.2	5.9	31.2	NEGATIVE	164.0	NK
2671T	T	T2cN0MX	Positive	slow	nf	y	7.0	60s	M	W	8.9	17.0	17.0	NEGATIVE	164.0	NK
28278T	T	T3AN0MX	Negative	none	nf	n	7.0	50s	M	U	4.0	N/A	N/A	NO	157.0	None
29671T	T	T3AN0MX	Negative	slow	nf	y	7.0	60s	M	W	8.9	17.4	15.4	NEGATIVE	155.0	NK
29825T	T	T3aN0MX	Negative	none	nf	n	7.0	50s	M	W	12.0	N/A	N/A	NEGATIVE	159.0	None
2HB568T	T	T3bN0MX	Negative	fast	f	y	7.0	60s	M	W	5.7	24.1	3.9	NEGATIVE	70.3	ADT, RT
2HB591T	T	T3bN1MX	Negative	fast	f	y	7.0	60s	M	W	18.3	1.5	3.8	POSITIVE FOR BONE AND HEPATIC METASTASIS	47.0	ADT, CHEMO
21B483T	T	T2bN0MX	Negative	fast	f	y	7.0	50s	M	W	6.2	1.7	1.9	NO	58.0	ADT, CHEMO
2K98-8378T	T	T3AN0MX	Positive	none	nf	n	7.0	60s	M	W	8.6	N/A	N/A	NO	158.0	None
33PR053T	T	T3bN1MX	Negative	fast	f	y	8.0	60s	M	W	21.0	1.0	0.4	bone metastasis	16.0	CHEMO
34PR227T	T	T3bN0MX	Negative	none	nf	n	7.0	60s	M	W	11.6	N/A	N/A	NO	123.0	None
34T	T	T2CN0MX	Positive	none	nf	n	7.0	50s	M	U	3.6	N/A	N/A	NO	159.0	None
3D994336T	T	T2bN0MX	Negative	none	nf	n	6.0	60s	M	W	6.6	N/A	N/A	NEGATIVE	164.0	None
3G989122T	T	T2bN0MX	Negative	none	nf	n	7.0	50s	M	W	9.0	N/A	N/A	NO	164.0	None
3K5772T	T	T3bN0MX	Negative	none	nf	n	7.0	60s	M	U	6.7	N/A	N/A	NO	160.0	None
3M-11462T	T	T3aN0MX	Negative	none	nf	n	7.0	50s	M	W	22.0	N/A	N/A	NEGATIVE	158.0	None
3Q-10614T	T	T3bN0MX	Negative	none	nf	n	7.0	70s	M	W	12.5	N/A	N/A	NO	77.0	None
4308T	T	T1CN0MX	Negative	none	nf	n	6.0	60s	M	W	12.4	N/A	N/A	NO	153.0	None

TABLE 7-continued

Clinical and pathological characteristics of 213 cases of prostate cancer from UPMC cohort

Sample	Type	TNM	Margin	Recurrence	Recurrence fast	Recurrence simple	Gleason	Age	Sex	Race	PSA pre-operative	Time to progession (Months)	PSADT (months)	Radiology follow-up	Length of follow-up (Months)	Additional Treatment
4336T	T	T1cN0MX	Positive	slow	nf	y	6.0	60s	M	W	2.5	21.7	22.0	NEGATIVE	165.0	NK
4L98-27086T	T	T3aN0MX	Negative	none	nf	n	7.0	60s	M	W	12.2	N/A	N/A	NO	78.0	None
5396T	T	T2bN1MX	Negative	none	nf	n	9.0	60s	M	W	8.9	N/A	N/A	NO	156.0	None
54IB289T	T	T2bN0MX	Negative	none	nf	n	6.0	50s	M	W	9.6	N/A	N/A	not done	89.0	None
562T	T	T2bN0MX	Negative	none	nf	n	6.0	60s	M	W	11.3	N/A	N/A	NO	157.0	None
56FB76T	T	T3bN0MX	Negative	none	nf	n	6.0	60s	M	W	6.6	N/A	N/A	not done	137.0	None
6647T	T	T3AN0MX	Negative	none	nf	y	7.0	40s	M	AA	6.1	95.6	45.5	NEGATIVE	150.0	NK
678T	T	T2bN0MX	Negative	none	nf	n	7.0	60s	M	W	5.3	N/A	N/A	NO	152.0	None
67R13T	T	T2bN0MX	Negative	none	nf	n	6.0	60s	M	W	10.8	N/A	N/A	NO	145.0	None
6837T	T	T3aN0MX	Negative	slow	nf	y	6.0	70s	M	W	10.4	87.4	15.4	NEGATIVE	155.0	NK
7221T	T	T3bN0MX	Negative	fast	f	y	7.0	50s	M	W	13.5	16.6	2.4	POSITIVE FOR BONE REETASTASIS	124.0	ADT, CHEMO, RT
7270T	T	T3BN1MX	Negative	none	nf	n	9.0	70s	M	W	15.9	N/A	N/A	NO	98.0	None
7504T	T	T3bN0MX	Positive	none	nf	n	9.0	70s	M	U	10.5	N/A	N/A	NO	143.0	None
78HB340T	T	T3bN0MX	Negative	ND	ND	ND	7.0	60s	M	W	9.6	N/A	N/A	not done	14.0	None
7943T	T	T3AN0MX	Positive	none	nf	n	7.0	60s	M	W	9.6	N/A	N/A	NO	137.0	None
828142T	T	T2bN0MX	Negative	none	nf	n	8.0	60s	M	W	7.4	N/A	N/A	NO	160.0	None
832972T	T	T2bN0MX	Negative	none	nf	n	10.0	60s	M	W	7.5	N/A	N/A	NO	160.0	None
842620T	T	T2bN0MX	Negative	none	nf	n	7.0	60s	M	W	7.7	N/A	N/A	NO	159.0	None
8432T	T	T2aN0MX	Positive	none	nf	n	7.0	50s	M	W	6.6	N/A	N/A	NO	166.0	None
84375T	T	T2bN0MX	Negative	none	nf	n	6.0	60s	M	W	6.8	N/A	N/A	NO	161.0	None
84876T	T	T2bN0MX	Negative	none	nf	n	7.0	60s	M	W	8.9	N/A	N/A	NO	160.0	None
849731T	T	T2bN0MX	Negative	none	nf	n	7.0	50s	M	W	6.1	N/A	N/A	NO	153.0	None
855327T	T	T2bN0MX	Negative	none	nf	n	6.0	60s	M	W	9.1	N/A	N/A	NO	137.0	None
8629T	T	T1CN0MX	Negative	none	nf	n	6.0	50s	M	W	6.5	N/A	N/A	NO	163.0	None
863176T	T	T3bN0MX	Negative	none	nf	n	8.0	60s	M	W	11.7	1.4	1.0	NO	151.0	ADT, CHEMO
8712362T	T	T2bN0MX	Negative	none	nf	n	8.0	50s	M	W	10.4	N/A	N/A	NO	155.0	None
8713205T	T	T2bN0MX	Negative	slow	nf	y	10.0	60s	M	W	8.3	12.0	18.3	NO	161.0	NK
8741T	T	T2bN0MX	Negative	none	nf	n	6.0	60s	M	W	9.1	N/A	N/A	NO	151.0	None
8433T	T	T3bN0MX	Negative	none	nf	n	8.0	60s	M	W	9.6	N/A	N/A	NO	160.0	None
9122T	T	T1CN0MX	Negative	none	nf	n	7.0	50s	M	W	13.0	N/A	N/A	NO	164.0	None
9210207T	T	T3bN0MX	Negative	slow	nf	y	8.0	60s	M	W	14.6	20.0	3.2	NO	105.0	NK
9217293T	T	T3bN0MX	Negative	slow	nf	y	8.0	60s	M	W	7.8	20.0	16.9	NO	132.0	NK
92SR293T	T	T2bN0MX	Negative	none	nf	n	6.0	50s	M	W	6.5	N/A	N/A	NO	155.0	None
9412443T	T	T3bN0MX	Negative	fast	f	y	8.0	50s	M	W	11.1	4.3	2.1	NO	78.0	ADT, CHEMO
9812033T	T	T2bN0MX	Negative	none	nf	n	6.0	50s	M	W	7.9	N/A	N/A	NO	165.0	None
9814481T	T	T3bN0MX	Negative	slow	nf	y	9.0	60s	M	W	11.3	38.0	21.0	NO	160.0	NK
98TA-83782T	T	T3bN0MX	Negative	none	nf	n	7.0	60s	M	W	13.2	N/A	N/A	NO	151.0	None
991199T	T	T3bN0MX	Negative	slow	nf	y	8.0	50s	M	W	15.5	15.0	24.0	NO	151.0	ADT, CHEMO
9927086T	T	T2BN0MX	Negative	none	nf	n	6.0	50s	M	W	9.5	N/A	N/A	NO	158.0	None
994308T	T	T1cN0MX	Negative	none	nf	n	6.0	60s	M	W	8.3	N/A	N/A	NO	160.0	None

TABLE 7-continued

Clinical and pathological characteristics of 213 cases of prostate cancer from UPMC cohort

Sample	Type	TNM	Margin	Recurrence	Recurrence fast	Recurrence simple	Gleason	Age	Sex	Race	PSA pre-operative	Time to progession (Months)	PSADT (months)	Radiology follow-up	Length of follow-up (Months)	Additional Treatment
995772T	T	T3bN0MX	Negative	none	nf	n	7.0	60s	M	W	8.7	N/A	N/A	NO	163.0	None
DB8237T	T	T2bN0MX	Negative	slow	nf	y	6.0	70s	M	W	6.3	46.0	26.0	NO	123.4	NK
FB120T	T	T3aN0MX	Negative	slow	nf	y	7.0	60s	M	W	61.1	1.3	20.8	NEGATIVE	94.9	NK
FB174T	T	T3aN0MX	Negative	fast	f	y	7.0	60s	M	W	6.9	30.5	3.2	NEGATIVE	94.7	ADT, CHEMO, RT
FB183T	T	T2cN0MX	Negative	slow	nf	y	7.0	60s	M	W	9.7	78.8	25.6	NO	99.1	NK
FB238T	T	T3bN0MX	Negative	slow	nf	y	7.0	60s	M	W	15.9	41.0	30.0	NO	101.7	NK
FB421T	T	T3aN0MX	Negative	fast	f	y	7.0	60s	M	W	4.5	1.3	4.4	POSITIVE FOR BONE METASTASIS	92.1	ADT
FB76T	T	T2cN0MX	Negative	none	nf	n	7.0	50s	M	W	6.5	N/A	N/A	not done	130.0	None
FB94T	T	T2cN0MX	Negative	slow	nf	y	7.0	60s	M	W	5.1	48.6	15.2	NEGATIVE	96.6	NK
GB195T	T	T2cN0MX	Negative	slow	nf	y	7.0	60s	M	W	10.1	53.2	23.8	NEGATIVE	65.2	RT
GB368T	T	T3aN0MX	Negative	slow	nf	y	7.0	50s	M	W	5.5	70.0	15.0	not done	112.0	None
GB400T	T	T3bN0MX	Negative	fast	f	y	7.0	60s	M	W	3.5	29.6	4.2	NEGATIVE	78.9	ADT, RT
HB021T	T	T2bN0MX	Negative	fast	f	y	6.0	50s	M	W	5.9	24.2	4.0	NEGATIVE	80.1	ADT, RT
HB033T	T	T2cN0MX	Negative	none	nf	n	7.0	50s	M	W	8.4	N/A	N/A	NO	87.0	None
HB207T	T	T3bN0MX	Negative	fast	f	y	9.0	60s	M	W	6.3	5.5	0.6	POSITIVE FOR BONE METASTASIS	74.7	ADT, CHEMO
HB235T	T	T3bN1MX	Negative	slow	nf	y	9.0	60s	M	W	4.6	1.3	20.8	POSITIVE FOR BONE METASTASIS	10.7	ADT, CHEMO
HB261T	T	T3aN0MX	Negative	none	nf	n	7.0	50s	M	W	5.4	N/A	N/A	NO	74.0	None
HB303T	T	T2cN0MX	Negative	none	nf	n	7.0	60s	M	W	31.3	N/A	N/A	not done	102.0	None
HB305T	T	T3bN0MX	Negative	fast	f	y	6.0	60s	M	W	10.1	1.4	3.9	NO	68.8	ADT, CHEMO
HB322T	T	T2cN0MX	Negative	none	nf	n	7.0	60s	M	W	4.9	N/A	N/A	not done	102.0	None
HB327T	T	T2cN0MX	Negative	none	nf	n	8.0	50s	M	W	9.5	N/A	N/A	not done	102.0	None
HB340T	T	T2cN0MX	Negative	ND	ND	ND	7.0	60s	M	W	9.6	N/A	N/A	not done	32.0	None
HB346T	T	T3aN0MX	Negative	none	nf	n	7.0	60s	M	W	17.2	N/A	N/A	not done	102.0	None
HB46T	T	T3bN0MX	Negative	slow	nf	y	8.0	60s	M	W	4.7	20.1	15.3	NO	69.1	NK
HB492T	T	T2cN0MX	Negative	slow	nf	y	7.0	50s	M	W	7.4	82.0	25.0	negative	99.0	None
HB504T	T	T3bN0MX	Positive	fast	f	y	8.0	50s	M	U	70.0	4.3	0.7	NEGATIVE	58.7	ADT, CHEMO
HB526T	T	T3bN0MX	Positive	fast	f	y	6.0	60s	M	W	8.7	1.4	2.7	POSITIVE FOR BONE METASTASIS	23.9	ADT, CHEMO
HB568T	T	T3bN0MX	Negative	fast	f	y	7.0	60s	M	W	4.4	22.4	4.2	NEGATIVE	68.2	ADT, RT
HB591T	T	T3bN1MX	Negative	fast	f	y	7.0	60s	M	W	17.6	1.3	3.6	POSITIVE FOR BONE AND HEPATIC METASTASIS	47.0	ADT, CHEMO
HB603T	T	T3aN1MX	Negative	slow	nf	y	7.0	60s	M	W	8.4	22.1	15.9	NO	70.7	
HB658T	T	T3bN0MX	Negative	none	nf	n	7.0	70s	M	W	20.6	N/A	N/A	not done	97.0	None
HB705T	T	T2cN0MX	Negative	none	nf	n	7.0	60s	M	W	9.8	N/A	N/A	not done	97.0	None
HB951T	T	T3bN1MX	Negative	fast	f	y	7.0	60s	M	W	23.1	15.9	4.0	POSITIVE FOR BONE AND HEPATIC METASTASIS	47.0	ADT, CHEMO

TABLE 7-continued

Clinical and pathological characteristics of 213 cases of prostate cancer from UPMC cohort

Sample	Type	TNM	Margin	Recurrence	Recurrence fast	Recurrence simple	Gleason	Age	Sex	Race	PSA pre-operative	Time to progession (Months)	PSADT (months)	Radiology follow-up	Length of follow-up (Months)	Additional Treatment
IB071T	T	T3aN0MX	Negative	fast	f	y	7.0	60s	M	W	2.6	4.3	1.6	POSITIVE FOR BONE METASTASIS	45.6	ADT, RT
IB110T	T	T2cN0MX	Negative	none	nf	n	8.0	60s	M	W	2.7	N/A	N/A	not done	94.0	None
IB111T	T	T2cN0MX	Negative	none	nf	n	7.0	60s	M	W	9.5	N/A	N/A	not done	94.0	None
IB112T	T	T3aN0MX	Negative	slow	nf	y	7.0	60s	M	W	4.7	55.8	30.6	NO	67.2	NK
IB134T	T	T3bN0MX	Negative	none	nf	n	9.0	70s	M	W	15.7	N/A	N/A	NO	77.0	None
IB136T	T	T3bN1MX	Negative	fast	f	y	8.0	50s	M	W	19.6	1.8	2.2	POSITIVE FOR BONE METASTASIS	69.2	ADT, CHEMO
IB180T	T	T2cN0MX	Negative	none	nf	n	7.0	60s	M	W	3.0	N/A	N/A	not done	93.0	None
IB273T	T	T2bN0MX	Negative	fast	f	y	7.0	50s	M	W	4.3	10.6	4.0	NEGATIVE	60.8	RT
IB289T	T	T2aN0MX	Negative	none	nf	n	7.0	60s	M	W	10.0	N/A	N/A	not done	91.0	None
IB298T	T	T3bN0MX	Negative	slow	nf	y	7.0	60s	M	W	5.3	34.3	20.4	NO	67.0	NK
IB362T	T	T3bN0MX	Negative	slow	nf	y	7.0	50s	M	W	18.9	4.6	16.0	NEGATIVE	65.2	RT
IB378T	T	T3bN0MX	Negative	none	nf	n	7.0	60s	M	W	2.8	N/A	N/A	not done	90.0	None
IB483T	T	T2bN0MX	Negative	fast	f	y	7.0	50s	M	W	5.2	1.4	1.7	NO	54.8	ADT, CHEMO
JB154T	T	T3bN0MX	Negative	fast	f	y	8.0	50s	M	U	70.0	3.5	0.9	NEGATIVE	58.7	ADT, CHEMO
JB197T	T	T3bN0MX	Positive	fast	f	y	7.0	50s	M	W	11.2	1.4	8.85 (death)	SINGLE FOCUS OF INCREASED ACTIVITY	48.4	ADT, CHEMO
JB426T	T	T2cN0MX	Negative	fast	f	y	7.0	60s	M	W	5.7	17.4	2.3	NEGATIVE	50.9	ADT, RT
JB770T	T	T2cN0MX	Negative	fast	f	y	8.0	60s	M	W	2.4	33.8	3.0	NEGATIVE	33.9	RT
KB170T	T	T3bN1MX	Negative	fast	f	y	7.0	70s	M	W	14.1	1.8	4.2	POSITIVE FOR NODAL METASTASIS	37.2	ADT
PR018ST	T	T3aN0MX	Positive	slow	nf	y	7.0	60s	M	W	9.0	78.0	55.0	NO	140.2	
PR053T	T	TURP	Negative	fast	f	y	TURP	60s	M	W	182.5	1.0	0.2	bone metastasis	15.0	ADT, CHEMO
PR079T	T	T3aN0MX	Positive	slow	nf	y	7.0	60s	M	W	5.1	95.3	17.3	NO	129.8	
PR227T	T	T2cN0MX	Negative	none	nf	n	7.0	60s	M	W	4.5	N/A	N/A	not done	135.0	None
PR236T	T	T3bN0MX	Negative	fast	f	y	10.0	60s	M	W	9.9	1.3	3.9	POSITIVE FOR BLASTIC METASTASIS	64.7	ADT, CHEMO
PR300T	T	T3bN1MX	Negative	fast	f	y	7.0	50s	M	W	20.3	71.5	3.9	NEGATIVE	98.5	NK
PR303T	T	T3bN0MX	Negative	slow	nf	y	6.0	70s	M	W	10.5	54.6	43.3	NO	79.7	NK
PR306T	T	T3bN0MX	Positive	slow	nf	y	7.0	60s	M	W	11.5	16.4	52.9	NEGATIVE	109.1	RT
PR310T	T	T3bN0MX	Negative	fast	f	y	7.0	60s	M	W	5.1	22.8	1.6	POSITIVE FOR BONE AND ILIAC METASTASIS	47.7	ADT, CHEMO, RT
PR375T	T	T3bN1MX	Negative	fast	f	y	7.0	50s	M	W	11.3	1.2	1.1	POSITIE FOR BONE AND PELVIC METASTASIS	114.9	ADT, CHEMO, RT
PR434T	T	T3aN0MX	Negative	slow	nf	y	7.0	60s	M	W	6.4	72.8	30.8	NO	137.6	RT
PR521T	T	T2bN0MX	Negative	slow	nf	y	7.0	50s	M	W	6.4	79.2	15.5	NO	126.2	RT
PR530T	T	T2cN0MX	Negative	ND	ND	ND	7.0	60s	M	W	4.4	N/A	N/A	Not Done	25.0	None
PR534T	T	T2bN0MX	Negative	none	nf	n	6.0	60s	M	W	8.4	N/A	N/A	not done	13.0	None

TABLE 7-continued

Clinical and pathological characteristics of 213 cases of prostate cancer from UPMC cohort

Sample	Type	TNM	Margin	Recurrence	Recurrence fast	Recurrence simple	Gleason	Age	Sex	Race	PSA pre-operative	Time to progession (Months)	PSADT (months)	Radiology follow-up	Length of follow-up (Months)	Additional Treatment
PR536T	T	T2bN0MX	Negative	none	nf	n	7.0	50s	M	W	5.4	N/A	N/A	not done	136.0	None
R10T	T	T3bN0MX	Negative	fast	f	y	8.0	60s	M	W	13.1	11.0	2.3	NO	74.0	ADT, CHEMO
R13T	T	T3bN0MX	Negative	none	nf	n	7.0	60s	M	W	10.4	N/A	N/A	NO	157.0	None
R16T	T	T2bN0MX	Negative	none	nf	n	7.0	50s	M	W	5.8	N/A	N/A	NO	159.0	None
R18T	T	T2bN0MX	Negative	none	nf	n	7.0	50s	M	W	9.1	N/A	N/A	NO	163.0	None
R19T	T	T3bN0MX	Negative	slow	nf	y	9.0	60s	M	W	13.8	2.0	1.1	NO	60.0	ADT, CHEMO
R26T	T	T3aN0MX	Negative	none	nf	n	7.0	60s	M	W	7.7	N/A	N/A	NO	146.0	None
R3T	T	T2bN0MX	Negative	none	nf	n	7.0	60s	M	W	7.1	N/A	N/A	NO	137.0	None
R57T	T	T3bN0MX	Negative	none	nf	n	7.0	50s	M	W	8.8	N/A	N/A	NO	107.0	None
R59T	T	T3bN0MX	Negative	none	nf	n	7.0	60s	M	W	9.8	N/A	N/A	NO	127.0	None
R61T	T	T3bN0MX	Negative	none	nf	n	7.0	60s	M	W	12.5	N/A	N/A	NO	160.0	None
SR9R57T	T	T2bN0MX	Negative	none	nf	n	7.0	60s	M	W	7.2	N/A	N/A	NO	161.0	None
TP08PP-S0721T	T	T3bN1MX	Negative	fast	f	y	9.0	50s	M	W	20.2	1.3	1.1	POSITIVE FOR BONE METASTASIS	17.0	ADT, CHEMO
TP08-S00530T	T	T3bN0MX	Negative	fast	f	y	7.0	60s	M	W	11.1	1.3	3.3	NEW LEFT EXTERNAL ILIAC LYMPH NODE; NO METASTASIS	37.2	ADT
TP08-S00542T	T	T2cN0MX	Negative	fast	f	y	7.0	50s	M	W	4.3	1.9	3.6	POSITIVE FOR BLASTIC AND HEPATIC METASTASIS	30.6	RT
TP09-S0006T	T	T3bN1MX	Negative	fast	f	y	8.0	50s	M	W	4.9	4.6	1.2	NEW SCLEROTIC FOCUS @T12	27.1	ADT
TP09-S0420T	T	T3bN1MX	Negative	fast	f	y	7.0	50s	M	W	14.6	1.4	3.7	NEGATIVE	29.1	ADT
TP09-S0704T	T	T4N1MX	Negative	fast	f	y	9.0	60s	M	W	55.0	29.3	1.9	not done	67.0	ADT, CHEMO
TP09-S0721T	T	T3bN1MX	Negative	fast	f	y	10.0	50s	M	W	29.3	1.4	0.9	POSITIVE FOR BONE METASTASIS	15.5	ADT, CHEMO
TP10PP-S0420T	T	T3bN1MX	Negative	fast	f	y	7.0	50s	M	W	15.8	1.7	3.3	NEGATIVE	30.6	ADT
TP10-S0638T	T	T3bN1MX	Negative	fast	f	y	10.0	50s	M	W	9.2	1.4	1.8	POSITIVE FOR BONE METASTASIS	149.6	ADT
TP10-S093T	T	T3aN0MX	Negative	slow	nf	y	7.0	60s	M	W	4.1	43.8	40.0	NO	133.3	RT
TP11PP-S0638T	T	T3bN1MX	Negative	fast	f	y	9.0	50s	M	W	11.3	1.6	1.9	POSITIVE FOR BONE METASTASIS	137.0	ADT
TP12-S0048T	T	T3aN0MX	Negative	ND	ND	ND	8.0	70s	M	W	7.9	ND	ND	Not Done	23.0	None
TP12-S0049T	T	T2cN0MX	Negative	ND	ND	ND	7.0	60s	M	W	13.6	ND	ND	Not Done	23.0	None
TP12-S0102T	T	T3aN1MX	Negative	ND	ND	ND	7.0	60s	M	W	10.7	ND	ND	Not Done	23.0	None
TP12-	T	T3aN0MX	Negative	ND	ND	ND	7.0	50s	M	W	4.2	ND	ND	Not Done	22.0	None

TABLE 7-continued

Clinical and pathological characteristics of 213 cases of prostate cancer from UPMC cohort

Sample	Type	TNM	Margin	Recurrence	Recurrence fast	Recurrence simple	Gleason	Age	Sex	Race	PSA pre-operative	Time to progession (Months)	PSADT (months)	Radiology follow-up	Length of follow-up (Months)	Additional Treatment
S0191T																
TP12-S0194T	T	T2cN0MX	Negative	ND	ND	ND	7.0	50s	M	AA	7.3	ND	ND	Not Done	22.0	None
TP12-S0246T	T	T2cN1MX	Negative	ND	ND	ND	7.0	60s	M	W	3.9	ND	ND	Not Done	22.0	None
TP12-S0337T	T	T2aN1MX	Negative	fast	f	y	7.0	60s	M	W	13.8	1.4	0.3	Bone/CT Scan(s) - negative	33.0	ADT
TP12-S0340T	T	T3bN1MX	Negative	fast	f	y	9.0	60s	M	W	5.5	7.4	2.6	Not Done	33.0	ADT
TP12-S0456T	T	T3aN1MX	Negative	ND	ND	ND	8.0	60s	M	W	6.0	ND	ND	Not Done	20.0	None
TP12-S0466T	T	T3bN1MX	Negative	fast	f	y	8.0	50s	M	W	6.1	1.4	0.2	negative	22.0	ADT
TP12-S0608T	T	T3aN1MX	Negative	fast	f	y	8.0	60s	M	W	20.3	1.5	0.8	not done	19.0	ADT
TP12-S0624T	T	T3bN1MX	Negative	fast	f	y	7.0	70s	M	W	3.3	1.4	2.0	not done	19.0	none
TP12-S0704T	T	T3aN0MX	Negative	ND	ND	ND	7.0	50s	M	W	5.0	N/A	N/A	not done	17.0	none
TP12-S0723T	T	T2cN0MX	Negative	ND	ND	ND	7.0	60s	M	W	5.4	ND	ND	Not Done	16.0	None
TP12-S0740T	T	T3bN0MX	Negative	fast	f	y	9.0	50s	M	W	25.0	1.6	0.5	Bone/CT Scan(s) - negative	30.0	None
TP12-S0765T	T	T3aN0MX	Negative	ND	ND	ND	7.0	50s	M	W	5.0	ND	ND	Not Done	17.0	None
TP12-S0770T	T	T3aN0MX	Negative	ND	ND	ND	7.0	40s	M	W	9.0	ND	ND	Not Done	19.0	None
TP12-S0786T	T	T3bN1MX	Negative	fast	f	y	7.0	60s	M	W	4.5	1.3	0.6	not done	30.0	ADT
TP12-S0789T	T	T3bN1MX	Negative	ND	ND	ND	7.0	60s	M	W	10.6	ND	ND	Not Done	17.0	None
TP12-S0790T	T	T3aN0MX	Negative	Fast	f	y	7.0	60s	M	W	24.2	11.7	3.7	Not Done	29.0	None
TP12-S0795T	T	T2cN0MX	Negative	ND	ND	ND	7.0	50s	M	W	2.4	ND	ND	Not Done	17.0	None
TP12-S0799T	T	T3aN0MX	Negative	ND	ND	ND	7.0	50s	M	W	6.4	ND	ND	CT Scan(s) - negative	17.0	None
TP12-S0803T	T	T2cNXMX	Negative	ND	ND	ND	7.0	60s	M	W	unknown	ND	ND	Not Done	17.0	None
TP12-S0805T	T	T2cN0MX	Negative	ND	ND	ND	7.0	50s	M	W	4.0	ND	ND	Not Done	22.0	None
TP12-S0816T	T	T3aN0MX	Negative	ND	ND	ND	7.0	50s	M	W	6.5	ND	ND	Not Done	17.0	None
TP12-S0915T	T	T3aNXMX	Negative	ND	ND	ND	7.0	60s	M	W	5.0	ND	ND	Not Done	16.0	None
TP12-S0916T	T	T3aN0MX	Negative	ND	ND	ND	7.0	60s	M	W	5.0	N/A	N/A	not done	16.0	none

TABLE 7-continued

Clinical and pathological characteristics of 213 cases of prostate cancer from UPMC cohort

Sample	Type	TNM	Margin	Recurrence	Recurrence fast	Recurrence simple	Gleason	Age	Sex	Race	PSA pre-operative	Time to progession (Months)	PSADT (months)	Radiology follow-up	Length of follow-up (Months)	Additional Treatment
TP12-S0918T	T	T3bN1MX	Negative	fast	f	y	9.0	70s	M	W	6.8	0.9	2.2	CT Scan(s) - negative	28.0	ADT
TP12-S0928T	T	T3aN0MX	Negative	ND	ND	ND	7.0	60s	M	W	5.3	ND	ND	Not Done	16.0	None
TP12-S0943T	T	T3aN1MX	Negative	fast	f	y	9.0	50s	M	W	10.3	9.1	3.1	Not Done	28.0	None
TP12-S0954T	T	T3bN0MX	Negative	fast	f	y	7.0	60s	M	W	15.7	1.5	0.4	not done	16.0	None
TP12-S0966T	T	T3aN0MX	Negative	ND	ND	ND	7.0	50s	M	W	12.2	ND	ND	Not Done	16.0	None
TP12-S0967T	T	T3aN0MX	Negative	ND	ND	ND	7.0	60s	M	W	6.0	N/A	N/A	Not Done	14.0	None
TP12-S0981T	T	T3bN0MX	Negative	ND	ND	ND	7.0	60s	M	W	56.4	ND	ND	Not Done	16.0	None
TP12-S0988T	T	T3aN0MX	Negative	ND	ND	ND	7.0	60s	M	W	16.6	ND	ND	Not Done	13.0	None
TP12-S1032T	T	T3aN0MX	Negative	ND	ND	ND	7.0	60s	M	W	9.2	ND	ND	Not Done	141.0	None
TP12-S1059T	T	T3aN0MX	Negative	fast	f	y	8.0	60s	M	W	10.6	1.3	0.4	not done	15.0	none
TP12-S1189T	T	T2cN0MX	Negative	ND	ND	ND	7.0	60s	M	W	18.5	ND	ND	Not Done	15.0	None
TP12-S1197T	T	T2cN0MX	Negative	ND	ND	ND	7.0	70s	M	W	5.0	ND	ND	Not Done	14.0	None
TP12-S1224T	T	T2cN0MX	Negative	ND	ND	ND	7.0	60s	M	W	4.9	ND	ND	Not Done	16.0	None
TP13-S0043T	T	T3aN0MX	Negative	fast	f	y	8.0	60s	M	W	22.0	1.5	0.2	NO	12.0	None
TP13-S0109T	T	T3bN1MX	Negative	fast	f	y	8.0	70s	M	W	21.5	1.6	1.1	NO	12.0	None
TP13-S0248T	T	T3bN1MX	Negative	fast	f	y	8.0	60s	M	W	6.8	2.1	0.5	NO	11.0	ADT
TP13-S0314T	T	T3aN0MX	Negative	fast	f	y	7.0	60s	M	W	3.6	7.8	2.0	NO	9.0	None
TP13-S0456T	T	T3aN0MX	Negative	fast	f	y	9.0	50s	M	W	29.9	1.9	1.9	NO	7.0	None
TP13-S0464T	T	T3bN1MX	Negative	fast	f	y	9.0	50s	M	W	10.0	1.1	0.3	NO	7.0	None

f-PSADT ≤ 4 months;
nf-PSADT ≥ 15 months;
y—yes;
n—no;
ADT—androgen deprivation therapy;
RT—radiation therapy;
Chemo—chemotherapy;
ND—not determined.

TABLE 8

Clinical and pathological characteristics of 30 cases of prostate cancer from Stanford cohort.

Sample	Age	Ethnicity	Preop RX	Pre-PSA	T	N	M	Path Grade	Angio	Margins
PC 19T	50s	Caucasian	None	4.42	T3a	N1	M0	4 + 5	Yes	Negative
PC 252T	60s	Caucasian	None	42	T4	N0	M0	3 + 4	Unknown	Positive
PC 265T	50s	African American	None	4.53	T2b	N0	M0	4 + 4	Unknown	Negative
PC 452T	60s	Caucasian	None	5.12	T2b	N0	M0	4 + 3	Unknown	Negative
PC 366T	50s	African American	Horm	4.01	T3b	N0	M0	4 + 3	Unknown	Negative
PC 538T	60s	Caucasian	None	10.7	T2b	N0	M0	3 + 4	No	Negative
PC 47T	50s	Caucasian	None	9.92	T2b	N0	M0	3 + 4	Unknown	Negative
PC 97T	50s	Caucasian	None	4.1	T2b	N0	M0	4 + 3	Unknown	Negative
PC 370T	50s	Caucasian	None	10.76	T3b	N1	M0	4 + 4	Yes	Negative
PC 405T	60s	Caucasian	None	15.44	T2b	N1	M0	3 + 4	Unknown	Negative
PC 448T	60s	Caucasian	None	7.1	T3b	N0	M0	3 + 4	Unknown	Negative
PC 485T	60s	Caucasian	None	5.91	T2b	N0	M0	3 + 4	Yes	Negative
PC 498T	50s	Caucasian	None	4.68	T2b	N0	M0	3 + 3	Unknown	Negative
PC 551T	40s	Caucasian	None	4.8	T2b	N0	M0	3 + 3	Unknown	Negative
PC 494T	60s	Caucasian	None	2.38	T2b	N0	M0	3 + 4	Unknown	Negative
PC 629T	70s	African American	None	3.2	T2b	N0	M0	3 + 3	Unknown	Negative
PC 643T	60s	Caucasian	None	7.16	T2b	N0	M0	3 + 4	No	Negative
PC 646T	60s	Caucasian	None	4.9	T2b	N0	M0	3 + 4	Unknown	Negative
PC 473T	60s	Asian	None	4.64	T2b	N0	M0	3 + 4	Unknown	Negative
PC 470T	70s	Caucasian	None	6.8	T2b	N0	M0	3 + 4	Unknown	Negative
PC 482T	70s	Caucasian	None	2.84	T2b	N0	M0	3 + 3	Unknown	Negative
PC 15T	40s	Caucasian	None	5.12	T2b	N0	M0	3 + 3	Unknown	Negative
PC 501T	60s	Caucasian	None	3.93	T2b	N0	M0	4 + 3	Unknown	Negative
PC 274T	60s	Caucasian	None	3.9	T2b	N0	M0	3 + 4	Unknown	Positive
PC 343T	60s	Caucasian	None	10.77	T2b	N0	M0	3 + 3	Unknown	Negative
PC 599T	40s	Caucasian	None	8.9	T2b	N0	M0	3 + 4	Unknown	Negative
PC 45T	50s	Caucasian	None	6.58	T2b	N0	M0	3 + 4	No	Negative
PC 86T	60s	Caucasian	None	2.1	T2b	N0	M0	3 + 4	Unknown	Negative
PC 99T	70s	Hispanic	None	6.26	T2b	N0	M0	3 + 4	Unknown	Negative
PC 85T	40s	Caucasian	None	4.8	T2a	N0	M0	3 + 4	Unknown	Positive

Sample	Months followup	Recurrence	Months to recurrent	PSADT	Relapse	Relapse fast	Relapse simple
PC 19T	116.2	Biochemical	19.13333333	4.11	fast	f	y
PC 252T	22.86666667	Biochemical	10.2	3.85	fast	f	y
PC 265T	20.76666667	Biochemical	2.77	3.89	fast	f	y
PC 452T	89.3	Biochemical	19.17	4.32	fast	f	y
PC 366T	82.7	Biochemical	12.33	9.04	Intermediate	nf	y
PC 538T	73	Biochemical	24.86666667	8.55	Intermediate	nf	y
PC 47T	64.66666667	Biochemical	37.6	98.58	slow	nf	y
PC 97T	117	Biochemical	61.13333333	>20	slow	nf	y
PC 370T	68.8	Biochemical	15.83	21.89	slow	nf	y
PC 405T	40.06666667	Biochemical	2.5	>20	slow	nf	y
PC 448T	72	Biochemical	35.63	>20	slow	nf	y
PC 485T	71.6	Biochemical	49.7	20.69	slow	nf	y
PC 498T	50.66666667	None	ND	n/a	ND	ND	ND
PC 551T	47.6	None	ND	n/a	ND	ND	ND
PC 494T	41.43333333	None	ND	n/a	ND	ND	ND
PC 629T	48.3	None	ND	n/a	ND	ND	ND
PC 643T	43.8	None	ND	n/a	ND	ND	ND
PC 646T	49	None	ND	n/a	ND	ND	ND
PC 473T	52.83333333	None	ND	n/a	ND	ND	ND
PC 470T	47.86666667	None	ND	n/a	ND	ND	ND
PC 482T	45.9	None	ND	n/a	ND	ND	ND
PC 15T	118	None	>60	n/a	none	nf	n
PC 501T	74.6	None	>60	n/a	none	nf	n
PC 274T	105.5	None	>60	n/a	none	nf	n
PC 343T	61.96666667	None	>60	n/a	none	nf	n
PC 599T	61.3	None	>60	n/a	none	nf	n
PC 45T	118.1	None	>60	n/a	none	nf	n

TABLE 8-continued

Clinical and pathological characteristics of 30 cases of prostate cancer from Stanford cohort.

PC 86T	105.6	None	>60	n/a	none	nf	n
PC 99T	120.6	None	>60	n/a	none	nf	n
PC 85T	98	None	>60	n/a	none	nf	n

f-PSADT ≤ 4 months;
nf-PSADT ≥ 5 months;
y—yes;
n—no;
ADT—androgen deprivation therapy;
RT—radiation therapy
Chemo—chemotherapy;
ND-not determined.

TABLE 9

Clinical and pathological characteristics of 36 cases of prostate cancer from Wisconsin cohort.

Sample ID	Age	Stage	Margin	Pre-operational PSA	Grade	PSA recurrence
W1	60s	T1C	+, and lymph node	12	3 + 3	yes
W2	50s	T1C	–	4.5	3 + 4	no
W3	50s	T3a	+	2.9	3 + 4	yes
W4	70s	T3a	+	5	3 + 4	no
W5	50s	T2A	+	5.1	3 + 4	yes
W6	60s	T2A	+, and lymph node	4.13	4 + 5	yes
W7	60s	T1C	–	5.2	3 + 3	yes
W8	40s	T1C	–	7	4 + 4	no
W9	60s	T1C	–	4.95	3 + 4	yes
W10	40s	T1C	+, and lymph node	42	3 + 4	yes
W11	40s	unknown	+	5	4 + 3	yes
W12	60s	D0	–	6.3	4 + 5	yes
W13	60s	unknown	–	4.3	3 + 4	yes
W14	50s	T2B	–	2.5	3 + 3	no
W15	70s	T2B	–	7.9	4 + 3	yes
W16	60s	T3A	+	4.2	3 + 4	no
W17	60s	T2C	+	5	3 + 4	no
W18	60s	T2C	+	5.6	3 + 4	yes
W19	60s	T2C	–	unknown	4 + 3	no
W20	60s	T2C	+	4.47	3 + 4	no
W21	60s	T2A	–	4	3 + 3	no
W22	60s	T3B	+	6.7	3 + 4	yes
W23	50s	T2C	–	5.7	3 + 4	no
W24	50s	T3A	–	5	3 + 4	no
W25	50s	T2C	–	5.4	3 + 4	no
W26	60s	T2C	–	4.6	3 + 4	no
W27	50s	T2C	–	4.1	3 + 3	no
W28	unknown	unknown	unknown	unknown	4 + 4	ND
W29	60s	T2C	+	4.6	3 + 4	no
W30	60s	unknown	unknown	unknown	5 + 5	no
W31	60s	T2c	–	4	4 + 5	Yes
W32	40s	T3b	+	27	4 + 5	Yes
W33	50s	unknown	unknown	unknown	4 + 4	Yes
W34	50s	T3b	+	3.7	4 + 5	Yes
W35	unknown	unknown	unknown	unknown	4 + 5	ND
W36	50s	unknown	unknown	unknown	4 + 4	ND

TABLE 10

The status of 8 fusion genes predicting prostate cancer recurrence on 90 training cohort from UPMC*.

Number of fusion	accuracy	sensitivity	specificity	Youden Inex
Panel of 8 fusion transcripts				
1	0.567	0.19	1	0.19
2	0.644	0.33	1	0.33
3	0.622	0.33	0.95	0.29
4	0.622	0.33	0.95	0.29

TABLE 10-continued

The status of 8 fusion genes predicting prostate cancer recurrence on 90 training cohort from UPMC*.

Number of fusion	accuracy	sensitivity	specificity	Youden Inex
5	0.644	0.38	0.95	0.33
6	0.711	0.5	0.95	0.45
7	0.689	0.5	0.91	0.40
8	0.711	0.58	0.89	0.47

TABLE 10-continued

The status of 8 fusion genes predicting prostate cancer recurrence on 90 training cohort from UPMC*.

Number of fusion	accuracy	sensitivity	specificity	Youden Inex
Panel of 8 fusion transcripts plus TMPRSS2-ERG				
1	0.589	0.42	0.79	0.20
2	0.622	0.48	0.79	0.27
3	0.6	0.48	0.74	0.22
4	0.6	0.48	0.74	0.22
5	0.611	0.5	0.74	0.24
6	0.656	0.58	0.74	0.32
7	0.633	0.58	0.69	0.27
8	0.656	0.63	0.69	0.32

*Using any fusion transcript as cutoff.

TABLE 11

The status of 8 fusion genes with or without TMPRSS2-ERG predicting prostate cancer recurrence*.

Cohort	accuracy	sensitivity	specificity
8 fusion transcript			
UPMC training	0.711	0.58	0.89
UPMC testing	0.705	0.51	0.95
Wisconsin	0.8	0.63	1
Stanford	0.762	0.67	0.89
Combined testing**	0.734	0.56	0.951
8 fusion transcript plus TMPRSS2-ERG			
UPMC training	0.656	0.63	0.69
UPMC testing	0.681	0.67	0.69
Wisconsin	0.767	0.69	0.86
Stanford	0.762	0.83	0.67
Combined testing**	0.712	0.70	0.73

*Using any fusion transcript as cutoff;
**Combining UPMC testing, Stanford and Wisconsin data set.

TABLE 12

Association of fusion transcript with clinical/pathological parameters.

	P value				
Fusion gene	Gleason	PSA (pre-operation)	Tumor stage	Lymph node	Nomogram
TMEM135-CCDC67	0.59	0.98	0.432	0.082	0.21
KDM4B-AC011523.2	0.64	0.726	0.688	0.588	0.588
MAN2A1-FER	0.781	0.721	0.679	0.140	1.07E−03
CCNH-C5orf30	0.14	0.313	0.254	0.059	0.156
TRMT11-GRIK2	0.012	0.227	5.38E−04	0.013	8.56E−03
SLC45A2-AMACR	0.566	0.441	0.022	0.181	0.015
MTOR-TP53BP1	0.993	0.57	0.731	1	0.775
LRRC59-FLJ60017	0.877	0.034	0.226	0.206	0.188
At least one	0.064	0.138	3.852e−3	4.77e−3	2.86E−04
TMPRSS2-ERG	0.869	0.306	0.642	0.042	0.325

TABLE 13

Gleason score prediction of recurrent status of 90 samples of UPMC training Cohort.

Score	accuracy	sensitivity	specificity	Youden index
6	0.5333333	1	0	0
7	0.6111111	0.95833333	0.2142857	0.17261905
8	0.6111111	0.39583333	0.8571429	0.25297619
9	0.5111111	0.16666667	0.9047619	0.07142857
10	0.4666667	0.02083333	0.9761905	−0.00297619

TABLE 14

Gleason score prediction of recurrent status of 229[!] samples of training and testing cohorts from UPMC, Stanford and Wisconsin*.

Cohort	accuracy	sensitivity	specificity
Gleason alone			
UPMC training	0.611	0.40	0.86
UPMC testing	0.602	0.41	0.85
Wisconsin	0.6	0.31	0.93
Stanford	0.571	0.25	1
Combined testing**	0.597	0.37	0.89
Gleason plus 8 fusion transcripts+			
UPMC training	0.722	0.65	0.81
UPMC testing	0.739	0.59	0.92
Wisconsin	0.9	0.81	1
Stanford	0.762	0.67	0.89
Combined testing**	0.777	0.65	0.94
Gleason plus 8 fusion transcripts plus TMPRSS2-ERG+			
UPMC training	0.644	0.73	0.55
UPMC testing	0.705	0.80	0.59
Wisconsin	0.833	0.88	0.79
Stanford	0.762	0.83	0.67
Combined testing**	0.741	0.82	0.65

*Using Gleason >=8 as cutoff;
+Using Gleason >=8 or presence of any fusion transcript as cutoff;
*Using <88 or presence of any fusion transcript or TMPRSS2-ERG as cutoff;
**Combining UPMC testing, Stanford and Wisconsin data set;
[!]Gleason score is not graded in one sample and not included in the analysis.

TABLE 15

Nomogram prediction of recurrent status of 90 samples of UPMC training Cohort.

Probability*	accuracy	sensitivity	specificity	Youden Index
0	0.4666667	0	1	0
1	0.4666667	0	1	0

TABLE 15-continued

Nomogram prediction of recurrent status of 90 samples of UPMC training Cohort.

Probability*	accuracy	sensitivity	specificity	Youden Index
2	0.4666667	0	1	0
3	0.4666667	0	1	0
4	0.4666667	0	1	0
5	0.4666667	0	1	0
6	0.4666667	0	1	0

TABLE 15-continued

Nomogram prediction of recurrent status of 90 samples of UPMC training Cohort.

Probability*	accuracy	sensitivity	specificity	Youden Index
7	0.4666667	0	1	0
8	0.4666667	0	1	0
9	0.4666667	0	1	0
10	0.4666667	0	1	0
11	0.4666667	0	1	0
12	0.4666667	0	1	0
13	0.4777778	0.02083333	1	0.02083333
14	0.4777778	0.02083333	1	0.02083333
15	0.4777778	0.02083333	1	0.02083333
16	0.4777778	0.02083333	1	0.02083333
17	0.4777778	0.02083333	1	0.02083333
18	0.4777778	0.02083333	1	0.02083333
19	0.4888889	0.04166667	1	0.04166667
20	0.4888889	0.04166667	1	0.04166667
21	0.4888889	0.04166667	1	0.04166667
22	0.4888889	0.04166667	1	0.04166667
23	0.4888889	0.04166667	1	0.04166667
24	0.4888889	0.04166667	1	0.04166667
25	0.5	0.0625	1	0.0625
26	0.5	0.0625	1	0.0625
27	0.5111111	0.08333333	1	0.08333333
28	0.5111111	0.08333333	1	0.08333333
29	0.5333333	0.125	1	0.125
30	0.5222222	0.125	0.97619048	0.10119048
31	0.5222222	0.125	0.97619048	0.10119048
32	0.5222222	0.125	0.97619048	0.10119048
33	0.5333333	0.14583333	0.97619048	0.12202381
34	0.5444444	0.16666667	0.97619048	0.14285714
35	0.5444444	0.16666667	0.97619048	0.14285714
36	0.5444444	0.16666667	0.97619048	0.14285714
37	0.5444444	0.16666667	0.97619048	0.14285714
38	0.5555556	0.1875	0.97619048	0.16369048
39	0.5555556	0.1875	0.97619048	0.16369048
40	0.5555556	0.1875	0.97619048	0.16369048
41	0.5555556	0.1875	0.97619048	0.16369048
42	0.5555556	0.1875	0.97619048	0.16369048
43	0.5777778	0.22916667	0.97619048	0.20535714
44	0.5888889	0.25	0.97619048	0.22619048
45	0.5888889	0.25	0.97619048	0.22619048
46	0.5888889	0.25	0.97619048	0.22619048
47	0.6	0.27083333	0.97619048	0.24702381
48	0.6	0.27083333	0.97619048	0.24702381
49	0.6	0.27083333	0.97619048	0.24702381
50	0.6111111	0.29166667	0.97619048	0.26785714
51	0.6111111	0.29166667	0.97619048	0.26785714
52	0.6111111	0.29166667	0.97619048	0.26785714
53	0.6222222	0.3125	0.97619048	0.28869048
54	0.6222222	0.3125	0.97619048	0.28869048
55	0.6222222	0.3125	0.97619048	0.28869048
56	0.6222222	0.3125	0.97619048	0.28869048
57	0.6333333	0.33333333	0.97619048	0.30952381
58	0.6444444	0.35416667	0.97619048	0.33035714
59	0.6444444	0.35416667	0.97619048	0.33035714
60	0.6555556	0.375	0.97619048	0.35119048
61	0.6555556	0.375	0.97619048	0.35119048
62	0.6555556	0.375	0.97619048	0.35119048
63	0.6444444	0.375	0.95238095	0.32738095
64	0.6333333	0.375	0.92857143	0.30357143
65	0.6333333	0.375	0.92857143	0.30357143
66	0.6444444	0.39583333	0.92857143	0.32440476
67	0.6555556	0.41666667	0.92857143	0.3452381
68	0.6555556	0.41666667	0.92857143	0.3452381
69	0.6555556	0.41666667	0.92857143	0.3452381
70	0.6777778	0.45833333	0.92857143	0.38690476
71	0.6777778	0.47916667	0.9047619	0.38392857
72	0.6777778	0.5	0.88095238	0.38095238
73	0.6888889	0.52083333	0.88095238	0.40178571
74	0.6888889	0.52083333	0.88095238	0.40178571
75	0.6888889	0.52083333	0.88095238	0.40178571
76	0.6888889	0.52083333	0.88095238	0.40178571
77	0.7	0.54166667	0.88095238	0.42261905
78	0.7	0.54166667	0.88095238	0.42261905
79	0.7	0.54166667	0.88095238	0.42261905
80	0.7111111	0.5625	0.88095238	0.44345238
81	0.7111111	0.5625	0.88095238	0.44345238
82	0.7111111	0.58333333	0.85714286	0.44047619
83	0.7	0.58333333	0.83333333	0.41666667
84	0.7	0.58333333	0.83333333	0.41666667
85	0.7111111	0.60416667	0.83333333	0.4375
86	0.7333333	0.64583333	0.83333333	0.47916667
87	0.7444444	0.66666667	0.83333333	0.5
88	0.7555556	0.6875	0.83333333	0.52083333
89	0.7333333	0.70833333	0.76190476	0.4702381
90	0.7222222	0.70833333	0.73809524	0.44642857
91	0.7111111	0.72916667	0.69047619	0.41964286
92	0.7	0.75	0.64285714	0.39285714
93	0.7111111	0.83333333	0.57142857	0.4047619
94	0.6777778	0.85416667	0.47619048	0.33035714
95	0.6888889	0.875	0.47619048	0.35119048
96	0.6777778	0.875	0.45238095	0.32738095
97	0.6222222	0.95833333	0.23809524	0.19642857
98	0.5444444	1	0.02380952	0.02380952
99	0.5333333	1	0	0
100	0.5333333	1	0	0

*Probability of PSA free survival for 5 years

TABLE 16

Nomogram prediction of recurrent status of 229[|]samples of training and testing cohorts from UPMC, Stanford and Wisconsin.

Cohort	accuracy	sensitivity	specificity
Nomogram alone*			
UPMC training	0.756	0.69	0.83
UPMC testing	0.75	0.80	0.69
Wisconsin	0.6	0.31	0.93
Stanford	0.619	0.38	1
Combined testing**	0.691	0.57	0.84
Nomogram plus 8 fusion transcripts[+]			
UPMC training	0.778	0.69	0.88
UPMC testing	0.807	0.76	0.87
Wisconsin	0.833	0.69	1
Stanford	0.81	0.75	0.89
Combined testing**	0.813	0.74	0.90
Nomogram plus 8 fusion transcripts plus TMPRSS2-ERG[+]			
UPMC training	0.656	0.63	0.69
UPMC testing	0.681	0.67	0.69
Wisconsin	0.767	0.69	0.86
Stanford	0.762	0.83	0.67
Combined testing**	0.719	0.62	0.84

*Using <88 as cutoff;

[+]Using <88 or any fusion transcript as cutoff;

[*]Using <88 or any fusion transcript or TMPRSS2-ERG as cutoff;

**Combining UPMC testing, Stanford and Wisconsin data set;

| -Gleason score is not graded in one sample and not included in the analysis.

TABLE 17

Putative fusion transcripts from benign prostate of healthy organ donors.

Fusion gene 1	Fusion_gene2	read pairs	Validation Status
SORBS1	RP11-476E15.3	25	
AHCY	RP11-292F22.3	25	
DCUN1D3	ERI2	12	
MACF1	KIAA0754	11	
C10orf68	CCDC7	11	RT-PCR and sequencing
RP11-166D19.1	BLID	7	
ASS1	ASS1P9	6	

TABLE 17-continued

Putative fusion transcripts from benign prostate of healthy organ donors.

Fusion gene 1	Fusion_gene2	read pairs	Validation Status
BACH1	BACH1-IT1	6	RT-PCR
MPDZ	RP11-272P10.2	5	
LIG3	RP5-837J1.2	4	
ACAD8	GLB1L3	4	RT-PCR
IGSF9B	RP11-259P6.1	3	
EYA1	RP11-1102P16.1	3	
TTC33	PRKAA1	3	RT-PCR
DNAH1	GLYCTK	3	
PSPC1	ZMYM5	3	
HSP90AB3P	RP11-759L5.2	3	
LSAMP	RP11-384F7.2	3	
RNF4	FAM193A	81	RT-PCR
AHCY	RP11-292F22.3	9	
LSAMP	RP11-384F7.2	8	
CBLL1	AC002467.7	4	
FNBP4	Y_RNA	4	
TBCE	RP11-293G6_A.2	4	
TRIM58	RP11-634B7.4	4	
DCUN1D3	ERI2	4	
PHPT1	MAMDC4	3	
TRIP6	SLC12A9	3	
NAT14	ZNF628	3	
TLL2	RP11-35J23.5	3	
UFSP2	Y_RNA	3	
TSPAN33	Y_RNA	3	
CADM3	DARC	3	
KIF27	RP11-213G2.3	3	
RABL6	KIAA1984	3	
ZNF615	ZNF350	3	
ZYG11A	RP4-631H13.2	3	
RP11-522L3.6	MTND4P32	3	
MTND3P10	AC012363.10	3	
RP11-464F9.1	BMS1P4	3	
RNF4	FAM193A	14	RT-PCR
GBP3	Y_RNA	3	
NACA	PRIM1	1	
AHCY	RP11-292F22.3	3	
GBP3	Y_RNA	3	
HARS2	ZMAT2	2	RT-PCR and sequencing
EED	C11orf73	1	RT-PCR
CNPY3	RP3-475N16.1	1	RT-PCR
RN7SL2	Metazoa_SRP	1	
SLC16A8	BAIAP2L2	2	RT-PCR
KLK4	KLKP1	2	RT-PCR and sequencing
ZNF137P	ZNF701	1	RT-PCR
AZGP1	GJC3	1	RT-PCR
USP7	RP11-252I13.1	1	
TRRAP	AC004893.11	1	
C6orf47	BAG6	1	RT-PCR
TTTY15	USP9Y	9	
AC005077.12	LINC00174	2	
ADCK4	NUMBL	2	
ZNF606	C19orf18	2	
SLC45A3	ELK4	3	RT-PCR and sequencing

6.6. References

1. Jemal A, Bray F, Center M M, Ferlay J, Ward E, Forman D. Global cancer statistics. *CA Cancer J Clin*. Feb. 4, 2012.
2. Siegel R, Naishadham D, Jemal A. Cancer statistics, 2012. *CA Cancer J Clin*. January-February 2012; 62(1):10-29.
3. Li H, Durbin R. Fast and accurate short read alignment with Burrows-Wheeler transform. *Bioinformatics*. Jul. 15, 2009; 25(14):1754-1760.
4. Trapnell C, Roberts A, Goff L, et al. Differential gene and transcript expression analysis of RNA-seq experiments with TopHat and Cufflinks. *Nat Protoc*. March 2012; 7(3):562-578.
5. Trapnell C, Williams B A, Pertea G, et al. Transcript assembly and quantification by RNA-Seq reveals unannotated transcripts and isoform switching during cell differentiation. *Nat Biotechnol*. May 2010; 28(5):511-515.
6. Trapnell C, Pachter L, Salzberg S L. TopHat: discovering splice junctions with RNA-Seq. *Bioinformatics*. May 1, 2009; 25(9):1105-1111.
7. Edgren H, Murumagi A, Kangaspeska S, et al. Identification of fusion genes in breast cancer by paired-end RNA-sequencing. *Genome Biol*. 12(1):R6.
8. Wei Zeng C-W F, Stefan Muller Arisona, Huamin Qu. Visualizing Interchange Patterns in Massive Movement Data. *Computer Graphics Forum*. 2013(32):271-280.
9. Luo R I, Yu Y P, Cieply K, et al. Gene expression analysis of prostate cancers. *Mol Carcinog*. January 2002; 33(1): 25-35.
10. Yu Y P, Landsittel D, Jing L, et al. Gene expression alterations in prostate cancer predicting tumor aggression and preceding development of malignancy. *J Clin Oncol*. Jul. 15, 2004; 22(14):2790-2799.
11. Ren B, Yu G, Tseng G C, et al. MCMI amplification and overexpression are associated with prostate cancer progression. *Oncogene*. Feb. 16, 2006; 25(7):1090-1098.
12. Yu Y P, Yu G, Tseng G, et al. Glutathione peroxidase 3, deleted or methylated in prostate cancer, suppresses prostate cancer growth and metastasis. *Cancer Res*. Sep. 1, 2007; 67(17):8043-8050.
13. Tomlins S A, Rhodes D R, Perner S, et al. Recurrent fusion of TMPRSS2 and ETS transcription factor genes in prostate cancer. *Science*. Oct. 28, 2005; 310(5748):644-648.
14. Berger M F, Lawrence M S, Demichelis F, et al. The genomic complexity of primary human prostate cancer. *Nature*. February 10; 470(7333):214-220.
15. Baca S C, Prandi D, Lawrence M S, et al. Punctuated evolution of prostate cancer genomes. *Cell*. April 25; 153(3):666-677.
16. Freedland S J, Humphreys E B, Mangold L A, et al. Death in patients with recurrent prostate cancer after radical prostatectomy: prostate-specific antigen doubling time subgroups and their associated contributions to all-cause mortality. *J Clin Oncol*. May 1, 2007; 25(13):1765-1771.
17. Antonarakis E S, Zahurak M L, Lin J, Keizman D, Carducci M A, Eisenberger M A. Changes in PSA kinetics predict metastasis-free survival in men with PSA-recurrent prostate cancer treated with nonhormonal agents: combined analysis of 4 phase II trials. *Cancer*. March 15; 118(6):1533-1542.
18. Sinclair P B, Sorour A, Martineau M, et al. A fluorescence in situ hybridization map of 6q deletions in acute lymphocytic leukemia: identification and analysis of a candidate tumor suppressor gene. *Cancer Res*. Jun. 15, 2004; 64(12):4089-4098.
19. Misago M, Liao Y F, Kudo S, et al. Molecular cloning and expression of cDNAs encoding human alpha-mannosidase II and a previously unrecognized alpha-mannosidase IIx isozyme. *Proc Natl Acad Sci USA*. Dec. 5, 1995; 92(25):11766-11770.
20. Krolewski J J, Lee R, Eddy R, Shows T B, Dalla-Favera R. Identification and chromosomal mapping of new human tyrosine kinase genes. *Oncogene*. March 1990; 5(3):277-282.
21. Prakash T, Sharma V K, Adati N, Ozawa R, Kumar N, Nishida Y, Fujikake T, Takeda T, Taylor T D: Expression

of conjoined genes: another mechanism for gene regulation in eukaryotes, PLoS One 2010, 5:e13284.

22. Youden W J: Index for rating diagnostic tests, Cancer 1950, 3:32-35.
23. Robin X, Turck N, Hainard A, Tiberti N, Lisacek F, Sanchez J C, Muller M: pROC: an open-source package for R and S+ to analyze and compare ROC curves, BMC Bioinformatics 12:77.
24. Towns W L, Begley T J: Transfer RNA methytransferases and their corresponding modifications in budding yeast and humans: activities, predications, and potential roles in human health, DNA Cell Biol 2012, 31:434-454.
25. Misago M, Liao Y F, Kudo S, Eto S, Mattei M G, Moremen K W, Fukuda M N: Molecular cloning and expression of cDNAs encoding human alpha-mannosidase II and a previously unrecognized alphamannosidase IIx isozyme, Proc Natl Acad Sci USA 1995, 92:11766-11770.
26. Fisher R P, Morgan D O: A novel cyclin associates with M015/CDK7 to form the CDK-activating kinase, Cell 1994, 78:713-724.
27. Yang H, Rudge D G, Koos J D, Vaidialingam B, Yang H J, Pavletich N P: mTOR kinase structure, mechanism and regulation, Nature 2013, 497:217-223.
28. Wang H, Luo K, Tan L Z, Ren B G, Gu L Q, Michalopoulos G, Luo J H, Yu Y P: p53-induced gene 3 mediates cell death induced by glutathione peroxidase 3, J Biol Chem 2012, 287:16890-16902.
29. Zhen Y, Sorensen V, Skjerpen C S, Haugsten E M, Jin Y, Walchli S, Olsnes S, Wiedlocha A: Nuclear import of exogenous FGF1 requires the ER-protein LRRC59 and the importins Kpnalphal and Kpnbeta1, Traffic 2012, 13:650-664.
30. Yang J, Jubb A M, Pike L, Buffa F M, Turley H, Baban D, Leek R, Gatter K C, Ragoussis J, Harris A L: The histone demethylase JMJD2B is regulated by estrogen receptor alpha and hypoxia, and is a key mediator of estrogen induced growth, Cancer Res 70:6456-6466.
31. Savolainen K, Kotti T J, Schmitz W, Savolainen T I, Sormunen R T, Ilves M, Vainio S J, Conzelmann E, Hiltunen J K: A mouse model for alpha-methylacyl-CoA racemase deficiency: adjustment of bile acid synthesis and intolerance to dietary methyl-branched lipids, Hum Mol Genet 2004, 13:955-965.

7. EXAMPLE 2: PTEN-NOLC1 FUSION GENES

Transcriptome sequencing was performed on 15 samples of prostate cancer from patients who experienced prostate cancer recurrence after radical prostatectomy. One of the candidate fusion gene transcripts is PTEN-NOLC1. To validate the fusion transcript, RT-PCRs using primers specific for PTEN-NOLC1 were performed on the prostate cancer sample that was positive for the fusion transcript, using the following primers:

(SEQ ID NO: 28)
5'-GCATTTGCAGTATAGAGCGTGC3'/

(SEQ ID NO: 29)
5'GTCTAAGAGGGAAGAGGCATTG3',

under the following conditions: 94° C. for 5', then 30 cycles of 94° C. for 10 seconds, 61° C. for 1 min and 72° C. for 3 min, followed by 10 min at 72° C. for extension. A 158 bp PCR product was generated. The PCR product was subsequently sequenced. PTEN-NOLC1 fusion transcript was confirmed (FIG. **13**A). To investigate the mechanism of PTEN-NOLC1 fusion transcript, Fluorescence In Situ Hybridizations (FISH) were performed using probes corresponding to 5'-end of PTEN genome (RP11-124B18) and 3'-end of NOLC1 genome (CTD-3082D22), respectively. In normal prostate epithelial cells, these 2 probes were hybridized to distinct separate locations in the genome due to more than 14 megabase separation of these 2 genes (FIG. **13**B). In contrast, these two signals appeared to merge to generate an overlapped signal in prostate cancer genome from a sample that is positive for PTEN-NOLC1 fusion transcript. Interestingly, non-fusion PTEN was virtually undetectable in this prostate cancer sample, suggesting that PTEN-NOLC1 fusion was accompanied with PTEN deletion in another allele. These results suggest that genome rearrangement is the underlying mechanism for PTEN-NOLC1 transcription. To investigate the clinical significance of PTEN-NOLC1 fusion, 215 prostate cancer samples were analyzed for PTEN-NOLC1 expression. Over 14% (31/215) prostate cancer samples were found to express PTEN-NOLC1 (FIG. **13**C). Among the positive samples, 77% (24/31, p=0.03) patients experienced prostate cancer recurrence. This indicates that PTEN-NOLC1 fusion is associated with poor clinical outcome. Interestingly, our analysis of lung adenocarcinoma, Glioblastoma multiforme, and hepatocellular carcinoma indicates that significant number of these cancers are also positive for PTEN-NOLC1 fusion: 35/38 glioblastoma multiformis, 3/20 hepatocellular carcinoma and 29/40 lung adenocarcinoma. These results suggest that PTEN-NOLC1 fusion may have broad implication for cancer development.

Expression of Pten-NOLC1 in NIH3T3 and PC3 Cells Increased Cell Growth.

To investigate whether PTEN-NOLC1 has pro-growth activity, we ligated PTEN-NOLC1 cDNA into pCDNA-FLAG vector to create pCDNA4-PTEN-NOLC1-FLAG. Subsequently, we transfected NIH3T3 and PC3 cells (a human prostate cancer cell line) with pCDNA4-PTEN-NOLC1-FLAG/pCDNA6. As shown in FIG. **27**B, induction of NIH3T3 and PC3 cells produces 10.3 ($p<0.01$) and 3.1 fold ($p<0.01$) increase of cell growth, respectively. These were accompanied with 2.3 fold ($p<0.01$) and 2.7 fold ($p<0.001$) increase of cell entry into S-phase in NIH3T3 and PC3 cells in cell cycle analysis (FIG. **27**C). Colony formation analyses indicate that expression of PTEN-NOLC1 produced 2.2 fold ($p<0.001$) higher numbers of colonies from single cell suspension for NIH3T3 cells than the un-induced controls and 2.7 fold ($p<0.01$) more colonies for PC3 cells when they were induced to express PTEN-NOLC1-FLAG (FIG. **27**D).

To investigate the subcellular localization of PTEN-NOLC1, NIH3T3 cells were transformed with pCDNA4-PTEN-NOLC1-FLAG/pCDNA6 were induced with tetracycline to express PTEN-NOLC1-FLAG. As shown in FIG. **27**A, most PTEN-NOLC1-FLAG was localized in the nucleus of the cells. This is contrary to cytoplasmic localization of PTEN. PTEN-NOLC1-FLAG was also detected in purified nucleus fraction. Without being bound to a particular theory, these results indicate that fusion formation with NOLC1 alters the subcellular localization of PTEN-NOLC1 from cytoplasm to nucleus.

8. EXAMPLE 3: THERAPEUTIC TARGETING AT FUSION TRANSCRIPT CONTAINING CHIMERA PROTEIN MAN2A1-FER

8.1. Results

MAN2A1-FER Likely Produces Activated FER Kinase.

MAN2A1-FER was present in prostate cancer, hepatocellular carcinoma and Glioblastoma multiforme. MAN2A1 is a Golgi enzyme required for conversion of high mannose to complex type structure of N-glycan for mature glycosylation of a membrane protein[1,2]. Little is known about its relation with human malignancies. On the other hand, FER, a tyrosine kinase, is a well-documented oncogene[3, 4]. Several studies showed that FER activate androgen receptor (AR) by phosphorylating Tyr223 in AR[5], and is essential for NFκB activation of EGFR[6]. Some studies indicate that FER is an essential component of stem cell tyrosine kinase 1 (STK1)[6] and mast cell growth factor receptor (kit)[7,8] signaling. Over-expression of FER is associated with poor clinical outcomes of breast cancer[9], renal cell carcinoma[10, 11], non-small cell lung cancer[12,13] and hepatocellular carcinoma[14]. The N-termini of many tyrosine protein kinases serve to constrain the kinase activity and are regulated by other molecules. Domains of some N-termini bind and select specific targets for the kinases. Removal of the N-terminus from a protein kinase may produce constitutively activated kinase activity that may alter the signaling pathways and generates uninhibited cell growth. The best analogy to MAN2A1-FER is BCR-Abl. When c-Abl is intact, its kinase activity is constrained. Removal of SH3 domain in c-Abl in the BCR-Abl fusion protein converts the mutant Abl tyrosine kinase into an oncogene that plays key role in developing acute lymphoblastic leukemia and chronic myelogenous leukemia. Wild type FER with intact SH2 domain is inactive in kinase activity when assayed in cell free system. In the fusion gene MAN2A1-FER, the N-terminus of FER suffers a loss of SH2 and FHC domain (FIG. **14**). These domains were replaced with glycoside hydrolase and α-mannosidase middle domain from MAN2A1. As a result, the kinase activity may be activated and substrate targets of FER tyrosine kinase may be altered.

MAN2A1-FER Expression Accelerates Cell Cycle Entry into S Phase and Increased Tyrosine Phosphorylation of EGFR in the Absence of EGFR Ligand.

To investigate whether MAN2A1-FER chimera protein is expressed in prostate cancer samples that contain MAN2A1-FER transcript, protein extracts from 5 prostate cancer samples positive for MAN2A1-FER RNA were analyzed using antibodies specific for MAN2A1 or FER. These results showed that the samples expressed a 115 Kd protein recognized by both MAN2A1 and FER antibodies (FIG. **22**). This protein is not detected in prostate cancer samples that are negative for MAN2A1-FER transcript.

When MAN2A1-FER was forced to express in RWPE1 cells, a non-transformed prostate epithelial cell line, it increase the proportion of cells in S phase by 4.6-5 fold ($p<0.001$). MAN2A1-FER was determined to be co-localized with Golgi protein in both immunofluorescence and sucrose gradient analysis, supporting the notion that MAN2A1-FER is primarily located in Golgi apparatus. Interestingly, expression of MAN2A1-FER increased tyrosine phosphorylation of EGFR in RWPE1 cells in the absence of EGFR ligand, suggesting that MAN2A1-FER may ectopically phosphorylate the EGFR extracellular domain. Thus, MAN2A1-FER may function as a transforming oncogene and possess intrinsic tyrosine kinase activity derived from its FER kinase domain. Not to be limited to any particular theory, the kinase domain of MAN2A1-FER may be the driver of its oncogenic activity through ectopic phosphorylation of transmembrane proteins such as EGFR.

Therapeutic Targeting at MAN2A1-FER Results in Specific Cell Death Prostate Cancer Cells Expressing MAN2A1-FER.

Based on the analyses above, we reason that the altered subcellular location and substrate specificity of FER kinase will create oncogenic activity of MAN2A1-FER. A large part of this oncogenic activity results from ectopic phosphorylation and activation of EGFR and its down-stream signaling pathways. Thus, we can intervene and disrupt the oncogenic pathways of MAN2A1-FER using 2 different approaches. The first approach is inhibiting the kinase activity of MAN2A1-FER by targeting MAN2A1-FER proteins using small molecules that can inhibit tyrosine kinase. Several small molecules specific for FER such as diaminopyrimidine TAE684, and pyrazologyridines WZ-4-49-8 and WZ-4-49-10, generic ALK/FER inhibitor crisotinib are available. Among these compound inhibitors, Crisotinib has been approved by FDA to treat advanced and metastatic non-small cell lung cancer positive for EML4-ALK, another tyrosine kinase fusion protein. The drug has been shown to be able to shrink tumor mass by at least 30% in most patients.

To investigate whether Crisotinib is also effective against MAN2A1-FER positive cancer cells, we transformed human prostate cancer cell line PC3 with pCDNA4-MAN2A1-FER-FLAG/pCDNA6 to express MAN2A1-FER fusion protein. These cells were treated with low dosage of Crisotinib for 24 hours. As shown in FIG. **22**, the treatment resulted in 31% cell death in MAN2A1-FER expressing cells, while it hardly killed the same type of cancer cells that do not express this fusion protein. A dosage effect analysis showed that expression of MAN2A1-FER lowers the cancer killing EC so by at least 2 magnitudes (~100 fold). Thus, it is reasonable to treat MAN2A1-FER positive prostate cancer with Crisotinib at a dosage that is not harmful to normal human cells.

The second approach is to target EGFR activation by EGFR inhibitors. These include erlotinib, cetuximab, bevacizumab, canertinib and bortezomib. Many of these drugs were FDA approved and is widely used in a variety of human solid tumors. To interrogate the effectiveness of EGFR activation interruption in treating prostate cancer, we treated MAN2A1-FER transformed PC3 cells with canertinib. As shown in FIG. **23**, the treatment also produced 34% cell death of cells expressing MAN2A1-FER. In contrast, the effect on cells not expressing MAN2A1-FER (Tet−) was minimal: The cell death level is similar to those untreated controls. These results suggest EGFR activation is one of the critical pathways for MAN2A1-FER oncogenic activity. Interesting, when we tried to intercept the down-streaming signaling molecule of EGFR, MEK, using an experimental drug AZD6244, the differential killing effect was largely moderated and vanished (data not shown). It suggests that other signaling pathways for EGFR may bypass MEK signaling.

8.2. References

1. Moremen K W, Robbins P W: Isolation, characterization, and expression of cDNAs encoding murine alpha-mannosidase II, a Golgi enzyme that controls conversion of high mannose to complex N-glycans, J Cell Biol 1991, 115:1521-1534.

2. Misago M, Liao Y F, Kudo S, Eto S, Mattei M G, Moremen K W, Fukuda M N: Molecular cloning and expression of cDNAs encoding human alpha-mannosidase II and a previously unrecognized alpha-mannosidase IIx isozyme, Proc Natl Acad Sci USA 1995, 92:11766-11770.
3. Hao Q L, Heisterkamp N, Groffen J: Isolation and sequence analysis of a novel human tyrosine kinase gene, Mol Cell Biol 1989, 9:1587-1593
4. Krolewski J J, Lee R, Eddy R, Shows T B, Dalla-Favera R: Identification and chromosomal mapping of new human tyrosine kinase genes, Oncogene 1990, 5:277-282.
5. Rocha J, Zouanat F Z, Zoubeidi A, Hamel L, Benidir T, Scarlata E, Brimo F, Aprikian A, Chevalier S: The Fer tyrosine kinase acts as a downstream interleukin-6 effector of androgen receptor activation in prostate cancer, Mol Cell Endocrinol 381:140-149.
6. Guo C, Stark G R: FER tyrosine kinase (FER) overexpression mediates resistance to quinacrine through EGF-dependent activation of NF-kappaB, Proc Natl Acad Sci USA 108:7968-7973.
7. Kwok E, Everingham S, Zhang S, Greer P A, Allingham J S, Craig A W: FES kinase promotes mast cell recruitment to mammary tumors via the stem cell factor/KIT receptor signaling axis, Mol Cancer Res 10:881-891.
8. Voisset E, Lopez S, Dubreuil P, De Sepulveda P: The tyrosine kinase FES is an essential effector of KITD816V proliferation signal, Blood 2007, 110:2593-2599.
9. Ivanova I A, Vermeulen J F, Ercan C, Houthuijzen J M, Saig F A, Vlug E J, van der Wall E, van Diest P J, Vooijs M, Derksen P W: FER kinase promotes breast cancer metastasis by regulating alpha6- and beta1-integrin-dependent cell adhesion and anoikis resistance, Oncogene 32:5582-5592.
10. Miyata Y, Kanda S, Sakai H, Greer P A: Feline sarcoma-related protein expression correlates with malignant aggressiveness and poor prognosis in renal cell carcinoma, Cancer Sci 104:681-686.
11. Wei C, Wu S, Li X, Wang Y, Ren R, Lai Y, Ye J: High expression of FER tyrosine kinase predicts poor prognosis in clear cell renal cell carcinoma, Oncol Lett 5:473-478.
12. Ahn J, Truesdell P, Meens J, Kadish C, Yang X, Boag A H, Craig A W: Fer protein-tyrosine kinase promotes lung adenocarcinoma cell invasion and tumor metastasis, Mol Cancer Res 11:952-963.
13. Kawakami M, Morita S, Sunohara M, Amano Y, Ishikawa R, Watanabe K, Hamano E, Ohishi N, Nakajima J, Yatomi Y, Nagase T, Fukayama M, Takai D: FER overexpression is associated with poor postoperative prognosis and cancer-cell survival in non-small cell lung cancer, Int J Clin Exp Pathol 6:598-612.
14. Li H, Ren Z, Kang X, Zhang L, Li X, Wang Y, Xue T, Shen Y, Liu Y: Identification of tyrosine-phosphorylated proteins associated with metastasis and functional analysis of FER in human hepatocellular carcinoma cells, BMC Cancer 2009, 9:366.
15. Zha S, Ferdinandusse S, Denis S, Wanders R J, Ewing C M, Luo J, De Marzo A M, Isaacs W B: Alpha-methylacyl-CoA racemase as an androgen-independent growth modifier in prostate cancer, Cancer Res 2003, 63:7365-7376.
16. Krastev D B, Slabicki M, Paszkowski-Rogacz M, Hubner N C, Junqueira M, Shevchenko A, Mann M, Neugebauer K M, Buchholz F: A systematic RNAi synthetic interaction screen reveals a link between p53 and snoRNP assembly, Nature cell biology 2011, 13:809-818.

9. EXAMPLE 4. ELIMINATION OF CANCER CELLS POSITIVE FOR FUSION TRANSCRIPTS THROUGH GENOME EDITING

Recent advances in genome editing using ZFN and CAS9 has made it possible to target a specific cancer genome sequence that is not present in normal cells. The mechanism of formation of fusion transcript is chromosome rearrangement. As a result, breakpoints in the chromosome are readily identified in a cancer genome. Normal cells do not have similar chromosome rearrangements, and are thus negative for the breakpoint. Targeting a specific breakpoint in the prostate cancer genome will likely generate an effective treatment for prostate cancer. Since the genomic breakpoint of CCNH-C5ORF30 and TMEM135-CCDC67 has been identified, genome editing technology targeting at the breakpoint of CCNH-C5orf30 or TMEM135-CCDC67 can be used to kill cancer cells.

As shown in FIG. **15**, genome recombination in prostate cancer case 3T produced a breakpoint in chromosome 5 that connect intron 6 of CCNH with intron 1 of C5orf30. The resulting breaking point is unique in prostate cancer case 3T. The breakpoint is positive in most prostate cancer tissues but negative for normal tissues from this patient. A guide RNA (gRNA) of 23 bp including protospacer adjacent motif (PAM) sequence is designed specific for the breakpoint region. The DNA sequence corresponding to this target sequence is artificially ligated into vector containing the remainder of gRNA and CAS9. This sequence is recombined and packaged into recombinant virus (Adenovirus or lentivirus). A promoterless Herpes Simplex Virus Type 1 (HSV-1) thymidine kinase is constructed into a shuttle vector for adenovirus along with splice tag sequence from intron/exon juncture of CCNH exon 7. A 500 bp sequence surrounding the CCNH-C5orf30 breakpoint from each side is also ligated into the shuttle vector in order to produce efficient homologous recombination to complete the donor DNA construction. The vector is recombined and packaged into AdEasy to generate recombinant viruses. These viruses are administered to patients or animals that have cancer positive for CCNH-C5orf30 fusion transcript. This leads to insertion of donor DNA into the target site (fusion breakpoint). Since HSV-1 TK in recombinant virus is promoterless, no transcription will occur if HSV-1 TK cDNA does not integrate into a transcription active genome. However, transcription of HSV-1 TK is active if HSV-1 TK is integrated into the target site of CCNH-C5orf30, since this transcript is readily detectable in the prostate cancer sample of this patient. When patient 3T takes ganciclovir or its oral homologue valganciclovir, the homologue is readily converted to triphosphate guanine analogue by HSV-1 TK and incorporated into the genomes of cancer cells. This leads to stoppage of DNA elongation in cells that are positive for CCNH-C5orf30. Since mammalian TK does not phosphorylate ganciclovir, ganciclovir is not converted to active (triphosphate) form in cells that are negative for HSV-1 TK protein. Thus, the impact of ganciclovir on normal cells is minimized.

The technique described above was applied to cells having the TMEM135-CCDC67 breakpoint. Since none of the fusion genes identified so far was present in prostate cancer cell lines, a TMEM135-CCDC67 genome breakpoint was created that is identical to the prostate cancer sample were analyzed. The expression of the TMEM135-CCDC67 break-

point was driven by a CMV promoter. Subsequently, a donor DNA was constructed that encompassed HSV-1 TK and the splicing sites of TMEM135 exon 14. When this donor DNA was co-transfected with a vector that expresses gRNA targeting at the TMEM135-CCDC67 breakpoint into PC3 cells containing this genome breakpoint, integration of TK into the genome was identified (FIG. **28**A). In contrast, when the same pairs of DNA were transfected into cells that do not contain the breakpoint, no integration of TK was found (data not shown). Treatment of PC3 cells without TMEM135-CCDC67 breakpoint has minimal cell death, while the same treatment of PC3 cells containing the breakpoint with ganciclovir resulted in 8 fold increase of cell death (FIG. **28**B). This is remarkable in considering only 5-10% transfection efficiency using conventional liposome method. Without being limited to a particular theory, these data suggest that almost all the cells receiving the DNA died when treated with ganciclovir, if they contain the breakpoint. In light of this promising result, both TMEM135-CCDC67-TK cassette and NicKase-gRNATMEM135-CCDC67-BrkPt DNA are now in the process of packaging into Adenovirus. We will infect the recombinant virus into these cells in the future experiments. This will dramatically improve the delivery efficiency in the subsequent animal study and probably human.

10. EXAMPLE 5: NOVEL FUSION TRANSCRIPTS ASSOCIATE WITH PROGRESSIVE PROSTATE CANCER

The analysis of an additional 68 prostate cancer samples by transcriptome sequencing leads to the discovery of 5 additional novel fusion transcripts present in prostate cancer. It is noted that significant number of prostate cancers contained no fusion transcripts in RNA sequencing. Even though extensive transcriptome sequencings were performed on 30 prostate cancer samples that prove non-recurrent for extended period of time, no viable fusion transcripts were identified in these samples using fusion catcher software. These 5 fusion transcripts were validated through Sanger sequencing of the RT-PCR products (FIG. **16**). The following primers were used:

ACPP-SEC13:

(SEQ ID NO: 30)
5'-TCCCATTGACACCTTTCCCAC/

(SEQ ID NO: 31)
5'-TGAGGCTTCCAGGTACAACAG;

CLTC-ETV1:

(SEQ ID NO: 32)
5'-GCCCAGTTGCAGAAAGGAATG/

(SEQ ID NO: 33)
5'-CTTGATTTTCAGTGGCAGGCC;

DOCK7-OLR1:

(SEQ ID NO: 34)
5'-GACTACGTCTCATGCCTTTCC/

(SEQ ID NO: 35)
5'-TTCTCATCAGGCTGGTCCTTC;

PCMTD1-SNTG:

(SEQ ID NO: 36)
5'-GATGTGGTGGAATATGCCAAGG/

(SEQ ID NO: 37)
5'-AAATCCATGTGCTGTGGCACC;

-continued

and

ZMPSTE24-ZMYM4:

(SEQ ID NO: 38)
5'-CGCAATGAGGAAGAAGGGAAC/

(SEQ ID NO: 39)
5'-CATAAATCTGGAATAGGGCTCAG.

10.1. Results

ZMPSTE24-ZMYM4 Fusion Genes.

This fusion transcript was discovered in a prostate cancer sample from a patient who experienced prostate cancer recurrence 1.8 month after radical prostatectomy. The patient's pelvic lymph nodes were positive for metastatic prostate cancer, while his primary cancer sample was graded with Gleason 7. In addition to ZMPSTE24-ZMYM4, his prostate cancer sample was also positive for CCNH-c5orf30. ZMPSTE24 is a zinc-metalloproteinase involved in post-translational proteolytic cleavage that coverts farnesylated prelamin A to form mature lamin A. Mutation of this protein is associated with mandibuloacral dysplasia[1]. It was suggested that ZMPSTE24 may be a mediator promoting invasive prostate cancer[2]. ZMYM4 is an anti-apoptotic gene whose function domain is located in the 3' untranslated region. Expression of ZMYM4 3' UTR has been shown to resist cell death induced by interferon γ through inhibition of AUF1 activity[3]. The fusion formation between ZMPSTE24 and ZMYM4 produces a truncation of 159 amino acids from the C-terminus of ZMPSTE24 and 1315 amino acids from the N-terminus of ZMYM4. Motif analysis suggests that ZMPSTE24-ZMYM4 fusion will delete about 50% of the peptidase domain from ZMPSTE24 and remove all zinc fingers from ZMYM4, but leave ZUF3504 (domain of unknown function) and apoptosis inhibitor domain intact (FIG. **17**). Thus, ZMPSTE24-ZMYM4 fusion may provide cancer cells an important tool to resist program cell death.

CLTC-ETV1 Fusion Genes.

CLTC-ETV1 was discovered in a prostate cancer sample that has Gleason's grade of 7. The patient experienced prostate cancer recurrence 22 months after radical prostatectomy, and had been rapidly progressing. In addition to CLTC-ETV1, the prostate cancer sample was also positive for TRMT11-GRIK2 fusion. CLTC is a major protein component of coated vesicles and coated pits, and is universally expressed. Its presence is essential for cell shape formation and cell motility. ETV1 is a transcription factor that was shown to over-express in prostate cancer. ETV1 had been shown to partner at least 12 different head genes in prostate cancer and Ewing's sarcoma[4,5]. However, most of these fusions do not produce a functional transcription factor from ETV1 due to frameshift in the fusion or few amino acids left after the fusion. In contrary, CLTC-ETV1 fusion preserves a largely intact transcription domain in ETV1, and probably represents the first example of potential functional ETV1 fusion in prostate cancer. CLTC-ETV1 fusion deletes 3 clathrin domains from CLTC (FIG. **18**). This may impair the function of CLTC for coated pit formation. ETV1 has been shown to be oncogenic in several organ systems[6-8]. The regulatory domain is located in the N-terminus. The regulatory domain contains MAPK phosphorylation site as well as ubiquitination site by COP1[9,10]. Truncation in the N-terminus of ETV1 eliminates all these regulatory elements from ETV1. Thus, the protein level CLTC-ETV1 may be increased due to less degradation and activity of ETV1 may become constitutive due to the lack of regulatory constraint

in the fusion protein. Since ETV1 has been shown to overexpress in many prostate cancers, CLTC-ETV1 fusion might be the underlying mechanism.

ACPP-SEC13 Fusion Genes.

The ACPP-SEC13 fusion transcript was discovered in a prostate cancer sample from patients who experienced recurrence but also had a slow rise of PSA with doubling time more than 20 months. The Gleason's grade is 7. The pathological examination reveals invasion into seminal vesicle by prostate cancer cells. ACPP is prostate specific acid phosphatase and is abundantly expressed in prostate acinar cells, while SEC13 belongs to the family of WD-repeat proteins, and is required for vesicle biogenesis from endoplasmic reticulum[11]. Recent studies suggest that SEC13 is a subunit of GATOR2, an octomeric GTPase activating protein. Inhibition of SEC13 suppresses mTOR activation[12]. In ACPP-SEC13 fusion, only the N-terminus 72 amino acids of ACPP is preserved, and over ⅔ of the phosphatase domain is truncated, while SEC13 loses 196 amino acids from its N-terminus and has 3 WD-repeat domains deleted (FIG. **19**). Due to the large truncation of critical domains in both proteins, it is expected that ACPP-SEC13 contains neither phosphatase nor GTPase-activation activity. Such loss of function may lead to hyperactivity of mTOR and may make it insensitive to amino acid deprivation. A potential targeted treatment for patients positive for ACPP-SEC13 might be using mTOR inhibitor since cancer cells may become hypersensitive to mTOR inhibitors when SEC13 is not functional.

DOCK7-OLR1 Fusion Genes.

DOCK7-OLR1 fusion transcript was discovered in a prostate cancer sample from a patient who experienced recurrent prostate cancer 30.5 months after the radical prostatectomy. However, the rise of PSA appeared rapid with PSADT less than 3 months. The prostate cancer Gleason's grade was 7, and there was no invasion into seminal vesicle or other adjacent organs at the time of surgery. The surgical margin was negative. It clearly suggests that some prostate cancer cells had escaped the primary location before the surgery. DOCK7 is a guanine nucleotide exchange factor involving in migration and cell polarization[13,14], while OLR1 is a low density lipoprotein receptor that belongs to the C-type lectin superfamily. OLR1 binds, internalizes and degrades oxidized low-density lipoprotein[15]. Unlike the above 3 fusion transcripts, DOCK7-OLR1 does not produce a chimera protein. Instead, separate translation of DOCK7 and OLR1 occurs from the fusion transcript. The fusion deleted a significant portion of cytokinesis domain of DOCK7 such that motility regulation by DOCK7 might be compromised. However, the fusion transcript will produce an intact OLR1 protein (FIG. **20**). OLR1 was implicated in Fas-mediated apoptosis. The functional significance of its expression under the control of DOCK7 promoter is to be investigated.

PCMTD1-SNTG1 Fusion Genes.

PCMTD1-SNTG1 fusion transcript was discovered in a prostate cancer sample from a patient who experienced recurrent prostate cancer 5.5 months after the radical prostatectomy. The rise of PSA was rapid with PSADT less than 3 months. The Gleason's grade is 9. Seminal vesicle invasion was identified in the prostatectomy sample. The prostate cancer sample is also positive for SLC45A2-AMACR and LRRC59-FLJ60017. PCMTD1 is Daspartate methyltransferase domain containing protein. The function of PCMTD1 has not been studied. SNTG1 is a member of the syntrophin family. SNTG1 belongs to peripheral membrane protein. Recent study suggests that SNTG1 may regulate diacylglycerol kinase zeta subcellular localization and regulates the termination of diacylglycerol signaling. Similar to DOCK7-OLR1 fusion, PCMTD1-SNTG1 fusion does not produce a chimera protein. PCMTD1-SNTG1 fusion produces a truncated PCMTD1. The truncation removes half of the methyl-transferase domain of PCMTD1. However, SNTG1 is intact (FIG. **21**). Since diacylglycerol kinase weakens protein kinase C activity by depleting the availability of diacylglycerol, higher level of SNTG1 might enhance PKC signaling If PCMDT1-SNTG1 fusion drives up the expression of SNTG1. Alternatively, impairing the function of PCMTD1 may have impact on cell metabolism and cell growth that are yet to be delineated.

10.2. References

1. Agarwal, A. K., Fryns, J. P., Auchus, R. J., and Garg, A. (2003) Zinc metalloproteinase, ZMPSTE24, is mutated in mandibuloacral dysplasia. *Human molecular genetics* 12(16), 1995-2001.
2. Parr-Sturgess, C. A., Tinker, C. L., Hart, C. A., Brown, M. D., Clarke, N. W., and Parkin, E. T. Copper modulates zinc metalloproteinase-dependent ectodomain shedding of key signaling and adhesion proteins and promotes the invasion of prostate cancer epithelial cells. *Mol Cancer Res* 10(10), 1282-1293.
3. Shchors, K., Yehiely, F., Kular, R. K., Kotlo, K. U., Brewer, G., and Deiss, L. P. (2002) Cell death inhibiting RNA (CDIR) derived from a 3'-untranslated region binds AUF1 and heat shock protein. 27. *The Journal of biological chemistry* 277(49), 47061-47072.
4. Clark, J. P., and Cooper, C. S. (2009) ETS gene fusions in prostate cancer. *Nat Rev Urol* 6(8), 429-439.
5. Jeon, I. S., Davis, J. N., Braun, B. S., Sublett, J. E., Roussel, M. F., Denny, C. T., and Shapiro, D. N. (1995) A variant Ewing's sarcoma translocation (7; 22) fuses the EWS gene to the ETS gene ETV1. *Oncogene* 10(6), 1229-1234.
6. Carver, B. S., Tran, J., Chen, Z., Carracedo-Perez, A., Alimonti, A., Nardella, C., Gopalan, A., Scardino, P. T., Cordon-Cardo, C., Gerald, W., and Pandolfi, P. P. (2009) ETS rearrangements and prostate cancer initiation. *Nature* 457(7231), E1; discussion E2-3.
7. Chi, P., Chen, Y., Zhang, L., Guo, X., Wongvipat, J., Shamu, T, Fletcher, J. A., Dewell, S., Maki, R. G., Zheng, D., Antonescu, C. R., Allis, C. D., and Sawyers, C. L. ETV1 is a lineage survival factor that cooperates with KIT in gastrointestinal stromal tumours. *Nature* 467 (7317), 849-853.
8. Jane-Valbuena, J., Widlund, H. R., Perner, S., Johnson, L. A., Dibner, A. C., Lin, W. M., Baker, A. C., Nazarian, R. M., Vijayendran, K. G., Sellers, W. R., Hahn, W. C., Duncan, L. M., Rubin, M. A., Fisher, D. E., and Garraway, L. A. An oncogenic role for ETV1 in melanoma. *Cancer research* 70(5), 2075-2084.
9. Vitari, A. C., Leong, K. G., Newton, K., Yee, C., O'Rourke, K., Liu, J., Phu, L., Vij, R., Ferrando, R., Couto, S. S., Mohan, S., Pandita, A., Hongo, J. A., Arnott, D., Wertz, I. E., Gao, W. Q., French, D.
10. M., and Dixit, V. M. COP1 is a tumour suppressor that causes degradation of ETS transcriptionfactors. *Nature* 474(7351), 403-406
11. Willardsen, M., Hutcheson, D. A., Moore, K. B., and Vetter, M. L. The ETS transcription factor Etv1 mediates FGF signaling to initiate proneural gene expression during *Xenopus laevis* retinal development. *Mechanisms of development* 131, 57-67

12. Enninga, J., Levay, A., and Fontoura, B. M. (2003) Sec13 shuttles between the nucleus and the cytoplasm and stably interacts with Nup96 at the nuclear pore complex. *Molecular and cellular biology* 23(20), 7271-7284.
13. Bar-Peled, L., Chantranupong, L., Cherniack, A. D., Chen, W. W., Ottina, K. A., Grabiner, B. C., Spear, E. D., Carter, S. L., Meyerson, M., and Sabatini, D. M. A Tumor suppressor complex with GAP activity for the Rag GTPases that signal amino acid sufficiency to mTORC1. *Science* (New York, N.Y. 340(6136), 1100-1106.
14. Watabe-Uchida, M., John, K. A., Janas, J. A., Newey, S. E., and Van Aelst, L. (2006) The Rac activator DOCK7 regulates neuronal polarity through local phosphorylation of stathmin/Op18. *Neuron* 51(6), 727-739.
15. Nellist, M., Burgers, P. C., van den Ouweland, A. M., Halley, D. I, and Luider, T. M. (2005) Phosphorylation and binding partner analysis of the TSC1-TSC2 complex. *Biochemical and biophysical research communications* 333(3), 818-826.

11. EXAMPLE 6: SLC45A2-AMACR FUSION GENES

11.1 Results

The fusion transcript of Solute carrier family 45, member 2-alpha-methylacyl-CoA racemase (SLC45A2-AMACR) produces a chimera protein with Nterminus 187 amino acids of SLC45A2 and the C-terminus 311 amino acids of AMACR. SLC45A2 is a transporter protein known to be overexpressed in melanoma[1], while AMACR is an enzyme involved in metabolism of branch fatty acid, and is known for its overexpression in several human malignancies. SLC45A2-AMACR replaces 5 transmembrane and cytosolic domains of SLC45A2 with an intact racemase domain from AMACR[2], while leaves the extracellular and the N-terminal transmembrane domains intact (FIG. **24**). Most of prostate cancer patients who were positive for SLC45A2-AMACR experienced prostate cancer recurrence within 5 years of surgical treatment. Previous studies suggest that AMACR is essential for optimal growth of prostate cancer cells in vivo. Knocking down of AMACR or treatment of prostate cancer with AMACR inhibitors resulted in death of cancer cells both in vitro and in vivo[3]. Formation of SLC45A2-AMACR generates ectopic racemase for fatty acid metabolism to support the growth of prostate cancer cells.

Transformation of Prostate Epithelial Cells with SLC45A2-AMACR Results in Dramatic Cell Growth and Transformation, Possibly Through Activation of SHIP2-Akt Pathway.

To investigate whether SLC45A2-AMACR chimera protein is expressed in prostate cancer samples that contain SLC45A2-AMACR transcript, protein extracts from 4 prostate cancer samples positive for SLC45A2-AMACR RNA were analyzed using antibodies specific for MAN2A1 or FER. The results showed that these samples expressed a 50 Kd protein recognized by both MAN2A1 and FER antibodies (FIG. **25**A). This protein was not detected in prostate cancer samples that were negative for SLC45A2-AMACR transcript. When SLC45A2-AMACR was forced to express in RWPE1 cells, a non-transformed prostate epithelial cell line, it increased the proportion of cells in S phase by an average of 8.7 fold ($p<0.001$). MTT assays showed a 7.5 fold increase of cell proliferation ($p<0.001$)(FIG. **25** E-F). SLC45A2-AMACR was determined to be localized in the plasma membrane by immunofluorescence staining and membranous fractionation analyses. This is in contrast to native AMACR, which is located primarily in the mitochondria/cytoplasm. To investigate what are the potential signaling molecules mediating SLC45A2-AMACR induced cell growth and DNA synthesis. Yeast-two hybrid screening of prostate Yeast two-Hybrid library using pBD-SLC45A2-AMACR was performed. After 3 rounds of metabolic screening, 15 unique clones that contain SLC45A2-AMACR binding proteins were identified. One of these clones encodes inositol polyphosphate phosphatase-like 1 (INPPL1, also called SHIP2). SHIP2 is a SH2 domain containing inositol phosphatase that converts PIP3(3,4,5) to PIP2(3,4). In contrast to Pten, which converts PIP3(3,4,5) to an inactive PIP2(4,5), PIP2(3,4) generated by SHIP2 has higher affinity binding with AKT than PIP3(3,4,5), and thus hyper-activate AKT pathway. The interaction between SLC45A2 and SHIP2 was validated by both yeast Two-hybrid co-transfection analysis and co-immunoprecipitation assays in SLC45A2-AMACR expressing cells (FIG. **25**G-H). Induction of SLC45A2-AMACR expression in 2 different clones of RWPE1 cells generated 2.1- and 2.3-fold higher level of PIP2(3,4), respectively. These results indicate that binding of SLC45A2-AMACR and SHIP2 leads to activation of SHIP2 phosphatase activity and probably AKT signaling pathway.

Therapeutic Targeting at SLC45A2-AMACR Using Racemase Inhibitor.

To investigate whether targeting SLC45A2-AMACR is a viable approach to treat prostate cancer, we chose 2 approaches: 1) To intercept SLC45A2-AMACR/SHIP2-Akt pathway with small molecules; and 2) to block the ectopic racemase activity of SLC45A2-AMACR with ebselen or trifluoro-ibuprofen. Surprisingly, both SHIP2 and MTOR inhibitors killed PC3 cells effectively, regardless whether they were transformed with SLC45A2-AMACR. Expression of SLC45A2-AMACR only moderately sensitized PC3 cells to Rapamycin. This is probably due to Pten negative status of PC3 cells such that Akt pathway is fully activated regardless the presence of SLC45A2-AMACR. On the other hand, when we applied ebselen, the potent inhibitor of racemase of AMACR, to SLC45A2-AMACR expressing PC3 cells, 5 fold higher sensitivity of cell growth inhibition was found for PC3 cells transformed with pCDNA4-SLC45A2-AMACR-FLAG/pCDNA6 over the controls. In contrast, non-transformed RWPE1 cells and NIH3T3 cells that expressed little AMACR was largely insensitive to ebselen killing (FIG. **26**). The differential sensitivity of normal cells versus cancer cells to AMACR inhibitors may prove very useful in treating prostate cancer positive for this fusion gene.

11.2. References

1. Misago, M., Liao, Y. F., Kudo, S., Eto, S., Mattei, M. G., Moremen, K. W., and Fukuda, M. N. (1995) Molecular cloning and expression of cDNAs encoding human alpha-mannosidase II and a previously unrecognized alpha-mannosidase IIx isozyme. Proceedings of the National Academy of Sciences of the United States of America 92(25), 11766-11770.
2. Krolewski, J. J., Lee, R., Eddy, R., Shows, T. B., and Dalla-Favera, R. (1990) Identification and chromosomal mapping of new human tyrosine kinase genes. Oncogene 5(3), 277-282.
3. Zha, S., Ferdinandusse, S., Denis, S., Wanders, R. J., Ewing, C. M., Luo, J., De Marzo, A. M., and Isaacs, W. B. (2003) Alpha-methylacyl-CoA racemase as an andro-

12. EXAMPLE 7: GENOME TARGETING AT THE CHROMOSOME BREAKPOINT OF A FUSION GENE RESULTED IN REMISSION OF XENOGRAFTED PROSTATE CANCERS

12.1 Introduction

Prostate cancer is the most frequent malignancies for men in the US. The mortality of prostate cancer reached 27,540 in 2014, the second most lethal cancer for men.[1] Treatment of prostate cancer, particularly of those metastatic prostate cancers remains problematic. As described above, a panel of fusion genes that are present in most prostate cancers have been shown to be recurrent and lethal.[2] The mechanism of these fusions is chromosome rearrangement. The expressions of these fusion genes are wide-spread among aggressive prostate cancers but are absent in normal tissues. Thus, targeting at these chromosome rearrangement breakpoints that create these fusion genes would provide a highly cancer specific approach to treat prostate cancers.

In this Example, $Cas9^{D10A}$ mediated genome editing was successfully used to insert Herpes Simplex Virus 1 thymidine kinase (HSV1-tk) into the chromosomal breakpoint of fusion gene TMEM135-CCDC67. Treatment of tumors harboring TMEM135-CCDC chromosome breakpoint with Ganciclovir led to cell death in cell culture and remission of xenografted prostate cancer in Severe Combined Immunodeficiency (SCID) mice.

12.2 Methods and Materials

Materials and Vector Construction.

All cell lines, including PC3 (prostate cancer), Du145 (prostate cancer) were purchased from American Type Cell Culture (Manassas, Va.). PC3 cells were cultured with F12K medium supplemented with 10% fetal bovine serum (InVitrogen, Carlsbad, Calif.). Du145 cells were cultured with modified Eagle medium supplemented with 10% fetal bovine serum (Invitrogen). Rabbit polyclonal anti-Cas9 antibodies were purchased from Clontech Inc., CA. Rabbit anti-HSV-1 TK polyclonal antibodies were purchased from Sigma Inc., OH. ABC kit was purchased from Vector Labs, Inc., OH.

Construction of Vector.

To construct the gRNA expression vector, sequences flanking the breakpoint region of TMEM135-CCDC67 were analyzed and gRNAs were designed using DNA 2.0 tool: https://www.dna20.com/eCommerce/cas9/input. Both gRNA− and gRNA+ were ligated into All-in-One NICKASENINJA® vector that also contains $Cas9^{D10A}$. The insert was then released by restriction with XbaI, and ligated into similarly restricted VQAd5 shuttle vector to create VQAd5-$Cas9^{D10A}$-$gRNA^{TMEM135int13}$-$gRNA^{CCDC67int9}$. The recombinant shuttle vector was then recombined with pAD5 virus to generate pAD5-$Cas9^{D10A}$-$gRNA^{TMEM135int13}$-$gRNA^{CCDC67int9}$ using a method previously described.[7]

To construct donor DNA recombinant virus, PCR was performed on pEGFP-N1 using the following primers:

(SEQ ID NO: 78)
GTACTCACGTAAGCTTTCGCCACCATGGTGAGCAAGG;
and

(SEQ ID NO: 79)
GACTCAGATGGGCGCCCTTGTACAGCTCGTCCATGCC.

The PCR product was restricted with KasI and HindIII, and ligated into similarly restricted pSELECT-zeo-HSV1tk vector to create pEGFP-HSV1-tk.

PCR was performed on the genome DNA from sample where TMEM135-CCDC67 fusion was discovered to obtain intron 13 sequence of TMEM135 using the following primers:

(SEQ ID NO: 80)
GACTCAGATGGCGGCCGCCTGTATTCTTTGTTTTACAGATTTGCTGTCAG
GGGTTAGATAGCTTGCCAG/

(SEQ ID NO: 81)
GTACTCACGTAAGCTTGAGCTAACATTACCAATGAGGC.

The PCR products were then restricted with NotI and HindIII, and ligated into similarly restricted pEGFPtk vector to create pTMEM135int13-EGFP-tk.

Subsequently, PCR was performed on the genome DNA from the sample where TMEM135-CCDC67 fusion was discovered to obtain intron 9 sequence of CCDC67 using the following primers:

(SEQ ID NO: 82)
GACTCAGATGGCTAGCAGTTCACTGAGTGTGCCATGC/

(SEQ ID NO: 83)
GTACTCACGTGAATTCCTATTCTGCCTGCTTGCATACCTTTTGTTTTGGT
TGCAGTATAGTGGGCTGAG.

The PCR was then restricted with NheI and EcoRI, and ligated into the similarly restricted pTMEM135int13-EGFP-tk vector to create pTMEM135int13-EGFP-tk-CCDC67int9. The vector was then restricted with EcoR1 and NotI and ligated into the similarly restricted pAdlox to create pAdlox-pTMEM135int13-EGFP-tk-CCDC67int9. The recombinant shuttle vector was then recombined with adenovirus to create pAd-TMEM135int13-EGFP-tk-CCDC67int9.

For the construction of pCMV-TMEM135-CCDC67 bp vector, PCR was performed on genome DNA from a prostate cancer sample that are positive for TMEM135-CCDC67 fusion using the following primers:

(SEQ ID NO: 84)
GACTCAGATGAAGCTTAAGAGCATGGGCTTTGGAGTC/

(SEQ ID NO: 85)
GTACTCACGTTCTAGACTGGAATCTAGGACTCTTGGC.

The PCR product was then sequenced to confirm the presence of TMEM135-CCDC67 breakpoint. The PCR product was digested with HindIII and XbaI, and ligated into similarly digested pCMVscript vector. The construct was subsequently transfected into PC3 and DU145 cells using lipofectamine 3000. Cells stably expressing TMEM135-CCDC67 breakpoint transcripts were selected by incubation of the transfected cells in medium containing G418 (200 μg/ml).

In Vitro Cas9 Target Cleavage Assays.

gRNA DNA sequence plus scaffold DNA sequence for + or − DNA strand were amplified from the all-in-one vector with the following primers:

(SEQ ID NO: 86)
GGCCAGTGAATTGTAATACGACTCACTATAGGGAGGCGGCACTCACTGAG
CTCTTTGCC/

-continued

(SEQ ID NO: 87)
AAAAAAAGCACCGACTCGGTGCCACTTTTTC for gRNA+ template, and

(SEQ ID NO: 88)
GGCCAGTGAATTGTAATACGACTCACTATAGGGAGGCGGTGTGGAAAGGA CGAAACACCG/

(SEQ ID NO: 89)
AAAAAAAGCACCGACTCGGTGCCACTTTTTC for gRNA-template.

The PCR products were in vitro transcribed using In Vitro Transcription kit from Ambion, CA, to obtain gRNA+ and gRNA− products. Cleavage assays were performed at 25° C. for 10 min and then 37° C. for 1 hour under the following condition: 1x Cas9 nuclease reaction buffer, 30 nM gRNA 3 nM DNA template and 30 nM Cas9 Nuclease, *S. pyogenes*. The cleaved DNA was visualized in 1% agarose gel electrophoresis.

TABLE 18

Primer sequences for PCR and RT-PCR.

Forward primer/ reverse primer	Forward primer/reverse primer
Genome BP PCR	GCCCATATATGGAGTTCCGCG (SEQ ID NO: 90)/ TCTGGCAAGCTATCTAACCCC (SEQ ID NO: 91)
RNA BP RT-PCR	AGCACAGAGACCCAGAAGGTC (SEQ ID NO: 92)/ AGGAGGAGGAGGAGGAGAAAG (SEQ ID NO: 93)
Genome β-actin PCR	TCTTTGCACTTTCTGCATGTCCCC (SEQ ID NO: 94)/ GTCCATCACGATGCCAGTGGTAC (SEQ ID NO: 95)
RNA β-actin RT-PCR	ATGATGATATCGCCGCGCTC (SEQ ID NO: 96)/ CACGATGGAGGGGAAGACG (SEQ ID NO: 97)
Pre-integration 5' end	GCCCATATATGGAGTTCCGCG (SEQ ID NO: 98)/ AGGCAAAGAGCTCAGTGAGTG (SEQ ID NO: 99)
Pre-integration 3' end	TGCCTCATTGGTAATGTTAGCTC (SEQ ID NO: 100)/ GGCGAATTGGGTACACTTACC (SEQ ID NO: 101)
CMV-EGFP PCR	ACTCACGGGGATTTCCAAGTC (SEQ ID NO: 102)/ AAGTCGTGCTGCTTCATGTGG (SEQ ID NO: 103)
HSV1-tk-CMV PCR	TGTTCTAGCCAAGAGGCTGAG (SEQ ID NO: 104)/ GGCGAATTGGGTACACTTACC (SEQ ID NO: 105)

Fluorescence Activated Cell Sorting (FACS) Analysis of Apoptotic Cells.

The assays were previously described.[8-16] Briefly, the cells treated with pAD5-Cas9^{D10A}-gRNA^{TMEM135int13}-gRNA^{CCDC67int9}/pAD-TMEM135int13-EGFP-tk-CDC67int9, and various concentrations of ganciclovir were trypsinized and washed twice with cold PBS. The cells were then resuspended in 100 μl of annexin binding buffer (Invitrogen), and incubated with 5 μl of phycoerythrin (PE)-conjugated annexin V and 1 μl of 100 ng/ml propidium iodide for 15 min in dark at room temperature. The binding assays were terminated by addition of 400 μl of cold annexin binding buffer. FACS analysis was performed using a BD-LSR-II flow cytometer (BD Science, San Jose, Calif.). The fluorescence stained cells were analyzed at the fluorescence emission at 533 nm (FL2). The negative control, cells with neither PE nor PI in the incubation medium, was used to set the background for the acquisition. UV treated cells were used as a positive control for apoptosis. For each acquisition, 10,000 to 20,000 cells were sorted based on the fluorescence color of the cells. WinMDI 2.9 software (freeware from Joseph Trotter) was used to further analyze the data.

Tumor Growth and Spontaneous Metastasis.

The xenografting procedure was described previously.[10, 14-19] Briefly, Approximately 2×10^7 viable PC3 and Du145 cells that contain TMEM135-CCDC67 breakpoint or control vector, suspended in 0.2 mL of Hanks' balanced salt solution (Krackeler Scientific, Inc., Albany, N.Y.) were subcutaneously implanted in the abdominal flanks of 48 SCID mice to generate one tumor per mouse. Mice were observed daily, and their body weight and tumor size were recorded weekly. Tumor size were measured on the diameter. Three weeks after xenografting, these mice were applied with pAD5-Cas9^{D10A}gRNA^{TMEM135int13}-gRNA^{CCDC67int9} and pAD-TMEM135int13-EGFP-tk-CCDC67int9 (5×10^{10} pfu), and treated with ganciclovir (80 mg/kg) or controls as indicated in FIG. 32 through intraperitoneal and local applications. After 7 weeks, mice that were applied with pAD5-cas9^{D10A}-gRNA^{TMEM135int13}-gRNA^{CCDC67int9}/pAD-TMEM135int13-EGFP-tk-CCDC67int9, and with ganciclovir were killed, and necropsies were performed. For mice treated with control reagents, necropsies were performed when mice died from the xenografted cancers. Serial sections of formalin-fixed, paraffin-embedded lung, brain, liver, kidney, vertebra, and lymph node specimens were collected, stained with hematoxylin and eosin, and examined microscopically. All animal procedures were approved by the University of Pittsburgh Institutional Animal Care and Use Committee.

Immunohistochemistry.

Immunohistochemistry was performed as described previously[19] with antibodies specific for HSV-1 TK (1:100 dilution) or for Cas9 (1:100 dilution). The antibody was omitted in negative controls. The sections were then incubated with horseradish peroxidase-conjugated anti-rabbit IgG for 30 minutes at room temperature (ABC kit from Vector Labs, Inc). Slides were then exposed to a 3,3'-diaminobenzidine solution to visualize immunostaining. Counterstaining was performed by incubating the slides in

1% Hematoxylin solution for 2 minutes at room temperature. The slides were then rinsed briefly in distilled water to remove excessive staining.

12.3 Results

One of the fusion genes discovered in prostate cancer is between transmembrane protein 135 (TMEM135) and coiled-coil domain containing 67 (CCDC67). The fusion gene was created due to a 6 MB deletion in the region of chromosome 11q14.2-21. The deletion joins intron 13 of TMEM135 with intron 9 of CCDC67 in chromosome 11 (FIG. **29**A). Such sequence joining creates a unique sequence breakpoint not present in normal tissues. This provides a unique target in cancer cells for therapeutic intervention. To target at this joining sequence, 2 gRNAs were designed to complement to the regions flanking the chromosomal breakpoint (FIG. **29**B). These gRNAs and $Cas9^{D10A}$ were ligated into VQAd5-CMV shuttle vector and recombined into pAD5 adenovirus to create pAD5-$cas9^{D10A}$-$gRNA^{TMEM135int13}$-$gRNA^{CCDC67int9}$. To provide a potential lethal gene for targeted cancer cells, cDNA of HSV-1 tk was ligated with enhanced green fluorescence protein (EGFP) cDNA in frame to create a chimeric gene EGFP-tk. The chimeric cDNA is promoterless, and was ligated with 584 bp of intron 13 sequence of TMEM135 at the 5' end and 561 bp of intron 9 sequence of CCDC67 at the 3' end. These sequences were subsequently ligated into PAdlox shuttle vector and recombined into adenovirus to create pADTMEM135int13-EGFP-tk-CCDC67int9. Such device is intended to produce single strand breaks at intron 13 of TMEM135 and intron 9 of CCDC67 in close proximity to the chromosome breakpoint and in different strands.

To examine whether the designed gRNA is adequate in recruiting Cas9 to produce DNA break at the targeted DNA, in vitro cleavage assays were performed on pCMV-TMEM135int13-CCDC67int9, using recombinant Cas9 from *S. pyogenes* and gRNA generated from in vitro transcription. As shown in FIG. **30**A, both gRNA− and gRNA+ cleaved the linearized pCMVTMEM135int13-CCDC67int9 at the correct locations and generated the expected 4317 and 3206 bp fragments for gRNA−, and 4414 and 3109 bp for gRNA+. To test whether pAD5-$Cas9^{D10A}$$gRNA^{TMEM135int13}$-$gRNA^{CCDC67int9}$ and pAD-TMEM135int13-EGFP-tk-CCDC67int9 induced integration of EGFP-tk into the TMEM135-CCDC67 breakpoint of the cancer genome, prostate cancer cell lines PC3 and DU145 were transfected with pCMV-TMEM135int13-CCDC67int9 such that the integrated vector would transcribe a RNA containing TMEM133-CCDC67 breakpoint under CMV 1E94 promoter (FIG. **30**B). When PC3 cells stably expressing TMEM133-CCDC67 breakpoint RNA were infected with pAD5-$Cas9^{D10A}$-$gRNA^{TMEM135int13}$-$gRNA^{CCDC67int9}$ and pAD-TMEM135int13-EGFP-tk-CCDC67int9, intensive EGFP-tk expression was identified in cells (green fluorescence) that also expressed $Cas9^{D10A}$-RFP (red fluorescence), while little EGFP-tk expression was found in cells that had minimal $Cas9^{D10A}$-RFP expression (FIGS. **30**C and D, Table 19), suggesting that the integration of EGFP-tk into the genome and the expression of EGFP-tk protein are dependent on $Cas9^{D10A}$-RFP. Similar finding was also observed in DU145 cells transformed with pCMV-TMEM135int13-CCDC67int9. In contrast, neither PC3 nor DU145 cells transformed with pCMVscript displayed significant expression of EGFP-tk (FIGS. **30**C and D, Table 19), suggesting that no integration of EGFP-tk occurred when TMEM135-CCDC67 breakpoint was absent. These results indicate that integration of EGFP-tk into the breakpoint of TMEM135-CCDC67 using $Cas9^{D10A}$ is highly specific. Few off-target events occurred.

TABLE 19

Chromosome breakpoint dependent integration and expression of EGFP-tk.

Samples	Treatment	$Cas9^{D10A}$-RFP+/ EGFP-tk+	$Cas9^{D10A}$-RFP+/ EGFP-tk+	$Cas9^{D10A}$-RFP+/ EGFP-tk+	Cas9D10A-RFP+/ EGFP-tk+
PC3 + pCMV-BP	Adeno*	16.9% ± 2.2	76.6% ± 3.5	0.5% ± 0.2	6.4% ± 0.5
PC3 + pCMV	Adeno*	1.0% ± 0.3	90.2% ± 5.6	0.2% ± 0.1	8.4% ± 1.5
DU145 + pCMV-BP	Adeno*	16.0% ± 1.7	80.1% ± 4.3	0.4% ± 0.1	4.4% ± 0.8
DU145 + pCMV	Adeno*	1.2% ± 0.3	95.7% ± 5.1	0.1% ± 0.1	3.1% ± 0.4

*Treatment include pAD5-$Cas9^{D10A}$-$gRNAT^{MEM135int13}$-$gRNA^{CCDC67int9}$ and pAD-TMEM135int13-EGFP-tk-CCDC67int9 at 10 multiplicity of infection;
pCMV-BP = pCMV-TMEM135int13-CCDC67int9;
pCMV = pCMVscript

Nucleotide homologues, such as guanine analogue 9-(1, 3-dihydroxy-2-propoxymethyl)guanine (ganciclovir)[20], is converted to triphosphates form by HSV-1 tk but not by its mammalian counterpart. Ganciclovir triphosphates blocks DNA synthesis. To examine whether cancer cells expressing EGFP-tk are susceptible to anti-Herpes drug such as ganciclovir, PC3 or DU145 cells expressing TMEM135-CCDC67 breakpoint were infected with pAD5-$Cas9^{D10A}$$gRNA^{TMEM135int13}$-$gRNA^{CCDC67int9}$ and pAD-TMEM135int13-EGFP-tk-CCDC67int9. These cells were exposed to various concentrations of ganciclovir. As shown in FIG. **31**A, at 0.075 μg/ml of ganciclovir, the killing of PC3 or DU145 cells reached 50% of its maximal level, and at 5 μg/ml, the killing was at the peak. At 5 μg/ml of ganciclovir, apoptosis of PC3 or DU145 cells containing the TMEM135-CCDC67 breakpoint and infected with pAD5-$Cas9^{D10A}$$gRNA^{TMEM135int13}$-$gRNA^{CCDC67int9}$ and pAD-TMEM135int13-EGFP-tk-CCDC67int9 was clearly visualized (FIG. **31**B and Table 20). No significant cell deaths were identified for cells containing no TMEM135-CCDC67 breakpoint, even though they were equally infected with these viruses and exposed to high concentrations of ganciclovir (up to 100 μg/ml, FIGS. **31**A and B). These findings indicate that the killing of cancer cells by ganciclovir is breakpoint dependent and is highly specific.

TABLE 20

Chromosome breakpoint dependent cancer cell killing by Ganciclovir.

Samples	Treatment	% Apoptosis
PC3 + pCMV-BP	Adeno + Gan*	20.6% ± 1.4
PC3 + pCMV	Adeno + Gan*	1.5% ± 0.2
DU145 + pCMV-BP	Adeno + Gan*	19.8% ± 0.7
DU145 + pCMV	Adeno + Gan*	1.2% ± 1.1

*Treatment of Adeno + Gan include pAD5-Cas9^{D10A}-gRNAT^{MEM135int13}-gRNA^{CCDC67int9} and pAD-TMEM135int13-EGFP-tk-CCDC67int9 at 10 multiplicity of infection and Ganciclovir at 1 μg/ml.
pCMV-BP = pCMV-TMEM135int13-CCDC67int9.
pCMV = pCMVscript

To examine whether such breakpoint dependent killing of cancer cells can be used as a treatment for cancer, PC3 or DU145 cells containing TMEM135-CCDC67 breakpoint were xenografted into the subcutaneous regions of severe combined immunodeficiency mice. The xenografted tumors were allowed to grow for 3 weeks to reach ~0.7 cm3 in size. These mice were then infected with pAD5-Cas9^{D10A}-gRNA^{TMEM135int13}-gRNA^{CCDC67int9} and pAD-TMEM135int13-EGFP-tk-CCDC67int9 (5×10^{10} pfu), and treated with ganciclovir (80 mg/kg). As shown in FIG. **32**A, mice xenografted with PC3 or DU145 cancer cells containing TMEM135-CCDC67 breakpoint experienced exponential growth of tumor if they were not treated properly. In contrast, if these tumors were treated with both viruses and ganciclovir, the mice experienced up to 30% shrinking of the tumor volumes. Integration of TMEM123int13-EGFP-tk-CCDC67int9 and expression of EGFP-tk were detected in PC3 or DU145 cells that contained TMEM135-CCDC67 breakpoint and treated with recombinant viruses (FIG. **33**). There was no incidence of metastasis detected in mice treated with pAD5-Cas9^{D10A}-gRNA^{TMEM135int13}-gRNA^{CCDC67int9}, pAD-TMEM135int13-EGFP-tk-CCDC67int9 and ganciclovir. However, PC3 or DU145 cells containing no TMEM135-CCDC67 breakpoint had 33-50% metastasis rate even treated with the recombinant viruses and ganciclovir (FIG. **32**B). Mice xenografted with PC3 or DU145 cells that contain TMEM135-CCDC67 breakpoint and treated with the recombinant viruses and ganciclovir had no mortality, while all control treated mice died within 7 weeks of tumor cells xenografting (FIG. **32**C). These experiments suggest that targeting fusion gene breakpoint in the cancer genome is an effective and highly specific approach to treat cancer.

12.4 Discussion

Chromosome rearrangement and deletion creates many cancer specific fusion genes.[21] These fusion genes either acquire additional function to drive the cancer progression or destroy genes that block the progression of cancer. TMEM135-CCDC7 is an example of latter such that the fusion eliminates the open-reading frame of CCDC67, a putative cancer suppressor and truncates 65 amino acids off the C-terminus of TMEM135, a protein widely expressed in most tissues but with unknown function. The impact of fusion genes on the function of genes that are involved is probably more dramatic than most missense point mutations. The fusion genes created in cancers represent a new stratum of novel functions developed by cancer cells. The presence of chromosome rearrangement-based fusion genes is the hallmark of human malignancies. As a result, targeting at fusion genes created by cancer cells will generate highly specific cancer cell killing but will spare the destruction of normal cells that do not contain the chromosome rearrangement.

The recent advances in precision cleavage of DNA by bacterial CRISPR/Cas system made it possible to target specific genome sequence with relatively high efficiency. The approach described herein appears highly specific, with average functional off-target rates being 1.3% in both PC3 and DU145 cells (EGFP-tk+ cells/Cas9^{D10A}-RFP+ cells in PC3+pCMV or DU145+pCMV cells, Table 18). Such precision specificity makes it possible to apply this approach to a clinical setting.

The current therapeutic approach to metastatic prostate cancer heavily relies on intervention of androgen receptor signaling pathway. However, such approach invariably leads to drug tolerance and refractory to drug treatment as cancer genome adjusts its gene expression pattern and develops new pathways to bypass the signaling blockade. The subsequent application of chemotherapy to androgen refractory prostate cancer may impact both cancer and normal tissues, and thus generally produces poor therapeutic outcomes. The genome approach may have significant advantage over chemotherapy because of its specificity for the cancer genome sequence. There is no appreciable cytotoxic side-effect of these recombinant viruses in either cell culture or animal model. The integration of EGFP-tk can be monitored by fluorescence imaging.

Furthermore, in the event of unwanted integration into the genome of healthy cells of critical location, the integrated EGFP-tk can be retrieved by Cre expression. In light of the toxic side-effect of small molecules targeting at protein molecules, genome therapeutic approach shown in this report may represent a more controlled, safe and probably minimal side-effect approach to treat human cancers.

12.5 References

1. Siegel, R. L., Miller, K. D., & Jemal, A. Cancer statistics, 2015. CA: a cancer journal for clinicians 65: 5-29.
2. Yu, Y. P., Ding, Y., Chen, Z., Liu, S., Michalopoulos, A., et al. (2014) Novel fusion transcripts associate with progressive prostate cancer. The American journal of pathology 184: 2840-2849.
3. Mojica, F. J., Diez-Villasenor, C., Garcia-Martinez, J., & Soria, E. (2005) Intervening sequences of regularly spaced prokaryotic repeats derive from foreign genetic elements. Journal of molecular evolution 60: 174-182.
4. Jinek, M., Chylinski, K., Fonfara, I., Hauer, M., Doudna, J. A., et al. A programmable dual-RNAguided DNA endonuclease in adaptive bacterial immunity. Science (New York, N.Y. 337: 816-821.
5. Esvelt, K. M., Smidler, A. L., Catteruccia, F., & Church, G. M. Concerning RNA-guided gene drives for the alteration of wild populations. eLife: e03401.
6. Ran, F. A., Hsu, P. D., Lin, C. Y., Gootenberg, J. S., Konermann, S., et al. Double nicking by RNAguided CRISPR Cas9 for enhanced genome editing specificity. Cell 154: 1380-1389.
7. Anderson, R. D., Haskell, R. E., Xia, H., Roessler, B. J., & Davidson, B. L. (2000) A simple method for the rapid generation of recombinant adenovirus vectors. Gene therapy 7: 1034-1038.
8. Wang, H., Luo, K., Tan, L. Z., Ren, B. G., Gu, L. Q., et al. (2012) p53-induced gene 3 mediates cell death induced by glutathione peroxidase 3. The Journal of biological chemistry 287: 16890-16902.

9. Zhu, Z. H., Yu, Y. P., Zheng, Z. L., Song, Y., Xiang, G. S., et al. (2010) Integrin alpha 7 interacts with high temperature requirement A2 (HtrA2) to induce prostate cancer cell death. The American journal of pathology 177: 1176-1186.

10. Shi, Y. K., Yu, Y. P., Tseng, G. C., & Luo, J. H. (2010) Inhibition of prostate cancer growth and metastasis using small interference RNA specific for minichromosome complex maintenance component 7. Cancer gene therapy 17: 694-699.

11. Luo, K. L., Luo, J. H., & Yu, Y. P. (2010) (−)-Epigallocatechin-3-gallate induces Du145 prostate cancer cell death via downregulation of inhibitor of DNA binding 2, a dominant negative helixloop-helix protein. Cancer science 101: 707-712.

12. Han, Y. C., Yu, Y. P., Nelson, J., Wu, C., Wang, H., et al. (2010) Interaction of integrin-linked kinase and miniature chromosome maintenance 7-mediating integrin {alpha}7 induced cell growth suppression. Cancer research 70: 4375-4384.

13. Zhu, Z. H., Yu, Y. P., Shi, Y. K., Nelson, J. B., & Luo, J. H. (2009) CSR1 induces cell death through inactivation of CPSF3. Oncogene 28: 41-51.

14. Yu, Y. P., Yu, G., Tseng, G., Cieply, K., Nelson, J., et al. (2007) Glutathione peroxidase 3, deleted or methylated in prostate cancer, suppresses prostate cancer growth and metastasis. Cancer research 67: 8043-8050.

15. Ren, B., Yu, Y. P., Tseng, G. C., Wu, C., Chen, K., et al. (2007) Analysis of integrin alpha7 mutations in prostate cancer, liver cancer, glioblastoma multiforme, and leiomyosarcoma. Journal of the National Cancer Institute 99: 868-880.

16. Yu, G., Tseng, G. C., Yu, Y. P., Gavel, T., Nelson, J., et al. (2006) CSR1 suppresses tumor growth and metastasis of prostate cancer. American Journal of Pathology 168: 597-607.

17. Han, Y. C., Zheng, Z. L., Zuo, Z. H., Yu, Y. P., Chen, R., et al. (2013) Metallothionein 1 h tumour suppressor activity in prostate cancer is mediated by euchromatin methyltransferase 1. The Journal of pathology 230: 184-193.

18. Ren, B., Yu, G., Tseng, G. C., Cieply, K., Gavel, T., et al. (2006) MCMI amplification and overexpression are associated with prostate cancer progression. Oncogene 25: 1090-1098.

19. Jing, L., Liu, L., Yu, Y. P., Dhir, R., Acquafondada, M., et al. (2004) Expression of myopodin induces suppression of tumor growth and metastasis. The American journal of pathology 164:1799-1806.

20. Smith, K. O., Galloway, K. S., Kennell, W. L., Ogilvie, K. K., & Radatus, B. K. (1982) A new nucleoside analog, 9-[[2-hydroxy-1-(hydroxymethyl)ethoxyl]methyl]guanine, highly active in vitro against herpes simplex virus types 1 and 2. Antimicrobial agents and chemotherapy 22: 55-61.

21. Luo, J. H., Liu, S., Zuo, Z. H., Chen, R., Tseng, G. C., et al. (2015) Discovery and Classification of Fusion Transcripts in Prostate Cancer and Normal Prostate Tissue. The American journal of pathology.

Various references are cited in this document, which are hereby incorporated by reference in their entireties herein.

SEQUENCE LISTING

<160> NUMBER OF SEQ ID NOS: 113

<210> SEQ ID NO 1
<211> LENGTH: 60
<212> TYPE: DNA
<213> ORGANISM: Artificial Sequence
<220> FEATURE:
<223> OTHER INFORMATION: Description of Artificial Sequence: Synthetic oligonucleotide

<400> SEQUENCE: 1

gcaaatacta tttcagaaac agcctatgag ggaaattttg gtgaagtata taagggcaca 60

<210> SEQ ID NO 2
<211> LENGTH: 25
<212> TYPE: RNA
<213> ORGANISM: Artificial Sequence
<220> FEATURE:
<223> OTHER INFORMATION: Description of Artificial Sequence: Synthetic oligonucleotide

<400> SEQUENCE: 2

cagccuauga gggaaauuuu gguga 25

<210> SEQ ID NO 3
<211> LENGTH: 27
<212> TYPE: RNA
<213> ORGANISM: Artificial Sequence
<220> FEATURE:
<223> OTHER INFORMATION: Description of Artificial Sequence: Synthetic oligonucleotide

<400> SEQUENCE: 3

ucaccaaaau uucccucaua ggcuguu 27

-continued

<210> SEQ ID NO 4
<211> LENGTH: 57
<212> TYPE: DNA
<213> ORGANISM: Artificial Sequence
<220> FEATURE:
<223> OTHER INFORMATION: Description of Artificial Sequence: Synthetic oligonucleotide

<400> SEQUENCE: 4

tccactacca tgccctcttc acaggtgtca tggagaaact ccagctgggc ccagaga 57

<210> SEQ ID NO 5
<211> LENGTH: 25
<212> TYPE: RNA
<213> ORGANISM: Artificial Sequence
<220> FEATURE:
<223> OTHER INFORMATION: Description of Artificial Sequence: Synthetic oligonucleotide

<400> SEQUENCE: 5

ugcccucuuc acagguguca uggag 25

<210> SEQ ID NO 6
<211> LENGTH: 27
<212> TYPE: RNA
<213> ORGANISM: Artificial Sequence
<220> FEATURE:
<223> OTHER INFORMATION: Description of Artificial Sequence: Synthetic oligonucleotide

<400> SEQUENCE: 6

cuccaugaca ccugugaaga gggcaug 27

<210> SEQ ID NO 7
<211> LENGTH: 63
<212> TYPE: DNA
<213> ORGANISM: Artificial Sequence
<220> FEATURE:
<223> OTHER INFORMATION: Description of Artificial Sequence: Synthetic oligonucleotide

<400> SEQUENCE: 7

tgtcagaatc caagtcaagt caggattcct tgttctggga atgtcagtgg aatctgctcc 60

tgc 63

<210> SEQ ID NO 8
<211> LENGTH: 25
<212> TYPE: DNA
<213> ORGANISM: Artificial Sequence
<220> FEATURE:
<223> OTHER INFORMATION: Description of Artificial Sequence: Synthetic oligonucleotide
<220> FEATURE:
<223> OTHER INFORMATION: Description of Combined DNA/RNA Molecule: Synthetic oligonucleotide

<400> SEQUENCE: 8

gucaggauuc cuuguucugg gaatg 25

<210> SEQ ID NO 9
<211> LENGTH: 27
<212> TYPE: RNA
<213> ORGANISM: Artificial Sequence
<220> FEATURE:
<223> OTHER INFORMATION: Description of Artificial Sequence: Synthetic oligonucleotide

-continued

<400> SEQUENCE: 9

cauucccaga acaaggaauc cugacuu 27

<210> SEQ ID NO 10
<211> LENGTH: 57
<212> TYPE: DNA
<213> ORGANISM: Artificial Sequence
<220> FEATURE:
<223> OTHER INFORMATION: Description of Artificial Sequence: Synthetic oligonucleotide

<400> SEQUENCE: 10

ttttaagact caccaagggc aaataagaag ccaactccaa caggtggaag agtacca 57

<210> SEQ ID NO 11
<211> LENGTH: 25
<212> TYPE: RNA
<213> ORGANISM: Artificial Sequence
<220> FEATURE:
<223> OTHER INFORMATION: Description of Artificial Sequence: Synthetic oligonucleotide

<400> SEQUENCE: 11

gacucaccaa gggcaaauaa gaagc 25

<210> SEQ ID NO 12
<211> LENGTH: 27
<212> TYPE: RNA
<213> ORGANISM: Artificial Sequence
<220> FEATURE:
<223> OTHER INFORMATION: Description of Artificial Sequence: Synthetic oligonucleotide

<400> SEQUENCE: 12

gcuucuuauu ugcccuuggu gagucuu 27

<210> SEQ ID NO 13
<211> LENGTH: 60
<212> TYPE: DNA
<213> ORGANISM: Artificial Sequence
<220> FEATURE:
<223> OTHER INFORMATION: Description of Artificial Sequence: Synthetic oligonucleotide

<400> SEQUENCE: 13

tgtcacagtt actagatata atgaaaatac ctggagtaga acagaaaaat tattatgtct 60

<210> SEQ ID NO 14
<211> LENGTH: 25
<212> TYPE: RNA
<213> ORGANISM: Artificial Sequence
<220> FEATURE:
<223> OTHER INFORMATION: Description of Artificial Sequence: Synthetic oligonucleotide

<400> SEQUENCE: 14

augaaaauac cuggaguaga acaga 25

<210> SEQ ID NO 15
<211> LENGTH: 27
<212> TYPE: RNA
<213> ORGANISM: Artificial Sequence
<220> FEATURE:
<223> OTHER INFORMATION: Description of Artificial Sequence: Synthetic oligonucleotide

-continued

<400> SEQUENCE: 15

ucuguucuac uccagguauu uucauua 27

<210> SEQ ID NO 16
<211> LENGTH: 60
<212> TYPE: DNA
<213> ORGANISM: Artificial Sequence
<220> FEATURE:
<223> OTHER INFORMATION: Description of Artificial Sequence: Synthetic oligonucleotide

<400> SEQUENCE: 16

aactacctgc actttgggga gcctaagtcc tggacagtaa gcaagcctgg atctgagaga 60

<210> SEQ ID NO 17
<211> LENGTH: 25
<212> TYPE: RNA
<213> ORGANISM: Artificial Sequence
<220> FEATURE:
<223> OTHER INFORMATION: Description of Artificial Sequence: Synthetic oligonucleotide

<400> SEQUENCE: 17

gagccuaagu ccuggacagu aagca 25

<210> SEQ ID NO 18
<211> LENGTH: 27
<212> TYPE: RNA
<213> ORGANISM: Artificial Sequence
<220> FEATURE:
<223> OTHER INFORMATION: Description of Artificial Sequence: Synthetic oligonucleotide

<400> SEQUENCE: 18

ugcuuacugu ccaggacuua ggcuccc 27

<210> SEQ ID NO 19
<211> LENGTH: 65
<212> TYPE: DNA
<213> ORGANISM: Artificial Sequence
<220> FEATURE:
<223> OTHER INFORMATION: Description of Artificial Sequence: Synthetic oligonucleotide

<400> SEQUENCE: 19

agcatctgga gttccgcctg ccggtggtat ttttgaatat gtggaatctg gcccaatggg 60

agctg 65

<210> SEQ ID NO 20
<211> LENGTH: 25
<212> TYPE: DNA
<213> ORGANISM: Artificial Sequence
<220> FEATURE:
<223> OTHER INFORMATION: Description of Artificial Sequence: Synthetic oligonucleotide
<220> FEATURE:
<223> OTHER INFORMATION: Description of Combined DNA/RNA Molecule: Synthetic oligonucleotide

<400> SEQUENCE: 20

ccgccugccg gugguauuuu ugaat 25

<210> SEQ ID NO 21
<211> LENGTH: 27
<212> TYPE: RNA
<213> ORGANISM: Artificial Sequence

-continued

<220> FEATURE:
<223> OTHER INFORMATION: Description of Artificial Sequence: Synthetic oligonucleotide

<400> SEQUENCE: 21

auucaaaaau accaccggca ggcggaa 27

<210> SEQ ID NO 22
<211> LENGTH: 68
<212> TYPE: DNA
<213> ORGANISM: Artificial Sequence
<220> FEATURE:
<223> OTHER INFORMATION: Description of Artificial Sequence: Synthetic oligonucleotide

<400> SEQUENCE: 22

ctgcttggat gagaagcagt gtaagcagtg tgcaaacaag gtgactggaa gcacctgctc 60

aatggctg 68

<210> SEQ ID NO 23
<211> LENGTH: 25
<212> TYPE: DNA
<213> ORGANISM: Artificial Sequence
<220> FEATURE:
<223> OTHER INFORMATION: Description of Artificial Sequence: Synthetic oligonucleotide
<220> FEATURE:
<223> OTHER INFORMATION: Description of Combined DNA/RNA Molecule: Synthetic oligonucleotide

<400> SEQUENCE: 23

acaaggugac uggaagcacc ugctc 25

<210> SEQ ID NO 24
<211> LENGTH: 27
<212> TYPE: RNA
<213> ORGANISM: Artificial Sequence
<220> FEATURE:
<223> OTHER INFORMATION: Description of Artificial Sequence: Synthetic oligonucleotide

<400> SEQUENCE: 24

gagcaggugc uuccagucac cuuguuu 27

<210> SEQ ID NO 25
<211> LENGTH: 68
<212> TYPE: DNA
<213> ORGANISM: Artificial Sequence
<220> FEATURE:
<223> OTHER INFORMATION: Description of Artificial Sequence: Synthetic oligonucleotide

<400> SEQUENCE: 25

aagccaaccg atacttttct ccaaatttta agacacagca ggatgccaat gcctcttccc 60

tcttagac 68

<210> SEQ ID NO 26
<211> LENGTH: 25
<212> TYPE: RNA
<213> ORGANISM: Artificial Sequence
<220> FEATURE:
<223> OTHER INFORMATION: Description of Artificial Sequence: Synthetic oligonucleotide

<400> SEQUENCE: 26

cuccaaauuu uaagacacag cagga 25

<210> SEQ ID NO 27
<211> LENGTH: 27
<212> TYPE: RNA
<213> ORGANISM: Artificial Sequence
<220> FEATURE:
<223> OTHER INFORMATION: Description of Artificial Sequence: Synthetic oligonucleotide

<400> SEQUENCE: 27

uccugcugug ucuuaaaauu uggagaa 27

<210> SEQ ID NO 28
<211> LENGTH: 22
<212> TYPE: DNA
<213> ORGANISM: Artificial Sequence
<220> FEATURE:
<223> OTHER INFORMATION: Description of Artificial Sequence: Synthetic primer

<400> SEQUENCE: 28

gcatttgcag tatagagcgt gc 22

<210> SEQ ID NO 29
<211> LENGTH: 22
<212> TYPE: DNA
<213> ORGANISM: Artificial Sequence
<220> FEATURE:
<223> OTHER INFORMATION: Description of Artificial Sequence: Synthetic primer

<400> SEQUENCE: 29

gtctaagagg gaagaggcat tg 22

<210> SEQ ID NO 30
<211> LENGTH: 21
<212> TYPE: DNA
<213> ORGANISM: Artificial Sequence
<220> FEATURE:
<223> OTHER INFORMATION: Description of Artificial Sequence: Synthetic primer

<400> SEQUENCE: 30

tcccattgac acctttccca c 21

<210> SEQ ID NO 31
<211> LENGTH: 21
<212> TYPE: DNA
<213> ORGANISM: Artificial Sequence
<220> FEATURE:
<223> OTHER INFORMATION: Description of Artificial Sequence: Synthetic primer

<400> SEQUENCE: 31

tgaggcttcc aggtacaaca g 21

<210> SEQ ID NO 32
<211> LENGTH: 21
<212> TYPE: DNA
<213> ORGANISM: Artificial Sequence
<220> FEATURE:
<223> OTHER INFORMATION: Description of Artificial Sequence: Synthetic primer

<400> SEQUENCE: 32

gcccagttgc agaaaggaat g 21

-continued

<210> SEQ ID NO 33
<211> LENGTH: 21
<212> TYPE: DNA
<213> ORGANISM: Artificial Sequence
<220> FEATURE:
<223> OTHER INFORMATION: Description of Artificial Sequence: Synthetic primer

<400> SEQUENCE: 33

cttgattttc agtggcaggc c 21

<210> SEQ ID NO 34
<211> LENGTH: 21
<212> TYPE: DNA
<213> ORGANISM: Artificial Sequence
<220> FEATURE:
<223> OTHER INFORMATION: Description of Artificial Sequence: Synthetic primer

<400> SEQUENCE: 34

gactacgtct catgcctttc c 21

<210> SEQ ID NO 35
<211> LENGTH: 21
<212> TYPE: DNA
<213> ORGANISM: Artificial Sequence
<220> FEATURE:
<223> OTHER INFORMATION: Description of Artificial Sequence: Synthetic primer

<400> SEQUENCE: 35

ttctcatcag gctggtcctt c 21

<210> SEQ ID NO 36
<211> LENGTH: 22
<212> TYPE: DNA
<213> ORGANISM: Artificial Sequence
<220> FEATURE:
<223> OTHER INFORMATION: Description of Artificial Sequence: Synthetic primer

<400> SEQUENCE: 36

gatgtggtgg aatatgccaa gg 22

<210> SEQ ID NO 37
<211> LENGTH: 21
<212> TYPE: DNA
<213> ORGANISM: Artificial Sequence
<220> FEATURE:
<223> OTHER INFORMATION: Description of Artificial Sequence: Synthetic primer

<400> SEQUENCE: 37

aaatccatgt gctgtggcac c 21

<210> SEQ ID NO 38
<211> LENGTH: 21
<212> TYPE: DNA
<213> ORGANISM: Artificial Sequence
<220> FEATURE:
<223> OTHER INFORMATION: Description of Artificial Sequence: Synthetic primer

<400> SEQUENCE: 38

cgcaatgagg aagaagggaa c 21

-continued

<210> SEQ ID NO 39
<211> LENGTH: 23
<212> TYPE: DNA
<213> ORGANISM: Artificial Sequence
<220> FEATURE:
<223> OTHER INFORMATION: Description of Artificial Sequence: Synthetic primer

<400> SEQUENCE: 39

cataaatctg gaatagggct cag 23

<210> SEQ ID NO 40
<211> LENGTH: 36
<212> TYPE: DNA
<213> ORGANISM: Artificial Sequence
<220> FEATURE:
<223> OTHER INFORMATION: Description of Artificial Sequence: Synthetic oligonucleotide

<400> SEQUENCE: 40

taaaagctaa agttaaatac ctgtttgaaa atggta 36

<210> SEQ ID NO 41
<211> LENGTH: 35
<212> TYPE: DNA
<213> ORGANISM: Artificial Sequence
<220> FEATURE:
<223> OTHER INFORMATION: Description of Artificial Sequence: Synthetic oligonucleotide

<400> SEQUENCE: 41

tcactcataa agaagagctt gaatttggaa atgac 35

<210> SEQ ID NO 42
<211> LENGTH: 32
<212> TYPE: DNA
<213> ORGANISM: Artificial Sequence
<220> FEATURE:
<223> OTHER INFORMATION: Description of Artificial Sequence: Synthetic oligonucleotide

<400> SEQUENCE: 42

atagctttga taaactgctc tccagaatgt tg 32

<210> SEQ ID NO 43
<211> LENGTH: 34
<212> TYPE: DNA
<213> ORGANISM: Artificial Sequence
<220> FEATURE:
<223> OTHER INFORMATION: Description of Artificial Sequence: Synthetic oligonucleotide

<400> SEQUENCE: 43

gccaactcac ccagattggc tgcaatgccg tcag 34

<210> SEQ ID NO 44
<211> LENGTH: 35
<212> TYPE: DNA
<213> ORGANISM: Artificial Sequence
<220> FEATURE:
<223> OTHER INFORMATION: Description of Artificial Sequence: Synthetic oligonucleotide

<400> SEQUENCE: 44

tgccaatact agtgtggctt ttcatggcct gccac 35

<210> SEQ ID NO 45

-continued

<211> LENGTH: 32
<212> TYPE: DNA
<213> ORGANISM: Artificial Sequence
<220> FEATURE:
<223> OTHER INFORMATION: Description of Artificial Sequence: Synthetic oligonucleotide

<400> SEQUENCE: 45

tcagaaacag cctatgaggg aaattttggt ga 32

<210> SEQ ID NO 46
<211> LENGTH: 37
<212> TYPE: DNA
<213> ORGANISM: Artificial Sequence
<220> FEATURE:
<223> OTHER INFORMATION: Description of Artificial Sequence: Synthetic oligonucleotide

<400> SEQUENCE: 46

gactcaccaa gggcaaataa gaagccaact ccaacag 37

<210> SEQ ID NO 47
<211> LENGTH: 42
<212> TYPE: DNA
<213> ORGANISM: Artificial Sequence
<220> FEATURE:
<223> OTHER INFORMATION: Description of Artificial Sequence: Synthetic oligonucleotide

<400> SEQUENCE: 47

taagcagtgt gcaaacaagg tgactggaag cacctgctca at 42

<210> SEQ ID NO 48
<211> LENGTH: 40
<212> TYPE: DNA
<213> ORGANISM: Artificial Sequence
<220> FEATURE:
<223> OTHER INFORMATION: Description of Artificial Sequence: Synthetic oligonucleotide

<400> SEQUENCE: 48

gcatctggag ttccgcctgc cggtggtatt tttgaatatg 40

<210> SEQ ID NO 49
<211> LENGTH: 39
<212> TYPE: DNA
<213> ORGANISM: Artificial Sequence
<220> FEATURE:
<223> OTHER INFORMATION: Description of Artificial Sequence: Synthetic oligonucleotide

<400> SEQUENCE: 49

ccagtcagtc aggattcctt gttctgggaa tgtcagtgg 39

<210> SEQ ID NO 50
<211> LENGTH: 40
<212> TYPE: DNA
<213> ORGANISM: Artificial Sequence
<220> FEATURE:
<223> OTHER INFORMATION: Description of Artificial Sequence: Synthetic oligonucleotide

<400> SEQUENCE: 50

gttactagat ataatgaaaa tacctggagt agaacagaaa 40

<210> SEQ ID NO 51
<211> LENGTH: 42

-continued

<212> TYPE: DNA
<213> ORGANISM: Artificial Sequence
<220> FEATURE:
<223> OTHER INFORMATION: Description of Artificial Sequence: Synthetic oligonucleotide

<400> SEQUENCE: 51

ccactaccat gccctcttca caggtgtcat ggagaaactc ca 42

<210> SEQ ID NO 52
<211> LENGTH: 47
<212> TYPE: DNA
<213> ORGANISM: Artificial Sequence
<220> FEATURE:
<223> OTHER INFORMATION: Description of Artificial Sequence: Synthetic oligonucleotide

<400> SEQUENCE: 52

aactacctgc actttgggga gcctaagtcc tggacagtaa gcaagcc 47

<210> SEQ ID NO 53
<211> LENGTH: 36
<212> TYPE: DNA
<213> ORGANISM: Artificial Sequence
<220> FEATURE:
<223> OTHER INFORMATION: Description of Artificial Sequence: Synthetic oligonucleotide

<400> SEQUENCE: 53

aatgtttaaa tttggaacgt ggactttggg gcaggt 36

<210> SEQ ID NO 54
<211> LENGTH: 30
<212> TYPE: DNA
<213> ORGANISM: Artificial Sequence
<220> FEATURE:
<223> OTHER INFORMATION: Description of Artificial Sequence: Synthetic oligonucleotide

<400> SEQUENCE: 54

taataatgaa cctagctacc ctaaactcct 30

<210> SEQ ID NO 55
<211> LENGTH: 34
<212> TYPE: DNA
<213> ORGANISM: Artificial Sequence
<220> FEATURE:
<223> OTHER INFORMATION: Description of Artificial Sequence: Synthetic oligonucleotide

<400> SEQUENCE: 55

tctcattatg ttgccgaagg ggatatcacc acca 34

<210> SEQ ID NO 56
<211> LENGTH: 35
<212> TYPE: DNA
<213> ORGANISM: Artificial Sequence
<220> FEATURE:
<223> OTHER INFORMATION: Description of Artificial Sequence: Synthetic oligonucleotide

<400> SEQUENCE: 56

ttttctccaa attttaagac acagcaggat gccaa 35

<210> SEQ ID NO 57
<211> LENGTH: 23
<212> TYPE: DNA

-continued

<213> ORGANISM: Artificial Sequence
<220> FEATURE:
<223> OTHER INFORMATION: Description of Artificial Sequence: Synthetic oligonucleotide

<400> SEQUENCE: 57

aaatttggaa cgtggacttt ggg 23

<210> SEQ ID NO 58
<211> LENGTH: 23
<212> TYPE: DNA
<213> ORGANISM: Artificial Sequence
<220> FEATURE:
<223> OTHER INFORMATION: Description of Artificial Sequence: Synthetic primer

<400> SEQUENCE: 58

gagaccatct tactggaagt tcc 23

<210> SEQ ID NO 59
<211> LENGTH: 21
<212> TYPE: DNA
<213> ORGANISM: Artificial Sequence
<220> FEATURE:
<223> OTHER INFORMATION: Description of Artificial Sequence: Synthetic primer

<400> SEQUENCE: 59

tggtactctt ccacctgttg g 21

<210> SEQ ID NO 60
<211> LENGTH: 21
<212> TYPE: DNA
<213> ORGANISM: Artificial Sequence
<220> FEATURE:
<223> OTHER INFORMATION: Description of Artificial Sequence: Synthetic primer

<400> SEQUENCE: 60

ttggcatgat agaccagtcc c 21

<210> SEQ ID NO 61
<211> LENGTH: 21
<212> TYPE: DNA
<213> ORGANISM: Artificial Sequence
<220> FEATURE:
<223> OTHER INFORMATION: Description of Artificial Sequence: Synthetic primer

<400> SEQUENCE: 61

cagcaccaag ggaatgtgta g 21

<210> SEQ ID NO 62
<211> LENGTH: 21
<212> TYPE: DNA
<213> ORGANISM: Artificial Sequence
<220> FEATURE:
<223> OTHER INFORMATION: Description of Artificial Sequence: Synthetic primer

<400> SEQUENCE: 62

gcgctgtcgt gtacccttaa c 21

<210> SEQ ID NO 63
<211> LENGTH: 22
<212> TYPE: DNA
<213> ORGANISM: Artificial Sequence

-continued

<220> FEATURE:
<223> OTHER INFORMATION: Description of Artificial Sequence: Synthetic primer

<400> SEQUENCE: 63

ggtaagggta gtattgggta gc 22

<210> SEQ ID NO 64
<211> LENGTH: 21
<212> TYPE: DNA
<213> ORGANISM: Artificial Sequence
<220> FEATURE:
<223> OTHER INFORMATION: Description of Artificial Sequence: Synthetic primer

<400> SEQUENCE: 64

ccagggctgg aattactatg g 21

<210> SEQ ID NO 65
<211> LENGTH: 21
<212> TYPE: DNA
<213> ORGANISM: Artificial Sequence
<220> FEATURE:
<223> OTHER INFORMATION: Description of Artificial Sequence: Synthetic primer

<400> SEQUENCE: 65

aagcaccagt ctgcacaatc c 21

<210> SEQ ID NO 66
<211> LENGTH: 21
<212> TYPE: DNA
<213> ORGANISM: Artificial Sequence
<220> FEATURE:
<223> OTHER INFORMATION: Description of Artificial Sequence: Synthetic primer

<400> SEQUENCE: 66

ttgatgtctg ctcccatcag g 21

<210> SEQ ID NO 67
<211> LENGTH: 21
<212> TYPE: DNA
<213> ORGANISM: Artificial Sequence
<220> FEATURE:
<223> OTHER INFORMATION: Description of Artificial Sequence: Synthetic primer

<400> SEQUENCE: 67

tgatatcgtg gccagctaac c 21

<210> SEQ ID NO 68
<211> LENGTH: 21
<212> TYPE: DNA
<213> ORGANISM: Artificial Sequence
<220> FEATURE:
<223> OTHER INFORMATION: Description of Artificial Sequence: Synthetic primer

<400> SEQUENCE: 68

aacacgccct acctgtactt c 21

<210> SEQ ID NO 69
<211> LENGTH: 21
<212> TYPE: DNA
<213> ORGANISM: Artificial Sequence
<220> FEATURE:

-continued

<223> OTHER INFORMATION: Description of Artificial Sequence: Synthetic primer

<400> SEQUENCE: 69

ctgagcaaag acagcaacac c 21

<210> SEQ ID NO 70
<211> LENGTH: 21
<212> TYPE: DNA
<213> ORGANISM: Artificial Sequence
<220> FEATURE:
<223> OTHER INFORMATION: Description of Artificial Sequence: Synthetic primer

<400> SEQUENCE: 70

tggaagttca agtcagcgca g 21

<210> SEQ ID NO 71
<211> LENGTH: 22
<212> TYPE: DNA
<213> ORGANISM: Artificial Sequence
<220> FEATURE:
<223> OTHER INFORMATION: Description of Artificial Sequence: Synthetic primer

<400> SEQUENCE: 71

gctgtctttg tgtgcaaact cc 22

<210> SEQ ID NO 72
<211> LENGTH: 21
<212> TYPE: DNA
<213> ORGANISM: Artificial Sequence
<220> FEATURE:
<223> OTHER INFORMATION: Description of Artificial Sequence: Synthetic primer

<400> SEQUENCE: 72

gtgactgctt ggatgagaag c 21

<210> SEQ ID NO 73
<211> LENGTH: 21
<212> TYPE: DNA
<213> ORGANISM: Artificial Sequence
<220> FEATURE:
<223> OTHER INFORMATION: Description of Artificial Sequence: Synthetic primer

<400> SEQUENCE: 73

ccagcatgca gcttttctga g 21

<210> SEQ ID NO 74
<211> LENGTH: 21
<212> TYPE: DNA
<213> ORGANISM: Artificial Sequence
<220> FEATURE:
<223> OTHER INFORMATION: Description of Artificial Sequence: Synthetic primer

<400> SEQUENCE: 74

agtaggcgcg agctaagcag g 21

<210> SEQ ID NO 75
<211> LENGTH: 21
<212> TYPE: DNA
<213> ORGANISM: Artificial Sequence
<220> FEATURE:
<223> OTHER INFORMATION: Description of Artificial Sequence: Synthetic

primer

<400> SEQUENCE: 75

gggacagtct gaatcatgtc c 21

<210> SEQ ID NO 76
<211> LENGTH: 24
<212> TYPE: DNA
<213> ORGANISM: Artificial Sequence
<220> FEATURE:
<223> OTHER INFORMATION: Description of Artificial Sequence: Synthetic primer

<400> SEQUENCE: 76

tcaagatcat tgctcctcct gagc 24

<210> SEQ ID NO 77
<211> LENGTH: 24
<212> TYPE: DNA
<213> ORGANISM: Artificial Sequence
<220> FEATURE:
<223> OTHER INFORMATION: Description of Artificial Sequence: Synthetic primer

<400> SEQUENCE: 77

tgctgtcacc ttcaccgttc cagt 24

<210> SEQ ID NO 78
<211> LENGTH: 37
<212> TYPE: DNA
<213> ORGANISM: Artificial Sequence
<220> FEATURE:
<223> OTHER INFORMATION: Description of Artificial Sequence: Synthetic primer

<400> SEQUENCE: 78

gtactcacgt aagctttcgc caccatggtg agcaagg 37

<210> SEQ ID NO 79
<211> LENGTH: 37
<212> TYPE: DNA
<213> ORGANISM: Artificial Sequence
<220> FEATURE:
<223> OTHER INFORMATION: Description of Artificial Sequence: Synthetic primer

<400> SEQUENCE: 79

gactcagatg ggcgcccttg tacagctcgt ccatgcc 37

<210> SEQ ID NO 80
<211> LENGTH: 69
<212> TYPE: DNA
<213> ORGANISM: Artificial Sequence
<220> FEATURE:
<223> OTHER INFORMATION: Description of Artificial Sequence: Synthetic primer

<400> SEQUENCE: 80

gactcagatg gcggccgcct gtattctttg ttttacagat ttgctgtcag gggttagata 60

gcttgccag 69

<210> SEQ ID NO 81
<211> LENGTH: 38
<212> TYPE: DNA
<213> ORGANISM: Artificial Sequence
<220> FEATURE:

-continued

<223> OTHER INFORMATION: Description of Artificial Sequence: Synthetic primer

<400> SEQUENCE: 81

gtactcacgt aagcttgagc taacattacc aatgaggc 38

<210> SEQ ID NO 82
<211> LENGTH: 37
<212> TYPE: DNA
<213> ORGANISM: Artificial Sequence
<220> FEATURE:
<223> OTHER INFORMATION: Description of Artificial Sequence: Synthetic primer

<400> SEQUENCE: 82

gactcagatg gctagcagtt cactgagtgt gccatgc 37

<210> SEQ ID NO 83
<211> LENGTH: 69
<212> TYPE: DNA
<213> ORGANISM: Artificial Sequence
<220> FEATURE:
<223> OTHER INFORMATION: Description of Artificial Sequence: Synthetic oligonucleotide

<400> SEQUENCE: 83

gtactcacgt gaattcctat tctgcctgct tgcatacctt ttgttttggt tgcagtatag 60

tgggctgag 69

<210> SEQ ID NO 84
<211> LENGTH: 37
<212> TYPE: DNA
<213> ORGANISM: Artificial Sequence
<220> FEATURE:
<223> OTHER INFORMATION: Description of Artificial Sequence: Synthetic primer

<400> SEQUENCE: 84

gactcagatg aagcttaaga gcatgggctt tggagtc 37

<210> SEQ ID NO 85
<211> LENGTH: 37
<212> TYPE: DNA
<213> ORGANISM: Artificial Sequence
<220> FEATURE:
<223> OTHER INFORMATION: Description of Artificial Sequence: Synthetic primer

<400> SEQUENCE: 85

gtactcacgt tctagactgg aatctaggac tcttggc 37

<210> SEQ ID NO 86
<211> LENGTH: 59
<212> TYPE: DNA
<213> ORGANISM: Artificial Sequence
<220> FEATURE:
<223> OTHER INFORMATION: Description of Artificial Sequence: Synthetic primer

<400> SEQUENCE: 86

ggccagtgaa ttgtaatacg actcactata gggaggcggc actcactgag ctctttgcc 59

<210> SEQ ID NO 87
<211> LENGTH: 31
<212> TYPE: DNA
<213> ORGANISM: Artificial Sequence

-continued

<220> FEATURE:
<223> OTHER INFORMATION: Description of Artificial Sequence: Synthetic primer

<400> SEQUENCE: 87

aaaaaaagca ccgactcggt gccacttttt c 31

<210> SEQ ID NO 88
<211> LENGTH: 60
<212> TYPE: DNA
<213> ORGANISM: Artificial Sequence
<220> FEATURE:
<223> OTHER INFORMATION: Description of Artificial Sequence: Synthetic primer

<400> SEQUENCE: 88

ggccagtgaa ttgtaatacg actcactata gggaggcggt gtggaaagga cgaaacaccg 60

<210> SEQ ID NO 89
<211> LENGTH: 31
<212> TYPE: DNA
<213> ORGANISM: Artificial Sequence
<220> FEATURE:
<223> OTHER INFORMATION: Description of Artificial Sequence: Synthetic primer

<400> SEQUENCE: 89

aaaaaaagca ccgactcggt gccacttttt c 31

<210> SEQ ID NO 90
<211> LENGTH: 21
<212> TYPE: DNA
<213> ORGANISM: Artificial Sequence
<220> FEATURE:
<223> OTHER INFORMATION: Description of Artificial Sequence: Synthetic primer

<400> SEQUENCE: 90

gcccatatat ggagttccgc g 21

<210> SEQ ID NO 91
<211> LENGTH: 21
<212> TYPE: DNA
<213> ORGANISM: Artificial Sequence
<220> FEATURE:
<223> OTHER INFORMATION: Description of Artificial Sequence: Synthetic primer

<400> SEQUENCE: 91

tctggcaagc tatctaaccc c 21

<210> SEQ ID NO 92
<211> LENGTH: 21
<212> TYPE: DNA
<213> ORGANISM: Artificial Sequence
<220> FEATURE:
<223> OTHER INFORMATION: Description of Artificial Sequence: Synthetic primer

<400> SEQUENCE: 92

agcacagaga cccagaaggt c 21

<210> SEQ ID NO 93
<211> LENGTH: 21
<212> TYPE: DNA
<213> ORGANISM: Artificial Sequence
<220> FEATURE:

-continued

<223> OTHER INFORMATION: Description of Artificial Sequence: Synthetic primer

<400> SEQUENCE: 93

aggaggagga ggaggagaaa g 21

<210> SEQ ID NO 94
<211> LENGTH: 24
<212> TYPE: DNA
<213> ORGANISM: Artificial Sequence
<220> FEATURE:
<223> OTHER INFORMATION: Description of Artificial Sequence: Synthetic primer

<400> SEQUENCE: 94

tctttgcact ttctgcatgt cccc 24

<210> SEQ ID NO 95
<211> LENGTH: 23
<212> TYPE: DNA
<213> ORGANISM: Artificial Sequence
<220> FEATURE:
<223> OTHER INFORMATION: Description of Artificial Sequence: Synthetic primer

<400> SEQUENCE: 95

gtccatcacg atgccagtgg tac 23

<210> SEQ ID NO 96
<211> LENGTH: 20
<212> TYPE: DNA
<213> ORGANISM: Artificial Sequence
<220> FEATURE:
<223> OTHER INFORMATION: Description of Artificial Sequence: Synthetic primer

<400> SEQUENCE: 96

atgatgatat cgccgcgctc 20

<210> SEQ ID NO 97
<211> LENGTH: 19
<212> TYPE: DNA
<213> ORGANISM: Artificial Sequence
<220> FEATURE:
<223> OTHER INFORMATION: Description of Artificial Sequence: Synthetic primer

<400> SEQUENCE: 97

cacgatggag gggaagacg 19

<210> SEQ ID NO 98
<211> LENGTH: 21
<212> TYPE: DNA
<213> ORGANISM: Artificial Sequence
<220> FEATURE:
<223> OTHER INFORMATION: Description of Artificial Sequence: Synthetic primer

<400> SEQUENCE: 98

gcccatatat ggagttccgc g 21

<210> SEQ ID NO 99
<211> LENGTH: 21
<212> TYPE: DNA
<213> ORGANISM: Artificial Sequence
<220> FEATURE:
<223> OTHER INFORMATION: Description of Artificial Sequence: Synthetic

primer

<400> SEQUENCE: 99

aggcaaagag ctcagtgagt g 21

<210> SEQ ID NO 100
<211> LENGTH: 23
<212> TYPE: DNA
<213> ORGANISM: Artificial Sequence
<220> FEATURE:
<223> OTHER INFORMATION: Description of Artificial Sequence: Synthetic primer

<400> SEQUENCE: 100

tgcctcattg gtaatgttag ctc 23

<210> SEQ ID NO 101
<211> LENGTH: 21
<212> TYPE: DNA
<213> ORGANISM: Artificial Sequence
<220> FEATURE:
<223> OTHER INFORMATION: Description of Artificial Sequence: Synthetic primer

<400> SEQUENCE: 101

ggcgaattgg gtacacttac c 21

<210> SEQ ID NO 102
<211> LENGTH: 21
<212> TYPE: DNA
<213> ORGANISM: Artificial Sequence
<220> FEATURE:
<223> OTHER INFORMATION: Description of Artificial Sequence: Synthetic primer

<400> SEQUENCE: 102

actcacgggg atttccaagt c 21

<210> SEQ ID NO 103
<211> LENGTH: 21
<212> TYPE: DNA
<213> ORGANISM: Artificial Sequence
<220> FEATURE:
<223> OTHER INFORMATION: Description of Artificial Sequence: Synthetic primer

<400> SEQUENCE: 103

aagtcgtgct gcttcatgtg g 21

<210> SEQ ID NO 104
<211> LENGTH: 21
<212> TYPE: DNA
<213> ORGANISM: Artificial Sequence
<220> FEATURE:
<223> OTHER INFORMATION: Description of Artificial Sequence: Synthetic primer

<400> SEQUENCE: 104

tgttctagcc aagaggctga g 21

<210> SEQ ID NO 105
<211> LENGTH: 21
<212> TYPE: DNA
<213> ORGANISM: Artificial Sequence
<220> FEATURE:
<223> OTHER INFORMATION: Description of Artificial Sequence: Synthetic primer

-continued

<400> SEQUENCE: 105

ggcgaattgg gtacacttac c 21

<210> SEQ ID NO 106
<211> LENGTH: 30
<212> TYPE: DNA
<213> ORGANISM: Artificial Sequence
<220> FEATURE:
<223> OTHER INFORMATION: Description of Artificial Sequence: Synthetic oligonucleotide

<400> SEQUENCE: 106

taataatgaa cctagctacc ctaaactcct 30

<210> SEQ ID NO 107
<211> LENGTH: 20
<212> TYPE: DNA
<213> ORGANISM: Artificial Sequence
<220> FEATURE:
<223> OTHER INFORMATION: Description of Artificial Sequence: Synthetic oligonucleotide

<400> SEQUENCE: 107

gtgaattcat tcatcataaa 20

<210> SEQ ID NO 108
<211> LENGTH: 31
<212> TYPE: DNA
<213> ORGANISM: Artificial Sequence
<220> FEATURE:
<223> OTHER INFORMATION: Description of Artificial Sequence: Synthetic oligonucleotide

<400> SEQUENCE: 108

actcagttag taaatgaagg agctggaaca t 31

<210> SEQ ID NO 109
<211> LENGTH: 28
<212> TYPE: DNA
<213> ORGANISM: Artificial Sequence
<220> FEATURE:
<223> OTHER INFORMATION: Description of Artificial Sequence: Synthetic oligonucleotide

<400> SEQUENCE: 109

actcagttag taaaaggagc tggaacat 28

<210> SEQ ID NO 110
<211> LENGTH: 30
<212> TYPE: DNA
<213> ORGANISM: Artificial Sequence
<220> FEATURE:
<223> OTHER INFORMATION: Description of Artificial Sequence: Synthetic oligonucleotide

<400> SEQUENCE: 110

gactgaatgc acatgccacc acacccggct 30

<210> SEQ ID NO 111
<211> LENGTH: 26
<212> TYPE: DNA
<213> ORGANISM: Artificial Sequence
<220> FEATURE:
<223> OTHER INFORMATION: Description of Artificial Sequence: Synthetic oligonucleotide

-continued

<400> SEQUENCE: 111

gactgaacat gccaccacac ccggct 26

<210> SEQ ID NO 112
<211> LENGTH: 20
<212> TYPE: DNA
<213> ORGANISM: Artificial Sequence
<220> FEATURE:
<223> OTHER INFORMATION: Description of Artificial Sequence: Synthetic oligonucleotide

<400> SEQUENCE: 112

cactcactga gctctttgcc 20

<210> SEQ ID NO 113
<211> LENGTH: 81
<212> TYPE: DNA
<213> ORGANISM: Artificial Sequence
<220> FEATURE:
<223> OTHER INFORMATION: Description of Artificial Sequence: Synthetic oligonucleotide

<400> SEQUENCE: 113

cctgtgaatt cattcatcat aaaataataa tgaacctagc taccctaaac tccttttaca 60

ctcactgagc tctttgcctg g 81

What is claimed is:

1. A kit for performing a genome editing technique in a prostate cancer cell comprising a fusion gene, wherein the kit comprises: (i) a vector comprising a nucleic acid encoding a Cas protein or a mutant thereof and one or more guide RNAs (gRNAs); and (ii) a vector comprising a donor nucleic acid and one or more targeting sequences, and wherein the fusion gene is selected from the group consisting of TRMT1 1-GRIK2, SLC45A2-AMACR, MTOR-TP53BP1, LRRC59-FLJ60017, TMEM135-CCDC67, KDM4B-AC011523.2, MAN2A1-FER, PTEN-NOLC1, CCNH-C5orf30, ZMPSTE24-ZMYM4, CLTC-ETV1, ACPP-SEC13, DOCK7-OLR1, PCMTD1-SNTG1 and a combination thereof, wherein the one or more gRNAs comprise one gRNA that is complementary to a region within one gene of the fusion gene and a second gRNA that is complementary to a region within a second gene of the fusion gene.

2. The kit of claim 1, wherein the fusion gene is TMEM135-CCDC67 or CCNH C5orf30.

3. The kit of claim 1, wherein the donor nucleic acid encodes a protein that induces cell death of the prostate cancer cell.

4. The kit of claim 3, wherein the protein that induces cell death is Herpes Simplex Virus 1 thymidine kinase.

5. The kit of claim 1, wherein the one or more targeting sequences are complementary to one or more sequences of the fusion gene to promote homologous recombination of and the insertion of the donor nucleic acid into the fusion gene.

6. The kit of claim 1, wherein the Cas protein or mutant thereof is a Cas 9 protein or a mutant thereof.

7. The kit of claim 6, wherein the Cas 9 protein or mutant thereof is $Cas9^{D10A}$.

8. The kit of claim 1, further comprising ganciclovir and/or valganciclovir.

9. The kit of claim 1, further comprising one or more nucleic acid primers, one or more nucleic acid probes and/or one or more antibodies for detecting the one or more fusion genes.

10. A kit for performing a genome editing technique in a prostate cancer cell comprising a fusion gene, wherein the kit comprises: (i) a vector comprising a nucleic acid encoding a Cas protein; (ii) a vector comprising a nucleic acid encoding one or more guide RNAs (gRNAs); and (iii) a vector comprising a donor nucleic acid and one or more targeting sequences, and wherein the fusion gene is selected from the group consisting of TRMT11-GRIK2, SLC45A2-AMACR, MTOR-TP53BP1, LRRC59-FLJ60017, TMEM135-CCDC67, KDM4B-AC011523.2, MAN2A1-FER, PTEN-NOLC1, CCNH-C5orf30, ZMPSTE24-ZMYM4, CLTC-ETV1, ACPP-SEC13, DOCK7-OLR1, PCMTD1-SNTG1 and a combination thereof, wherein the one or more gRNAs comprise one gRNA that is complementary to a region within one gene of the fusion gene and a second gRNA that is complementary to a region within a second gene of the fusion gene.

11. The kit of claim 10, wherein the fusion gene is TMEM135-CCDC67 or CCNH C5orf30.

12. The kit of claim 10, wherein the donor nucleic acid encodes a protein that induces cell death of the prostate cancer cell.

13. The kit of claim 12, wherein the protein that induces cell death is Herpes Simplex Virus 1 thymidine kinase.

14. The kit of claim 10, wherein the one or more targeting sequences are complementary to one or more sequences of the fusion gene to promote homologous recombination of and the insertion of the donor nucleic acid into the fusion gene.

15. The kit of claim 10, wherein the Cas protein or mutant thereof is a Cas 9 protein or a mutant thereof.

16. The kit of claim 15, wherein the Cas 9 protein or mutant thereof is $Cas9^{D10A}$.

17. The kit of claim 10, further comprising ganciclovir and/or valganciclovir.

18. The kit of claim 10, further comprising one or more nucleic acid primers, one or more nucleic acid probes and/or one or more antibodies for detecting the one or more fusion genes.

* * * * *